RELAP5/MOD3.2.2 Gamma Assessment for Pressurized Thermal Shock Applications

RELAP5/MOD3.2.2 Gamma Assessment for Pressurized Thermal Shock Applications

Prepared by:
C. D. Fletcher[†], D. A. Prelewicz[†] , W. C. Arcieri[†]

Contributors:
M. A. Bolander[†], D. L. Mlynarczyk[†], K. C. Wagner[§], R. Anderson[‡], J. Cajigas[‡]

Michael B. Rubin, NRC Project Manager

[†]ISL, Inc.
11140 Rockville Pike
Rockville, MD 20852

[‡]Applied Analysis Corp.
2525 N. Fremont Ave.
Idaho Falls, ID 83415

[§]Innovative Technology Solutions, Inc..
400 West Gowe St.
Kent, WA 98032

Division of Systems Analysis and Regulatory Effectiveness
Office of Nuclear Regulatory Research
U.S. Nuclear Regulatory Commission
Washington, DC 20555-0001

ABSTRACT

The RELAP5/MOD 3.2.2Gamma computer code has been used to simulate overcooling and/or pressurization events that have the potential to result in pressurized thermal shock (PTS) in the reactor vessels of pressurized water reactors. An assessment of this code version is reported here to establish the suitability of the computer code for analyzing transients that may be significant PTS risk contributors. Code assessment principally consists of performing calculations for a specific test in an experimental facility and comparing the calculated results to the measured data from the experimental facility.

Prior assessment of the RELAP5 code series has been performed for a wide variety of transients over the 20-year development history of the code.   Many of these assessments focused on loss-of-coolant accidents (LOCAs) where the purpose of the analysis is to demonstrate core integrity during postulated licensing basis transients. For LOCAs, conditions in the core region are of principal interest. In contrast, for PTS related transients the focus is on the temperature and pressure conditions in the reactor vessel downcomer. Hence the assessment reported here focuses on comparing RELAP5 results with experimental data for conditions in the downcomer. Note that LOCA can be an important risk contributor to PTS and so assessments using LOCA tests remain relevant.

This report presents assessments that demonstrate the suitability of the code for analyzing PTS transients.

FOREWORD

The reactor pressure vessel is exposed to neutron radiation during normal operation. Over time, the vessel steel becomes progressively more brittle in the region adjacent to the core. If a vessel had a preexisting flaw of critical size *and* certain severe system transients occurred, this flaw could propagate rapidly through the vessel, resulting in a through-wall crack. The severe transients of concern, known as pressurized thermal shock (PTS), are characterized by rapid cooling (i.e., thermal shock) of the internal reactor pressure vessel surface that may be combined with repressurization. The simultaneous occurrence of critical-size flaws, embrittled vessel, and a severe PTS transient is a very low probability event. The current study shows that U.S. pressurized-water reactors do not approach the levels of embrittlement to make them susceptible to PTS failure, even during extended operation well beyond the original 40-year design life.

Advancements in our understanding and knowledge of materials behavior, our ability to realistically model plant systems and operational characteristics, and our ability to better evaluate PTS transients to estimate loads on vessel walls have shown that earlier analyses, performed some 20 years ago as part of the development of the PTS rule, were overly conservative, based on the tools available at the time. Consistent with the NRC's Strategic Plan to use best-estimate analyses combined with uncertainty assessments to resolve safety-related issues, the NRC's Office of Nuclear Regulatory Research undertook a project in 1999 to develop a technical basis to support a risk-informed revision of the existing PTS Rule, set forth in Title 10, Section 50.61, of the *Code of Federal Regulations* (10 CFR 50.61).

Two central features of the current research approach were a focus on the use of realistic input values and models and an *explicit* treatment of uncertainties (using currently available uncertainty analysis tools and techniques). This approach improved significantly upon that employed in the past to establish the existing 10 CFR 50.61 embrittlement limits. The previous approach included unquantified conservatisms in many aspects of the analysis, and uncertainties were treated *implicitly* by incorporating them into the models.

This report is one of a series of 21 reports that provide the technical basis that the staff will consider in a potential revision of 10 CFR 50.61. The risk from PTS was determined from the integrated results of the Fifth Version of the Reactor Excursion and Leak Analysis Program (RELAP5) thermal-hydraulic analyses, fracture mechanics analyses, and probabilistic risk assessment. The current study used the RELAP5 code to calculate the thermal-hydraulic response of three nuclear power plants for a wide spectrum of transients and accidents of possible PTS significance. To validate the RELAP5 code, a wide range of assessment cases were performed, and this assessment is the subject of the current report. The results were used to determine the accuracy and uncertainty of RELAP5 in predicting pressure, temperature, and heat transfer to the wall of the reactor vessel, which were the thermal-hydraulic boundary conditions required for fracture mechanics analyses. The assessment results showed that RELAP5 can be used with confidence for calculating plant responses to PTS transients.

Brian W. Sheron, Director
Office of Nuclear Regulatory Research
U.S. Nuclear Regulatory Commission

v

CONTENTS

LIST OF FIGURES

LIST OF TABLES

EXECUTIVE SUMMARY

This report documents assessments of the RELAP5/MOD3.2.2Gamma computer code for simulating PTS-significant thermal-hydraulic behavior in PWRs. These assessments are accomplished by comparing the results from RELAP5/MOD3.2.2Gamma simulations of tests performed in experimental facilities which are scaled physical representations of PWRs with the measured test data. The assessment focuses on the reactor vessel downcomer fluid temperature and RCS pressure, which are the most important parameters for evaluating PTS risk. The comparisons indicate the strengths and weaknesses of the computer code for simulating the physical behavior.

The RELAP5 PTS assessments use data from six experiments in four different separate-effects experimental facilities and from 12 experiments in five different integral-effects experimental facilities. The separate-effects experiments specifically address: (1) pressurizer draining and filling, (2) critical break flow, (3) steam and water behavior in the reactor vessel lower plenum and downcomer regions during the end-of-blowdown and refill periods of LBLOCAs, and (4) single-phase, two-phase and reflux cooling mode loop natural circulation phenomena under primary-side and secondary-side degraded inventory conditions. These represent phenomena that are significant for the prediction of the important PTS parameters. The integral-effects experiments address phenomena in coolant-system configurations specifically representing the geometries of Westinghouse, Combustion Engineering and Babcock & Wilcox PWR plant designs. The integral-effects tests simulated PWR behavior under conditions expected during small, medium and large break LOCAs, stuck-open pressurizer SRV events and feed-and-bleed cooling operation scenarios. These sequence categories make up the majority of the risk-dominant sequences in the PTS evaluation study for the Oconee-1, Beaver Valley-1 and Palisades PWRs.

The results of the 18 assessment cases generally indicated good and excellent agreement between the RELAP5 calculations and the measured test data. The average uncertainty in predicting the RCS pressure is characterized as +0.2 MPa [+29 psi]. The average uncertainty in predicting the reactor vessel downcomer fluid temperature is characterized as +10 K [+18EF].

ABBREVIATIONS

ACRS	Advisory Committee on Reactor Safeguards
ADS	automatic depressurization system
AFW	auxiliary feedwater
B&W	Babcock and Wilcox
CE	Combustion Engineering
CFT	core flood tank
CL	cold leg
CMT	core makeup tank
ECC	emergency core coolant
ECCS	emergency core coolant system
EFW	emergency feedwater
HFP	hot full power
HL	hot leg
HPI	high pressure injection
HZP	hot zero power
ISP	International Standard Problem
IRWST	In-containment Refueling Water Storage Tank
LBLOCA	large break loss-of-coolant accident
L/D ratio	length-to-diameter ratio
LOCA	loss-of-coolant accident
LOFT	Loss of Fluid Test
LPI	low pressure injection
MFW	main feedwater
MIST	Multi-Loop Integral Systems Test
MIT	Massachusetts Institute of Technology
NC	natural circulation
OTSG	once-through steam generator
PIRT	phenomena identification and ranking table
PORV	power operated relief valve
PRA	probabilistic risk assessment
PRHR	Passive Residual Heat Removal
PTS	pressurized thermal shock
PWR	pressurized-water reactor
RCP	reactor coolant pump
RCS	reactor coolant system
ROSA	Rig of Safety Assessment

SBLOCA   small break loss-of-coolant accident
SG   steam generator
SRV   safety relief valve

UPTF   Upper Plenum Test Facility
USNRC   U.S. Nuclear Regulatory Commission

ABBREVIATIONS

ACRS	Advisory Committee on Reactor Safeguards
ADS	automatic depressurization system
AFW	auxiliary feedwater
B&W	Babcock and Wilcox
CE	Combustion Engineering
CFT	core flood tank
CL	cold leg
CMT	core makeup tank
ECC	emergency core coolant
ECCS	emergency core coolant system
EFW	emergency feedwater
HFP	hot full power
HL	hot leg
HPI	high pressure injection
HZP	hot zero power
ISP	International Standard Problem
IRWST	In-containment Refueling Water Storage Tank
LBLOCA	large break loss-of-coolant accident
L/D ratio	length-to-diameter ratio
LOCA	loss-of-coolant accident
LOFT	Loss of Fluid Test
LPI	low pressure injection
MFW	main feedwater
MIST	Multi-Loop Integral Systems Test
MIT	Massachusetts Institute of Technology
NC	natural circulation
OTSG	once-through steam generator
PIRT	phenomena identification and ranking table
PORV	power operated relief valve
PRA	probabilistic risk assessment
PRHR	Passive Residual Heat Removal
PTS	pressurized thermal shock
PWR	pressurized-water reactor
RCP	reactor coolant pump
RCS	reactor coolant system
ROSA	Rig of Safety Assessment

SBLOCA   small break loss-of-coolant accident
SG   steam generator
SRV   safety relief valve

UPTF   Upper Plenum Test Facility
USNRC   U.S. Nuclear Regulatory Commission

1. INTRODUCTION

Pressurized thermal shock (PTS) refers to a condition in the reactor vessel of a pressurized water reactor (PWR) where a combination of cold water and high pressure can lead to a brittle fracture of the reactor vessel wall. PTS risk increases as a PWR continues operating; flaws in the reactor vessel wall become more susceptible to failure as a function of cumulative neutron absorption.

PTS risk-significant transients primarily involve a period of relatively rapid energy removal from the primary coolant system followed by a relatively quiescent period where pressure and temperature conditions do not rapidly change. During the period of energy removal, the primary coolant system temperatures decline. Depending on the type of transient, this cooldown can be due to the combined effects of loss of high-energy coolant (through a break or valve), excessive heat removal by the secondary coolant system and injection of low temperature coolant from the emergency core cooling systems (ECCS). In some transients, late primary coolant system repressurization can occur due to an event such as re-closure of a stuck-open relief valve or simply from refilling the system. Many events feature single-phase flow in the primary coolant loops once the quiescent period is reached. For some events, notably events where no break in the primary system is postulated, single-phase flow conditions will exist in the primary coolant loops throughout the event, so that complex two-phase flow phenomena will play no role. However, thermal hydraulic conditions are quite variable during PTS risk-significant transients, depending on the nature of the transient. It is noted that some phenomena such as cold leg thermal stratification cannot be modeled by a one-dimensional code such as RELAP5. However, these phenomena are found to have a minimal effect on the reactor vessel downcomer temperature and pressure.

Because of the wide variation in thermal-hydraulic conditions that can occur in PTS transients, a phenomena identification and ranking table (PIRT) exercise was conducted to identify the most important phenomena affecting PTS in PWRs. Two independent PTS PIRT exercises have been conducted, one before and one after the evaluation of PTS results in the current PTS evaluation study. The results from both PTS PIRTs are shown in Table 1-1. Many of the items on the PIRT list are strictly related to specific plant operator actions and/or hardware availability or failure criteria. As such, these items are mostly not relevant for code assessments using data from scaled experimental facilities.

The PIRT was used to focus the assessment by defining the following list of parameters; data covering these parameters are, to varying degrees, available from the scaled experimental facilities. The assessments presented here emphasize comparisons between calculated and measured data for:

- Break flow
- Pressurization
- Natural circulation/flow stagnation
- Boiling-condensation mode/ Reflux condensation
- Mixing in the downcomer
- Condensation, mixing and stratification in the cold leg
- Integral system response

These phenomena were selected because of their primary or secondary importance for the PTS figures of merit (reactor vessel downcomer fluid temperature, pressure and wall heat transfer coefficient). Three phenomena of most importance to PTS significant transients were identified. Natural circulation/flow stagnation is particularly significant because if loop flow continues, warm

(average coolant system temperature) fluid is flushed through the reactor vessel downcomer, while if it stagnates the effects of cold ECCS water are seen immediately and directly in the downcomer. Integral system response is important because the ECCS injection behavior (flow rates, timings, and to some extent temperatures) are functions of the overall system behavior (mainly pressure, but also various levels and temperatures). Pressurization is itself a primary figure of merit in the PTS analyses. The other phenomena were selected because of their influence on the main phenomena or because they represent potentially significant downcomer localized effects.

This report documents assessments of the RELAP5/MOD3.2.2Gamma computer code (Reference 1-1) for simulating PTS-significant thermal-hydraulic behavior in PWRs. These assessments are accomplished by comparing the results from RELAP5/MOD3.2.2Gamma simulations of tests performed in experimental facilities which are scaled physical representations of PWRs with the measured test data. The comparisons indicate the strengths and weaknesses of the computer code for simulating the physical behavior. To the extent feasible, the RELAP5 facility models used to simulate the experiments for the assessments were constructed to be consistent with the RELAP5 plant models used to perform the plant simulations for the PTS study. The objectives of this consistency are to minimize the influence of model nodalization as a variable in the comparative analyses and to assure that the code experimental assessment results are based on models that are representative of the plant models used in the PTS study.

Practical limitations affect the extent of modeling consistency that can be achieved. No RELAP5 system models of plants or experiments were developed in their entirety for the PTS study. Existing RELAP5 system models originally developed at national laboratories or by commercial organizations were used as starting points for the PTS plant and experimental facility models. These original model developments typically occurred ten or more years ago and documentation on the facilities and models varies widely from case to case. On the other hand, much similarity is generally evident among the starting-point test facility and plant system models. This similarity comes because models of different facilities often were developed by the same organization and also because the various organizations frequently shared their experiences regarding the requirements for developing acceptable system models. To the extent possible, independent reviews of models were performed to assure their adequacy and accuracy.

Within this environment, it was endeavored to use models with nodalization schemes and selections of key user input options that are as similar as possible for the PTS study. As an example regarding nodalization similarity, models employing 3 cells and 5 cells to model the cold leg would be considered similar, while models employing 3 cells and 40 cells for that purpose would not. Because of its importance for the PTS study, it was attempted to use reactor vessel downcomer nodalization as similar as possible among the models. However, constraints on achieving this similarity relate to: (1) unique, facility-specific configuration issues, (2) the availability of adequate current facility configuration information and (3) prioritization considerations, for example where schedule and economic aspects of a task may dictate that an extensive modification of a model can not be justified in the context of the significance of doing so. In addition to nodalization, there are many user option selections pertinent to RELAP5 system models. The key user option selections for the PTS analysis are to employ the Henry-Fauske critical flow model at locations representing breaks and relief valves and to disable momentum flux in the reactor vessel downcomer region of models where the downcomer is represented using a two-dimensional nodalization scheme.

Table 1-2 summarizes the RELAP5 nodalizations of the system experimental facility models used for the assessments in this report. For reference the table also includes comparable nodalization

information for the RELAP5 plant models used in the PTS study. In addition to the nodalization of fluid volumes, consistent modeling of heat structures is used. Models typically employ heat structures to represent not only core fuel rods and steam generator tubes, but also the passive structures of a facility such as piping walls and internal components. Because of scale effects, heat losses to containment typically are not represented in the plant models but are represented in subscale experimental facility models where heat loss effects can be significant.

The assessments in this report are separated based on whether the experiment produced separate effects or integral effects test data. Separate effects tests typically simulate the behavior in only specific components of a PWR reactor coolant system, such as the pressurizer, or the specific detailed behavior of a subset of PWR components under unique operating conditions. Separate effects experiments are controlled by setting thermal-hydraulic boundary conditions on the test components that generally represent those expected in the PWR system in certain situations (for example the pressurizer inlet flow rate and temperature during an insurge event). The separate effects assessments are presented in Section 2. Integral effects tests simulate the behavior of an entire PWR reactor coolant system and as such the boundary conditions imposed in the test are generally the same as imposed on the PWR system (for example, core power, reactor coolant pump speed, pressurized pressure and steam turbine inlet pressure). The integral effects assessments are presented in Section 3. The assessment conclusions are given in Section 4 and references are provided in Section 5.

Table 1-1   Phenomena Identification and Ranking Table for Pressurized Thermal Shock in Pressurized Water Reactors

Old Rank	New Rank	Description	Comments
6	1	Break flow/size (or valve capacity)	Importance of LBLOCA has increased, pressure is less important
1 & 3	2	ECCS flow rate (Accumulator, HPI, LPI)	State on/off, shutoff head of pumps, accumulator initial pressure
	3	Operator actions	Includes operating procedures, RCP trip, HPI throttling, feedwater isolation, etc.
	4	Time of stuck valve re-closure	Pressurizer safety relief valves which re-close after sticking open
9	5	Plant initial state	Hot Full Power vs. Hot Zero Power Operation
	6	Break location	Primary LOCA (hot leg, cold leg), MSLB (Inside/outside containment, upstream/downstream MSIVs), SGTR

Old Rank	New Rank	Description	Comments
	7	Unique plant features/design	Difference in steam generator design, # of loops, vent valves, etc.
	8	Vessel to downcomer fluid heat transfer	Affects the rate at which heat is transferred from the vessel wall to the downcomer fluid
5	9	ECCS temperatures	Seasonal/operational variations
	10	Sump recirculation	ECCS temperature/flow changes after RWST drained
19	11	Feedwater control (or failure)	Post trip main feedwater behavior for Oconee, steam generator overfeed events
18	12	Feedwater Temperature	Oconee (using emergency feedwater instead of main feedwater during transient)
2	13	Reactor vessel wall heat conduction	In conjunction with vessel to downcomer fluid heat transfer, affects the rate at which heat is transferred from the vessel wall to the downcomer fluid. Important particularly in those situations when heat transfer from the wall is conduction limited
11	14	Loop flow upstream of HPI	Scenario dependent, not as important for LBLOCAs
12	15	ECCS-Reactor coolant system mixing in cold legs	Affects potential for formation of cold plumes in the downcomer. Ranking lowered due to Oregon State University data

Old Rank	New Rank	Description	Comments
4	16	Flow distribution in downcomer	Affects mixing and potential for formation of cold plumes in the downcomer. Ranking lowered due to Oregon State University data
8	17	Jet behavior, cold leg pipe to downcomer	Ranking lowered due to Oregon State University data
13	18	Loop temperature upstream of the location of the safety injection junction	Scenario dependent, important for MSLB, not for LBLOCA
20	19	Steam generator energy exchange	
21	20	Timing of manual reactor coolant pump trips	
17	21	Interphase condensation & non-condensables	RELAP5 overprediction of condensation
14	22	Downcomer to core inlet bypass	Ranking lowered, less important for LBLOCAs
15	23	Downcomer to upper plenum bypass	Ranking lowered, less important for LBLOCAs
16	24	Upper head HTC under voided conditions	Ranking lowered, less important for LBLOCAs
22	--	Combined with new #7	
7	--	HPI temp (replaced with ECCS temperatures)	
10	--	Combined with old #2	

Table 1-2 Summary of RELAP5 Nodalization Schemes Employed in the Experimental Facility and Plant System Models in the PTS Study

Facility and Experiment Type(s)	Reactor Vessel Downcomer Cells	Core Cells	Steam Generator Cells	Hot Leg Cells	Pump-to-Vessel Cold Leg Cells	Pzr Cells
UPTF Test 6-131 Interphase condensation, steam back-flow in vessel	2 azimuth, 4 axial	N/A	N/A	N/A	3	N/A
UPTF Test 1-21 Fluid-Fluid Mixing in Downcomer	8 azimuth 10 axial	N/A	N/A	N/A	3	N/A
Semiscale Tests S-NC-02 and S-NC-03 Coolant loop natural circulation flow	1 azimuth, 11 axial The downcomer in the facility is a pipe	6	9 upflow, 9 downflow	8	5	N/A
ROSA-IV Tests SB-CL-18 and SB-HL-06 SBLOCAs with minimal cold leg asymmetries	1 azimuth, 14 axial	8	4 upflow, 4 downflow	3	4	8
ROSA/AP600 Tests APCL03 and APCL09 SBLOCAs, which ADS operation effectively changes into LBLOCAs	6 azimuth, 12 axial	8	4 upflow, 4 downflow	3	4	8
LOFT Test L2-5 LBLOCA	2 azimuth, 6 axial	12	4 upflow, 4 downflow	6	3	8
LOFT Test L3-7 SBLOCA	1 azimuth, 8 axial	6	4 upflow, 4 downflow	6	8	8

Facility and Experiment Type(s)	Reactor Vessel Downcomer Cells	Core Cells	Steam Generator Cells	Hot Leg Cells	Pump-to-Vessel Cold Leg Cells	Pzr Cells
LOFT Test L3-1 MBLOCA	1 azimuth, 8 axial 6 azimuth, 8 axial Assessment performed with both configurations	6	4 upflow, 4 downflow	6	8	8
APEX Tests APEX-CE-13 and APEX-CE-05 Stuck open pressurizer relief valve, HPI injection into stagnant loop	8 azimuth, 7 axial	6	4 upflow, 4 downflow	4	3	8
Full-Scale Plants Oconee, Beaver Valley, Palisades	6 azimuth, 8 to 10 axial	6	4 upflow, 4 downflow for U-tube SGs 10 axial for once-through SGs	3 to 4	3 to 4	8 to 10

2. SEPARATE EFFECTS TESTS

RELAP5 was assessed against measured data from seven separate-effects tests in four different experimental facilities to evaluate code capabilities for predicting key phenomena for the PTS applications. These separate effects assessments included Marviken tests for evaluating critical flow behavior, MIT pressurizer facility tests for evaluating steam condensation rate and critical heat transfer behavior, UPTF facility tests for evaluating condensation, steam-water flow and fluid-fluid mixing behavior and Semiscale tests for evaluating coolant loop natural circulation behavior. The RELAP5 assessments for these separate effects experiments are presented in this section.

2.1   Marviken Tests 22 and 24

The RELAP5 code includes critical flow models that are activated by setting an optional junction control flag. For all junctions where the critical flow model is active, the code determines whether flow dominated by choking effects or flow dominated by friction effects would be the most limiting and restricts the flow accordingly. The RELAP5/MOD3.2.2Gamma code employed in the PTS applications utilizes the Henry-Fauske critical flow model to determine the flow through breaks and valves during periods when critical flow is predicted.

Assessments of the RELAP5 Henry-Fauske critical flow model were performed based on experimental data obtained from two tests conducted in the Marviken facility. Marviken was a full-scale critical flow test fabricated from a pressure vessel that originally was part of the Marviken power plant. The Marviken vessel has an inside diameter of 5.22 m [17.12 ft], an overall length of 24.55 m [80.5 ft] and an internal volume of 420 m^3 [14,830 ft^3]. A discharge pipe connects the bottom of the pressure vessel to a test nozzle with a restricted flow area and a rupture disk assembly. The diameter of the discharge pipe is 0.752 m [2.47 ft] and the nozzle configuration varies from test to test. The facility is readied for the tests by pressurizing the vessel and establishing the desired temperature profile within it. Breaking the rupture disk and allowing the vessel to blow down through the nozzle to atmospheric pressure begins the tests. Marviken tests are part of the separate-effects problem set that is typically included in RELAP5 developmental assessment activities.

The two cases used for RELAP5 PTS assessment were Marviken Tests 22 and 24. The initial test conditions for the two tests were similar. Initial vessel pressures were 4.93 MPa [715 psia] in Test 22 and 4.96 MPa [719 psia] in Test 24 and initial vessel levels were 19.64 m [64.43 ft] in Test 22 and 19.88 m [65.22 ft] in Test 24. Initial vessel temperatures for the two tests also were very similar, with the fluid at the bottom the vessel about 32 K [58°F] subcooled relative to the steam dome temperature. Both tests used rounded-entrance test nozzles with a 0.5 m [1.64 ft] diameter. The main difference between these two tests was the nozzle L/D ratio, which was 1.5 for Test 22 and 0.33 for Test 24. Because of the difference in the L/D of the nozzle design, the data from Test 22 (L/D of 1.5) is most useful for assessing saturated critical flow while Test 24 (L/D of 0.33) is most useful for assessing subcooled critical flow. Test 22 is documented in Reference 2-1 and Test 24 is documented in Reference 2-2.

Simulations for the two Marviken cases were performed using the RELAP5/MOD3.2.2Gamma code. The RELAP5 nodalization represented the vessel using 39 hydrodynamic volumes and the discharge pipe using six hydrodynamic volumes. The Henry-Fauske critical flow model was activated at the break nozzle junction and the same critical flow parameters (discharge coefficient of 0.92 and thermal non-equilibrium constant of 3.5) used in the RELAP5 PTS plant applications were used for these assessment calculations. Figures 2-1 and 2-2 show a schematic of the

Marviken test rig, the RELAP5 nodalization employed and the initial vessel temperature profiles for Tests 22 and 24.

Comparisons of the calculated and measured data for vessel pressure and discharge mass flow at the nozzle outlet are presented in Figures 2-3 and 2-4 for Test 22 and in Figures 2-5 and 2-6 for Test 24. The assessment results for the two tests are similar, although the RELAP5 calculation for Test 22 compared somewhat better with the test data than was the case for Test 24. In the vessel pressure comparisons, RELAP5 underpredicts the measured pressures by up to 0.8 MPa [116 psi] over the first 20 to 25 s of the tests and the predictions are much better after that time. In the discharge flow comparisons, RELAP5 underpredicts the measured flow by up to about 20% over the first 20 to 25 s and then overpredicts the measured flow by up to about 20% afterward.

The divergences between the calculated and measured responses for Marviken may stem from numerical diffusion behavior that affects the calculated fluid conditions. Numerical diffusion results because discrete spatial nodalizations are employed with RELAP5 (as well as other thermal-hydraulic systems codes). Although the initial temperature distribution inside the tank may been correctly modeled, once the blowdown begins numerical diffusion can overpredict the rate at which hot fluid in the upper tank region is convected downward, thus affecting both the thermal distribution within the tank and the fluid conditions at the break nozzle. The divergences seen in the Marviken comparisons over the first few seconds of the tests tend to support this view. The measured data show an immediate drop in the vessel pressure (caused by the arrival of the depressurization wave) followed by a substantial pressure recovery (caused by fluid flashing effects). The calculated data also show the immediate drop in pressure, but the pressure recovery is much smaller. The mixing effects of numerical diffusion could cause this difference because in the calculation the hottest liquid is mixed with cooler liquid in the upper cells of the tank, leading to lower liquid temperatures and lower pressures at which the fluid flashes. In other words, numerical diffusion lowers the temperature of the hottest fluid in the tank. The lower calculated pressures then lead to underpredicted discharge flows because the differential pressure between the vessel and the atmosphere is smaller in the calculation than in the test.

Since numerical diffusion is influenced to some extent by the nodalization employed, a discussion in that regard is needed. First, although the geometry is the same, one should not consider the Marviken tests as representative of PWR pressurizer blowdown situations. PWR pressurizers are saturated systems while the conditions in the Marviken vessel are highly subcooled. The thermal mixing effects described above are therefore not pertinent for PWR pressurizers. Prior experience with PWR pressurizer modeling indicates that the eight-to-ten hydrodynamic cells in the tank used to represent the pressurizers in the PTS plant analysis models is sufficient to adequately simulate the pressurizer blowdown and refill behavior processes. The many separate and integral system test assessments in this report confirm this view. Second, the Marviken assessment does suggest that numerical diffusion may affect the simulation of break flow processes in general. Consider, for example, a cold leg break LOCA simulation. The entire RELAP5 RCS system model, with its many hydrodynamic cells and distribution of fluid conditions is more complex but nevertheless very analogous to the Marviken vessel with its distribution of fluid conditions. Furthermore, the number of hydrodynamic cells used between the pressurizer steam space (where flashing occurs) and the PWR cold leg break location is comparable to the number of cells used in the Marviken test simulations. The Palisades RELAP5 system model employs 33 cells between the steam space at the top of the pressurizer and the cold leg break location. This compares with 45 cells between the top of the vessel and the break nozzle in the Marviken RELAP5 model. Therefore, the deviations between calculated and measured data listed above for the Marviken tests may be taken as

indications of the uncertainties generally involved in RELAP5 predictions of break flow for the PTS applications.

The pressure and discharge mass flow comparisons for the Marviken tests are judged to demonstrate fair-to-good agreement between the RELAP5-calculated and measured data. It is noted that a spectrum of break sizes was thoroughly investigated for each plant evaluated in the PTS study. Ten different break diameters from 2.54 cm [1 in] to 57.5 cm [22.63 in] in equal flow-area increments were analyzed. Since the entire range of possible LOCA break sizes has been directly included in the plant analysis, the effects of uncertainties related to the RELAP5 break flow models on the results of the PTS evaluation are significantly reduced.
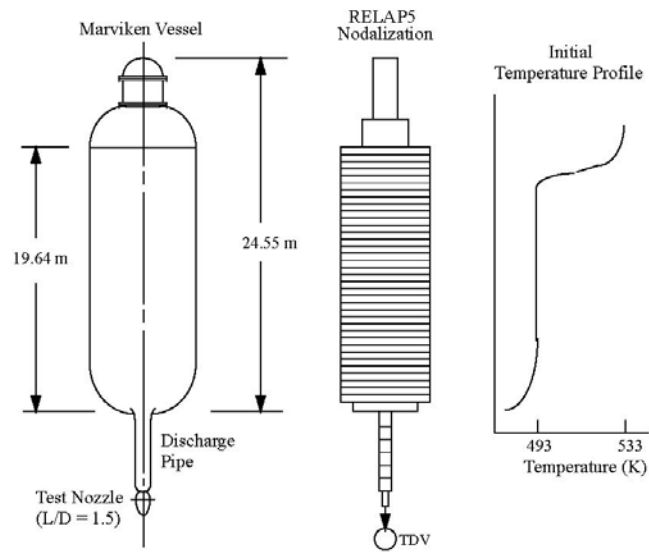
Figure 2-1   Test Schematic, RELAP5 Nodalization and Initial Temperature Profile for Marviken Test 22
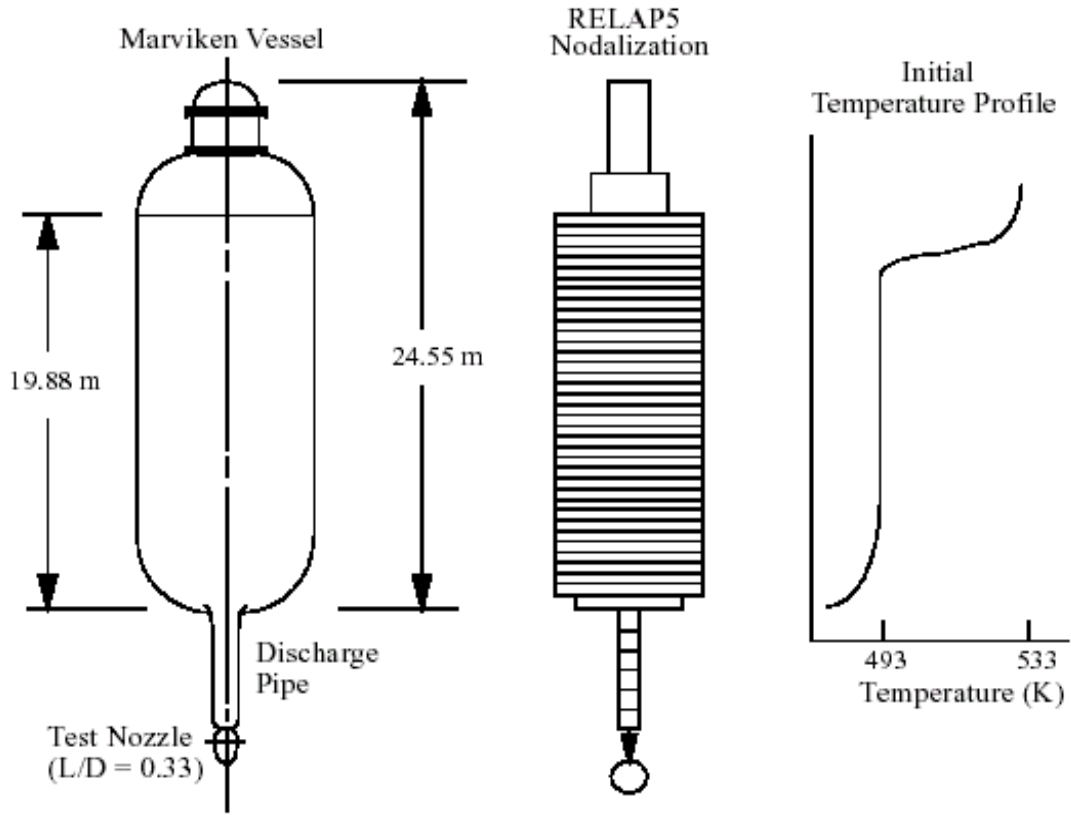
Figure 2-2   Test Schematic, RELAP5 Nodalization and Initial Temperature Profile for Marviken Test 24
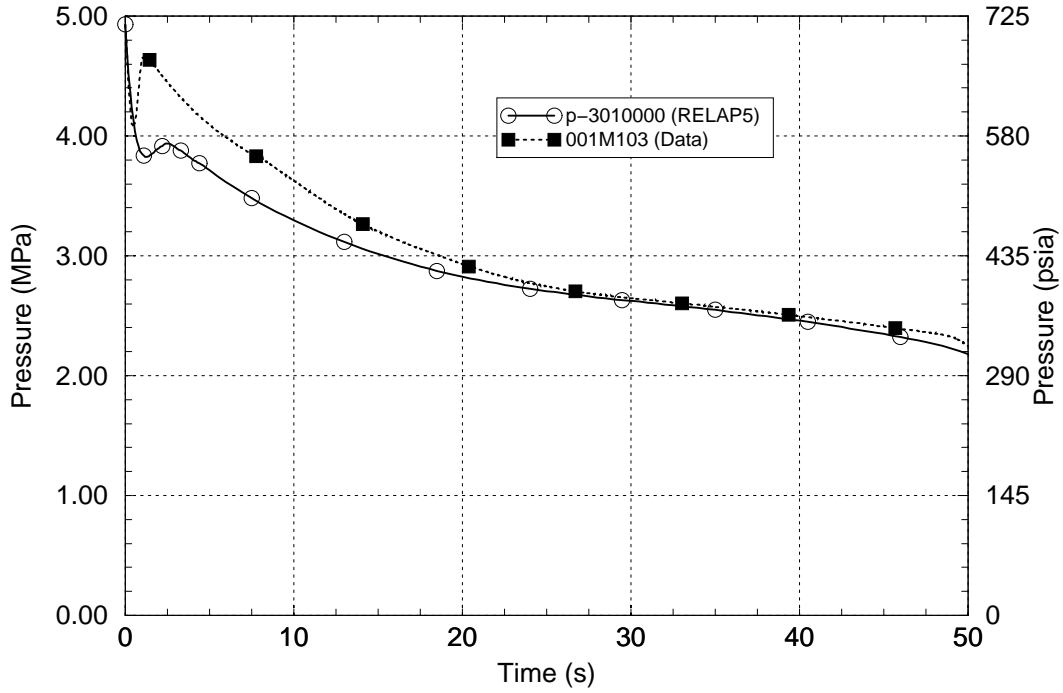
Figure 2-3   Pressure at Top of Vessel – Marviken Test 22
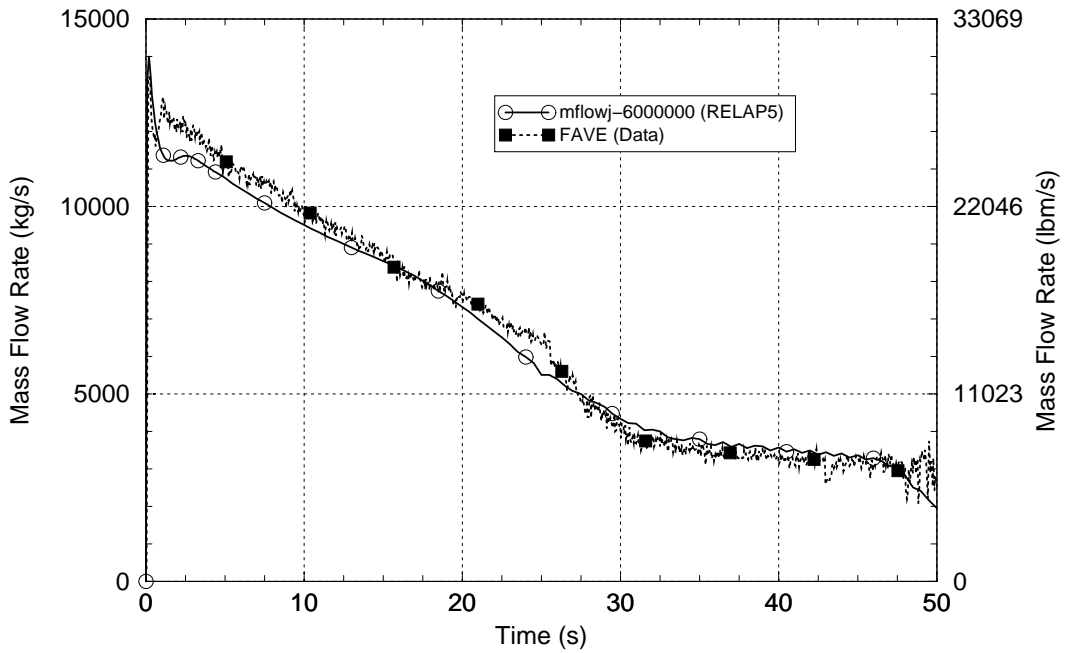
Figure 2-4   Mass Flow at Nozzle Outlet – Marviken Test 22
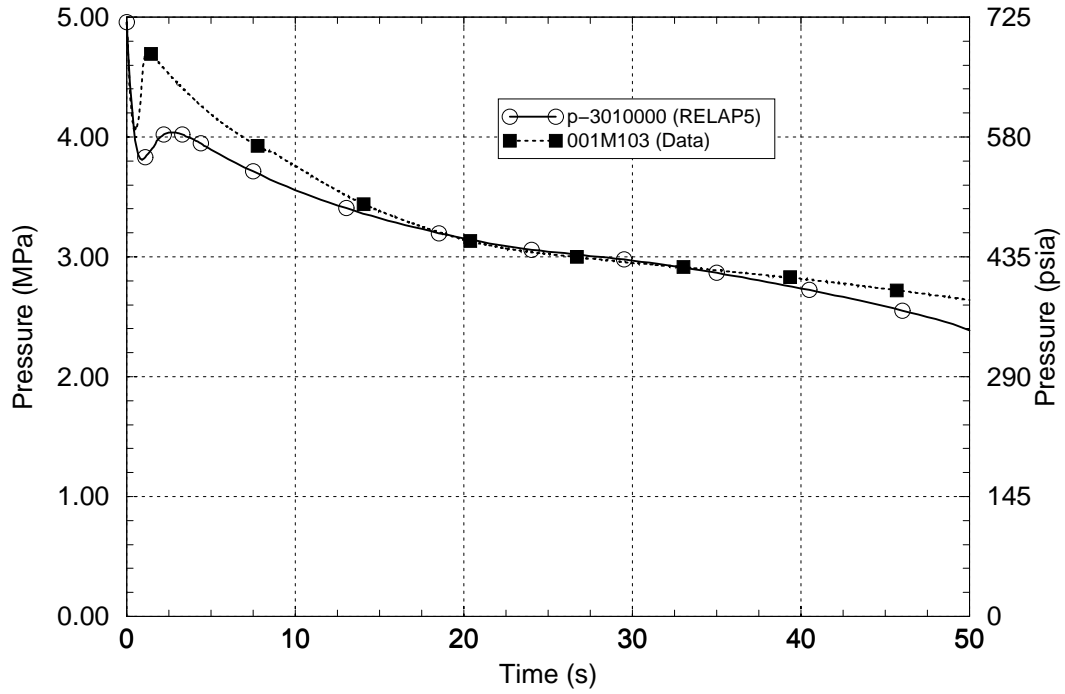
Figure 2-5   Pressure at Top of Vessel – Marviken Test 24
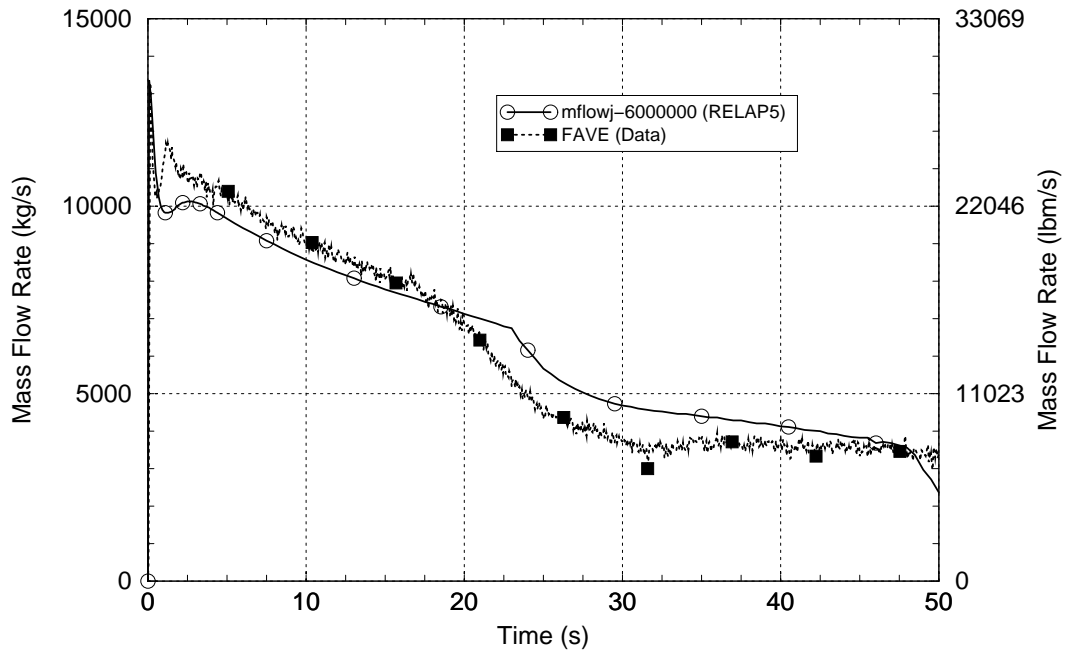
Figure 2-6   Mass Flow at Nozzle Outlet – Marviken Test 24

2.2 MIT Pressurizer Test ST4

Tests simulating pressurized water reactor pressurizers under inflow and outflow conditions have been performed at MIT by Saedi and Griffith [Ref. 2-4]. The MIT pressurizer was a small-scale, low-pressure representation of a pressurizer. The vessel representing the pressurizer was 1.14 m [3.74 ft] tall with an inner diameter of 0.203 m [0.667 ft]. Figure 2-7 is a schematic of the test facility. Test ST4 was initialized with 0.432 m [1.41 ft] of saturated water at a pressure of 0.493 MPa [71.5 psia] under quiescent conditions. Subcooled water was injected into the tank for 41 s, increasing the water level of the tank at approximately 1 cm/s [0.394 in/s]. The initial subcooling of the injected water was 129 K [232°F]. The steam in the upper part of the vessel was compressed. As the saturation temperature rose, the vessel walls became subcooled and film condensation occurred.

The vessel was modeled as a vertical pipe component with 10 fluid cells, which is typical of the nodalization used in the plant models. A time dependent junction was used to inject liquid into the bottom of the pipe at a rate determined from the test data. Perfect insulation was assumed on the outside of the pipe surface, the same assumption as used for the PTS analyses. The water level was initially in the fourth cell from the bottom (the void fraction in that cell was 0.22).

Prediction of pressurizer pressure requires accurate models of wall heat transfer, as well as interfacial liquid-steam heat transfer. The RELAP5 calculations of the steam condensation rate at the vessel wall, heat transfer to the wall and the interfacial heat transfer between the stratified liquid and the vapor above the liquid were assessed by comparing predictions to test data from test ST4. Mixing of incoming cold water with hot water present in the system will affect the system pressure prediction and is a potentially important phenomenon. This test is one of the separate-effects problems included in the RELAP5 Developmental Assessment. See Reference 2-5 for further information on this test.
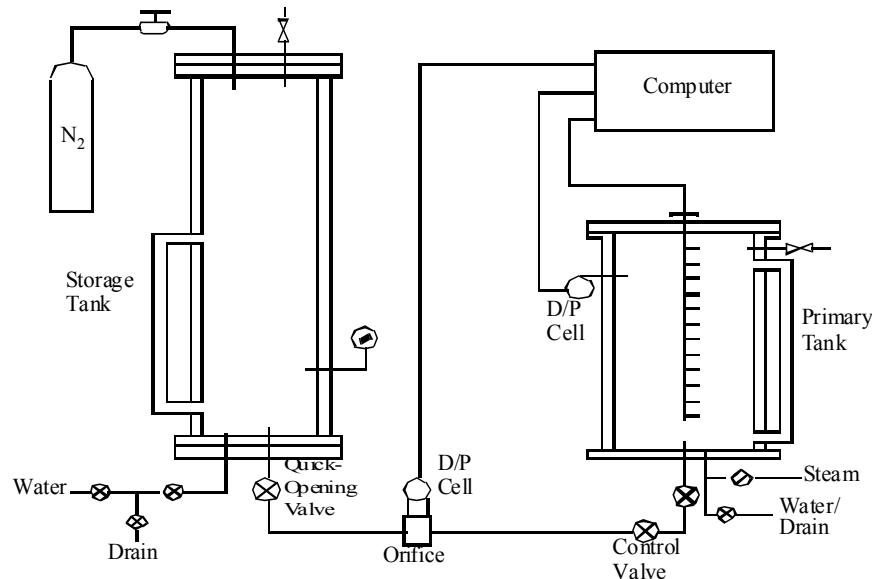
Figure 2-7   Schematic of MIT Pressurizer Test Facility

A comparison of the measured pressure rise to the RELAP5-calculated value is shown in Figure 2-8. Initially, pressure increased due to compression of the steam volume above the water surface. As the pressure increased, the saturation temperature also increased. During the insurge period up to 41 s, RELAP5 overpredicts the pressure. The main reason for the overprediction is neglect of environmental heat losses, which are significant for this small facility. However, heat loss to the environment is also neglected for all of the PTS plant models. Overall, RELAP5 captured the trend displayed by the test data quite well. It should be noted that this test was conducted at low pressure conditions, much lower than the operating pressure of a PWR plant.

The measured and predicted axial temperature profiles in the fluid and wall at 35 s into the insurge transient are shown in Figures 2-9 and 2-10, respectively. The experimenters noted that the radial temperature variation in the pressurizer fluid was negligible. It is apparent that RELAP5 predictions of the temperature changes are quite accurate, with the exception that there is more "smearing" of the temperature profile. A lumped parameter code will artificially mix the fluid as it flows from one node to the next. Since this mixing may lower the temperature of the liquid in the node with the liquid-vapor interface, condensation at the surface could be overpredicted. However, the effect on pressure response from this mixing is not significant. Sensitivity studies by Shumway, et. al. [Ref. 2-5] showed that wall condensation, rather than inter-phase heat transfer, plays the dominant role in determining the pressure response. It is noted that Shumway's RELAP5 results differ from those shown in this report because an estimate of heat losses to the environment were included in Shumway's analysis. It is noted that the magnitude of heat losses to the environment was not well known for this experiment.
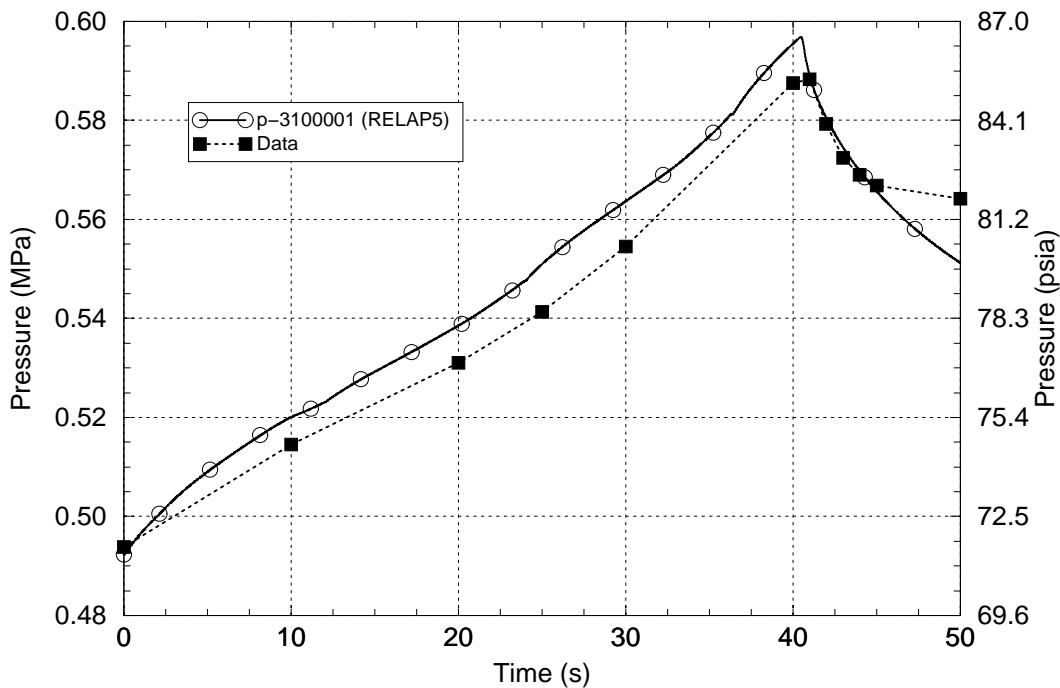
Figure 2-8   Comparison of Measured and Predicted Pressure Rise
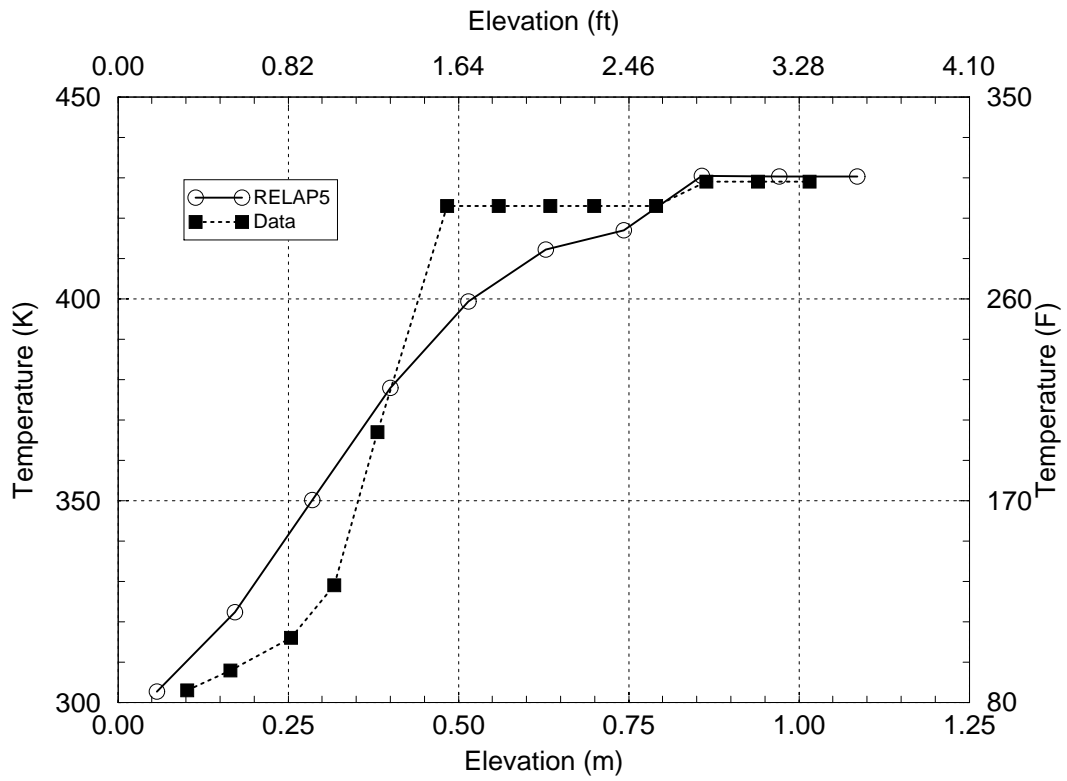
Figure 2-9   Comparison of Measured and Predicted Fluid Temperature Profiles at 35 Seconds
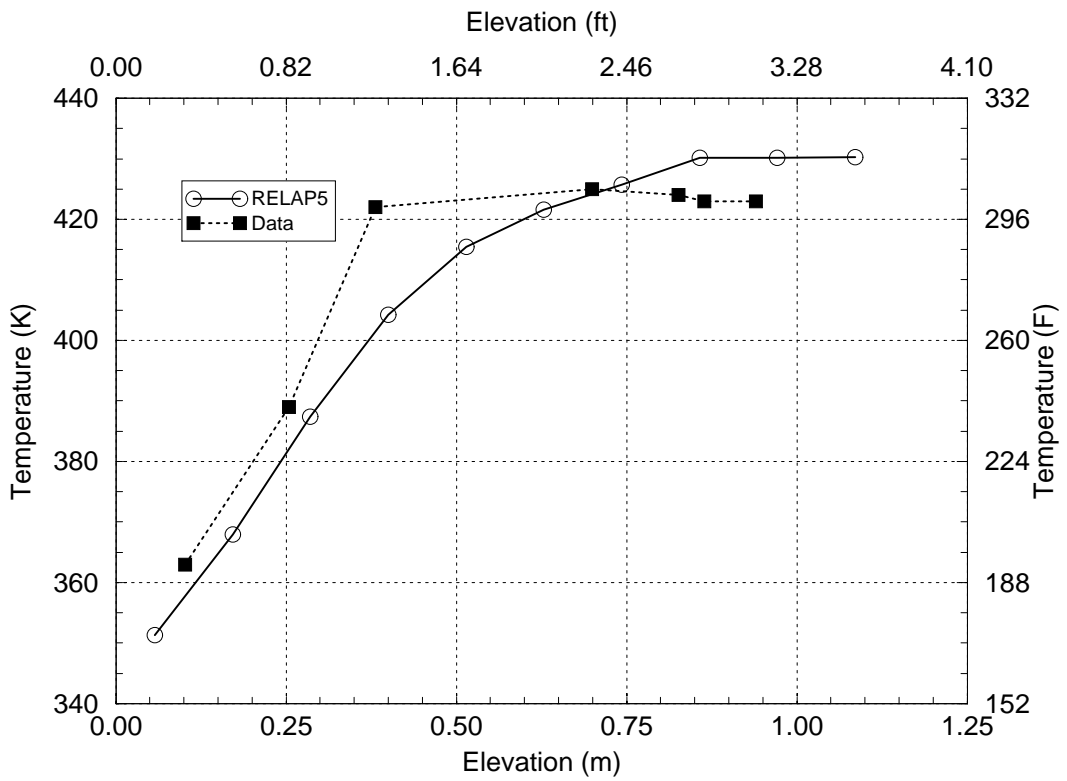
Figure 2-10   Comparison of Measured and Predicted Wall Temperature Profiles at 35 Seconds

2.3   Upper Plenum Test Facility, Test 6, Run 131

Large break LOCA events were found to contribute to PTS risk, so experiments relevant to LBLOCA were included in this assessment. The Upper Plenum Test Facility (UPTF) is a full-scale model of a four-loop 1300 MWe PWR. Components included in this facility are the reactor vessel, downcomer, lower plenum, core simulation, upper plenum, and four loops with pump and steam generator simulation, as shown in the schematic drawing in Figure 2-11. The test vessel, core barrel, and internal structures are a full-size representation of a PWR with four full-scale hot and cold legs simulating three intact loops and a broken loop. Further information on this test is found in Reference 2-6.

RELAP5 assessment was performed for two UPTF tests, the first of which is Run 131 of UPTF Test 6. This test is a separate-effects test to investigate the steam-water interaction phenomenon in the lower plenum and downcomer during the end-of-blowdown and refill portions of a large-cold leg break LOCA. For this test, the loops were closed off at the pump simulators, so the RELAP5 model included only the cold legs downstream of the pump simulators, as shown in the noding diagram in Figure 2-12. Run 131 was started by injecting steam through the core and steam generator simulators. All of this steam flows through the core, so the RELAP5 model begins at the core, with steam injected into the top of the core.
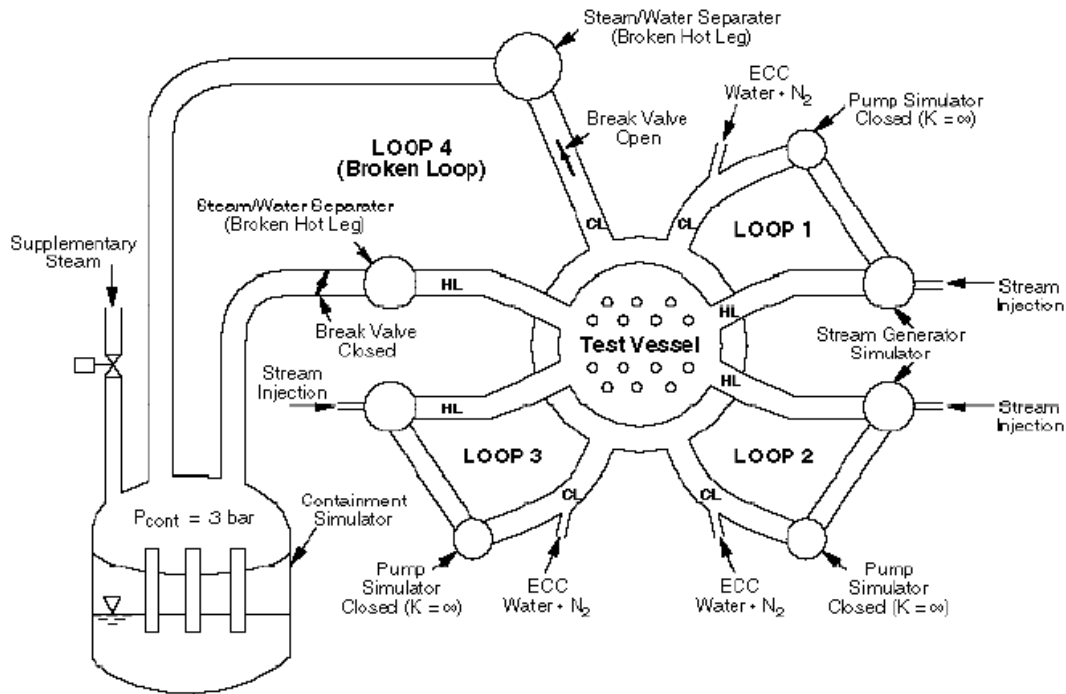
Figure 2-11   Schematic of the UPTF Test Facility
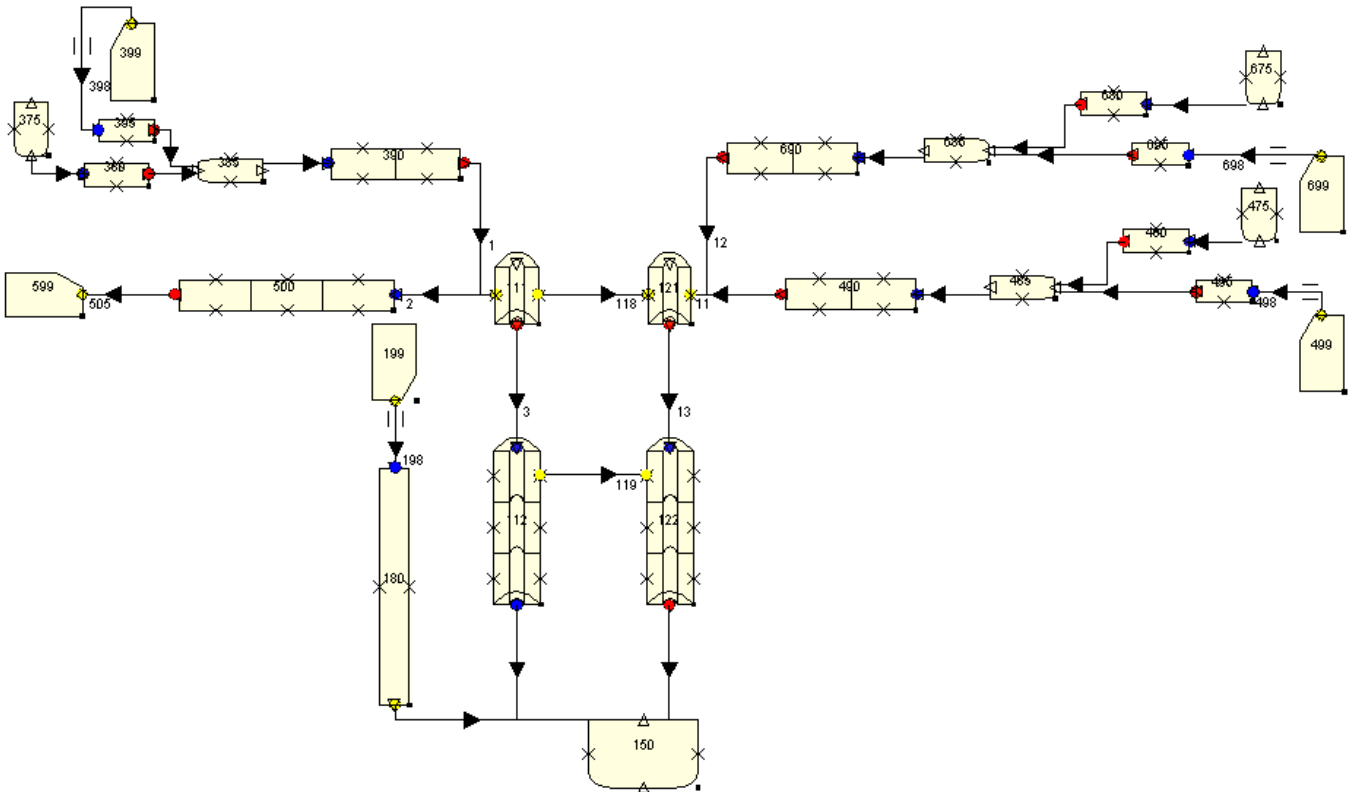
Figure 2-12   RELAP5 Noding Diagram - UPTF Test Facility, Test 6, Run 131

The injected steam flowed upward through the downcomer (nodes 112, 122) toward the broken cold leg (node 500). The steam flow was kept constant during the test. After the steam flow came to an almost steady condition, slightly subcooled emergency cooling water was injected into the cold legs of the three intact loops. This occurred at approximately 13 s after the steam flow was initiated. The same flow rate, 482 kg/s [1060 lbm/s] was injected into each loop. The test was started at an initial vessel pressure of 0.258 MPa [37.4 psia] at a temperature of 458 K [364°F]. The emergency core cooling accumulator pressure was 1.95 MPa [283 psia]. The emergency core cooling water temperature was 392 K [246°F]. At about 80 s, the steam and emergency injection flow were turned off.

Figure 2-13 shows a comparison of the calculated and measured pressure in the downcomer. These results show generally good agreement between the code predictions and the test results. During the initial phase of the event RELAP5 slightly underpredicts the pressure, and then slightly overpredicts pressure after the start of emergency coolant injection. Later in the event, the code pressure prediction is slightly low. A number of factors affect the prediction, including the modeling of flow resistances, condensation of steam and break flow.   At these low pressures, the temperature is more significant than pressure in determining PTS risk, so this slight underprediction is not an important factor.

A comparison of the RELAP5 predicted lower plenum liquid level and the test data is shown in Figure 2-14. Again, there is fairly good agreement between the test results and the code prediction. According to Reference 2-6, the test data showed a water level of 0.4 m [1.31 ft] in the lower plenum prior to the start of ECC injection, even though no water was initially stored in the lower plenum. The experimenters attributed this anomaly to dynamic pressure effects. When comparing RELAP5 predictions to data in Figure 2-14, 0.4 meters [1.31 ft] was subtracted from the measured data. Note that RELAP5 underpredicts the amount of water delivered to the lower plenum. This is conservative for ECCS calculations, but is potentially nonconservative for PTS calculations.

The more significant factor for this large break LOCA case is prediction of downcomer fluid temperatures. Figure 2-15 shows a comparison of RELAP5 predicted liquid temperature with experimental data. The RELAP5 prediction is located 2.92 m [9.59 ft] below the cold leg centerline in the downcomer channel that contains one intact cold leg and the broken cold leg. The thermocouples for the measured data are located 2.25 m [7.36 ft] below each intact cold leg nozzle centerline. The data show brief decreases in temperature, apparently due to droplets hitting the thermocouples as water penetrates the downcomer. There is always a quick return to the bulk fluid temperature as the thermocouples dry out. The bulk condition is near saturation. The RELAP5 pressure prediction is slightly low, so the corresponding saturation temperature will also be low. As a result, the RELAP5 predicted bulk temperature is generally a few degrees lower than the measured bulk temperature, which is conservative for PTS applications.

Overall, it is concluded that the RELAP5 predictions are fairly close to the UPTF experimental results. Over the period of the experiment, the average variation between the RELAP5 calculated and measured downcomer fluid temperature is 8 K [15°F].
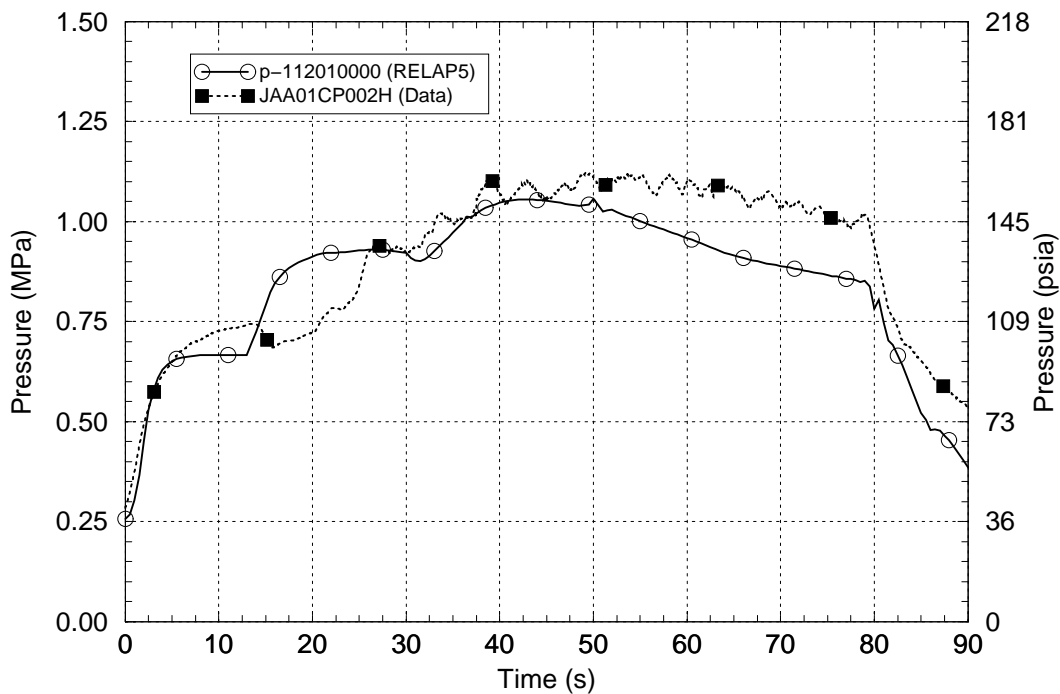
Figure 2-13   Downcomer Pressure - UPTF Test 6 - Run 131
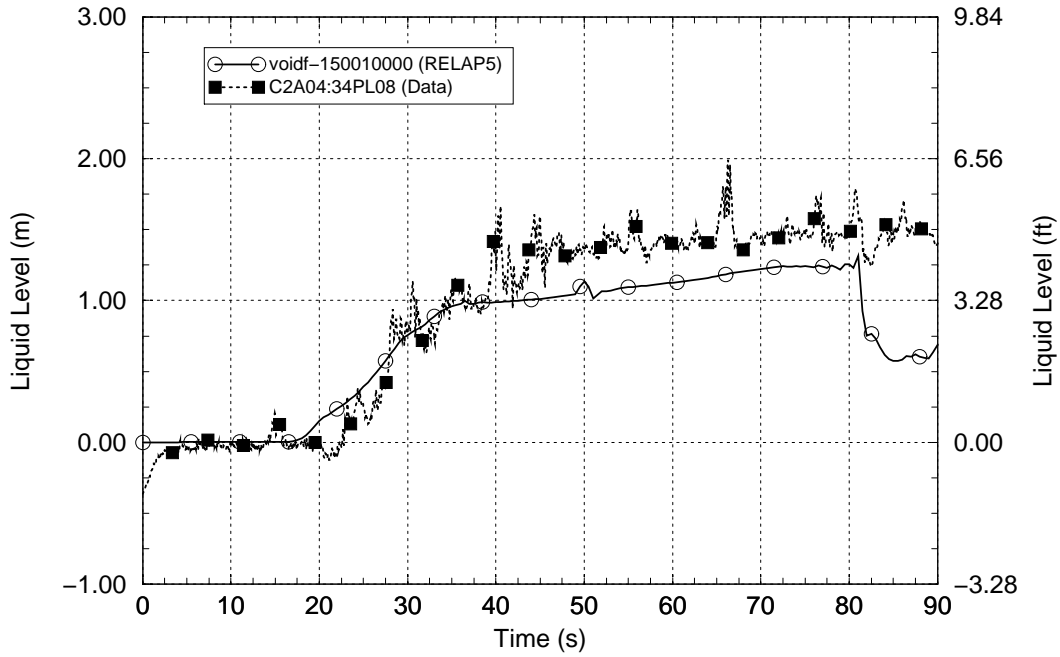
Figure 2-14   Lower Plenum Liquid Level - UPTF Test 6 - Run 131
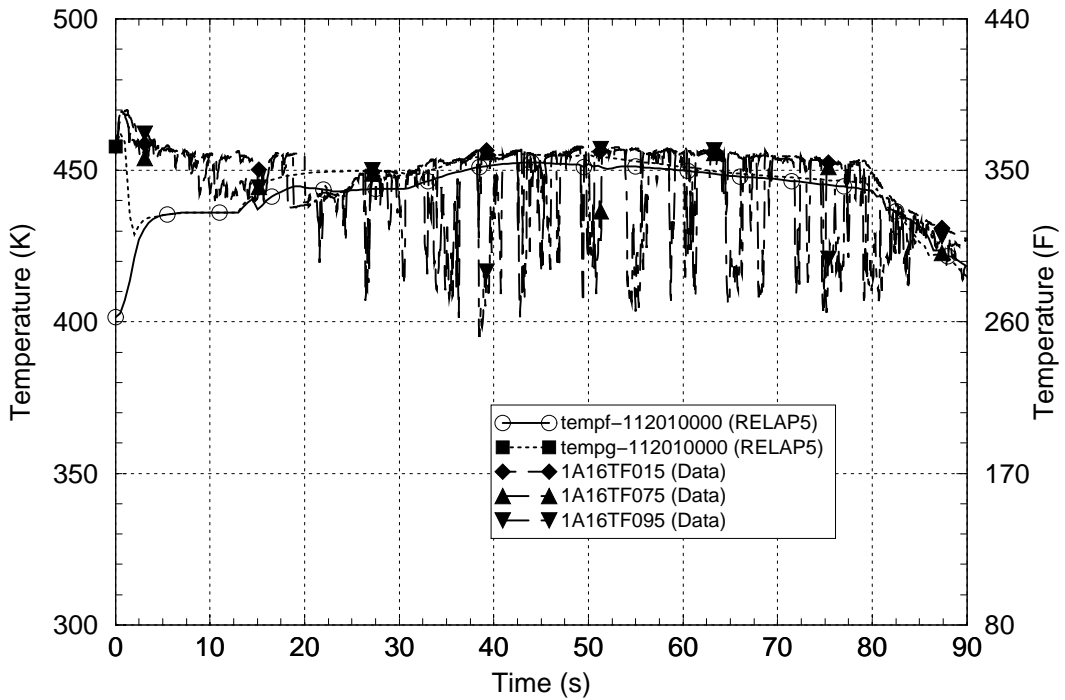
Figure 2-15   Downcomer Fluid Temperature - UPTF Test 6 - Run 131

2-14

2.4   Upper Plenum Test Facility, Test 1, Run 21

The Upper Plenum Test Facility (UPTF) Facility is described in Section 2.3. Two UPTF tests were used in the assessment of RELAP5 for the PTS application. The second UPTF test, Test No. 1 is a quasi-steady state, separate effects experiment run with blocked break valves and pump simulators. The purpose of the experiment is to provide data for investigating liquid-liquid mixing phenomena and the development of the fluid and wall temperature fields in the cold leg and downcomer regions of a PWR. The test is initiated from stagnant conditions with the reactor vessel, cold legs, hot legs and pump loop seals completely filled with hot water, 456 K [361°F], at 1.8 MPa [261 psia]. Cold ECC water at 305 K [90°F] is injected into one cold leg. Water is allowed to flow out of the test system through an opening in one hot leg. The system pressure is controlled steady at its initial value. Test 1 is run using five different ECC injection rates from 5 to 70 kg/s [11 to 154 lbm/s]. Test 1, Run 21 with an ECC injection rate of 40 kg/s [88 lbm/s] is selected for the RELAP5 PTS application assessment. This flow rate approximates the per-loop ECC flow expected from PWR high pressure injection and accumulator systems when the reactor coolant system pressure is the same as in the experiment. During Run 21, the ECC injection flow commenced at 126 s and the test was terminated at 2,790 s. The complete experimental procedure and the results for UPTF Test 1 are provided in the experiment data report, Reference 2-7.

The RELAP5 simulation of UPTF Test 1, Run 21 is performed using the RELAP5/MOD3.2.2Gamma code. The UPTF model employed is similar to the one shown for UPTF Test 6 in Figure 2-12, except that the axial and azimuthal nodalization of the reactor vessel downcomer region is significantly expanded in order to provide sufficient resolution in the calculated solution to allow for an adequate comparison with the measured data from this test. The axial nodalization of the downcomer region below the cold legs was expanded from three to nine cells, while the azimuthal nodalization was expanded from two to eight sectors. The eight sectors correspond to the azimuth locations of the four cold leg and four hot leg nozzles around the circumference of the reactor vessel. Consistent modifications are made both to the hydrodynamic and heat structure features of the model. In addition, the core-side nodalization was expanded upward and model junctions added between the upper plenum and upper downcomer regions to represent the PWR upper reactor vessel core bypass flow paths. Circulating flows between the upper plenum and downcomer through these bypass paths can influence the downcomer thermal behavior.   With these changes, the downcomer region of the UPTF model is nodalized consistently with the approach taken in the plant models used for the PTS applications. The RELAP5 model was initialized with stagnant conditions and at the pressures and temperatures described above for Test 1, Run 21.

Figures 2-16 through 2-19 compare the measured and RELAP5-calculated reactor vessel downcomer fluid temperature responses for UPTF Test 1, Run 21. Comparisons are made at elevations within the downcomer corresponding to the top, middle and bottom of the core active fuel region. The circumferential locations of the comparisons are denoted by the azimuth sector of the downcomer associated with the reactor vessel cold leg (CL) and hot leg (HL) penetrations. The ECC water is injected only into Cold Leg 2; data identified as "CL2" therefore represents the downcomer sector directly below the nozzle through which the cold water enters the vessel. Data shown with other cold leg or hot leg identifiers are for other sectors around the circumference of the downcomer.

Figure 2-16 compares the calculated and unfiltered measured fluid temperatures at an elevation corresponding to the top of the core heated length. The measured test data is oscillatory in the sector below Cold Leg 2, with amplitudes as large as 55 K (99°F). The measured test data in the

other two sectors is smooth. This oscillatory thermocouple response likely represents the physical experiment behavior and is indicating that (rather than a steady stream of cold water) pockets of cold water are intermittently falling through (and in the process displacing) the warmer water initially in the downcomer. That the process appears to be intermittent rather than steady indicates that the cold water injection rate is less than that required to support a vertical channel of cold water that steadily flows downward through the downcomer. Figure 2-16 shows that the oscillation amplitude decays over the test period. While unfiltered data is not shown for the lower elevations, the oscillation amplitudes there also decay significantly with elevation. The maximum oscillation amplitude at the mid-core elevation is 44 K (79°F) and at the core-bottom elevation it is 30 K (54°F).   Figure 2-17 presents the same comparison as in Figure 2-16, except with the measured test data is averaged over the previous 30 s interval. The two figures indicate that at the core-top elevation RELAP5 overpredicts the average fluid temperature in the downcomer sector below Cold Leg 2 and underpredicts it in the other sectors. The RELAP5 temperature prediction is seen to well represent the peak, not the average, temperature of the oscillations in the sector below Cold Leg 2.

Comparisons of filtered measured and RELAP5-calculated downcomer fluid temperatures are provided in Figure 2-18 at the mid-core elevation and in Figure 2-19 at the core-bottom elevation. RELAP5 predictive capabilities at these lower elevations are similar to those observed at the core-top elevation, with RELAP5 overpredicting the temperature in the Cold Leg 2 sector and underpredicting it in the other sectors. Comparing Figures 2-17 through 2-19, the RELAP5 temperature overprediction in the Cold Leg 2 sector is seen to become smaller at the mid-core elevation and smaller still at the at the core-bottom elevation.

Figure 2-20 compares the measured and calculated reactor vessel wall inside surface temperatures at the core-top elevation (comparisons at the mid-core and core-bottom elevations are similar). The wall temperature comparisons are consistent with the fluid temperature comparisons, with RELAP5 overpredicting the temperature in the Cold Leg 2 sector and underpredicting it in the other sectors.

The code-to-data comparisons indicate that RELAP5 is moderately overpredicting fluid mixing among the azimuthal sectors of the water-filled downcomer. RELAP5 permits only one temperature for the liquid phase and one temperature for the steam phase within each hydrodynamic cell. For the unstable situation in which cold water resides over warm water, this code limitation prevents simulating pockets of cold water intermittently falling through the warm water, a behavior that appears to be present in the experiment beneath the Cold Leg 2 nozzle. Instead, RELAP5 routes some of the cold water into the other downcomer sectors. Hence RELAP5 overpredicts the time-averaged temperature in the Cold Leg 2 sector and underpredicts the temperatures in the other sectors.

The RELAP5 downcomer fluid temperature prediction capabilities for this test are summarized as follows. The measured and calculated data for the Cold Leg 2 and Cold Leg 4 sectors at the mid-core elevation in Figure 2-18 are compared as a representation of an average code-to-data downcomer temperature differences over the elevation span of the core. As compared with the mid-core elevation, Figures 2-17 and 2-19 show that the code-data differences are larger at the core-top elevation and smaller at the core-bottom elevation. In the downcomer sector into which cold water is injected, RELAP5 underpredicted the measured temperature by a maximum of 1.8 K [3.2°F] and overpredicted it by a maximum of 13.1 K [23.6°F]. In the other downcomer sectors, RELAP5 underpredicted the measured temperature by a maximum of 8.4 K [15.1°F] and a minimum of 3.1 K [5.6°F]. If the Cold Leg 2 and Cold Leg 4 sector data are combined together to represent an average for the entire downcomer region, over the total test period RELAP5

underpredicted the measured downcomer temperature by an average of 4.4 K [7.9°F] and varied from the measured downcomer temperature by an average of 2.2 K [4.0°F].

The assessment of RELAP5/MOD3.2.2 Gamma using experimental data from UPTF Test 1, Run 21 indicates that the code is capable of acceptably simulating the behavior of the average reactor vessel downcomer fluid temperature, which is one of the key PTS parameters.
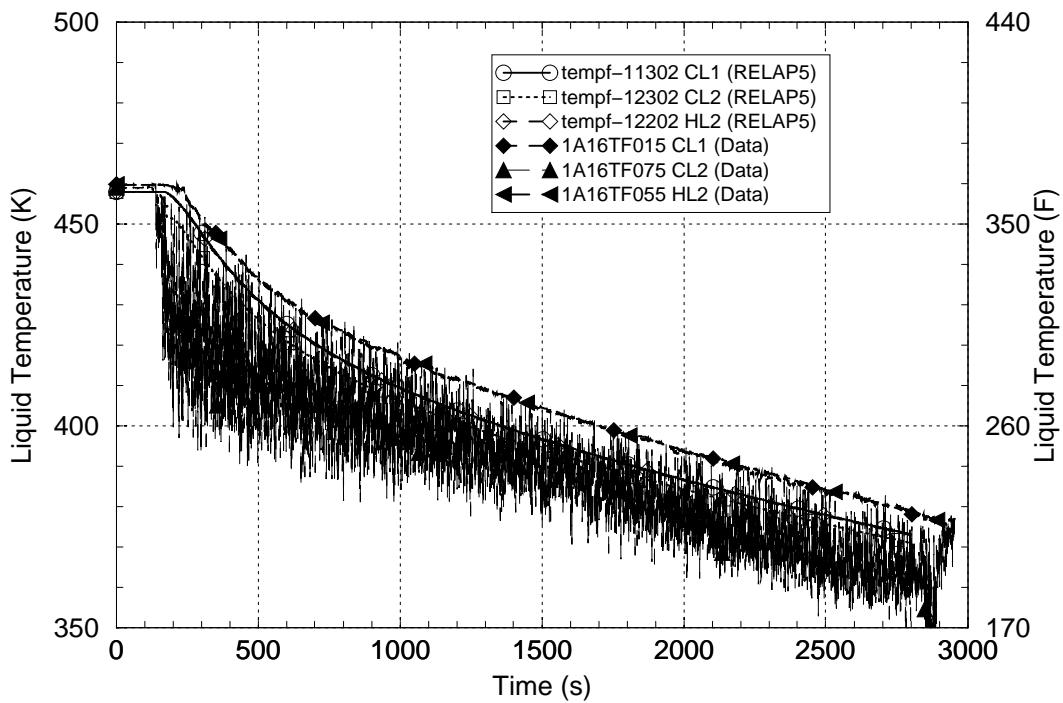
Figure 2-16 Unfiltered Downcomer Fluid Temperatures at Core-Top Elevation - UPTF Test 1 - Run 21
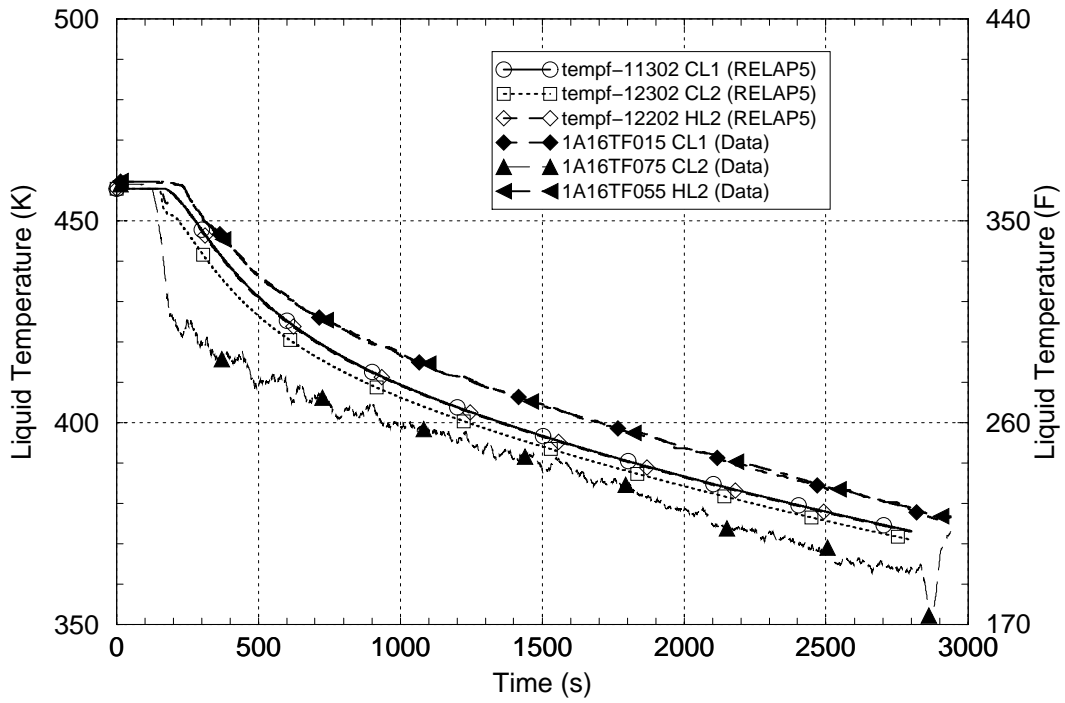
Figure 2-17 Downcomer Fluid Temperatures at the Core-Top Elevation - UPTF Test 1 - Run 21
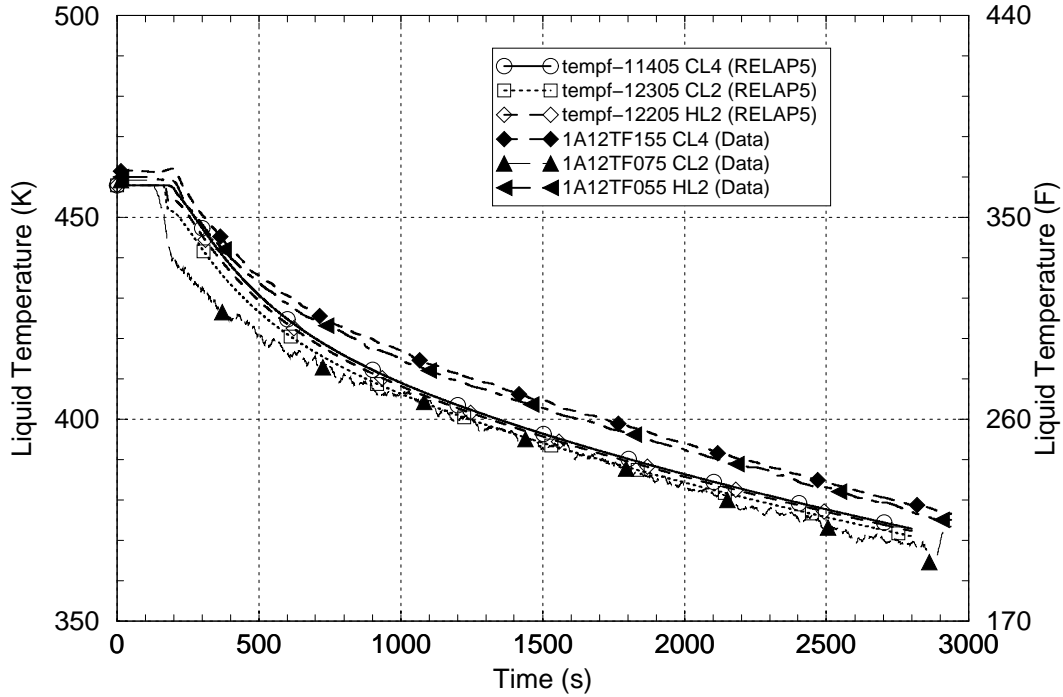
Figure 2-18 Downcomer Fluid Temperatures at the Mid-Core Elevation - UPTF Test 1 - Run 21

2-18
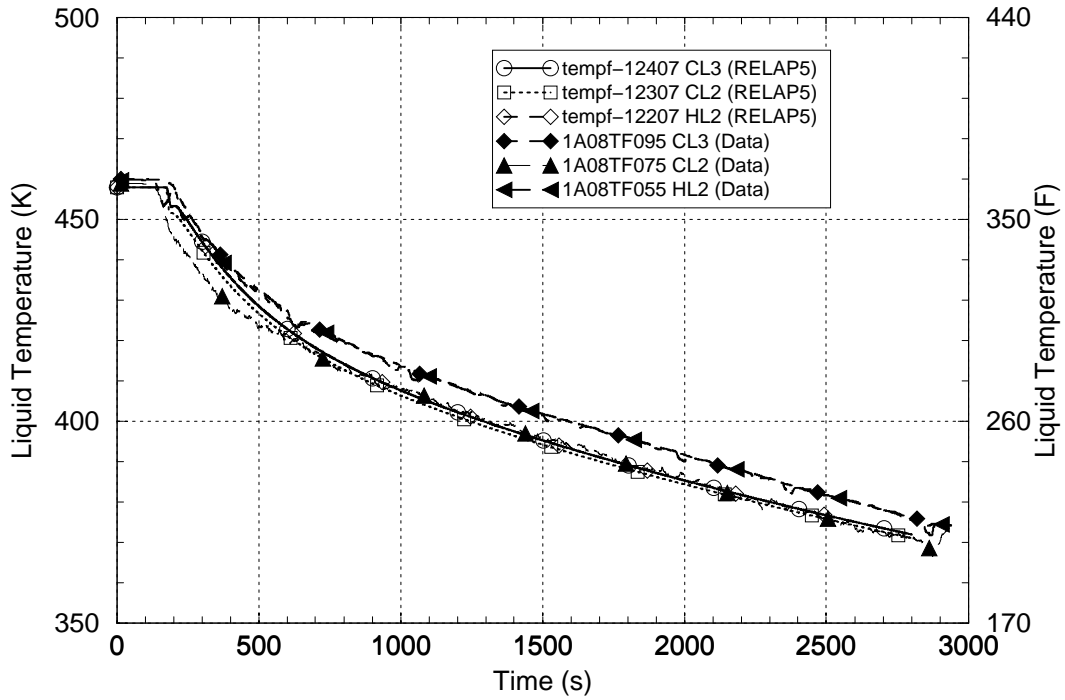
Figure 2-19 Downcomer Fluid Temperatures at the Core-Bottom Elevation - UPTF Test 1 - Run 21
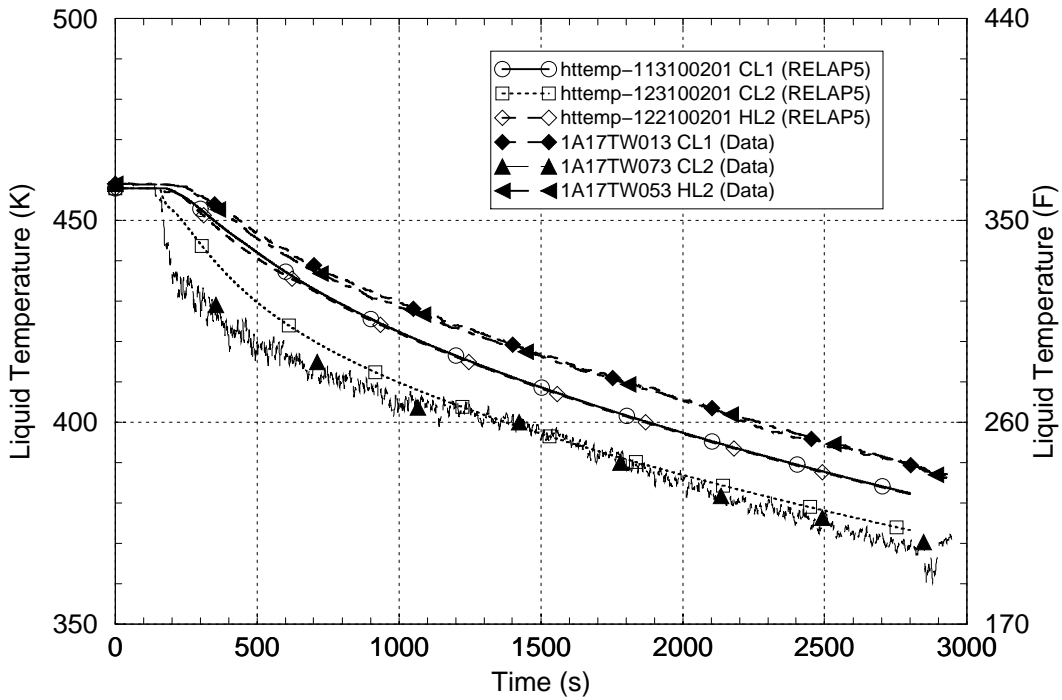
Figure 2-20 Reactor Vessel Wall Inside Surface Temperatures at the Core-Top Elevation - UPTF Test 1 - Run 21

2.5   Semiscale Mod-2A Tests S-NC-02 and S-NC-03

Experiments were performed in the Semiscale Mod-2A test facility (Reference 2-8) to evaluate steady-state single-phase, two-phase, and reflux cooling mode coolant loop natural circulation phenomena that are pertinent for SBLOCA sequences. This Semiscale facility was a small-scale model of the primary system of a four-loop PWR plant. The scaling factor is 1:1705. The complete Semiscale facility simulated all major components of a PWR coolant system, including steam generators, a reactor vessel with downcomer, reactor coolant pumps, a pressurizer and hot and cold leg coolant loop piping. The Semiscale natural circulation experiments utilized a single-loop configuration where the intact loop pump was replaced with a spool piece containing an orifice that simulated the hydraulic resistance of a locked pump rotor. The vessel was also modified to ensure a uniform heat up of the entire system and to avoid condensation effects in the vessel upper head region. These assessments are included in the separate effects section of this report (rather than in the integral effects section) because data were collected only for selected parameters and because only a portion of the full Semiscale test facility was actively used. A schematic of the single-loop Semiscale test facility configuration is shown in Figure 2-21.

Two Semiscale Mod-2A tests, S-NC-02 and S-NC-03, were selected for use in assessing RELAP5 capabilities for the PTS application. The RELAP5 nodalization of the Semiscale test facility is shown in Figure 2-22. The procedures and results for these tests are documented in Reference 2-9. Both tests investigated coolant loop natural circulation behavior, the existence or loss of which is important for the PTS application because of influences on the reactor vessel downcomer fluid temperature. If coolant loop natural circulation is present, the cold ECCS injection flow mixes with and is warmed by the coolant loop flow prior to entering the reactor vessel downcomer. However, if coolant loop natural circulation flow slows or stops, then the effects of the cold ECCS injection flow are felt more directly in the reactor vessel downcomer. Therefore, the slowing and interruption of coolant loop natural circulation flow are particularly significant from the perspective of the PTS application. This slowing and interruption may come from depletion of primary coolant system inventory (in which case liquid inventory within the SG tubes is insufficient to support the full flow rate) or from depletion of the SG secondary inventory (in which case SG heat removal capability is lost).

Test S-NC-02 investigates the steady-state coolant loop natural circulation flow rate as a function of primary-side mass inventory. Single-phase, two-phase, and reflux cooling modes are examined in this test by varying the core power (30, 60 and 100 kW) and the primary-side system mass inventory while holding the steam generator secondary-side conditions steady. A total of 17 separate steady-state conditions with different primary-side inventories, ranging from 100% to 61.2% of the full or maximum inventory, were used for Test S-NC-02.

Figure 2-23 displays the primary-side mass flow rate obtained as a function of primary coolant system mass inventory and overlays the results obtained with RELAP5/MOD3.2.2Gamma with the measured data. The following discussion compares the calculated and measured results, starting from the 100% primary inventory condition and working downward through the range of inventories investigated in the test.

The calculated and measured results compare well over the 100% to 97% inventory range, which the represents conditions of PWR single-phase coolant loop natural circulation.
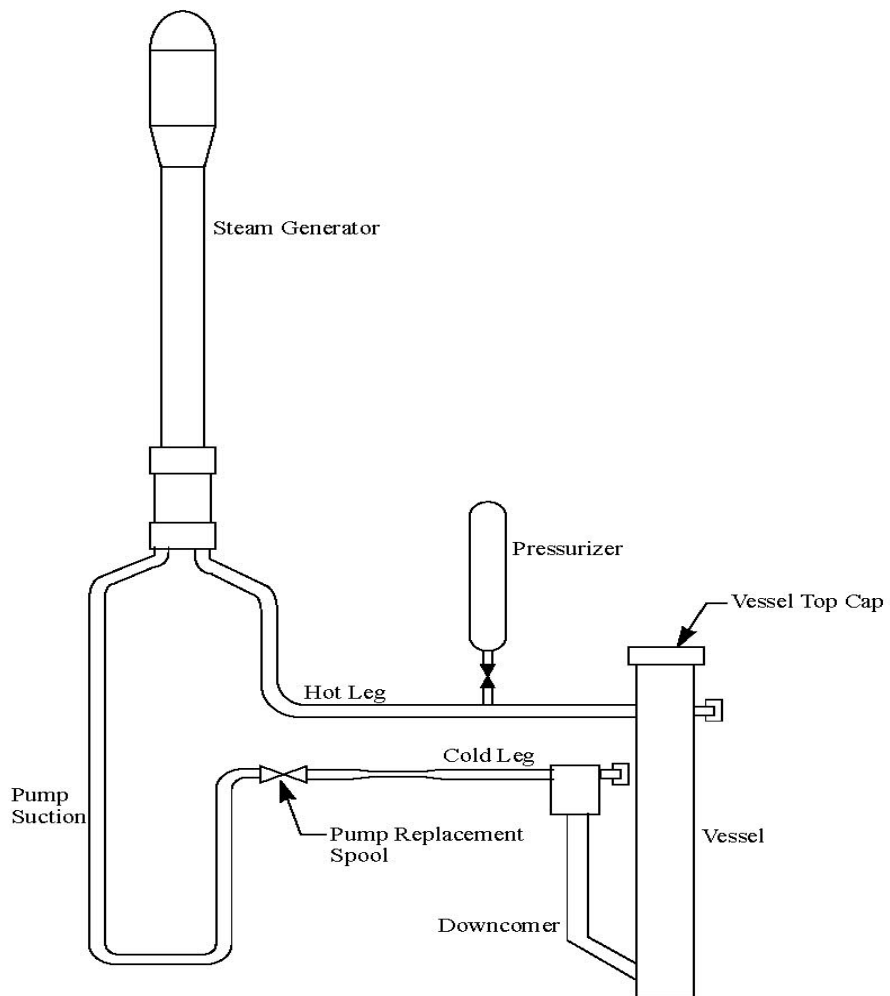
Figure 2-21   Schematic of the Semiscale Mod-2A Single-Loop Test Configuration
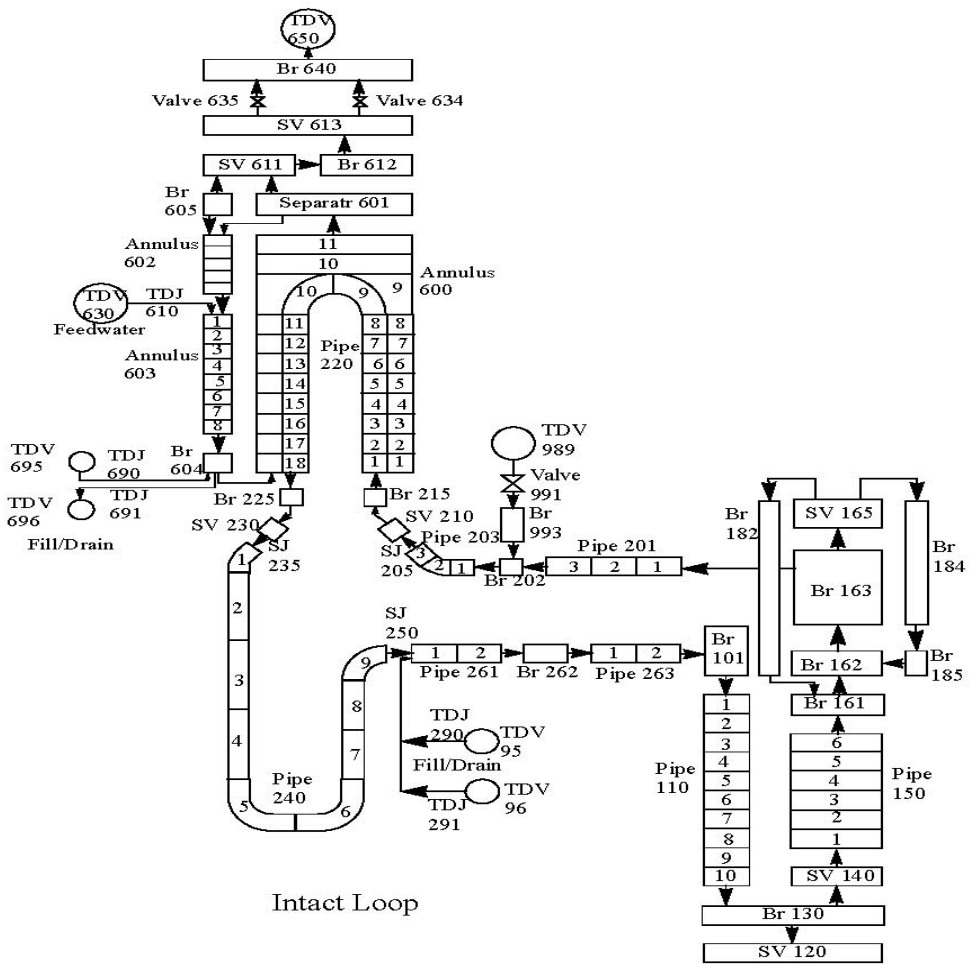
Figure 2-22   RELAP5 Nodalization of the Semiscale Mod-2A Test Facility
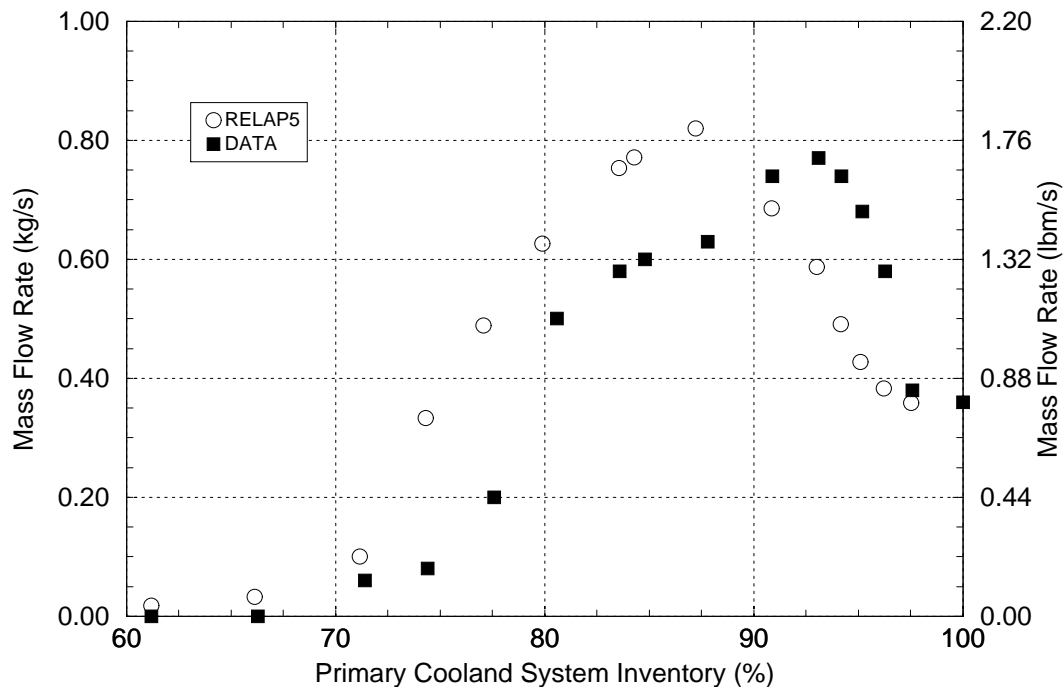
**Figure 2-23   Cold Leg Mass Flow as a Function of Primary Coolant System Inventory –
Semiscale Test S-NC-02**

Test conditions representing PWR two-phase coolant loop natural circulation are shown for inventories between 97% and 70%. As the inventory drops below 97%, the core boiling rate increases and the upflow sides of the SG U-tubes become more voided. (The term "upflow side" refers to the portion of the tube length in which flow is directed upward during normal plant operation). This tube voiding increases the buoyancy driving head for coolant loop natural circulation. The downflow side of the U-tubes remains liquid-filled, and it is the difference in fluid densities between the downflow and upflow sides of the U-tubes that creates the buoyancy driving head. The circulation rate increase begins at a 97% inventory in both the test and calculation. Flow rate peaks are seen at inventories of about 92% in the test and about 88% in the calculation and the peak flow rate is well-predicted with RELAP5. A flow peak is formed because, as the inventory continues to drop, eventually the downflow side of the SG tube starts to void and this reduces the buoyancy driving head and the natural circulation flow rate. The difference between the inventories at which the flow peaks are formed in the test and calculation is believed to be caused by an overprediction of interphase drag. An overpredicted drag tends to sweep more liquid upward through the tubes in the calculation than in the test, thus requiring a lower inventory to be reached in order to cause the onset of tube downflow-side voiding. For inventories between about 90% and 70%, the calculated mass flow rate was greater than in the test. This difference was found to result from the temperature of the liquid in the downflow side of the tube becoming about 2 K [3.6°F] colder in the calculation than in the test, perhaps due to an overprediction of wall condensation.

The calculated cold leg flow rate compares well with the measured data for conditions representing PWR coolant loop reflux cooling conditions. Reflux cooling was observed to occur over the inventory range from 70% to 61.2% in the test. It is noted that the RELAP5-calculated reflux

2-23

cooling mass flow rate was oscillatory and that the average of the calculated values is compared with the measured values on the plot.

Test S-NC-03 examines primary-side two-phase natural circulation behavior under varying SG secondary-side mass inventory conditions. A constant core power of 62 kW and a constant primary-side inventory (91.8% of full inventory) that represents a condition of two-phase natural circulation were used for this test. The secondary-side mass inventory was lowered in nine steps, thereby reducing the effective SG tube heat transfer area and the primary-side flow rate was measured at each of the steps.

Figure 2-24 shows the primary-side mass flow rate as a function of SG tube heat transfer area. Reducing the heat transfer area from 100% to 55% resulted in only a minor reduction in the primary-side flow rate. This behavior is seen in the test and calculation and results because the core power for the test represents only a small fraction of the scaled core power while the SGs have been designed to remove the full scaled core power. The SG heat transfer area available at the full secondary inventory is therefore more than ample to remove the core power used in the test. As the secondary inventory continues to be reduced, however, a point is eventually reached where the SG heat transfer process (and thereby the primary-side flow) is degraded by further reduction of the effective SG tube heat transfer area. The comparison shows good agreement between the measured and calculated primary-side flow rates at effective tube heat transfer areas above 55% and a good prediction of the transition to the degraded conditions at the lower effective heat transfer areas.
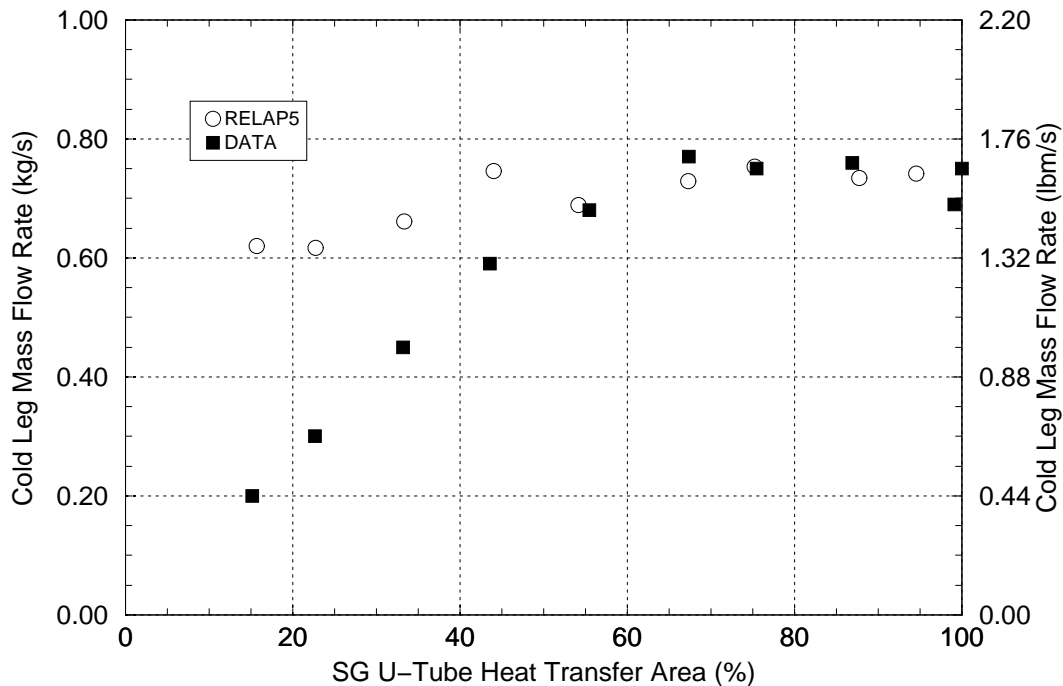
Figure 2-24   Cold Leg Mass Flow as a Function of SG Tube Active Heat Transfer Area – Semiscale Test S-NC-03

Below 55% effective tube heat transfer area the code is seen to overpredict the primary-side mass flow rate. The test data in this range show oscillatory behavior and only the average of the measured behavior is shown in the figure. The experimental uncertainty in the primary-side flow rate caused by the oscillations is about +0.15 kg/s [+0.33 lbm/s]. Therefore, the code overpredicts the primary-side flow rate even when this uncertainty in the measured data is considered. As was the case for reduced primary-side inventory test above, this overprediction is believed to be caused by an overprediction of interphase drag inside the SG tubes.

RELAP5 well-predicted the two Semiscale natural circulation tests for the conditions associated with higher primary- and secondary-side coolant system inventories. The code also predicted well the transitions to lower primary-side flow rates resulting from reduced primary- and secondary-side inventories. However, at reduced primary- and secondary-side inventories, the code generally tended to overpredict the primary-side flow rate and these overpredictions are believed to result from an overprediction of interphase drag.

An overprediction of the primary-side flow rate generally is non-conservative from the viewpoint of a PTS analysis. Since the temperature of the coolant loop flow typically is much higher than the ECCS injection temperature, then the faster the coolant loop flows the warmer a mixture of the coolant loop and ECCS temperatures becomes. The figures in this section indicate that under degraded inventory conditions the primary-side flow rate may be overpredicted by a factor of about two.

To judge the significance of this coolant loop flow overprediction for PTS, one must compare the relative flow rates of the ECCS and primary loops. As an example, consider Palisades Case 2 from the PTS plant evaluation, a 3.591 cm [1.414 in] diameter break in the pressurizer surge line. In this SBLOCA analysis case, the primary coolant system depressurizes to about 6.6 MPa [957 psia] and the loss of coolant inventory is not sufficient to interrupt coolant loop natural circulation. At 4,000 s into the event sequence, under coolant loop natural circulation conditions the coolant loop flow rate (per cold leg) is 84.6 kg/s [186.5 lbm/s] and the coolant loop temperature (coming from the SGs) is 499.6 K [439.6°F]. The HPI flow rate (per cold leg) is 13.4 kg/s [29.5 lbm/s] and the HPI fluid temperature is 314.3 K [106.1°F]. Mixing the coolant loop and HPI flows together, the temperature of the fluid entering the reactor vessel is 474.3 K [394.0°F]. Next, if one considers that the coolant loop flow rate may be overpredicted by a factor of two and repeats the mixing calculation using a coolant loop flow rate of 42.3 kg/s [93.3 lbm/s], the resulting temperature of the fluid entering the reactor vessel is 455.0 K [359.3°F]. Therefore, the effect on the temperature of the fluid entering the reactor vessel of overpredicting the natural circulation flow rate is estimated at 19.3 K [34.7°F]. This is the maximum effect expected based on steady flows. However, the PTS sequences are transients of which only brief periods of loop flow overprediction are occasionally encountered. The effects of any loop flow underprediction are automatically included in the assessments of RELAP5 for transient events in integral effects in Section 3.

3. INTEGRAL EFFECTS TESTS

RELAP5 was assessed against 12 integral-effects systems tests to evaluate code capabilities for predicting key PTS phenomena in the experimental data. The tests used for the assessments were performed in the ROSA-IV, ROSA/AP600, OSU-APEX, LOFT and MIST experimental facilities. The code assessments for the integral-effects systems tests are discussed in this section.

3.1   ROSA-IV Test SB-CL-18

The ROSA-IV experimental facility (Reference 3-1) is a 1/48 volume-scaled, full-pressure representation of a 3423-MW$_t$ Westinghouse-type four-loop PWR. The facility utilizes a full-height electrically-heated core. The four PWR coolant loops are represented with two equal-volume loops in the test facility. The components of the facility that are included are the hot leg, steam generator, reactor coolant pump (RCP), cold leg, pressurizer (on the "intact" loop) and emergency core coolant (ECC) systems: high pressure injection (HPI), low pressure injection (LPI) and accumulators. Figure 3-1 shows the layout of the ROSA-IV experimental facility.

ROSA-IV Test SB-CL-18 represents a 5%, 15.24 cm [6 in] equivalent diameter scaled break on the side of the cold leg with the reactor in full-power operation. The HPI and auxiliary feedwater (AFW) systems are assumed to fail. A loss of offsite power, resulting in tripping of all RCPs, is assumed to occur at the time of reactor scram. This experiment was the subject of International Standard Problem 26 (ISP-26, Reference 3-2) in which 18 organizations from 14 countries performed simulations of the experiment using eight different computer codes. The most recent RELAP5 code version used in the International Standard Problem exercise was RELAP5/MOD2.5.

A simulation of ROSA-IV Test SB-CL-18 was performed using the RELAP5/MOD3.2.2Gamma code. The nodalization diagram for the RELAP5 ROSA-IV facility model is shown in Figure 3-2. Table 3-1 lists the initial conditions for the test; the comparison shows good agreement between the measured and RELAP5-calculated initial condition data. A tabulated comparison of the measured and RELAP5-calculated sequences of events for this test is presented in Table 3-2. The code predictions of the loop seal clearing, main core uncovering and accumulator injection times are excellent. A minor core uncovering and rod heat up was observed from 120 s to 150 s in the experiment that was not predicted in the calculation. Overall, the comparison between the calculated and measured event sequence timing is excellent.

Plotted comparisons of the RELAP5 calculation system response with the experimental data are shown for phenomena pertinent for PTS in Figures 3-3 through 3-9.

The break flow comparison is shown in Figure 3-3. The calculated and measured data are in excellent agreement. The large declines in both curves at about 150 s result from steam reaching the break as a result of loop seal clearing phenomena.

The pressurizer pressure comparison is shown in Figure 3-4. The calculated and measured data are in excellent agreement. The code moderately overpredicted the RCS pressure from about 450 s to 750 s as a result of underpredicting the accumulator injection rate with its attendant condensation effects as discussed below.

The Loop A and B flow comparisons are shown in Figures 3-5 and 3-6. The declines in loop flow reflect tripping of the RCPs and transition to loop natural circulation observed in the experiment and are well-predicted by the code. The cause of the offset between the calculated and measured data

after about 250 s is not known, but likely is related to referencing or biasing of the instrumentation. The loss of loop natural circulation flow, as indicated by the RCS pressure falling below the SG pressures is well predicted (see Table 3-2).

The Loop B cold leg fluid density comparison is shown in Figure 3-7. The experimental information shown reflects densitometer data at the top, middle and bottom of the cold leg pipe while the calculated information reflects an average over the entire pipe cross section. The calculated and measured behaviors are in excellent agreement over the period when the RCS is draining, from 0 to 450 s. After the accumulator injection begins at about 450 s, the measured data reflect water residing in the lower half of the cold leg. Only a very minor increase in the calculated density is indicated during the accumulator injection period, reflecting both an underprediction of the accumulator injection rate and the one-dimensional nature of the cold leg modeling. The accumulator fluid is passed more directly to the reactor vessel in the calculation than is seen in the test data.

The Loop B accumulator discharge rate is shown in Figure 3-8; the code significantly underpredicts the accumulator injection rate. A comparison of the reactor vessel downcomer fluid temperatures at elevations corresponding to the top and bottom of the core is shown in Figure 3-9. The test data exhibit little azimuthal temperature variation (less than 1 K [2°F]); test data shown are for an azimuth location between the Hot Leg A and Cold Leg B orientations. The measured and calculated downcomer fluid temperature data are in good agreement at the elevation corresponding to the top of the core. However the code overpredicts the downcomer temperature at the elevation corresponding to the bottom of the core. Both the measured and calculated temperatures show some heating of the downcomer fluid between the top and bottom core elevations, however that fluid heating is greater in the calculation than in the test. Excluding the period when the code underpredicts the accumulator discharge rate, the downcomer fluid temperature overprediction at the bottom core elevation is characterized as about 8 K [14°F].

The overall system behavior during periods when accumulators are injecting is particularly challenging for computer codes to predict. The rapid influx of cold water into the RCS leads to significant condensation effects, which in turn lead to lower RCS pressures and higher accumulator injection rates. This process, whose rate feeds upon itself, is therefore quite sensitive to the prediction of condensation effects. The behavior of the process is seen in the responses of RCS pressure in Figure 3-4 and accumulator injection rate in Figure 3-8. The accumulator injection rate is higher and the pressure is lower in the test than in the calculation. However, the pressure difference is relatively small and there is no major impact on the other key parameter for PTS, the downcomer fluid temperature. Therefore, the results of this assessment are favorable regarding RELAP5/MOD3.2.2Gamma capabilities for predicting PTS phenomena.

As an aside which furthers understanding of the accumulator injection process, a preliminary version of the calculation reported here was presented to the Thermal-Hydraulic Subcommittee of the Advisory Committee on Reactor Safeguards on December 11, 2002. That preliminary calculation exhibited significant overprediction (rather than underprediction) of the accumulator injection rate and underprediction (rather than overprediction) of the RCS pressure and vessel downcomer temperature. Subsequently, an input error in the preliminary calculation was uncovered through comparison with data in the ISP-26 report, Reference 3-2. Specifically, ambiguous information regarding the referencing of the level led to specifying too low of an initial accumulator level in the preliminary calculation. As a result, the initial accumulator gas volume was too large, causing the accumulator pressure to decline too slowly as its liquid contents were discharged. This

effect sustained a large accumulator-to-RCS pressure difference during the injection period, which resulted in significant overprediction of the accumulator injection rate.

In summary, an assessment of RELAP5/MOD3.2.2 Gamma using experimental data from ROSA-IV Test SB-CL-18 indicates that the code is capable of acceptably simulating the behavior of the key PTS parameters. For this test, RELAP5 underpredicted the measured downcomer temperature by a maximum of 13 K [23°F] and overpredicted it by a maximum of 17 K [31°F]. Over the full test period, RELAP5 overpredicted the measured downcomer temperature by an average of 2.4 K [4.3°F] and varied from the measured downcomer temperature by an average of 3.2 K [5.8°F].

General View of LSTF

1. Simulated core
2. Reactor pressure vessel
3. Hot leg
4. Cold leg
5. Crossover leg
6. RCS pump
7. Pressurizer
8. Steam generator
9. Accumulator
10. ACC piping
11. HPIS piping
12. RHR piping
13. Pressure control vent valve
14. Relief valve
15. Break initiation valve
16. N2 supply valve
17. Feed water control valve
18. Feed water line
19. Main steam line
20. Feed water pump
21. Jet condenser
22. Main steam valve
23. Cooling tower line
24. Steam generator tubes
25. Break flow storage tank
26. Safety valve

Figure 3-1   Layout of the ROSA-IV Experimental Facility
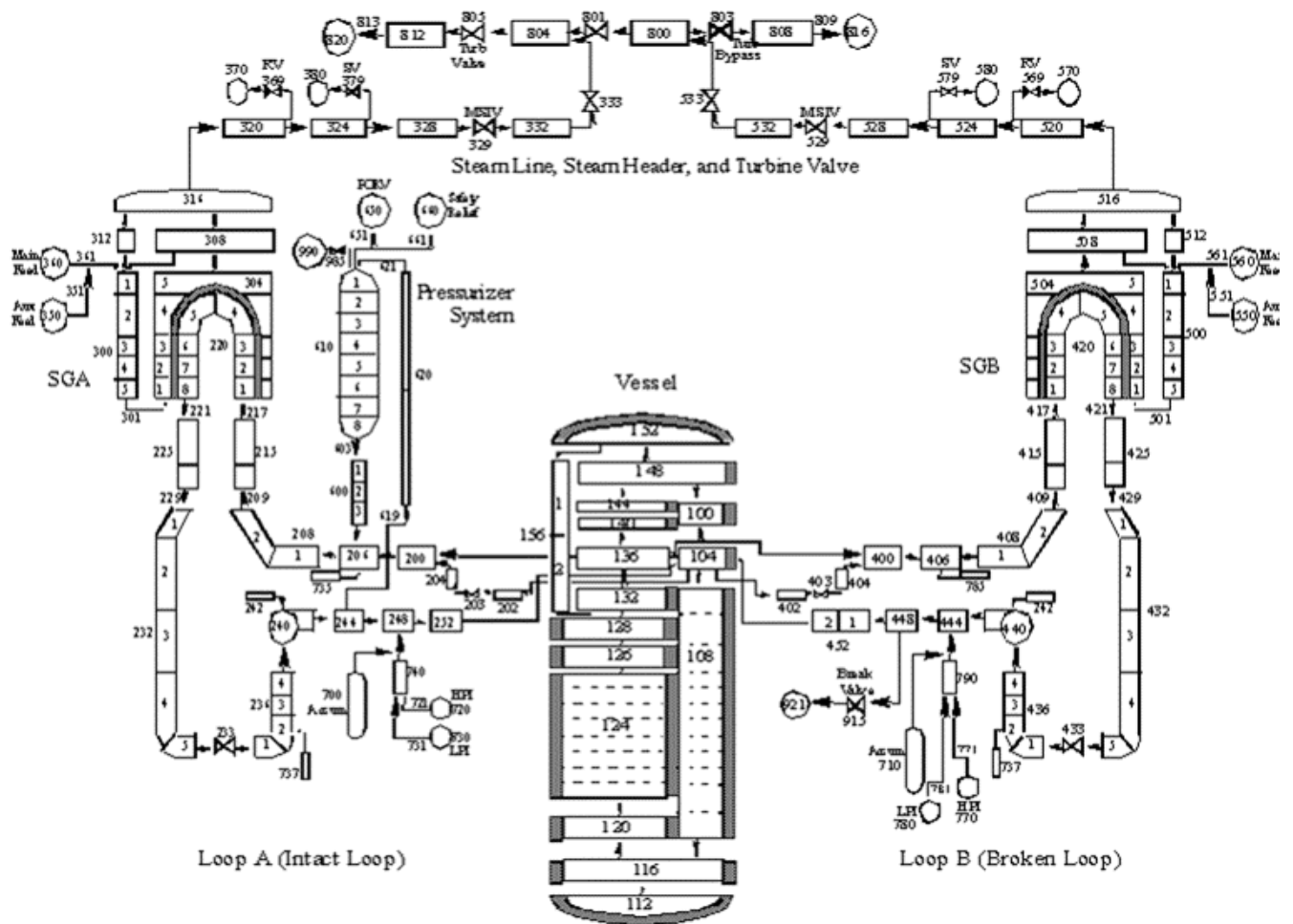
Figure 3-2   Nodalization of the RELAP5 ROSA-IV Facility Model

Table 3-1 Comparison of Measured and Calculated Initial Conditions for ROSA-IV Test SB-CL-18

Parameter	Initial Condition	
	Measured	RELAP5
Core power	10.0 MW	10.0 MW
Pressurizer pressure	15.5 MPa [2250 psia]	15.515 MPa [2250 psia]
Hot leg temperature	599.0 K [618.5°F]	599.07 K [618.7°F]
Cold leg temperature	563.5 K [554.6°F]	563.55 K [554.7°F]
Pressurizer level	2.7 m [8.8 ft]	2.963 m [9.7 ft]
Total primary coolant loop flow	48.7 kg/s [107.0 lbm/s]	48.99 kg/s [107.8 lbm/s]
SG 1 pressure	7.3 MPa [1058.7 psia]	7.216 MPa [1046.6 psia]
SG 2 pressure	7.4 MPa [1073.3 psia]	7.219 MPa [1047.0 psia]
SG 1 level	10.8 m [35.4 ft]	9.150 m [30.0 ft]
SG 2 level	10.6 ft [34.8 ft]	9.151 m [30.0 ft]

Table 3-2 Summary of Measured and Calculated Sequences of Events for ROSA-IV Test SB-CL-18

Event Description	Event Time (s)	
	Measured	RELAP5
Break opens	0	0
Scram signal	10	8.3
Safety injection signal	12	9.0
Steam line valve closes	14	8.3
Feedwater flow stops	16	10
First core uncovering begins	120	Not Predicted
Loop seal clearing	140	148
Primary pressure falls below secondary (both loops)	180	170
Reactor coolant pumps stop	265	271
Second core uncovering begins	420	422
Accumulator injection flow begins	455	470

Figure 3-3   Break Flow – ROSA-IV SB-CL-18
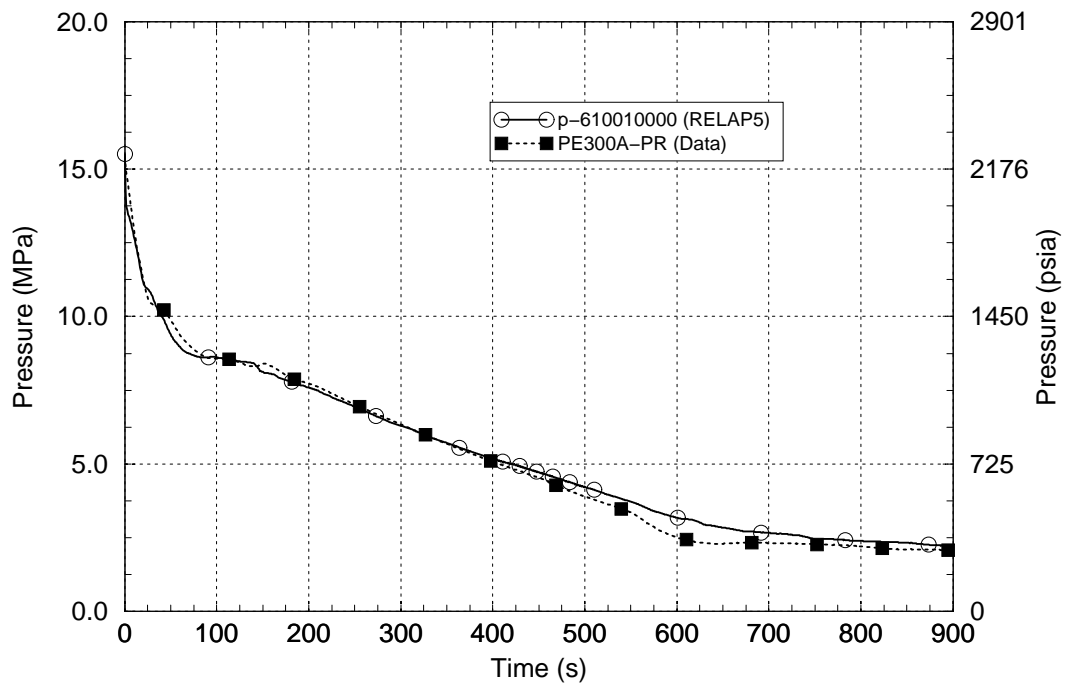
Figure 3-4   Pressurizer Pressure – ROSA-IV SB-CL-18

Figure 3-5   Loop A Pump Suction Cold Leg Flow – ROSA-IV SB-CL-18

Figure 3-6   Loop B Pump Suction Cold Leg Flow – ROSA-IV SB-CL-18

Figure 3-7   Loop B Pump Discharge Cold Leg Fluid Density – ROSA-IV SB-CL-18
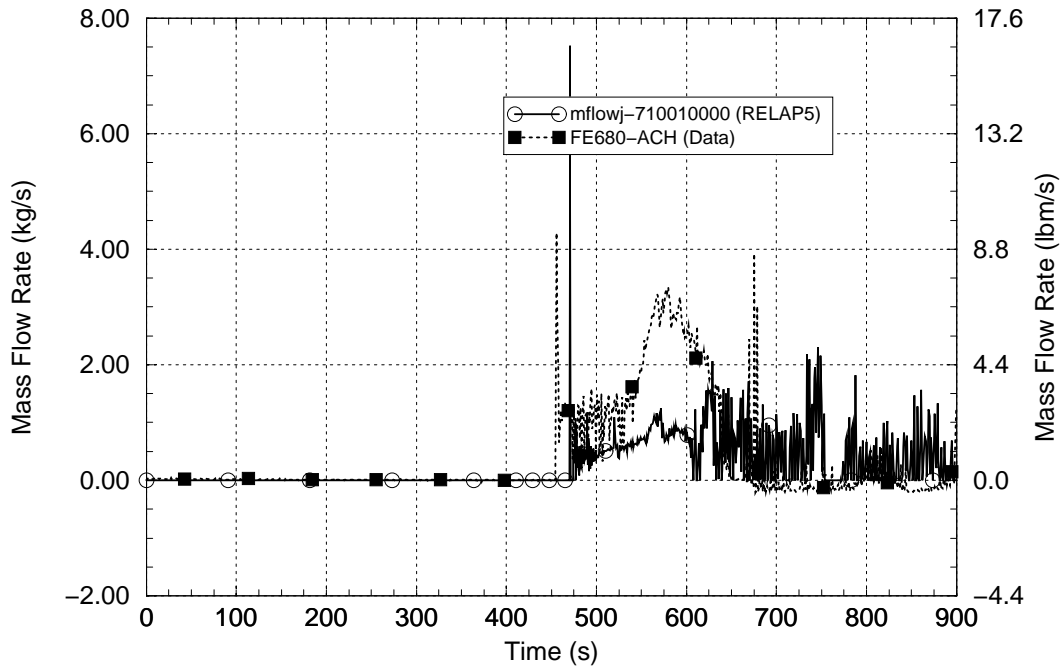
Figure 3-8   Loop B Accumulator Discharge Flow – ROSA-IV SB-CL-18
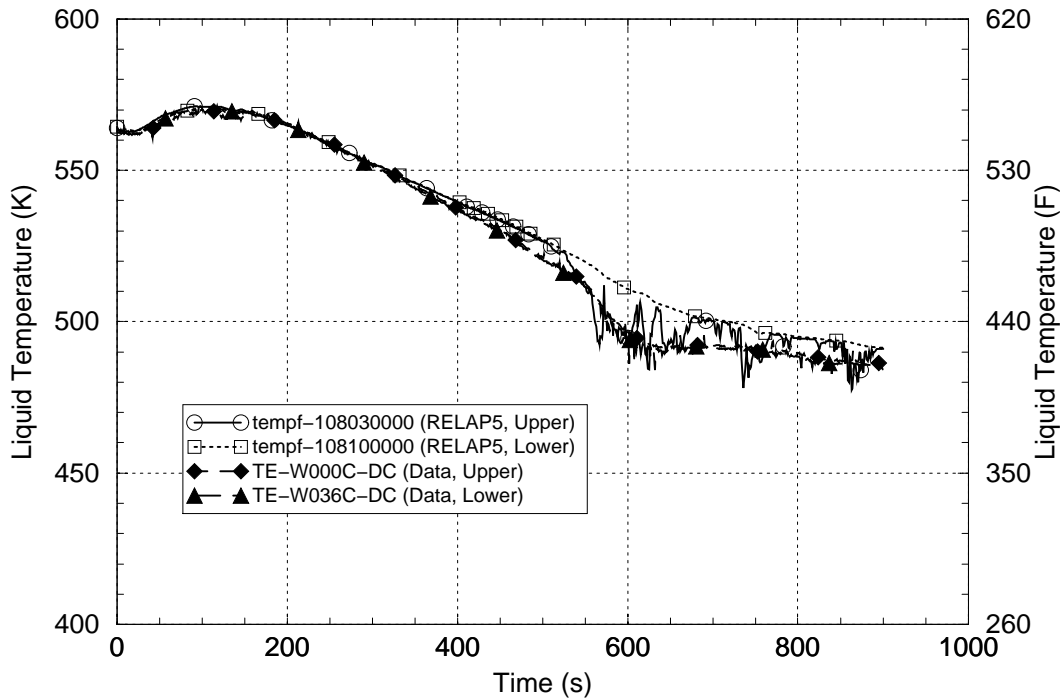
Figure 3-9   Reactor Vessel Downcomer Fluid Temperatures – ROSA-IV SB-CL-18

3.2   ROSA-IV Test SB-HL-06

See Section 3.1 for a basic description of the ROSA-IV experimental facility. The facility underwent minor modifications between the performance of Tests SB-CL-18 and SB-HL-06.   Those modifications, primarily relating to the core reactor region, are described in Reference 3-3.

ROSA-IV Test SB-HL-06 represents a 0.5%, 5.08 cm [2 in] equivalent diameter scaled break on the top of a hot leg with the reactor in full-power operation. The break is located in non-pressurizer loop Hot Leg B. The HPI and AFW systems are assumed to fail. A loss of offsite power, resulting in tripping all RCPs, is assumed to occur at the time of reactor scram. Once core uncovering and heat up started, the pressurizer PORV was opened to depressurize the primary coolant system and initiate accumulator injection.

A simulation of ROSA-IV Test SB-HL-06 was performed using the RELAP5/MOD3.2.2Gamma code. The nodalization diagram for the RELAP5 ROSA-IV facility model is shown in Figure 3-2. Table 3-3 lists the initial conditions for the test; the comparison shows good agreement between the measured and RELAP5-calculated data.

A tabulated comparison of the measured and RELAP5-calculated sequences of events for this test is presented in Table 3-4. The code predictions of voiding in the hot and cold legs and cessation of coolant loop natural circulation flow are in good overall agreement with the test. However, the loss of loop natural circulation in one loop was predicted too early while in the other loop it was predicted too late. The timing of core uncovering and heat up was well predicted with the code. To partially normalize comparisons between the code and test during the latter portion of the event sequence, the pressurizer PORV was opened at the same time in the calculation as in the test. Following the opening of the PORV, the RCS depressurization to the accumulator flow initiation

pressure was more rapid in the calculation than in the test and as a result, accumulator flow initiation occurred earlier in the calculation than in the test.

Table 3-3 Comparison of Measured and Calculated Initial Conditions for ROSA-IV Test SB-HL-06

Parameter	Initial Condition	
	Measured	RELAP5
Core power	10.0 MW	10.0 MW
Pressurizer pressure	15.52 MPa [2250 psia]	15.412 MPa [2235 psia]
Hot leg temperature	598.1 K [616.9°F]	598.84 K [618.2°F]
Cold leg temperature	562.4 K [552.6°F]	563.56 K [554.7°F]
Pressurizer level	2.73 m [8.96 ft]	2.930 m [9.61 ft]
Total primary coolant loop flow	48.7 kg/s [107.1 lbm/s]	49.296 kg/s [108.5 lbm/s]
SG 1 pressure	8.03 MPa [1164.6 psia]	7.216 MPa [1046.6 psia]
SG 2 pressure	7.82 MPa [1134.2 psia]	7.219 MPa [1047.0 psia]
SG 1 level	10.3 m [33.8 ft]	9.151 m [30.0 ft]
SG 2 level	10.3 m [33.8 ft]	9.151 m [30.0 ft]

Table 3-4 Summary of Measured and Calculated Sequences of Events for ROSA-IV Test SB-HL-06

Event Description	Event Time (s)	
	Measured	RELAP5
Break opens	0	0
Scram signal	87	94
Steam line valve closes	90	94
Feedwater flow stops	92	95
Initiation of core power decay	110	110
Vapor appears in hot legs	200	150
Reactor coolant pumps stop	341	350
Vapor appears in cold legs	800	840
Loop A natural circulation stops	1,200	1,700
Loop B natural circulation stops	1,900	1,700
Core heat up begins	5,680	5,200
Pressurizer PORV opened	5,806	5,806[1]
Primary pressure falls below secondary (both loops)	5,808	5,660
Accumulator injection begins	6,425	6,070

1 – The time of PORV opening in the RELAP5 calculation was set to agree with that in the test.

Overall, the comparison between the calculated and measured sequence of events timing is good.

Plotted comparisons of the RELAP5 calculation system response with the experimental data are shown for phenomena pertinent for PTS in Figures 3-10 through 3-17.

The break flow comparison is shown in Figure 3-10. The calculated break flow is moderately higher than observed in the test. The pressurizer pressure comparison is shown in Figure 3-11. Despite the difference in break flow, the calculated and measured pressure data are in excellent agreement, which implies that the measured break flow data may be particularly inaccurate or that the temperature of liquid at the break may be too low in the calculation.

The Loop A and B flow comparisons are shown in Figures 3-12 and 3-13. The early declines in the loop flow rates reflect the tripping of the RCPs and transition to loop natural circulation. This behavior was well-predicted by the code. The loss of loop natural circulation flow also was well predicted by the code (although in the calculation this occurred somewhat too early in Loop A and late in Loop B). In both the experiment and calculation, the RCS pressure remained above the SG pressures out to near the time when the pressurizer PORV was opened, see Table 3-4.

The differential pressures in the up-flow sides of the Loop A and Loop B SG U-tubes are shown in Figures 3-14 and 3-15. These data reflect the amount of liquid residing in the tubes; the declining values indicate a countercurrent draining of liquid from the tubes into the SG inlet plena and hot legs. Three experimental curves representing the data from three different tubes in the test facility are plotted. The code model employs only one tube flow path per SG and the data for it are also plotted. The differences between these differential pressure data for the calculation and test are consistent with the timing differences in loop natural circulation flow loss described above.

A comparison of the reactor vessel downcomer fluid temperatures at elevations of the top and bottom of the core is shown in Figure 3-16. The test data show little azimuth variation (less than 2 K [3.6°F]); the data are shown for an azimuth location between the Hot Leg A and Cold Leg B orientations. Prior to the time when the PORV is opened, the calculated and measured data are in excellent agreement, reflecting the saturated conditions present during the first part of the test. When the PORV is opened, the RCS pressure declines faster in the calculation than in the test (Figure 3-11), resulting in greater accumulator injection flow and colder vessel downcomer temperatures. There is some disagreement in the measured and calculated initial depressurization rates. Possible explanations for the faster depressurization in the calculation are that: (1) the modeled PORV is oversized, (2) the hot leg break becomes plugged with water during this period in the test but not in the calculation (as suggested by the comparison in Figure 3-10) and (3) the RCS inventory at the time the PORV opens is larger in the test than in the calculation (also as suggested by the comparison in Figure 3-10).

At 8,000 s, there is a large drop in the measured downcomer temperature and a corresponding drop in the measured pressure. This behavior is caused by a rapid movement of water into the pressurizer as shown in Figure 3-17. Condensation effects inside the tank resulting from an influx of cold water perhaps drive this pressurizer filling. The depressurization caused when the pressurizer fills leads to a rapidly increasing accumulator flow and the drop in the measured downcomer temperature seen in Figure 3-16. None of this specific behavior was observed in the calculation.
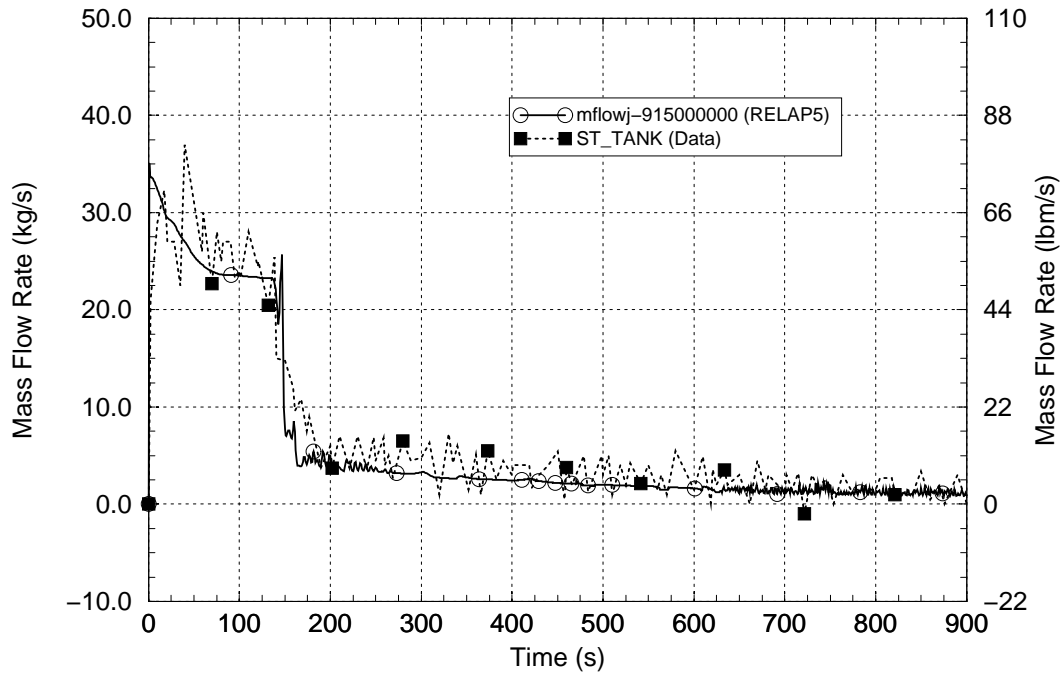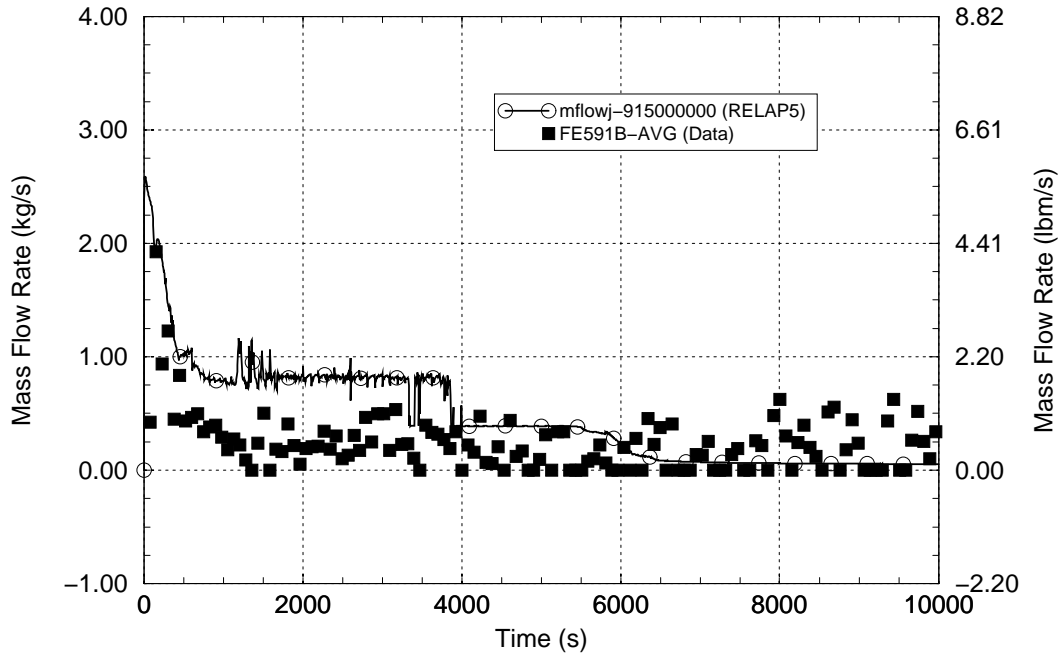
**Figure 3-10   Break Flow – ROSA-IV SB-HL-06**
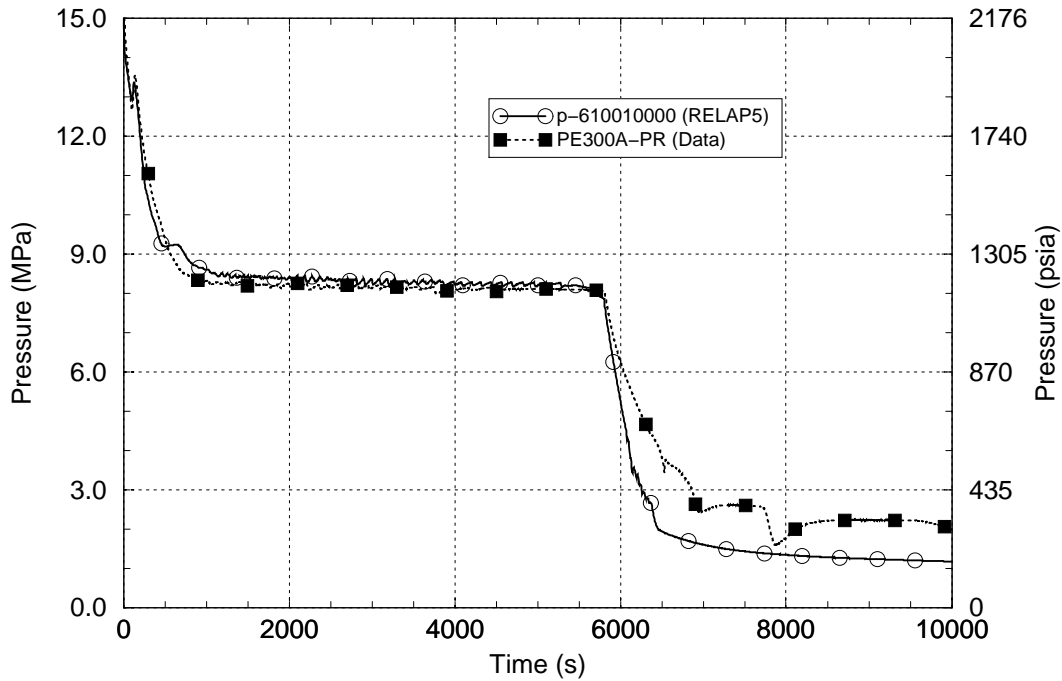
Figure 3-11   Pressurizer Pressure – ROSA-IV SB-HL-06
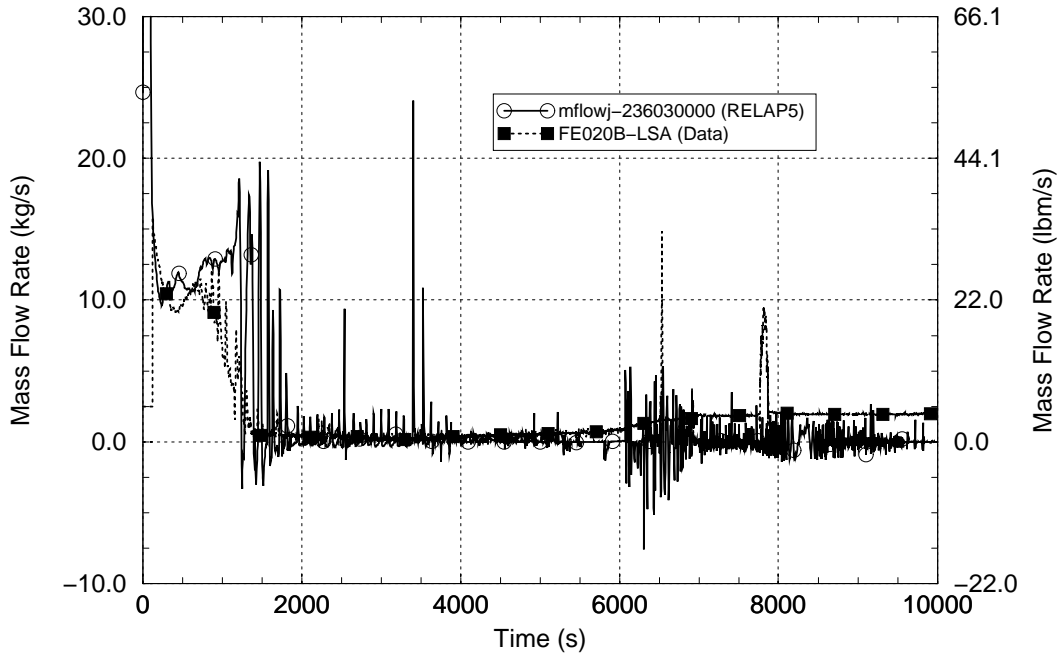
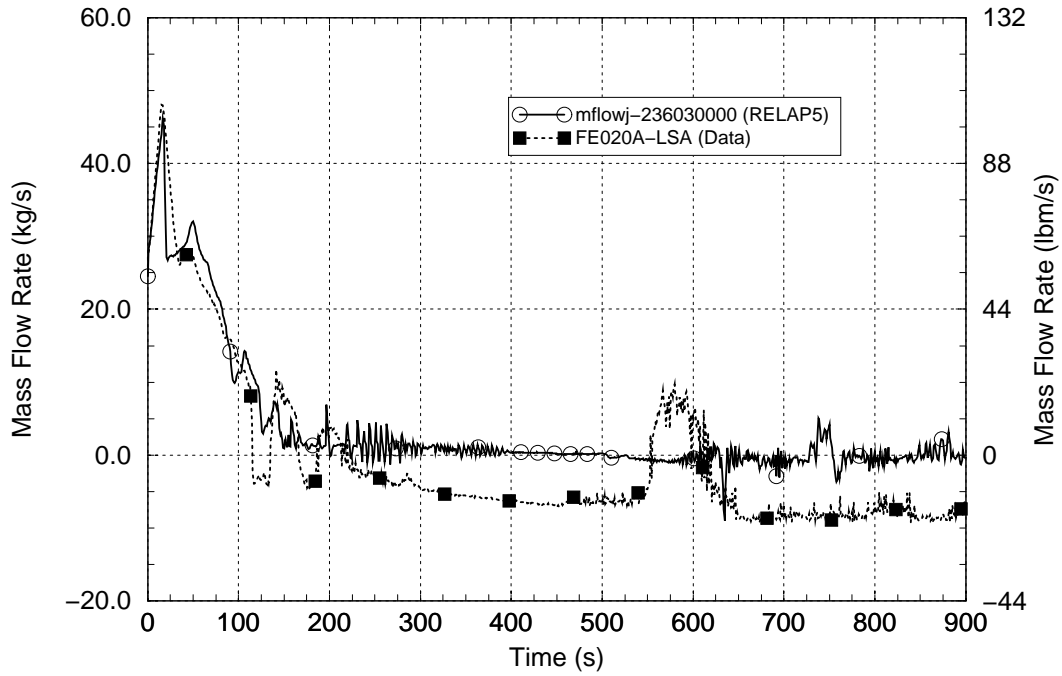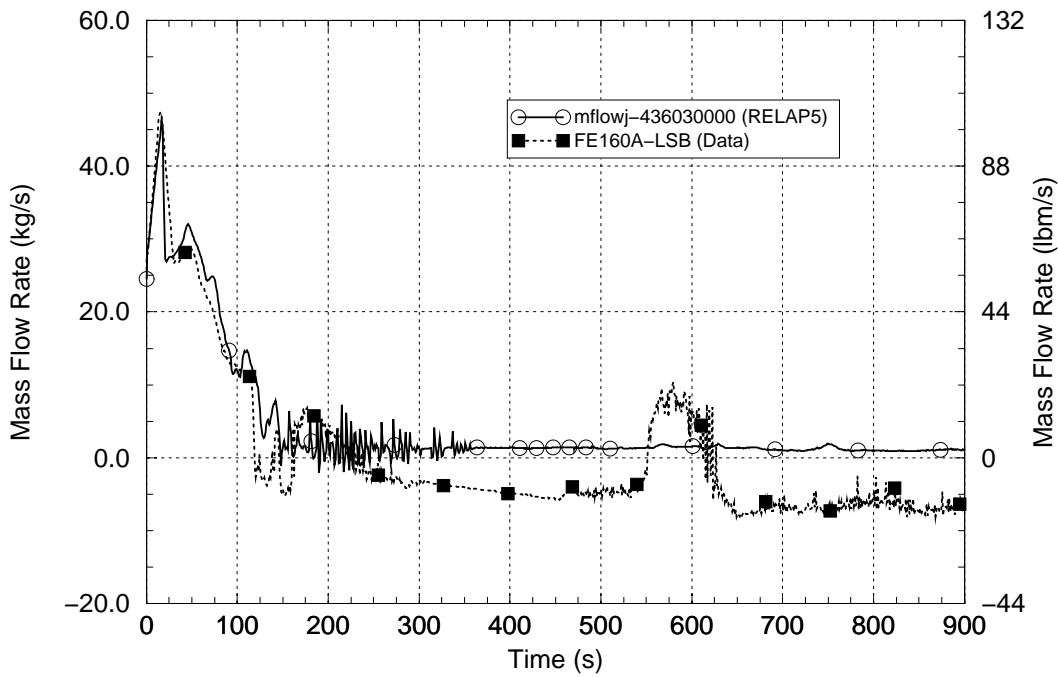**Figure 3-12   Loop A Pump Suction Cold Leg Flow – ROSA-IV SB-HL-06**

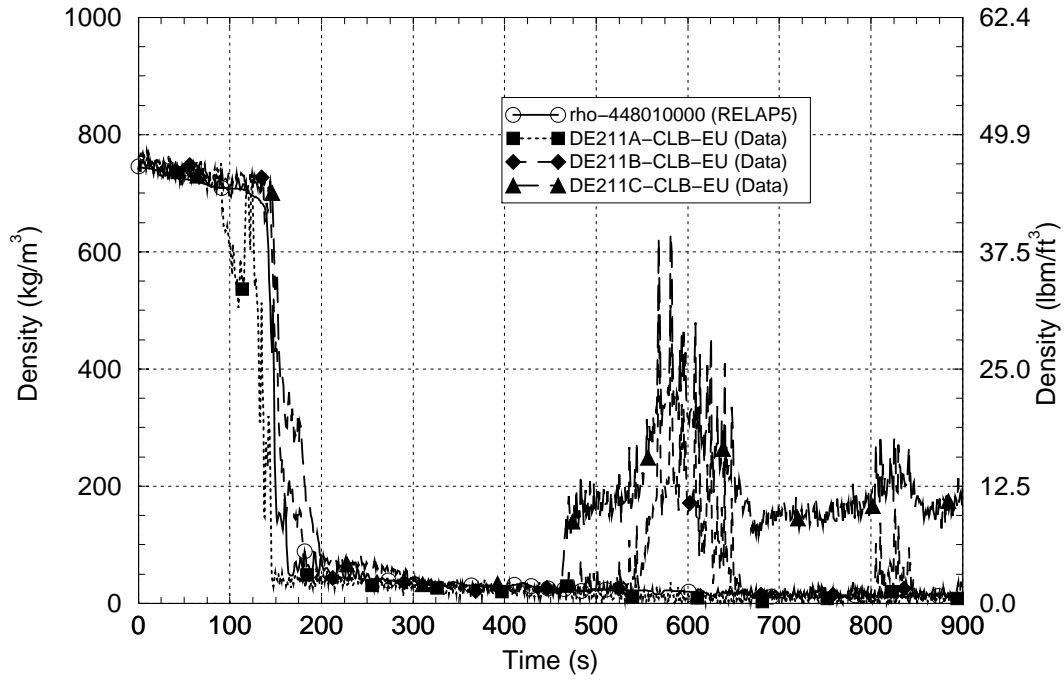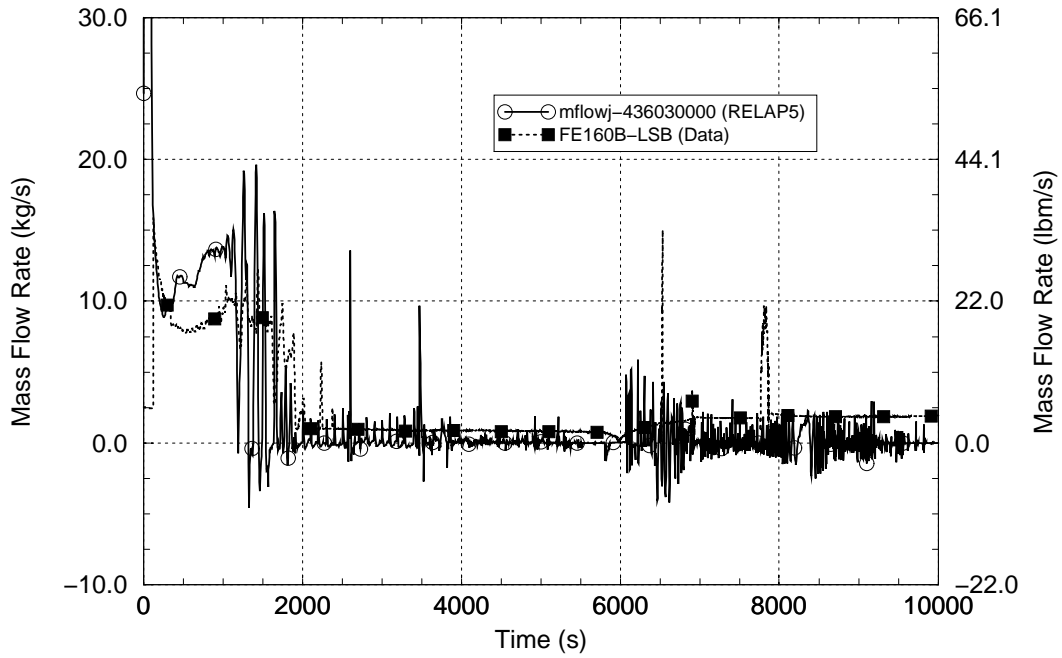**Figure 3-13   Loop B Pump Suction Cold Leg Flow – ROSA-IV SB-HL-06**
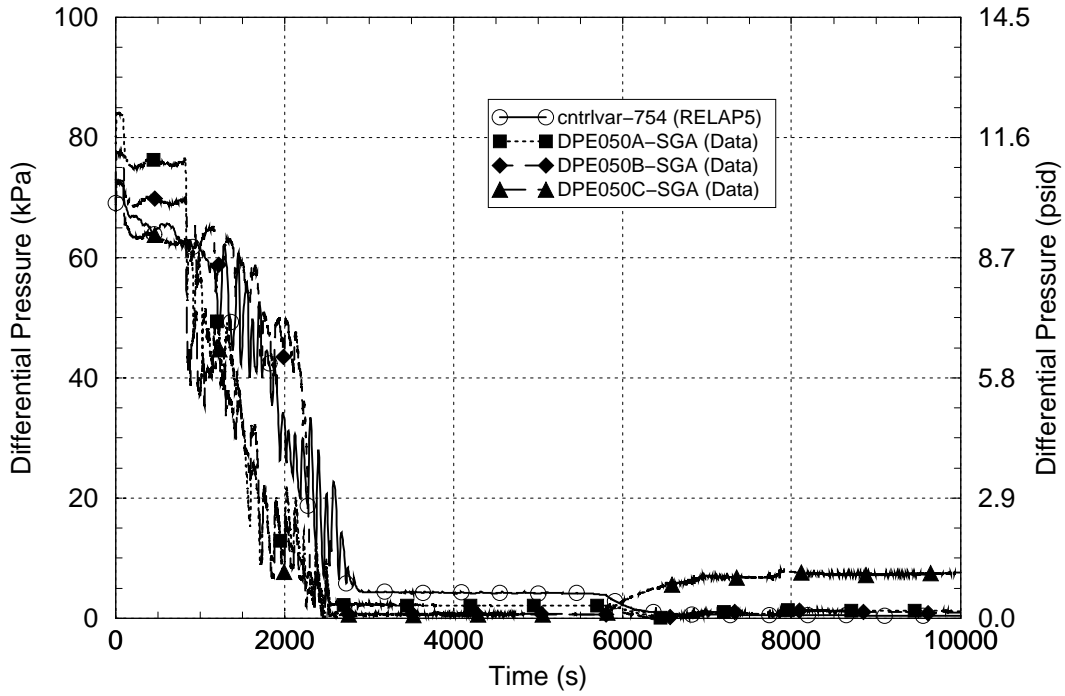
Figure 3-14   SG A U-Tube Up-flow Side Differential Pressure – ROSA-IV SB-HL-06
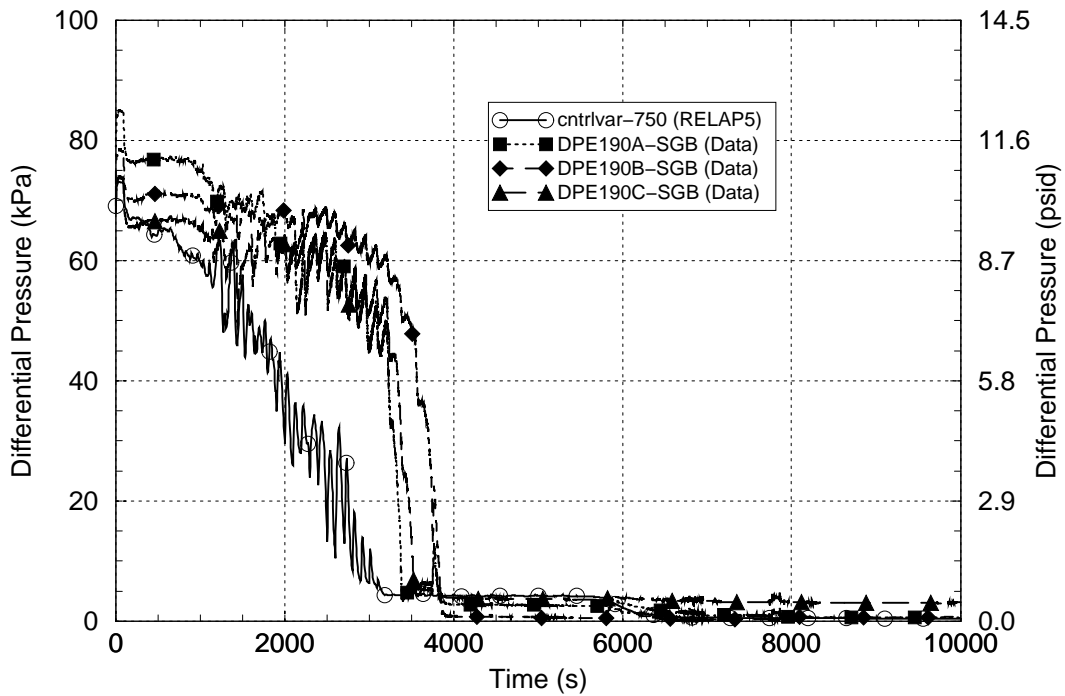
Figure 3-15   SG B U-Tube Up-flow Side Differential Pressure – ROSA-IV SB-HL-06
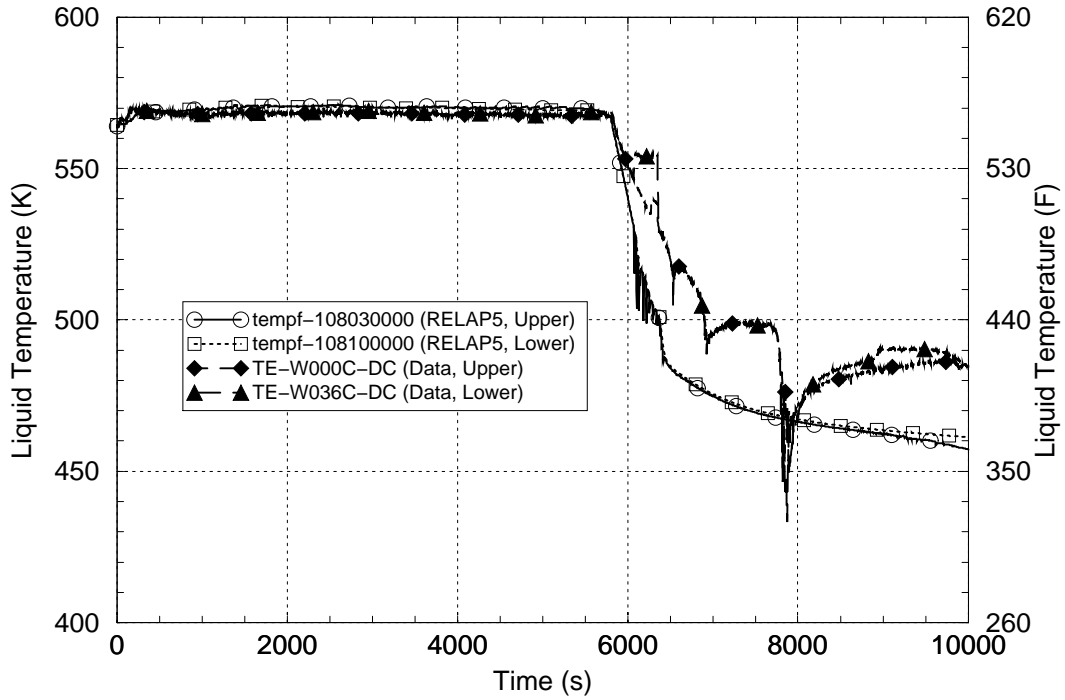
Figure 3-16 Reactor Vessel Downcomer Fluid Temperatures – ROSA-IV SB-HL-06
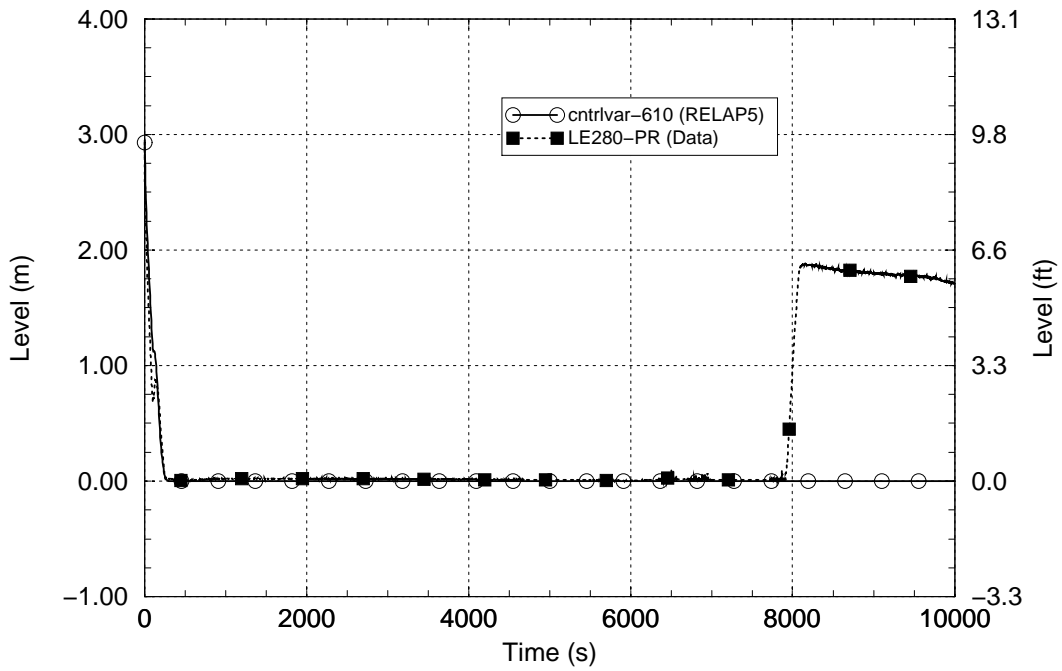
Figure 3-17 Pressurizer Level – ROSA-IV SB-HL-06

In summary, minor differences between calculated and measured behavior were observed in this assessment but none are considered to be serious predictive deficiencies. Loop flow stagnation was calculated somewhat too early in one loop and too late in the other loop; this difference may be caused by limitations of one-dimensional modeling of the loops. When the PORV is opened, the calculated depressurization was faster and smoother than observed in the test; this may be related to sizing of the modeled valve or differences in the RCS inventory or its distribution at the beginning of the depressurization period. The assessment of RELAP5/MOD3.2.2 Gamma using experimental data from ROSA-IV Test SB-HL-06 indicates that the code is capable of acceptably simulating the behavior of the key PTS parameters. For this test, RELAP5 underpredicted the measured downcomer temperature by a maximum of 53 K [95°F] and overpredicted it by a maximum of 35 K [63°F]. Over the full test period, RELAP5 underpredicted the measured downcomer temperature by an average of 8.9 K [16°F] and varied from the measured downcomer temperature by an average of 11 K [20°F].

3.3   ROSA/AP600 Test AP-CL-03

The ROSA/AP600 facility (Reference 3-4) is a 1/30 volume-scaled, full-pressure representation of a Westinghouse AP600 PWR. The facility utilizes a full-height electrically heated core. The two AP600 coolant loops are represented with two equal-volume loops. Components that are included in the loops are the hot leg, steam generator, one reactor coolant pump (as compared with two pumps in the plant design), one cold leg (compared with two in the plant design), pressurizer (on one coolant loop), and core makeup tanks (CMTs) on the opposite loop. The Passive Residual Heat Removal (PRHR) system, the Automatic Depressurization System (ADS), and the In-containment Refueling Water Storage Tank (IRWST) are also included. Figure 3-18 shows the layout of the ROSA/AP600 experimental facility.

There are many differences between the configurations of existing PWRs, for which PTS risk is being evaluated, and the AP600 plant configuration that is represented by the ROSA/AP600 facility. Specifically, the AP600 CMT, PRHR and IRWST components are not present in existing PWRs. However, comparison of RELAP5-calculated and measured test data for two ROSA/AP600 small break LOCA experiments are included in the PTS assessment matrix because they feature behavior that includes the pooling of cold liquid in the cold leg and the reactor vessel downcomer regions that is similar to that found in existing PWRs. Further, these regions in the experimental facility are particularly well-instrumented for providing measured data on the distributions of liquid and liquid temperatures. Assessments using experiments in the ROSA/AP600 facility provide a direct indication of code prediction capabilities for simulating the RCS pressure and reactor vessel downcomer fluid temperature responses, which are key parameters for PTS as described in Section 1.

Test AP-CL-03 (Reference 3-5) is a 0.1%, 2.54 cm [1 in] diameter scaled break on the bottom of the cold leg in the CMT loop. The reactor is operating at full power when the break opens. An additional failure, where one of the two ADS-4 valves on the CMT loop fails to open, is also assumed.

A simulation of ROSA/AP600 Test AP-CL-03 was performed using the RELAP5/MOD3.2.2Gamma code. The nodalization diagram for the RELAP5 ROSA/AP600 facility model is shown in Figure 3-19. Table 3-5 lists the initial conditions for the test; the comparison shows good agreement between the measured and RELAP5-calculated data. A tabulated comparison of the measured and calculated sequences of events is presented in Table 3-6. The comparison shows

excellent agreement in the measured and calculated event timing for this complex accident sequence.

Figure 3-20 shows the pressurizer pressure comparison. The measured and calculated pressures compare well down to a pressure of about 5 MPa [725 psia]. Afterward, the pressure declined faster in the calculation than in the test. The CMT B level comparison is shown in Figure 3-21. The rate of CMT level decline in the calculation is seen to be similar to that in the experiment, but the CMT level reached the ADS actuation setpoint level 478 s earlier in the calculation than in the test. The earlier ADS activation in the calculation is evident in the pressurizer pressure comparison. A refill of CMT B occurred between 7,000 s and 8,000 s during the experiment. This refill behavior was not calculated by the code.
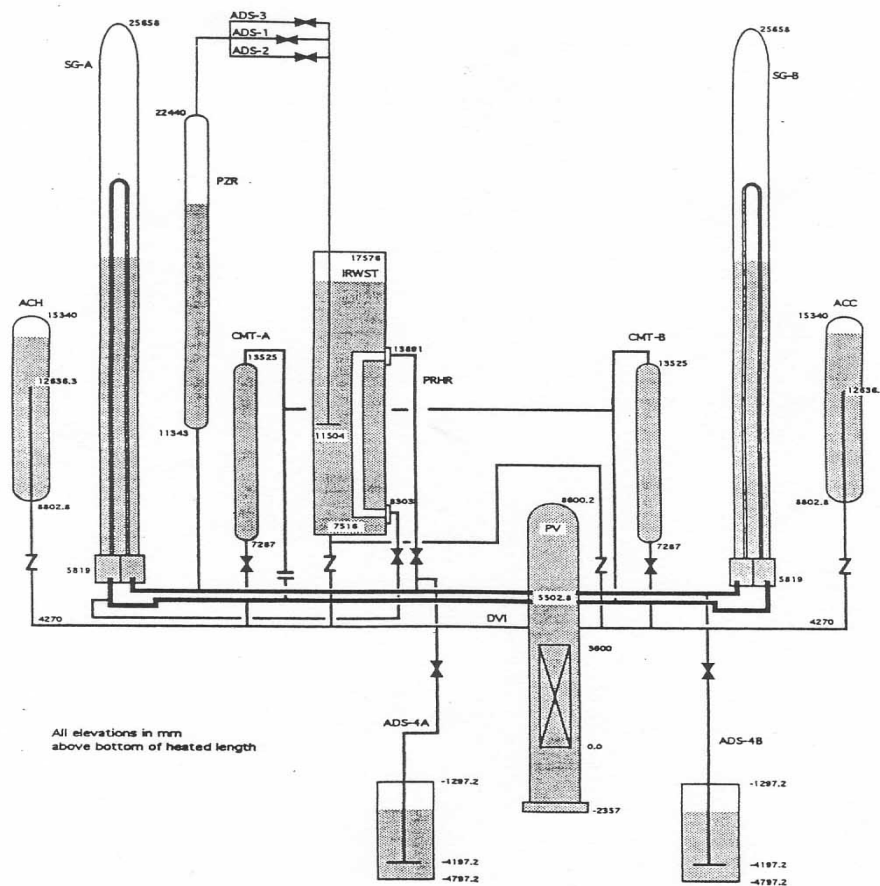
Figure 3-18   Layout of the ROSA/AP600 Experimental Facility
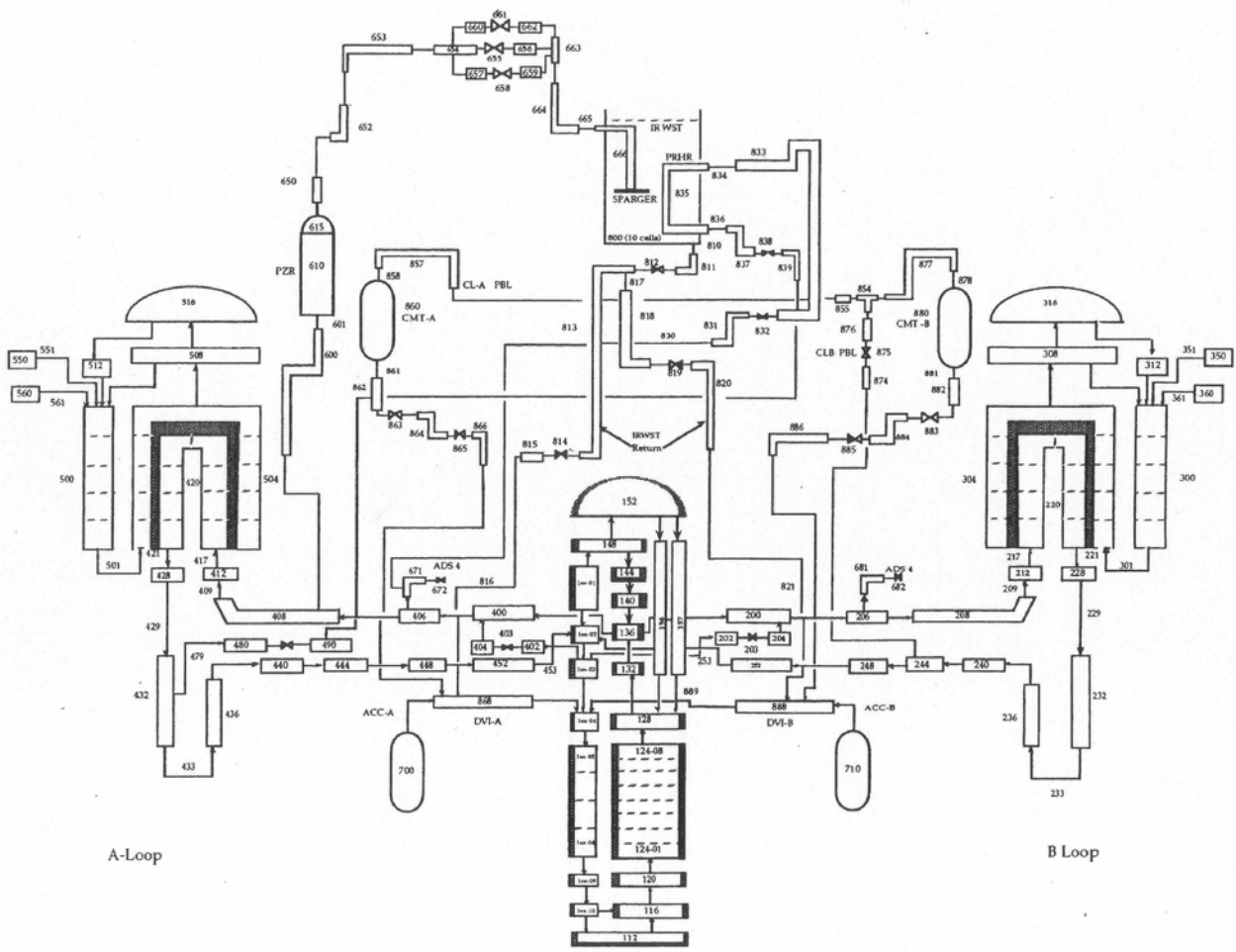
Figure 3-19   Nodalization of the RELAP5 ROSA/AP600 Facility Model

Table 3-5   Comparison of Measured and Calculated Initial Conditions for ROSA/AP600 Test AP-CL-03

Parameter	Initial Condition	
	Measured	RELAP5
Core power	9.97 MW	9.97 MW
Pressurizer pressure	15.5 MPa [2250 psia]	15.464 MPa [2248 MPa]
Hot leg temperature	587.5 K [597.8°F]	587.07 K [597.05°F]
Cold leg temperature	550.0 K [530.3°F]	549.93 K [530.2°F]
Pressurizer level	6.22 m [20.41 ft]	6.284 m [206.2 ft]
Total primary coolant loop flow	50.4 kg/s [110.8 lbm/s]	50.528 kg/s [111.2 lbm/s]
SG pressure	5.90 MPa [855.7 psia]	5.900 MPa [855.7 psia]

Table 3-6   Summary of Measured and Calculated Sequences of Events for ROSA/AP600 Test AP-CL-03

Event Description	Event Time (s)	
	Measured	RELAP5
Break opens	0	0
CMT recirculation begins	158	137
PRHR flow begins	159	137
Reactor scram, reactor coolant pumps tripped	178	152
S signal	203	163
Loss of natural circulation in pressurizer loop	463	470
Primary pressure falls below pressurizer loop SG pressure	696	1,181
Primary pressure falls below CMT loop SG pressure	805	611
Loss of natural circulation in CMT loop	1,115	1,080
Accumulator injection begins	1,934	1,900
CMT draining begins	2,198	2,196
ADS-1 valve opened	3,533	3,055
ADS-4 valves opened	4,450	3,853
IRWST injection begins	4,978	4,246
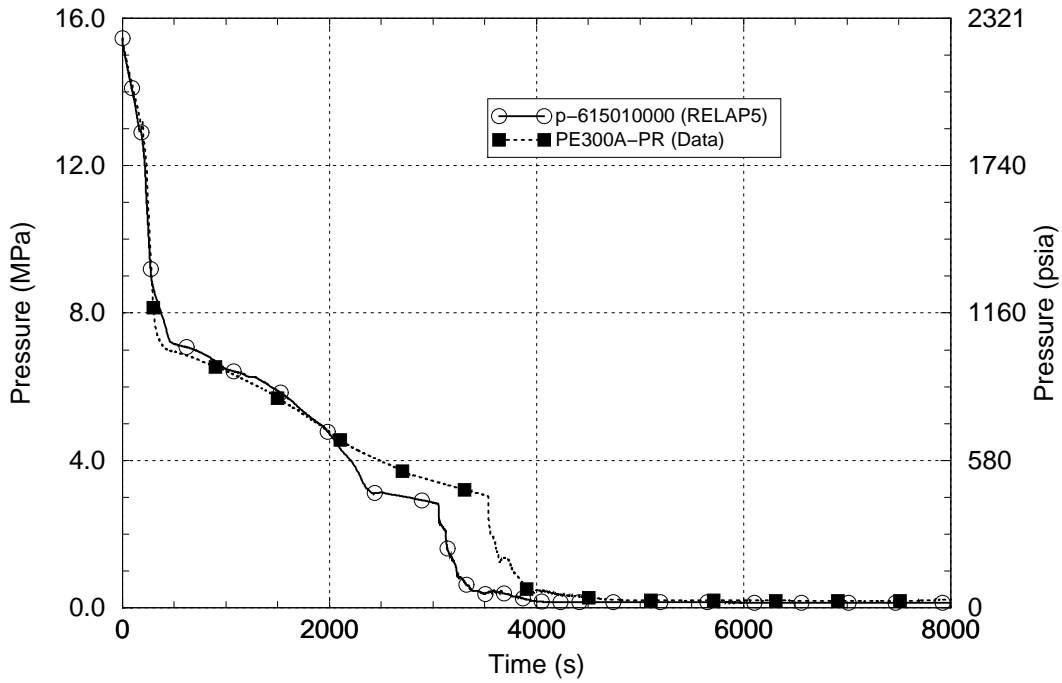
Figure 3-20   Pressurizer Pressure – ROSA/AP600 AP-CL-03
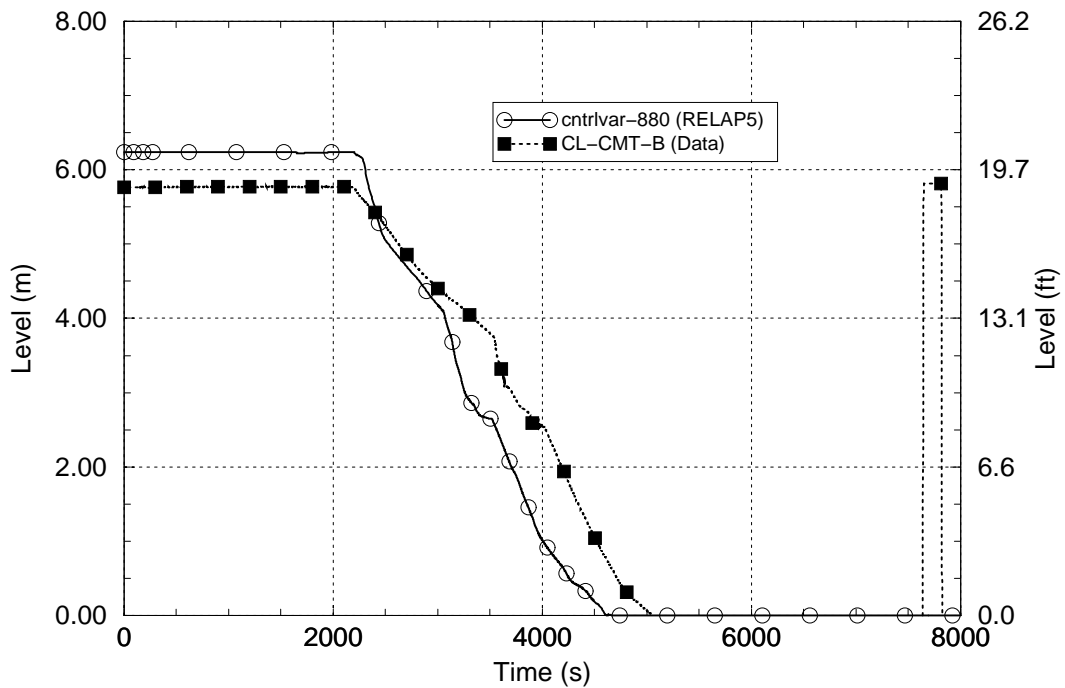
Figure 3-21   CMT B Level – ROSA/AP600 AP-CL-03

3-20

Figures 3-22 and 3-23, respectively, compare the pressurizer loop and CMT loop pump-suction cold leg flow rate responses. The timing of the stagnation of coolant loop natural circulation is seen to be excellently predicted by RELAP5 for both coolant loops. The loop flow stagnation times also correlate reasonably with the times when the RCS pressure falls below the SG pressures as shown in Table 3-6.

Figures 3-24 and 3-25, respectively, compare the pressurizer loop and CMT loop pump-discharge cold leg fluid temperature responses (near the reactor vessel). The experimental data were obtained using vertical rakes of thermocouples over the span from the top to bottom of the cold leg diameter. These figures indicate that there was considerable thermal stratification of the liquid in the cold legs of the test facility, with cooler water running underneath warmer water. This behavior cannot be simulated with a code such as RELAP5, which uses one-dimensional modeling for piping regions such as the cold legs. The calculated fluid temperature prediction reflects only the temperature of the cold water flowing through the cold leg toward the reactor vessel.

Figures 3-26 through 3-29 compare the fluid temperature responses in the upper and lower reactor vessel downcomer regions on the CMT-loop and pressurizer-loop sides of the downcomer. Despite the lack of a RELAP5 modeling capability for simulating thermal stratification in the cold legs, the comparisons in these figures demonstrate that RELAP5 can predict well the reactor vessel downcomer fluid temperature cooldown rates observed in the experiment.

During the cooldown period (first 4000 s), the downcomer temperature response comparisons indicate a consistent bias for the code-calculated temperatures to be slightly higher (by at most 15 K [27°F]) than the measured temperatures. Some of this bias may be related to the cold leg thermal stratification modeling situation discussed above. However, most of the bias is believed to result from the difference in calculated and measured PRHR system discharge temperatures shown in Figure 3-30. The figure shows that the calculation overpredicted the measured PRHR discharge temperature by up to 25 K [45°F]. The modeling of the PRHR system, which is immersed within the IRWST, is particularly challenging because of IRWST thermal stratification effects. The code model therefore tended to underpredict the effectiveness of the PRHR heat exchange process, resulting in warmer water entering the RCS from the PRHR system and finding its way to the reactor vessel downcomer.

The differences between the calculated and measured downcomer temperature behavior during the second half of the transient sequence in Figures 3-26 through 3-29 are related to the differences in IRWST injection behavior shown in Figure 3-31. The onset of IRWST injection was earlier in the calculation than in the experiment because, as shown in Figure 3-20: (1) the calculated ADS activation time was earlier, (2) the RCS pressure was lower in the calculation than in the experiment at the time of ADS activation and (3) the ADS was somewhat more effective in depressurizing the RCS in the calculation than in the test.

In summary, this assessment indicates that the complex system behavior and timing for the test are well predicted with RELAP5. The RELAP5 prediction of coolant loop flow stagnation and draining are in good agreement with the test data. The RELAP5 prediction of the reactor vessel downcomer cooldown behavior is in excellent agreement with the measured data. The test data exhibits cold leg thermal stratification behavior that cannot be simulated with a one-dimensional code such as RELAP5. However, the assessment indicates that the effects of this limitation on the reactor vessel downcomer liquid temperatures are minimal. The assessment of RELAP5/MOD3.2.2 Gamma using experimental data from ROSA/AP600 Test AP-CL-03 indicates that the code is capable of acceptably simulating the behavior of the key PTS parameters. For this test, RELAP5

underpredicted the measured downcomer temperature by a maximum of 72 K [130°F] and overpredicted it by a maximum of 59 K [106°F]. Over the full test period, RELAP5 overpredicted the measured downcomer temperature by an average of 2.2 K [4.0°F] and varied from the measured downcomer temperature by an average of 19 K [34°F].
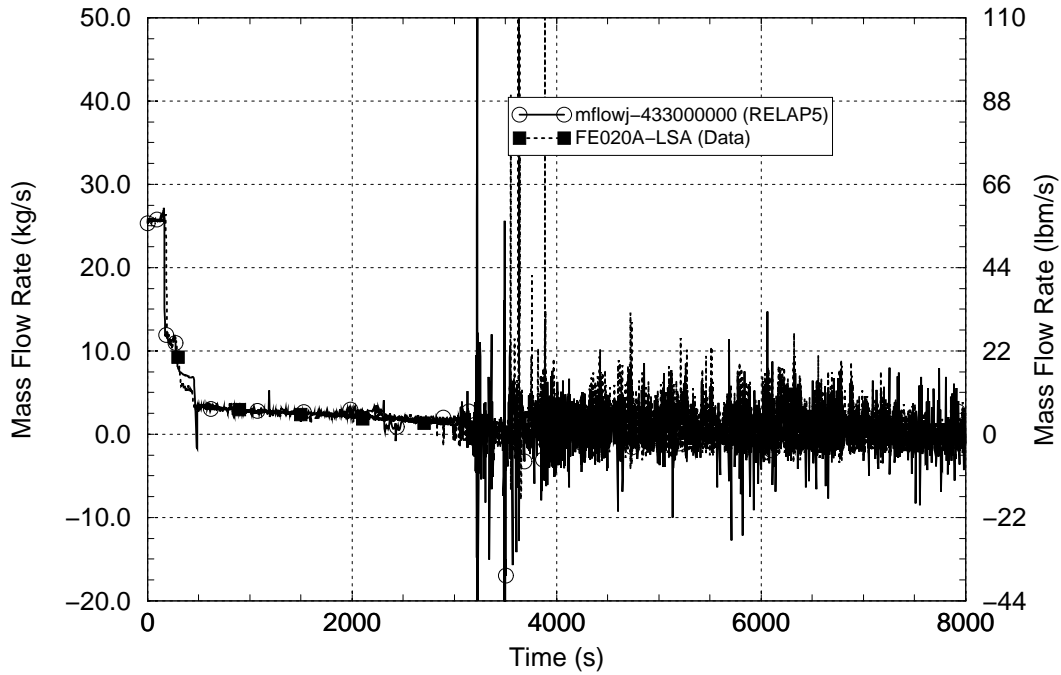
Figure 3-22   Pressurizer Loop Cold Leg Flow – ROSA/AP600 AP-CL-03
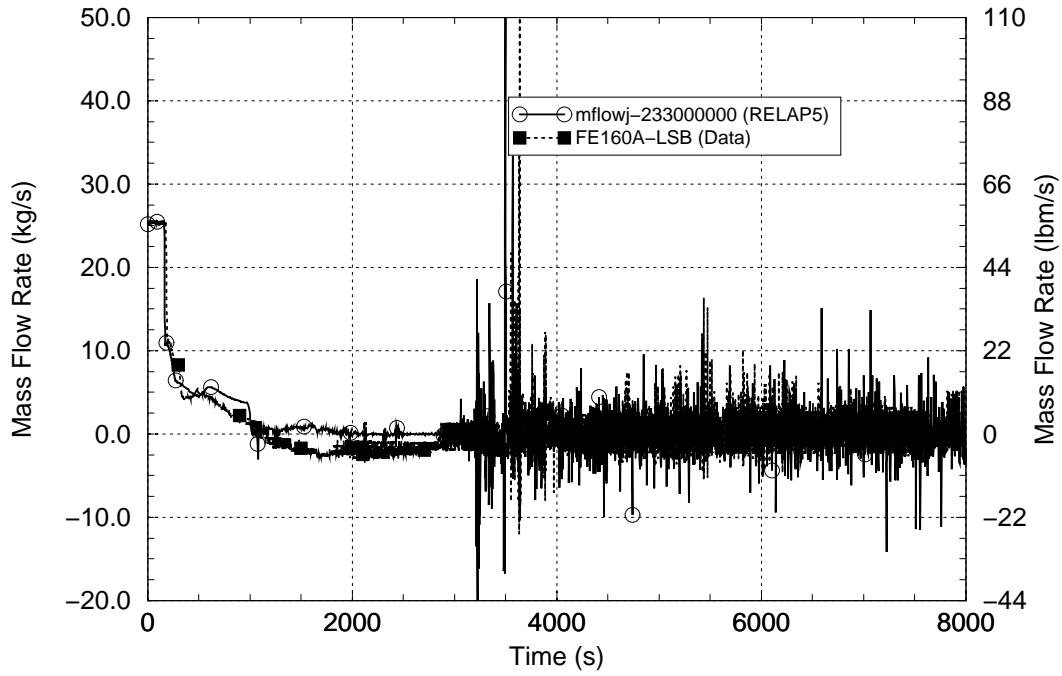
Figure 3-23   CMT Loop Cold Leg Flow – ROSA/AP600 AP-CL-03

Figure 3-24   Pressurizer Loop Cold Leg Temperatures – ROSA/AP600 AP-CL-03

Figure 3-25   CMT Loop Cold Leg Temperatures – ROSA/AP600 AP-CL-03

Figure 3-26   Upper Downcomer Temperature (CMT Loop Side) – ROSA/AP600 AP-CL-03

Figure 3-27   Lower Downcomer Temperature (CMT Loop Side) – ROSA/AP600 AP-CL-03

Figure 3-28   Upper Downcomer Temperature (Pressurizer Loop Side) – ROSA/AP600 AP-CL-03

**Figure 3-29   Lower Downcomer Temperature (Pressurizer Loop Side) – ROSA/AP600
AP-CL-03**
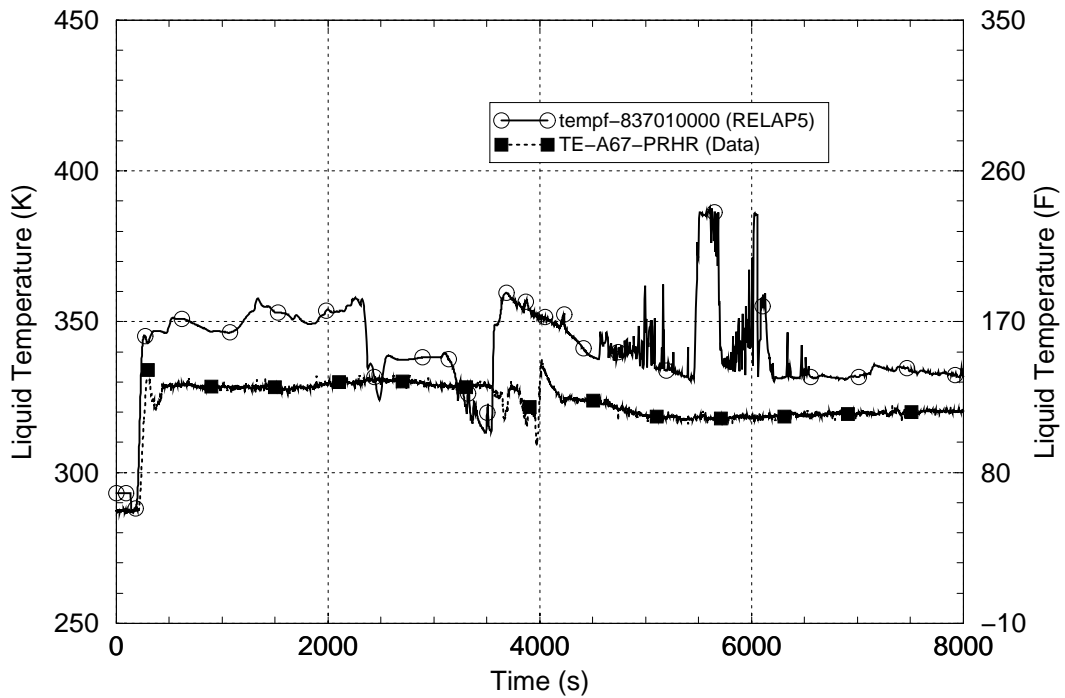
Figure 3-30   PRHR Discharge Temperature – ROSA/AP600 AP-CL-03
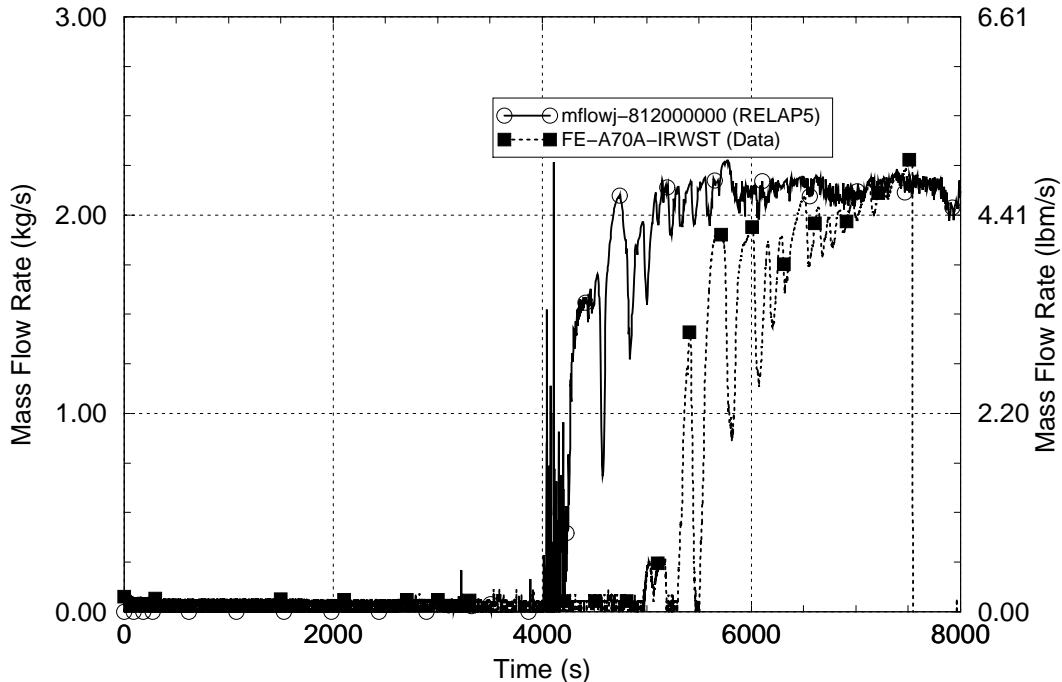
Figure 3-31   Total IRWST Injection Flow – ROSA/AP600 AP-CL-03

3.4   ROSA/AP600 Test AP-CL-09

The ROSA/AP600 experimental facility was previously described in Section 3.3; Figure 3-18 shows the facility layout.

Test AP-CL-09 (Reference 3-6) represents a 0.1%, 2.54 cm [1 in] diameter scaled break on the bottom of the cold leg in the core makeup tank (CMT) loop with the reactor operating at full power. This test is similar to Test AP-CL-03, described in Section 3.3, except additional failures of several passive safety systems are assumed. The additional failures represented in this test are: both CMT discharge valves fail closed, one-half of the valves in each ADS stage fail closed, ADS (normally activated on low CMT level) is activated 30 minutes after the low-low pressurizer pressure signal occurs, the check valves in the accumulator and IRWST discharge lines on the CMT loop fail closed and only one-half of the PRHR heat exchanger tubes are used.

A simulation of ROSA/AP600 Test AP-CL-09 was performed using the RELAP5/MOD3.2.2Gamma code.   The nodalization diagram for the RELAP5 ROSA/AP600 facility model is shown in Figure 3-19.   Table 3-7 lists the initial conditions for the test; the comparison shows good agreement between the measured and RELAP5-calculated data. A tabulated comparison of the measured and calculated sequences of events is presented in Table 3-8. The comparison shows excellent agreement in the measured and calculated event timing for this complex accident sequence.

The calculated and measured pressurizer pressures are shown in Figure 3-32. The comparison indicates excellent agreement between the calculation and the test data.

The calculated and measured pressurizer-loop and CMT-loop pump-discharge cold leg fluid temperatures are shown in Figures 3-33 and 3-34, respectively. As with Test AP-CL-03, the data

for Test AP-CL-09 exhibit considerable thermal stratification within the liquid-filled cold legs; the RELAP5 model cannot simulate this effect. This difference was found to cause the different coolant loop flow stagnation behavior between the experiment and calculation that is listed in Table 3-4. In the experiment, the CMT loop stagnated first and the pressurizer loop stagnated second. The opposite loop stagnation behavior is seen in the calculation. Although the order in which the loops stagnated was different, the timings of the first and second loop stagnations in the test and calculation are very similar. If used as an alternate indication of stagnation, the times when the RCS pressure falls below the SG pressures in Table 3-8 suggest that the order in which the loops stagnate is the same in the test and calculation.

Figures 3-35 through 3-38 compare the fluid temperature responses in the upper and lower reactor vessel downcomer regions on the CMT-loop and pressurizer-loop sides of the downcomer. Despite the lack of a RELAP5 modeling capability for simulating thermal stratification in the cold legs and the resulting effect on the order in which the loops stagnated, the comparisons in these figures demonstrate that RELAP5 can predict well the reactor vessel downcomer fluid temperature cooldown rates observed in the experiment. RELAP5 moderately overpredicted the cooldown rate during the pre-ADS portion of the sequence. The cooldown rate during the ADS blowdown period was excellently predicted. During the later part of the sequence, the minor differences between the calculated and measured downcomer temperatures relate to the difference in the calculated and measured IRWST injection fluid temperatures shown in Figure 3-39.

In summary, this assessment indicates that the complex system behavior and timing for the test are well predicted with RELAP5. The RELAP5 timing of coolant loop flow stagnation is in good agreement with the test data, although the order in which the loops stagnated in the test and calculation was reversed. The RELAP5 prediction of the reactor vessel downcomer cooldown behavior is in excellent agreement with the measured data. The test data exhibits cold leg thermal stratification behavior that cannot be simulated with a one-dimensional code such as RELAP5. However, the assessment indicates that the effects of this limitation on the reactor vessel downcomer liquid temperatures are minimal. For this test, RELAP5 underpredicted the measured downcomer temperature by a maximum of 32 K [57°F] and overpredicted it by a maximum of 39 K [71°F]. Over the full test period, RELAP5 overpredicted the measured downcomer temperature by an average of 1.1 K [2.0°F] and varied from the measured downcomer temperature by an average of 9.0 K [16°F]. The assessment of RELAP5/MOD3.2.2 Gamma using experimental data from ROSA/AP600 Test AP-CL-09 indicates that the code is capable of acceptably simulating the behavior of the key PTS parameters.

Table 3-7   Comparison of Measured and Calculated Initial Conditions for ROSA/AP600 Test AP-CL-09

Parameter	Initial Condition	
	Measured	RELAP5
Core power	10.2 MW	10.2 MW
Pressurizer pressure	15.49 MPa [2250 psia]	15.911 MPa [2307.7 psia]
Hot leg temperature	590.0 K [602.3°F]	589.92 K [602.2°F]
Cold leg temperature	552.0 K [533.9°F]	551.99 K [533.9°F]
Reactor vessel upper head temperature	588.0 K [598.7°F]	588.44 K [599.5°F]
Pressurizer level	6.8 m [22.3 ft]	6.354 m [20.8 ft]
Total primary coolant loop flow	49.0 kg/s [107.8 lbm/s]	49.18 kg/s [108.2 lbm/s]
SG pressure	6.10 MPa [884.7 psia]	6.098 MPa [884.4 psia]
SG secondary mass (per SG)	1,690 kg [3,718 lbm]	1,688 kg [3,714 lb]

Table 3-8   Summary of Measured and Calculated Sequences of Events for ROSA-AP600 Test AP-CL-09

Event Description	Event Time (s)	
	Measured	RELAP5
Break opens	0	0
Reactor scram, steam line valve closes, reactor coolant pumps tripped, PRHR activated, CVCS pump injection begins	183	173
S signal	203	173
Loss of natural circulation in the CMT loop	500	1,972
Primary pressure falls below CMT loop SG pressure	770	1,228
Loss of natural circulation in the pressurizer loop	1,650	740
Primary pressure falls below pressurizer loop SG pressure	1,984	1,967
ADS-1 valve opened	1,985	1,950
Accumulator injection begins	2,190	2,056
ADS-4 valves opened	3,486	3,150
IRWST injection begins	3,990	4,000
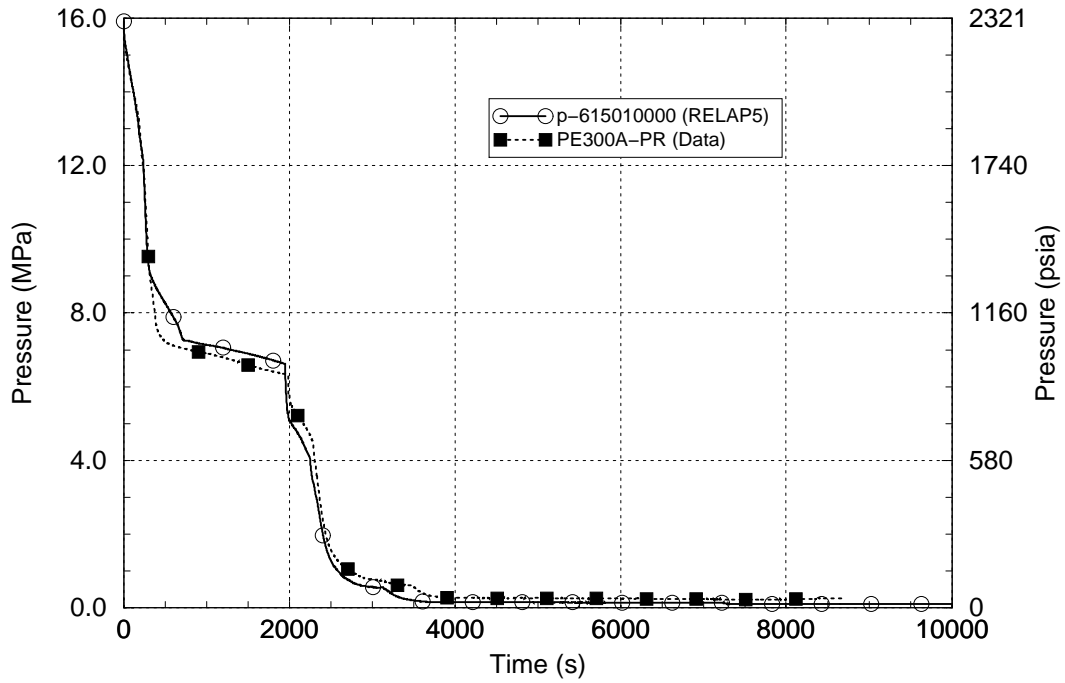
Figure 3-32   Pressurizer Pressure – ROSA/AP600 AP-CL-09
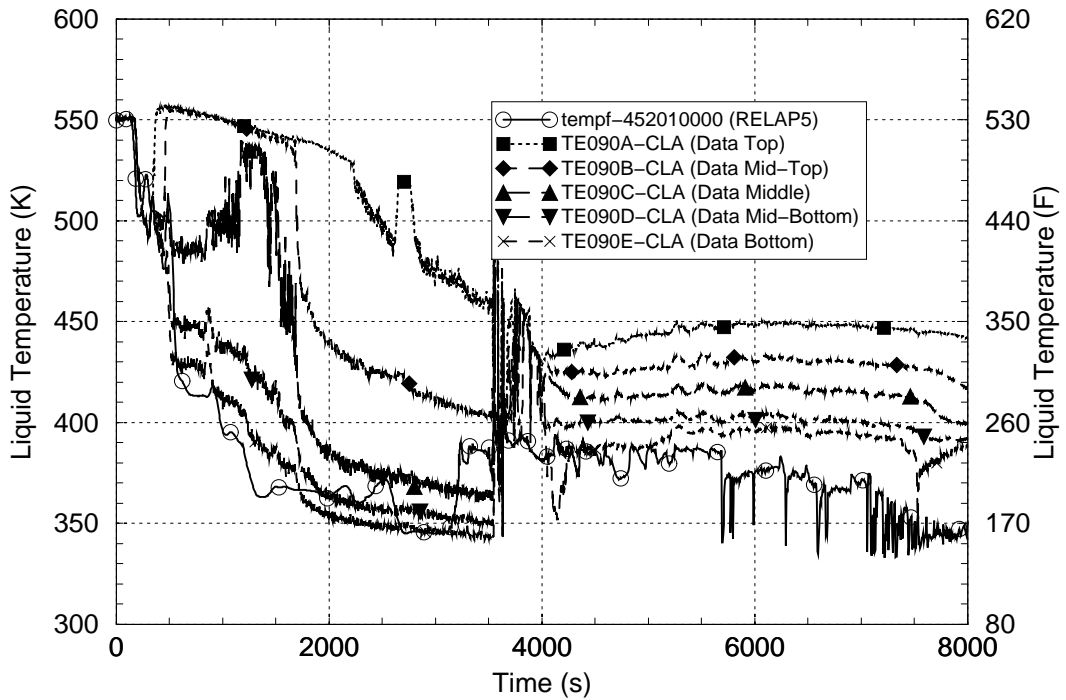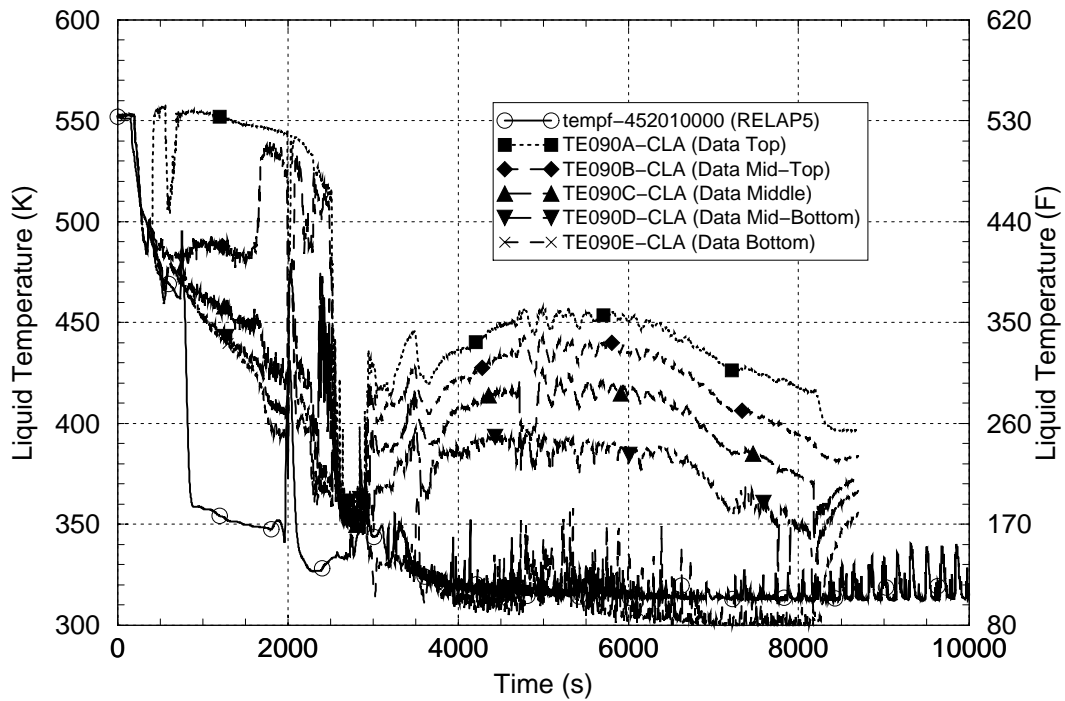

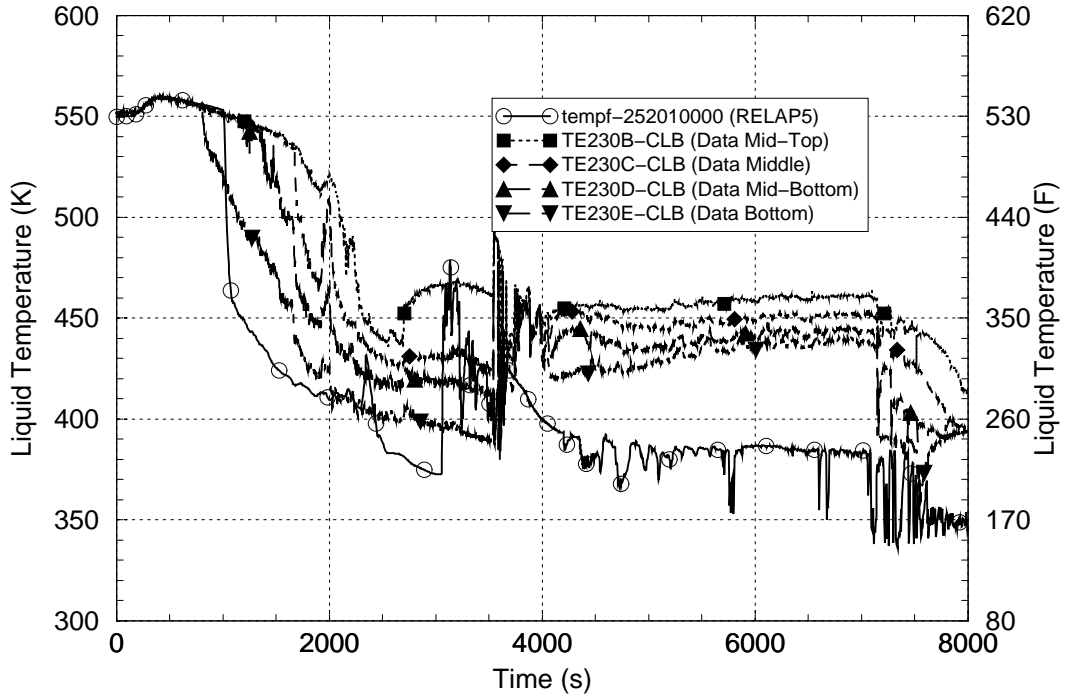**Figure 3-33   Pressurizer Loop Cold Leg Fluid Temperatures – ROSA/AP600 AP-CL-09**
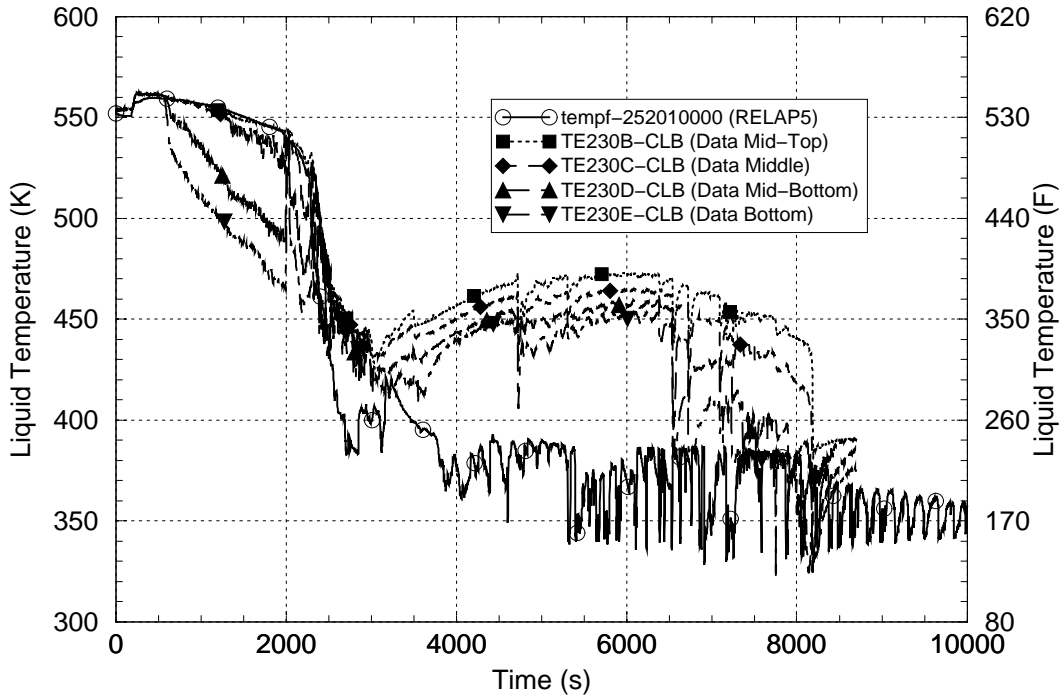
Figure 3-34   CMT Loop Cold Leg Fluid Temperatures – ROSA/AP600 AP-CL-09
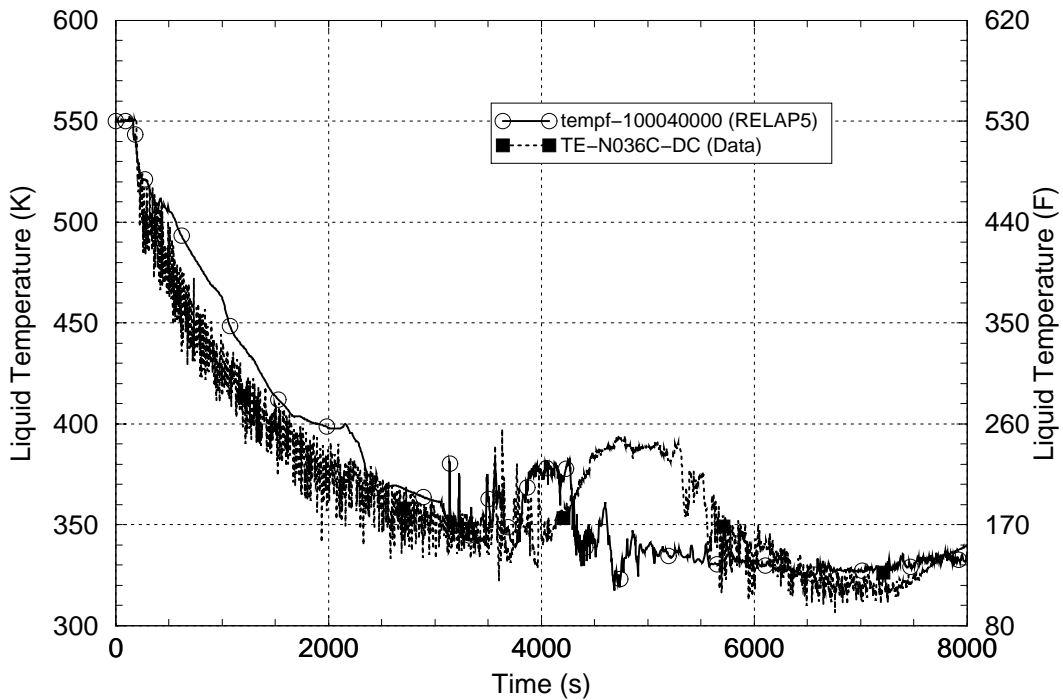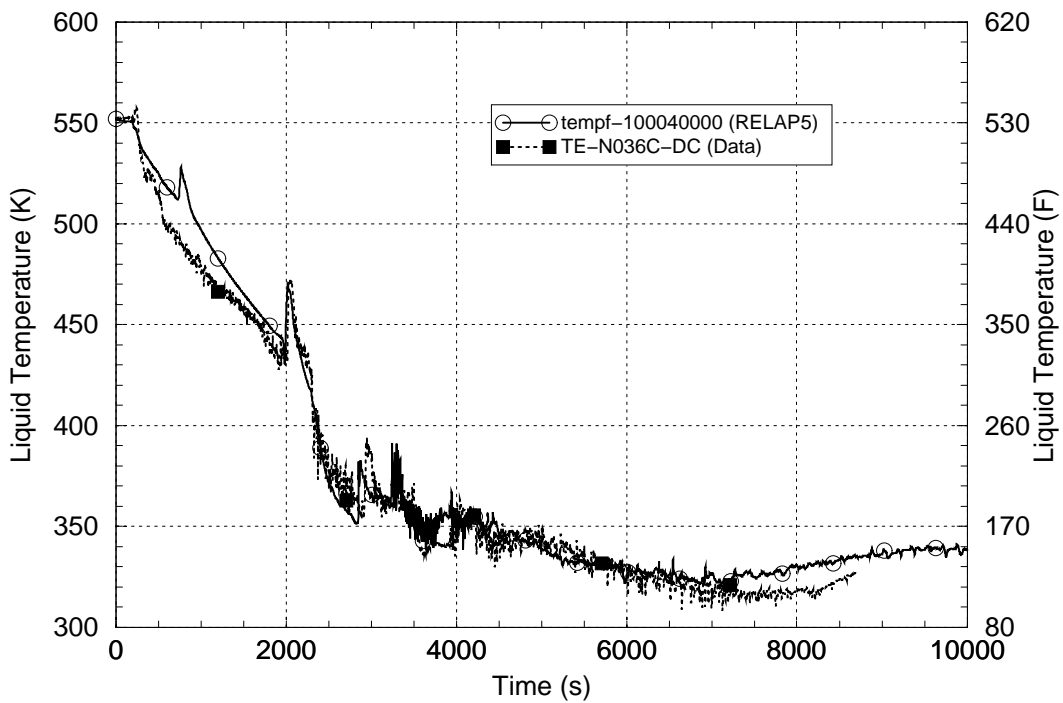

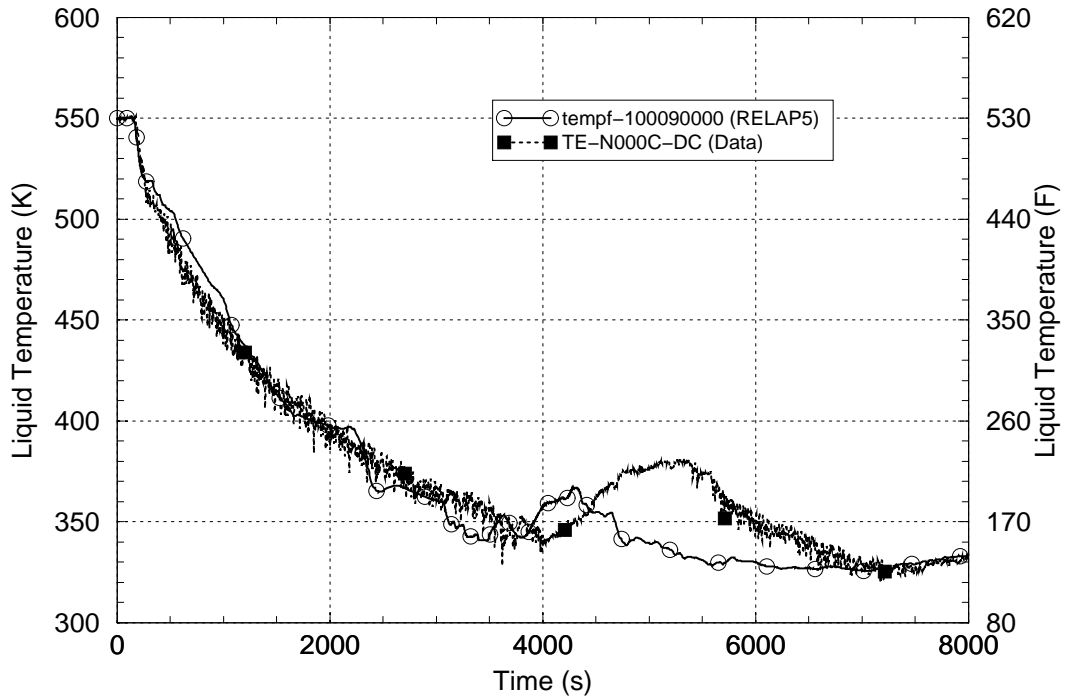**Figure 3-35   Upper Downcomer Temperature (CMT Loop Side) – ROSA/AP600 AP-CL-09**
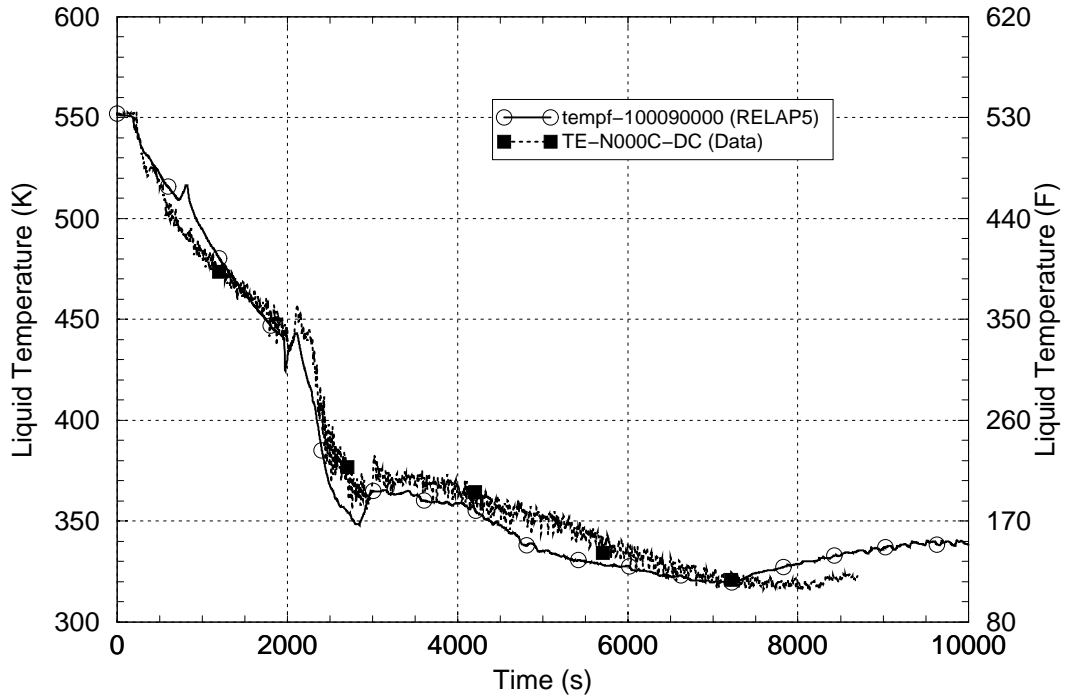
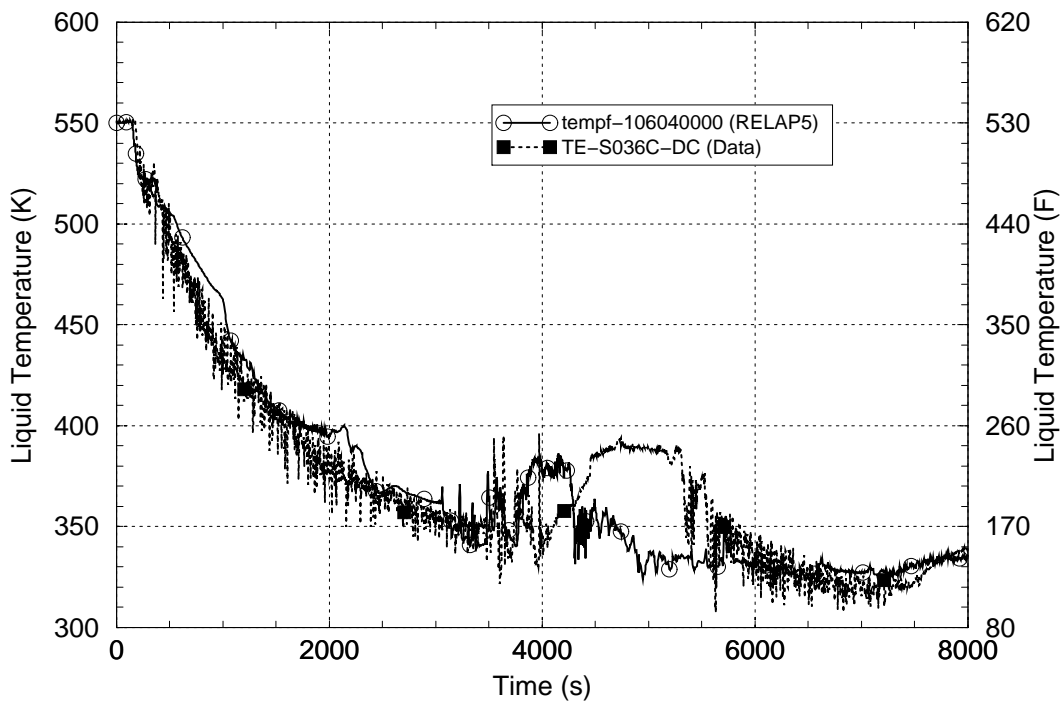**Figure 3-36   Lower Downcomer Temperature (CMT Loop Side) – ROSA/AP600 AP-CL-09**
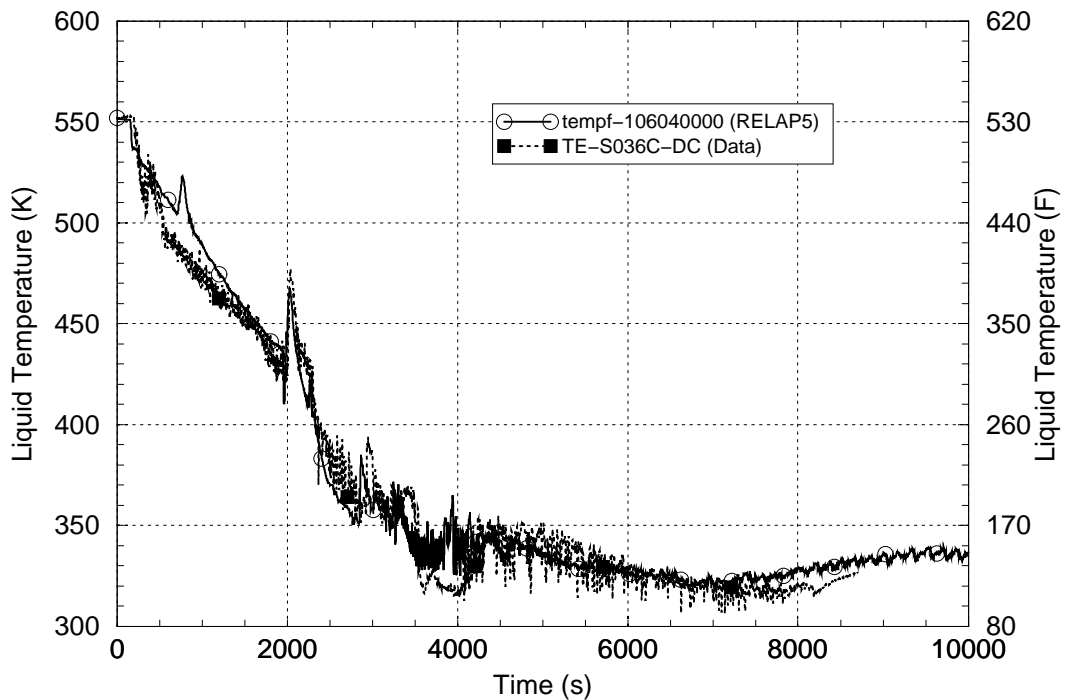
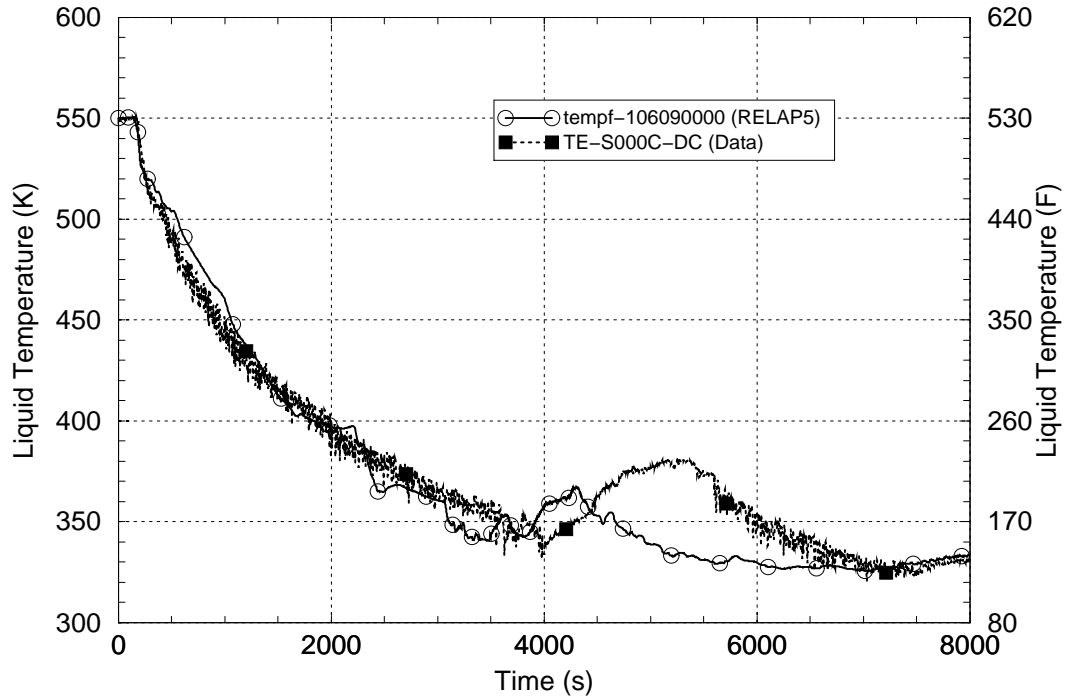**Figure 3-37   Upper Downcomer Temperature (Pressurizer Loop Side) – ROSA/AP600 AP-CL-09**
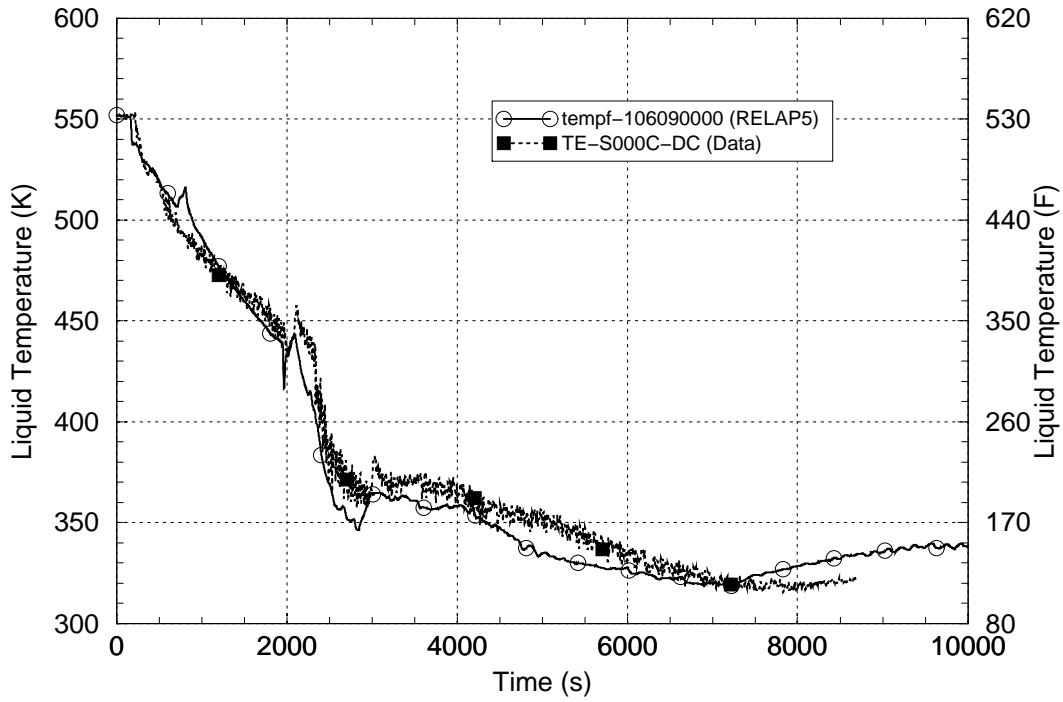
**Figure 3-38   Lower Downcomer Temperature (Pressurizer Loop Side) – ROSA/AP600 AP-CL-09**
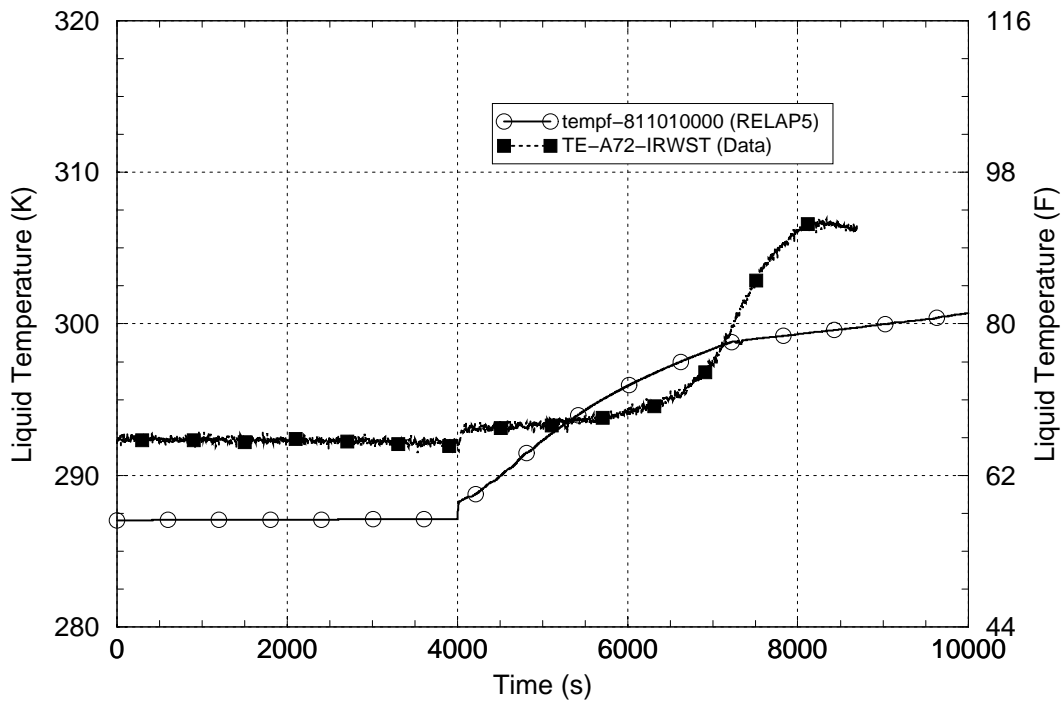
**Figure 3-39   IRWST Injection Temperature – ROSA/AP600 AP-CL-09**

3.5   APEX Test APEX-CE-13

A series of experiments was conducted in the APEX facility operated by Oregon State University. The APEX facility is a ¼-height scale low-pressure integral systems facility configured to model the thermal-hydraulic phenomena in plants of Combustion Engineering (CE) design. A schematic of the experimental facility is shown in Figure 3-40. The purpose of these tests was to investigate mixing of fluid injected from the HPI system within the cold leg and the downcomer regions. Of particular importance is ensuring that strong plumes of cold water entering the downcomer through the cold legs do not persist into the downcomer region adjacent to the core in order to support the adequacy of the one-dimensional treatment of the temperature boundary condition in the probabilistic fracture mechanics code FAVOR. A second goal is to elucidate the onset of loop-flow stagnation, which is generally necessary to achieve low temperatures in the reactor vessel downcomer region (because the loss of forced coolant loop flow results in pooling of cold HPI water locally in cold leg and downcomer regions).

Test APEX-CE-13 (Reference 3-7) simulates a stuck-open pressurizer safety relief valve event that occurs with the reactor in full power operation; the stuck-open valve is assumed to subsequently re-close. This transient is typical of one class of PTS-significant events and can be an important risk contributor due to the RCS repressurization that results from valve re-closure and the continued injection of HPI fluid during the period after the plant has cooled down. The test was initiated from full-power steady-state conditions. The ADS-2 valve was opened at the start of the transient to simulate the stuck-open pressurizer safety relief valve. Shortly thereafter, power to the reactor coolant pumps was tripped, the HPI system was activated and the reactor core power was shifted to the decay-heat mode. The ADS-2 valve was kept open for an hour and then was closed. The test was terminated about 20 minutes later, after the reactor coolant system had refilled.

Test APEX-CE-13 was initiated from a RCS pressure of 2.65 MPa [385 psia] and a core power of 610 kW. The initial cold leg temperature was 480 K [403°F]. The initial steam generator pressures were 1.71 MPa (249 psia) and the initial secondary system liquid levels were 38.6 cm [15.2 in]. The initial pressurizer level was 53.8 cm [21.2 in].

A simulation of Test APEX-CE-13 was performed using the RELAP5/MOD3.2.2Gamma code. Nodalization diagrams for the APEX RELAP5 model are shown in Figures 3-41 and 3-42. The model included an eight-sector two-dimensional nodalization scheme in the reactor vessel downcomer.   Table 3-9 lists the initial conditions for the test; the comparison shows good agreement between the measured and RELAP5-calculated data. A summary of the measured and calculated sequences of events is presented in Table 3-10. Note that all events listed in the table are manual actions experienced during the test, which is why the calculated and measured event times in the table agree exactly.

The calculated and measured pressurizer pressure responses are compared in Figure 3-43. The initial pressure decline in the calculation is seen to be about 0.15 MPa [22 psi] less than that in the test. Figures 3-44 and 3-45, respectively, compare the RCS fluid temperature responses in the cold leg and reactor vessel downcomer regions. The fluid temperature comparisons show excellent agreement between the calculated and measured data in the cold leg, but in the downcomer (at an elevation corresponding to the middle of the core) the initial drop in the measured temperature is seen to be about 10 K [18°F] greater than the drop in the calculated temperature. Little azimuth

temperature variation is seen, both in the test and in the calculation, around the periphery of the downcomer. Data are shown for two azimuth locations, one in the sector containing the DV1-2 nozzle and the other in the sector containing the Cold Leg 3 nozzle. These differences in the pressure and downcomer temperature comparisons over the first 1,300 s of the test period are consistent in that the higher pressure in the calculation led to less HPI flow and thereby warmer downcomer temperatures.
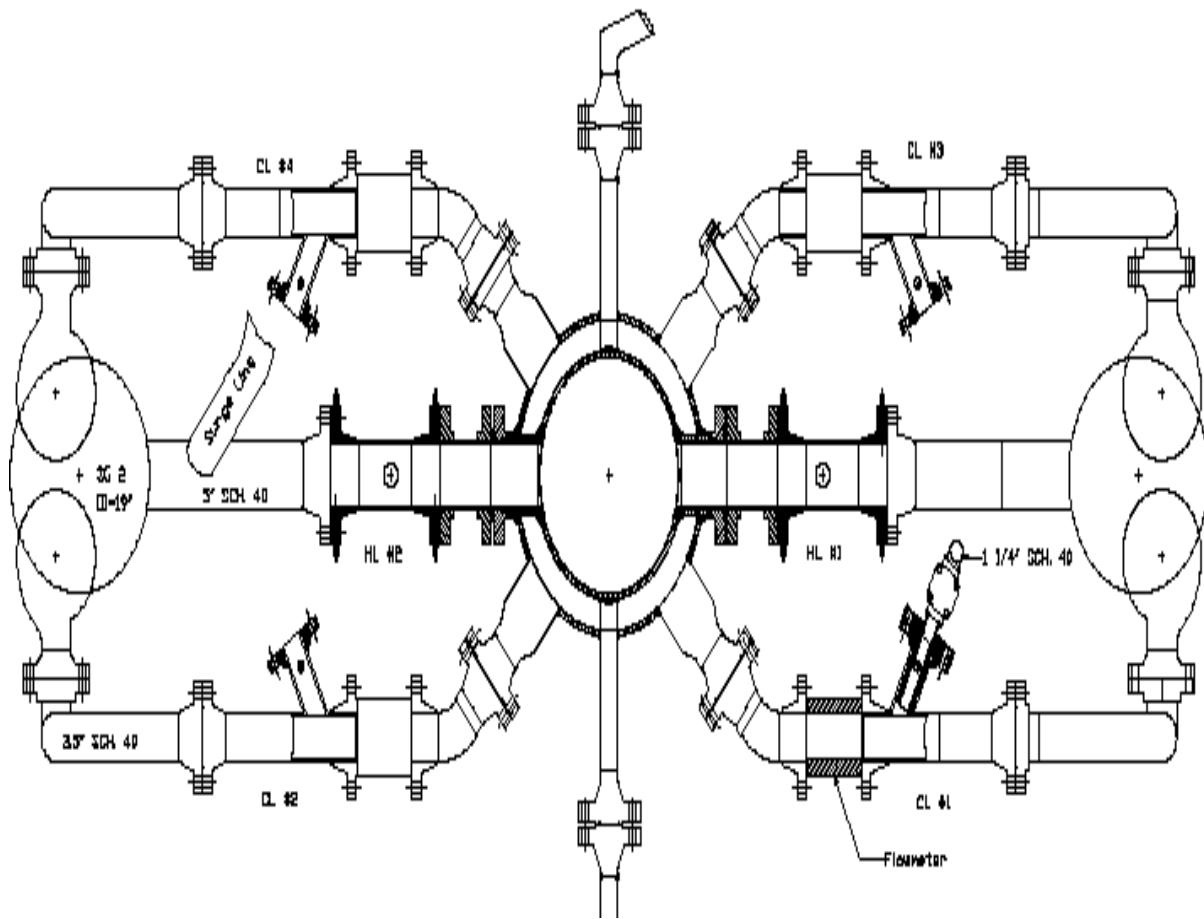
Figure 3-40   Schematic of APEX-CE Experimental Facility
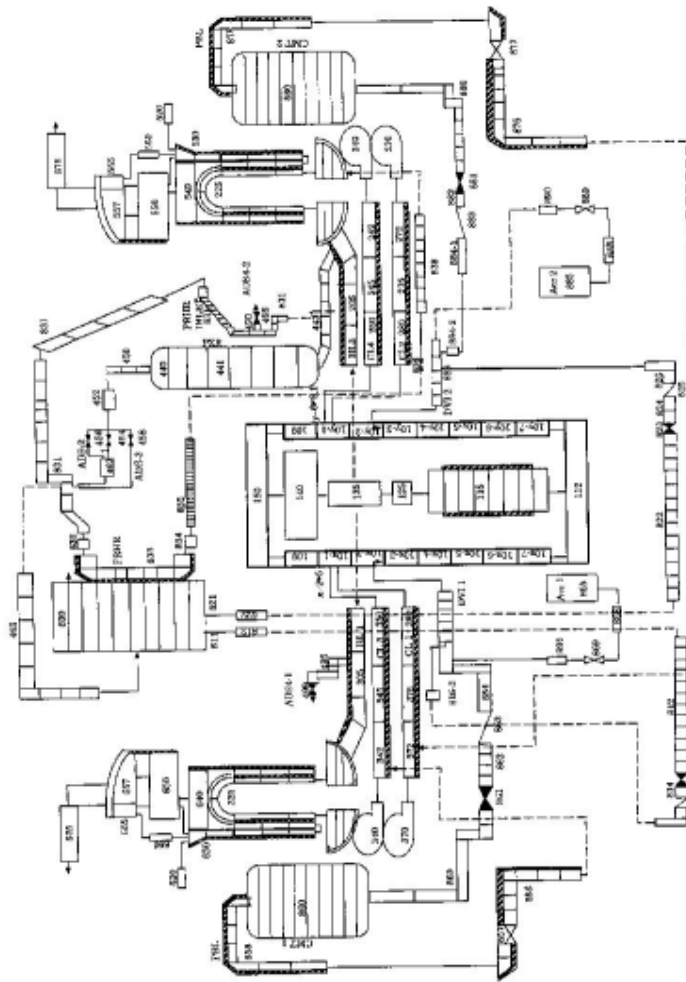
Figure 3-41   Nodalization of the RELAP5 APEX Facility Model
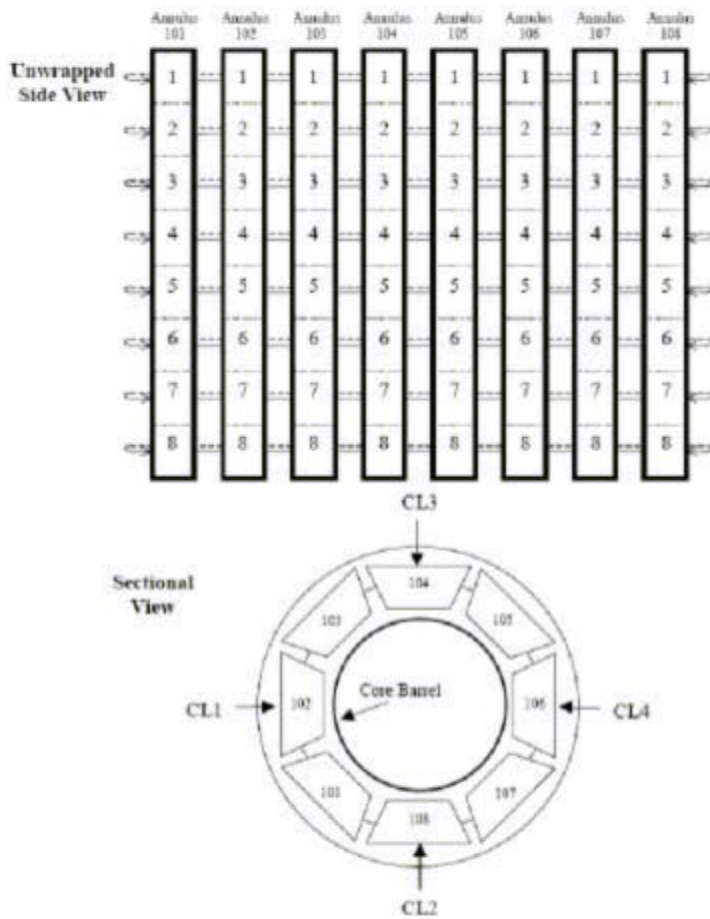
Figure 3-42   Nodalization of the RELAP5 APEX Reactor Vessel Region Model

Table 3-9   Comparison of Measured and Calculated Initial Conditions for APEX-CE-13 Test

Parameter	Initial Condition	
	Measured	RELAP5
RCS Pressure	2.65 MPa [384.4 psia]	2.65 MPa [384.4 psia]
Core Power	610 kW	610 kW
Cold Leg Temperature	480 K [404°F]	480 K [404°F]
SG 1 Pressure	1.71 MPa [248.0 psia]	1.70 MPa [248.6 psia]
SG 2 Pressure	1.71 MPa [248.0 psia]	1.70 MPa [246.6 psia]
SG 1 Level	38.6 cm [15.2 in]	32.8 cm [12.9 in]
SG 2 Level	38.6 cm [15.2 in]	32.8 cm [12.9 in]
Pressurizer Level	53.8 cm [21.2 in]	50.5 cm [19.9 cm]

Table 3-10   Summary of Measured and Calculated Sequences of Events for APEX-CE-13 Test

Event Description	Event Time (s)	
	Measured	RELAP5[a]
Pressurizer SRV opened	0	0
Scram signal (core power decay)	0	0
HPI flow starts	0	0
RCP #1 and #4 tripped	4.2	4.2
RCP #2 and #3 tripped	20.8	20.8
Turbine stop valves closed	18.0	18.0
Pressurizer SRV closed	3,589	3,589
End of test and calculation	4,800	4,800

a – All of the calculated event times in this table represent boundary conditions on the calculation.
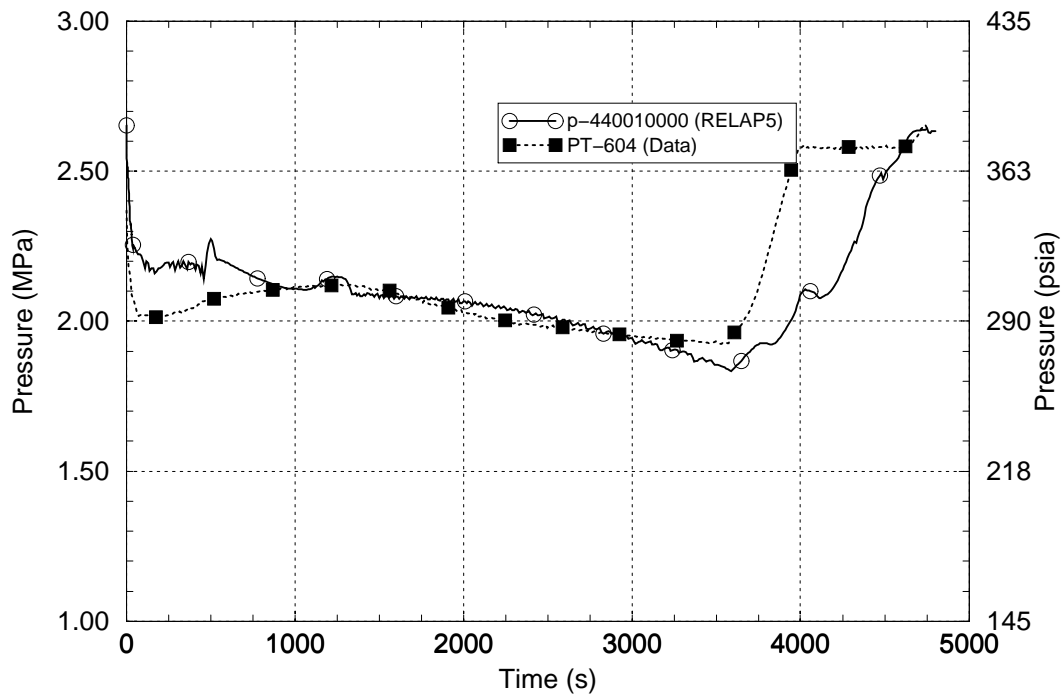
Figure 3-43 Pressurizer Pressure – APEX-CE-13
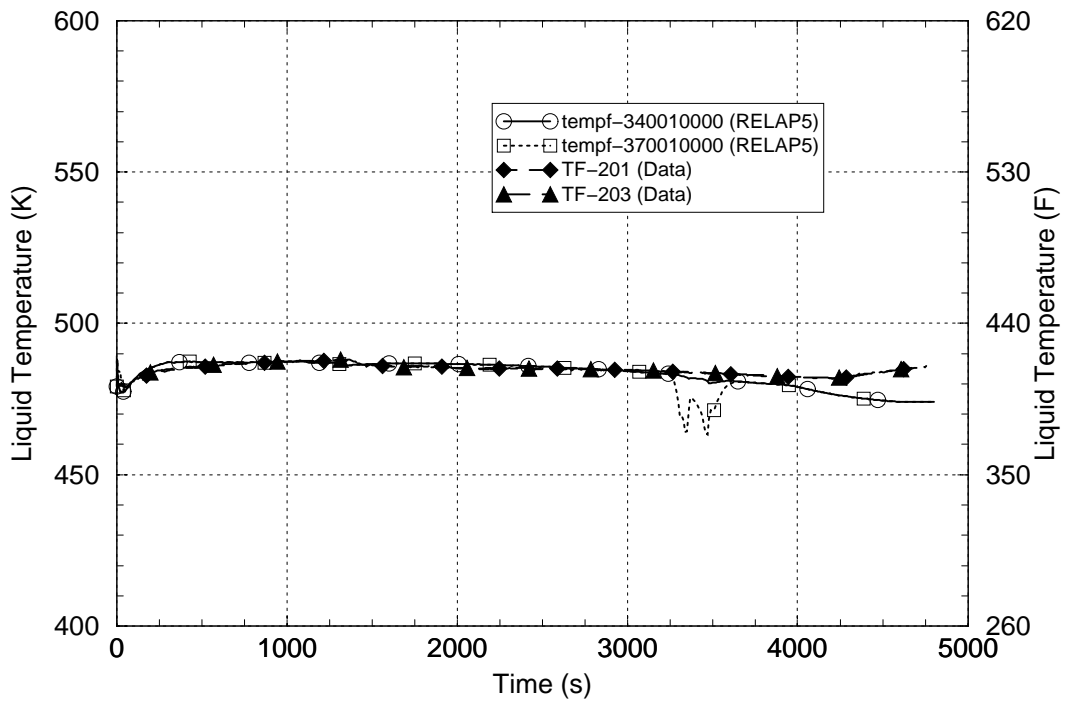
Figure 3-44 CMT Loop Cold Leg Fluid Temperatures – APEX-CE-13
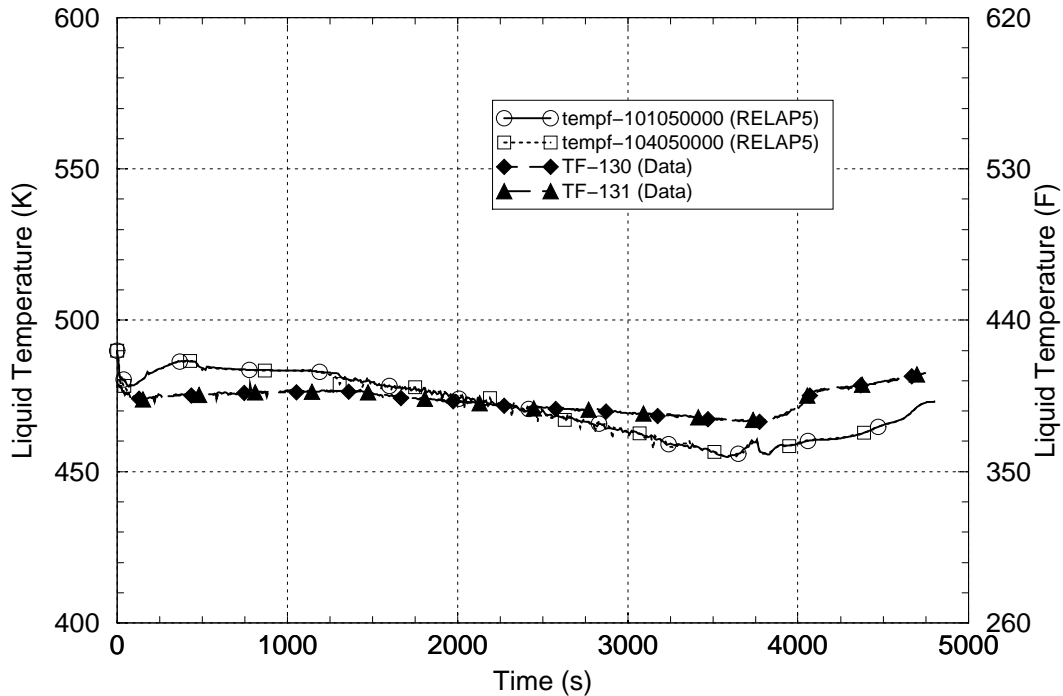
Figure 3-45   Reactor Vessel Downcomer Fluid Temperatures – APEX-CE-13

Differences between the measured and calculated data over the first part of the test (up to 1,300 s) are related to system heat loss effects. Heat losses (including a complex distribution of heat loss among the external component boundaries) are represented in the APEX-CE RELAP5 system model. However, comparison of the measured and calculated results for this test indicates that the actual facility heat loss is likely much greater than that modeled. Figure 3-46, which compares the measured and calculated SG 1 pressure responses, shows that about 1,300 s was required for the secondary pressure to reach the relief valve opening setpoint pressure in the test, but that only about 300 s was required in the calculation. Thus, both the primary and secondary system pressure response comparisons display hotter conditions in the calculation than in the test, an indication that heat losses are generally underpredicted with the model.

After 1,300 s, the calculated RCS pressure is seen to decline to, and then fall below the measured pressure and this leads to more HPI flow and cooler downcomer temperatures in the calculation than in the test. By the time the ADS-2 valve was closed, the disagreement in the downcomer temperatures had reversed, with the calculated temperature becoming about 10 K [18 °F] below the measured temperature.

The pressurizer level comparison is shown in Figure 3-47. An excellent agreement between the calculated and measured levels is seen during the period when the ADS-2 valve is open. The flow out the ADS-2 valve on the top of the pressurizer swells the mixture level upward inside the pressurizer tank, thus resulting in a mostly-full pressurizer condition in both the experiment and calculation.
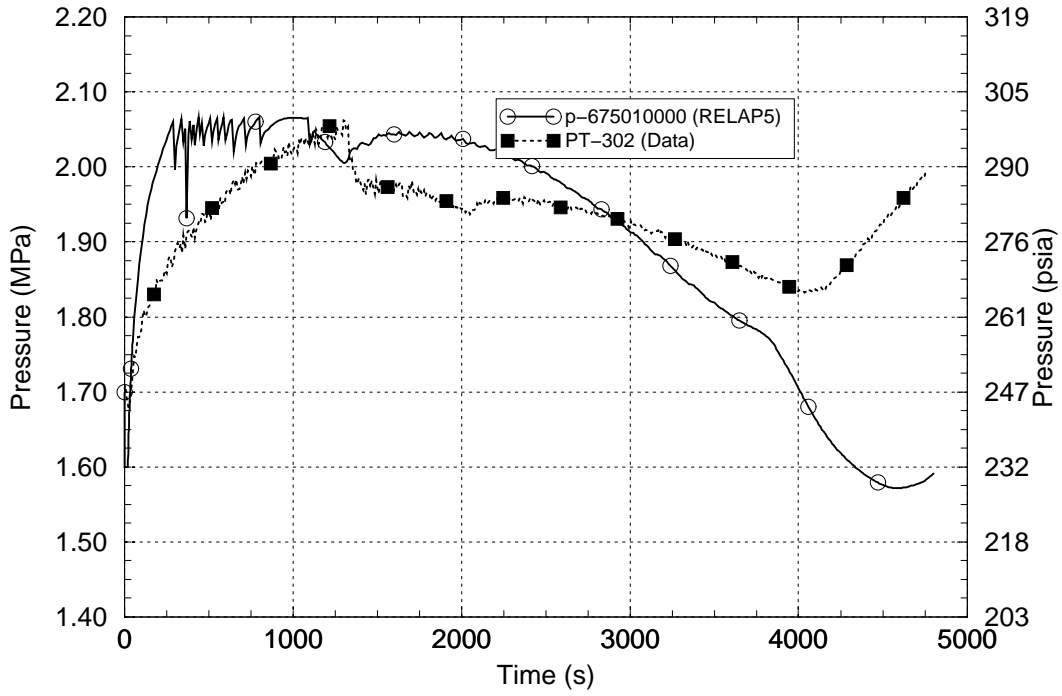
Figure 3-46   SG 1 Pressures – APEX-CE-13
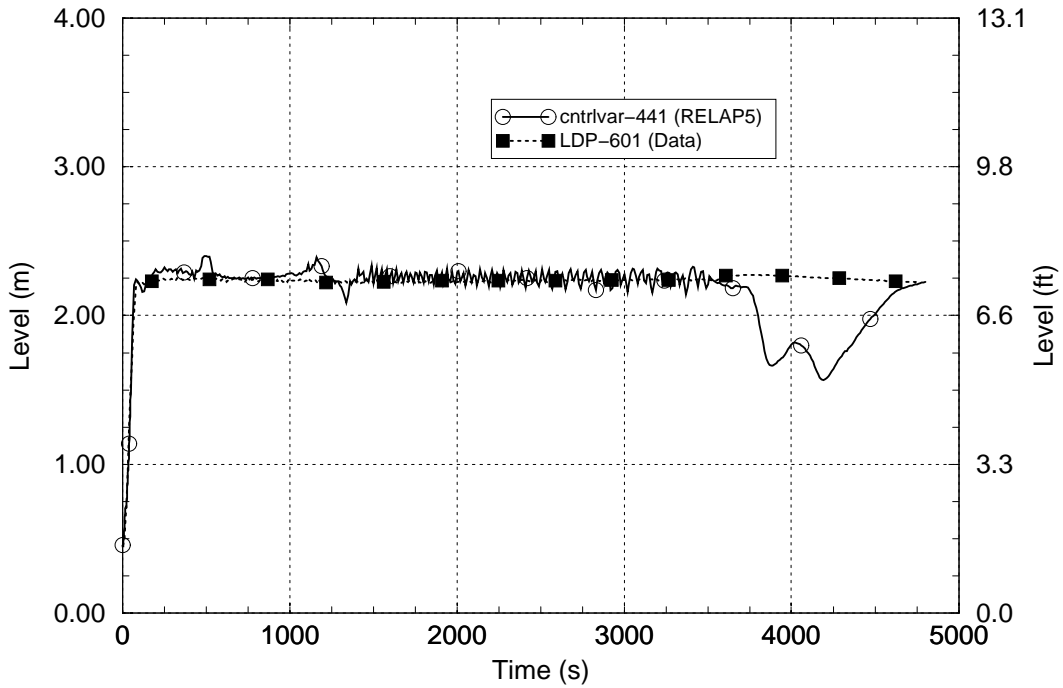
Figure 3-47   Pressurizer Level – APEX-CE-13

The ADS-2 valve vapor and liquid volumetric flow comparisons are shown in Figures 3-48 and 3-49, respectively. These figures show that RELAP5 generally overpredicted the vapor flow rate by a factor of about two and the liquid flow rate by a factor of about four. This overprediction is to some extent caused by the underprediction of system heat loss described above. The two figures also show that the average measured vapor and liquid flow rates are relatively constant during the entire time when the valve is open, but that the average calculated vapor flow rate tended to rise and the average calculated liquid flow rate tended to fall over time. This behavior suggests that in the test a steady distribution of voids existed within the pressurizer but in the calculation the distribution instead was changing, with the void at the top of the pressurizer increasing over time. The higher ADS-2 valve flow rates in the calculation eventually led to more RCS depressurization, lower RCS mass and cooler RCS temperatures in the calculation than in the experiment.

The drop in the calculated pressurizer level seen shortly after the valve closed (see Figure 3-47) represents a downward slumping of RCS inventory that could no longer be supported without the upward flow toward the valve. This slumping is not seen in the measured pressurizer level. Because of the greater ADS-2 valve flow in the calculation, at the time the valve was closed more void existed below the bottom of the pressurizer (such as in the surge line, hot leg and reactor vessel upper plenum and upper head regions) in the calculation than in the test.

Figures 3-43, 3-45 and 3-47 show that when the ADS-2 valve was closed, the calculated and measured reactor coolant system conditions were moderately different, with cooler RCS temperatures and more voiding seen in the calculation than in the experiment. This difference delayed the RCS repressurization and made the repressurization rate moderately lower in the calculation than in the experiment. The steam space present at the start of the repressurization was larger in the calculation than in the test and the cooler water in the calculation led to more condensation than in the test.

The adequate prediction of experimental facility heat loss effects with systems codes is particularly difficult. The difficulty grows for small-scale test facilities such as APEX because core powers are low and the system heat losses represent significant contributors to the overall system heat balances. The difficulty also grows for long transients such as Test APEX-CE-13 because the effects of incorrectly-simulated heat loss are integrated to produce large errors in system energy and its distribution. These principles are understood when modeling small-scale systems, but the necessary data to support the total heat loss represented and its distribution in a model are typically not available. The effects of these heat loss considerations are significantly reduced when modeling full-scale plants, where the power-to-volume and power-to-surface area ratios are much larger.

In summary, this assessment indicates that the major differences between the calculated and measured data for Test APEX-CE-13 are likely due to inadequate modeling of system heat loss effects that led to an overprediction of the ADS-2 valve liquid and vapor flow rates. At the time when the ADS-2 valve was closed, the RCS was cooler and more voided in the calculation than in the experiment. The RCS pressurization following closure of the ADS-2 valve was both delayed and slower in the calculation than in the test. These differences between calculation and test are considered moderate and the significance of the differences for the modeling of full-scale plants is considered minor. The RELAP5 prediction of the reactor vessel downcomer fluid temperature behavior is in good agreement with the measured data. For this test, RELAP5 underpredicted the measured downcomer temperature by a maximum of 17 K [31°F] and overpredicted it by a maximum of 12 K [22°F]. Over the full test period, RELAP5 underpredicted the measured

downcomer temperature by an average of 2.2 K [3.9°F] and varied from the measured downcomer temperature by an average of 7.4 K [13°F].

The assessment of RELAP5/MOD3.2.2 Gamma using experimental data from Test APEX-CE-13 indicates that the code is capable of acceptably simulating the behavior of the key PTS parameters.
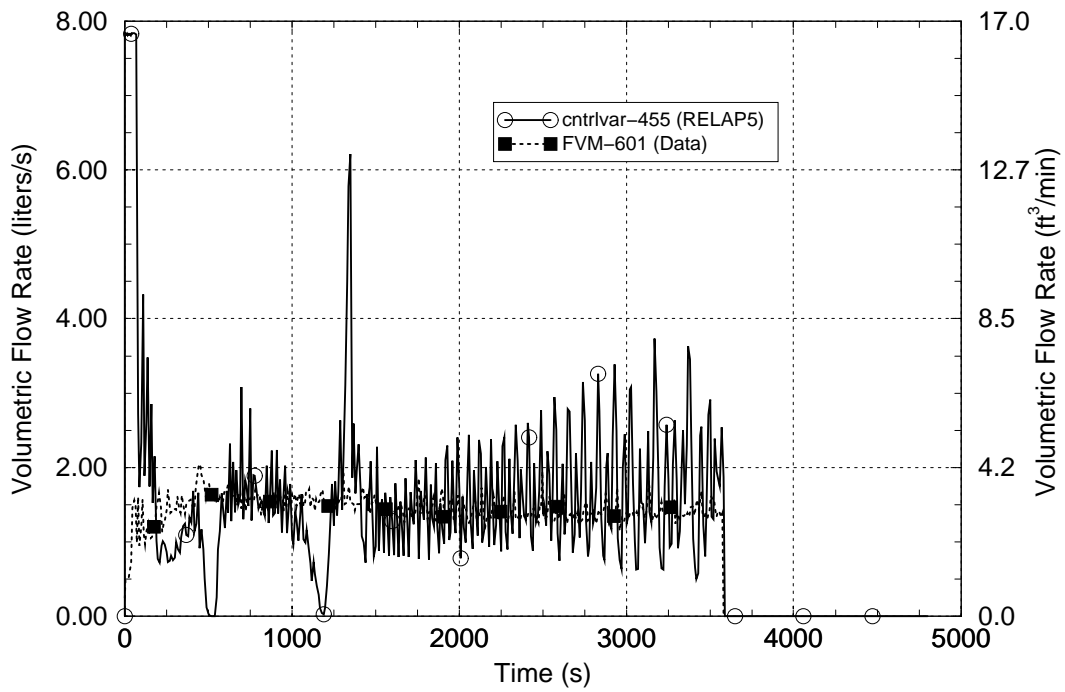
Figure 3-48   ADS-2 Valve Vapor Volumetric Flow Rate – APEX-CE-13
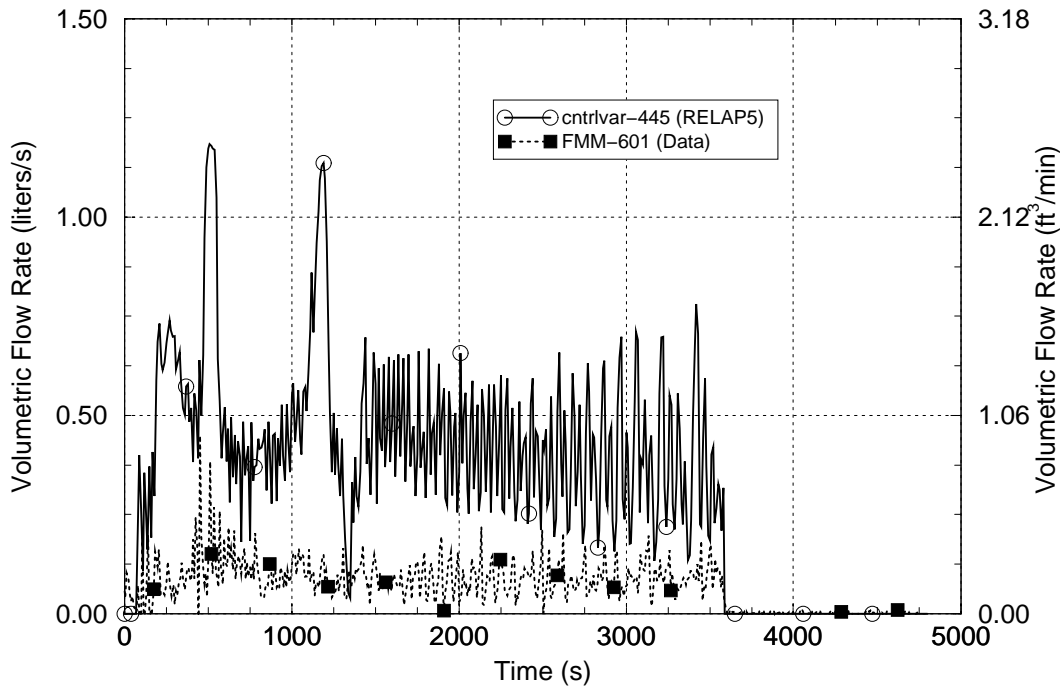
Figure 3-49   ADS-2 Valve Liquid Volumetric Flow Rate – APEX-CE-13

3.6   APEX TEST APEX-CE-05

The APEX facility is described in Section 3.5. The purpose of Test APEX-CE-05 (Reference 3-8) is to obtain baseline mixing data for stagnant coolant loop conditions in an experimental configuration representing the Combustion Engineering designed Palisades nuclear power plant. To perform the test, normal operating pressures and temperatures in the reactor coolant system are first established. The steam generators, reactor coolant pumps and reactor core heaters are then secured to establish stagnant conditions in the reactor coolant loops and high pressure safety injection flow is started into each of the four cold legs of the facility. A drain valve on the pressurizer is opened to accommodate the high pressure injection which is added to the reactor coolant system and control the pressurizer level between 50 and 55 inches. Of primary interest for this test are the thermal characteristics of the reactor coolant system as it cools down from the effects of the cold fluid injection.

For this assessment, a RELAP5 simulation of Test APEX-CE-05 is performed using the RELAP5/MOD3.2.2Gamma code. The RELAP5 model nodalization for Test APEX-CE-05 is the same as that used for Test APEX-CE-13 and shown in Figures 3-41 and 3-42. The model includes an eight-sector two-dimensional nodalization scheme in the reactor vessel downcomer region.

A 1,200 s RELAP5 steady state calculation was run to establish initial conditions for the transient test calculation.   Table 3-11 compares the measured initial conditions for the test with the RELAP5-calculated conditions at the end of the steady-state calculation. Since the reactor coolant system is stagnant at the beginning of the test, the RELAP5-calculated initial conditions are very close to those input at the beginning of the steady state run and the comparison between the measured and calculated initial conditions is excellent.

A RELAP5 calculation for the 4,229 s period of the APEX-CE-05 experiment was run starting from the conditions present at the end of the RELAP5 steady state calculation. A comparison of the measured and calculated sequences of events is presented in Table 3-12. Except for the first opening of the pressurizer drain valve, all events in the table represent boundary conditions on the calculation.

Results of the RELAP5 calculation and comparisons with the measured data for the test are shown in Figures 3-50 through 3-59.

The calculated and measured high pressure injection flow rates into Cold Leg 1 are compared in Figure 3-50. The injection is begun at 186 s in both the test and calculation. The measured high pressure injection flow rate data are used as boundary conditions on the calculation. The Cold Leg 1 injection flow rates shown in the figure are typical of the Cold Leg 2 and 3 injection flow rates as well. The Cold Leg 4 injection flow rates are slightly higher (by up to 6%) than the flow rates in the other three loops. In the model, the injection rates for each of the cold legs is modeled individually, matching the injection flow behavior for each loop in the experiment.

The calculated and measured high pressure injection fluid temperatures are compared in Figure 3-51. As with the injection flow rates, the measured injection fluid temperature is used as a boundary condition on the calculation. The trend of the data in the figure over the first 300 s reflects the initiation of the injection flow at 186 s and the sweep-out of fluid initially in the injection lines, which is at a slightly warmer temperature than the fluid in the tank from which the injection water is drawn.

Figure 3-52 compares the measured and calculated pressures in the upper head of the reactor vessel. Figure 3-53 compares the measured and calculated secondary pressures in Steam Generator 1; the comparison for Steam Generator 2 is similar. The offset between the measured and calculated initial steam generator pressures results from an unresolved inconsistency in the test data report between the tabulated and plotted pressure data. The primary and secondary system pressure comparisons indicate somewhat more steam generator heat removal in the calculation (after 1,000 s, when the coolant loops have again stagnated) leading to less need for reactor coolant system pressure relief in the calculation than in the test. Both the test and calculation indicate an opening and closing of the pressurizer drain valve, maintaining the pressurizer level within the narrow control band. Reference 3-8 discusses the operation of a pressurizer vent valve (in addition to the pressurizer drain valve). However, details regarding the size and operation of this vent valve are not known and, unlike the drain valve, it was not included in the RELAP5 model. For the purposes of this assessment the comparisons of the calculated and measured reactor coolant system pressures is considered acceptable. The simulation of the reactor vessel downcomer fluid temperature (the parameter of most significance) is not affected by the primary and secondary coolant system pressure differences seen in these figures.

Over the test period, relatively small variations are noted in the measured fluid temperature responses in both the axial and azimuth directions within the reactor vessel downcomer. Figure 3-54 overlays the measured fluid temperatures in the downcomer directly beneath the four cold leg nozzles at three different elevations. The thermocouples for the data channels with suffix "1.3D-2" are located 1.3 cold leg diameters below the cold leg centerlines (in other words, at a distance 80% of the 3.5 in cold leg diameter below the bottom of the cold leg pipe penetration on the reactor vessel). Data channels with suffix "8D-2" are located eight cold leg diameters below the cold leg centerline, at an elevation approximating the core top elevation. The data channels without a suffix are located at an elevation corresponding to the bottom of the core. The largest variations

among these data channels (with a maximum of 43 K [78°F]) are in the axial direction. These variations are related to the time required for fluid to flow through the full length of the downcomer, with the top of the downcomer first seeing the effect of the cold water injection and with the downward spreading of the cold water in cycles with a period of about 10 s. Around the periphery of the downcomer (including regions both under and between the cold leg nozzle orientations) the test data exhibit maximum variations of 9 K [16°F] at the downcomer elevation corresponding to the core top and 5 K [9°F] at the elevation corresponding to the core bottom. Overall, these are small temperature differences and the measured temperature data shown in Figure 3-54 are considered tightly clustered.

Figure 3-55 shows the RELAP5-calculated downcomer fluid temperatures at the locations corresponding to the thermocouples for the measured data in Figure 3-54. As with the measured data, small fluid temperature variations are noted in the axial and azimuth directions within the downcomer. The RELAP5-calculated downcomer temperatures are more tightly clustered than the measured temperatures, with variations indicated up to 7 K [13°F] in the axial direction and 3 K [6°F] in the azimuth direction.

A comparison of the calculated and measured fluid temperatures at a representative location in the downcomer is shown in Figure 3-56. Data are shown for a location under Cold Leg 1 at an elevation corresponding to the top of the core. The comparison shows very good agreement between the calculated and measured temperatures until about 2,000 s. Afterward, RELAP5 underpredicted the measured temperature by up to 16 K [29°F]. Over the full length of the test period, RELAP5 underpredicted the downcomer fluid temperature by an average of 5 K [9°F].

A number of modeling changes were applied in an attempt to improve the comparison of the calculated and measured temperatures. Reasonable variations in the modeled system heat losses were found to provide no significant benefit in this respect.

Figure 3-57 shows the calculated flow rates between the injection nozzles and reactor vessel in the four cold legs. The figure indicates some minor back flow in the cold legs prior to the start of the high pressure injection flow at 186 s, followed by a forward flow surge when the injection is initiated. This flow surge dissipates by about 800 s, when the flow rates have declined to near the 0.088 L/s [1.4 gpm] injection rate in each cold leg. The figure also shows circulations between the two cold legs on the same coolant loop that periodically appear and decay. Cold Legs 1 and 3 are situated on one coolant loop and Cold Legs 2 and 4 are situated on the other coolant loop. It is also noted that the directions of these periodic flows alternate, with one cold leg flowing in the reverse direction during one cycle and then the other cold leg flowing in the reverse direction during the subsequent cycle. Multiple cycles involving Cold Legs 1 and 3 are indicated in the figure. In addition to the circulation behavior shown in these figures, a minor circulation upward through the core and downward through the bypass at the top of the reactor vessel into the downcomer is calculated. This bypass circulation flow peaks at about 0.13 l/s [2 gpm] at 700 s and then decays away by 3,200 s. These cold leg and reactor vessel bypass circulations are driven by buoyancy differences created by cold and warm water residing over the same elevation spans in parallel vertical paths within the flow loops.

Figure 3-58 shows the measured cold leg flow responses in three of the cold legs during the test; no reliable flow data for the fourth cold leg is available. The test data show a period of reverse flow in Cold Legs 2 and 4 that is comparable in timing and magnitude to the RELAP5-calculated reverse flows during this period in the four cold legs. The test data also show a flow surge in Cold Leg 1 that is very similar in timing and magnitude to the flow surges seen in Figure 3-57 for all cold legs

in the RELAP5 calculation. Although the test data do not show the large-magnitude periodic circulations between the cold legs on the same coolant loop that are seen in the calculation, more minor periodic oscillations are seen in the experiment up to about 2,200 s.

Both the calculation (Figure 3-57) and experiment (Figure 3-58) indicate an involvement in the mixing process of reactor coolant system fluid not directly situated in the flow path between the cold water injection sites and the pressurizer drain valve. The importance of involving this fluid in the mixing process is demonstrated using a RELAP5 sensitivity calculation which was performed as follows. The base RELAP5 calculation described above was repeated, except that large artificial losses to flow in the reverse direction were added in the pump-suction region piping of each cold leg. This modeling change prevents the circulation of fluid (seen in Figure 3-57) between the two cold legs situated on the same coolant loop (with one cold leg flowing in the forward direction and the other cold leg flowing in the reverse direction). Figure 3-59 compares the results from both calculations with the test data for the fluid temperature at a representative reactor vessel downcomer location. The figure shows that excluding the cold leg fluid upstream of the reactor coolant pumps from the mixing process results in cooler water residing within the downcomer. In the sensitivity calculation, RELAP5 underpredicted the measured downcomer fluid temperature by a maximum of 22 K [40°F] and over the full test period by an average of 13 K [23°F].

It is noted that this cold leg circulation issue has been a concern for the PTS plant calculations for transients that result in stagnant coolant loop conditions (primarily loss-of-coolant accidents that are sufficiently large to interrupt coolant loop natural circulation). As a result of this concern, the RELAP5 plant simulations performed for these types of PTS events have employed the artificial high reverse flow loss approach for plants with designs featuring two cold legs per coolant loop. The results from this assessment indicate that the PTS calculations performed in this manner are conservative (i.e., result in a lower downcomer temperature) when compared to calculations performed without the artificial flow losses. The downcomer fluid temperature conservatism resulting from using large artificial reverse flow losses in the pump-suction cold legs is estimated to be 8 K [14°F], based on the differences in results between the base and sensitivity RELAP5 calculations for Test APEX-CE-05.

In summary, the assessment of RELAP5 using data from experiment APEX-CE-05 indicates that the code underpredicts the reactor vessel downcomer fluid temperature for a situation involving injection of cold water into stagnant coolant loops. For this test, RELAP5 underpredicted the measured downcomer temperature by a maximum of 16 K [27°F] and overpredicted it by a maximum of 12 K [22°F]. Over the full test period, RELAP5 underpredicted the measured downcomer temperature by an average of 5.0 K [9.0°F] and varied from the measured downcomer temperature by an average of 7.0 K [13°F]. The average underprediction increases to 13 K [23°F] if large artificial reverse flow losses are used in the pump-suction cold legs of the model.

Table 3-11   Comparison of Measured and Calculated Initial Conditions for Test APEX-CE-05

Parameter	Initial Condition	
	Measured	RELAP5
Reactor Power	0 MW	0 MW
Coolant Loop Mass Flow Rates	0 kg/s [0 lbm/s]	0 kg/s [0 lbm/s]
Pressurizer Pressure	2.65 MPa [385 psia]	2.65 MPa [384.7 psia]
Cold Leg Temperature	490.4 K [423.0°F]	492.0 K [426.0°F]
Hot Leg Temperature	490.4 K [423.0°F]	490.9 K [423.9°F]
Pressurizer Level	127 cm [50 in]	127.05 cm [50.02 in]
SG 1 Pressure	2.08 MPa [301 psia]	2.07 MPa [300.7 psia]
SG 2 Pressure	2.08 MPa [301 psia]	2.07 MPa [300.7 psia]
SG 1 Wide Range Level	227.73 cm [89.66 in]	225.09 cm [88.62 in]
SG 2 Wide Range Level	226.97 cm [89.36 cm]	224.97 cm [88.57 in]

Table 3-12   Summary of Measured and Calculated Sequences of Events for Test APEX-CE-05

Event Description	Event Time (s)	
	Measured	RELAP5
Experiment begins	0	0
High pressure injection flow started	186	186
Pressurizer drain valve first opened	318	230
Experiment terminated	4,229	4,229
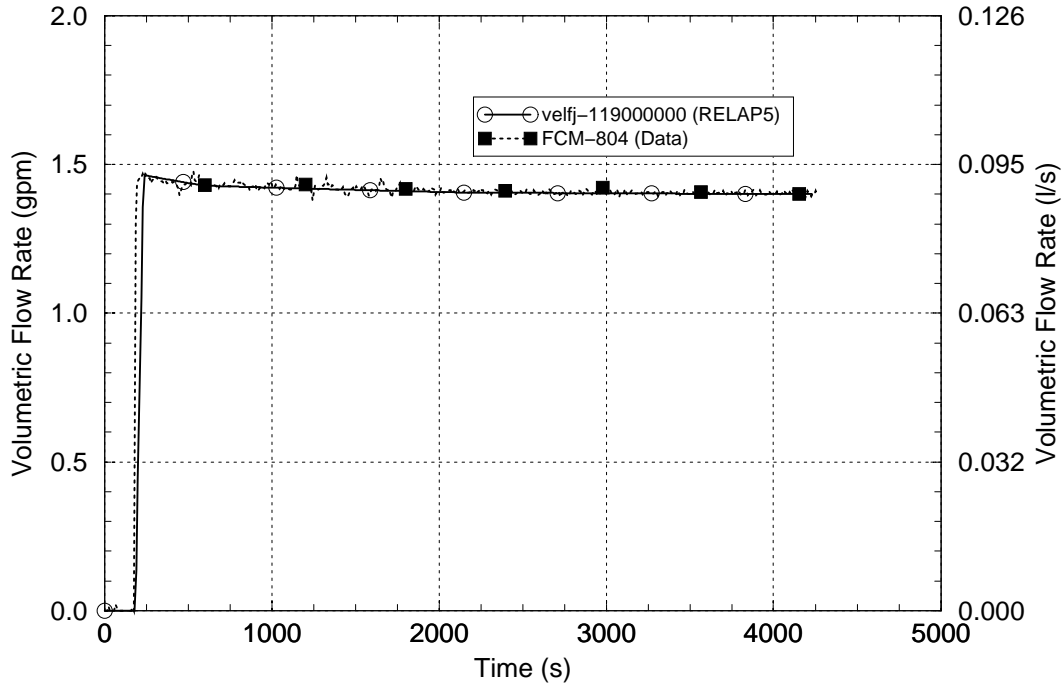
Figure 3-50 High Pressure Injection Flow Rate for Cold Leg 1 - APEX-CE-05
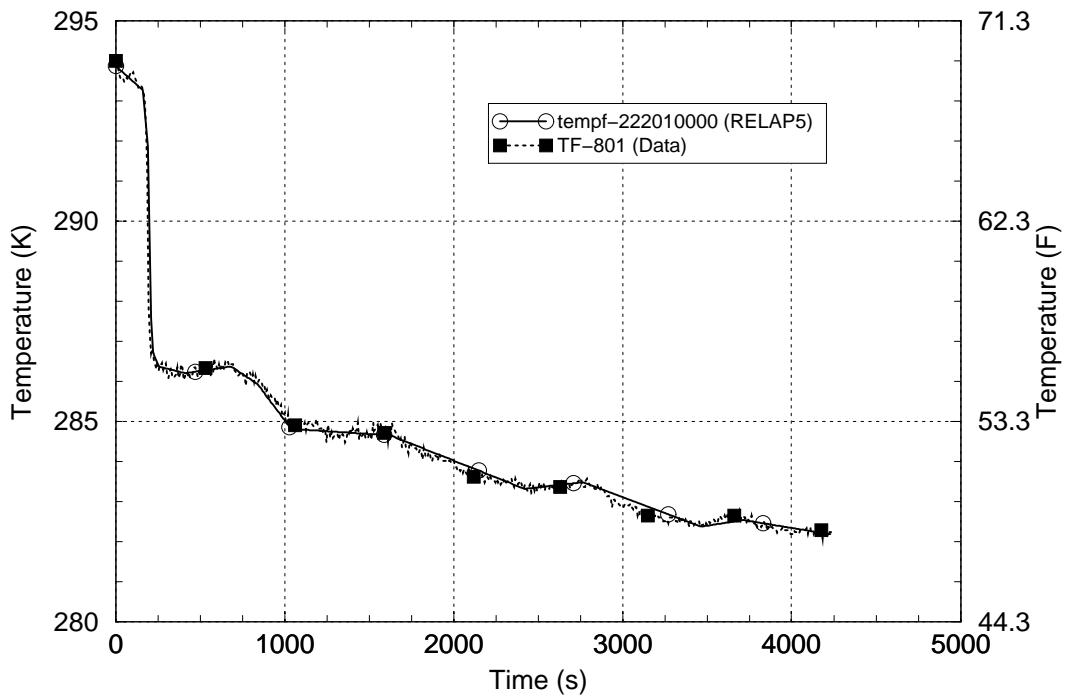
Figure 3-51 High Pressure Injection Fluid Temperature - APEX-CE-05
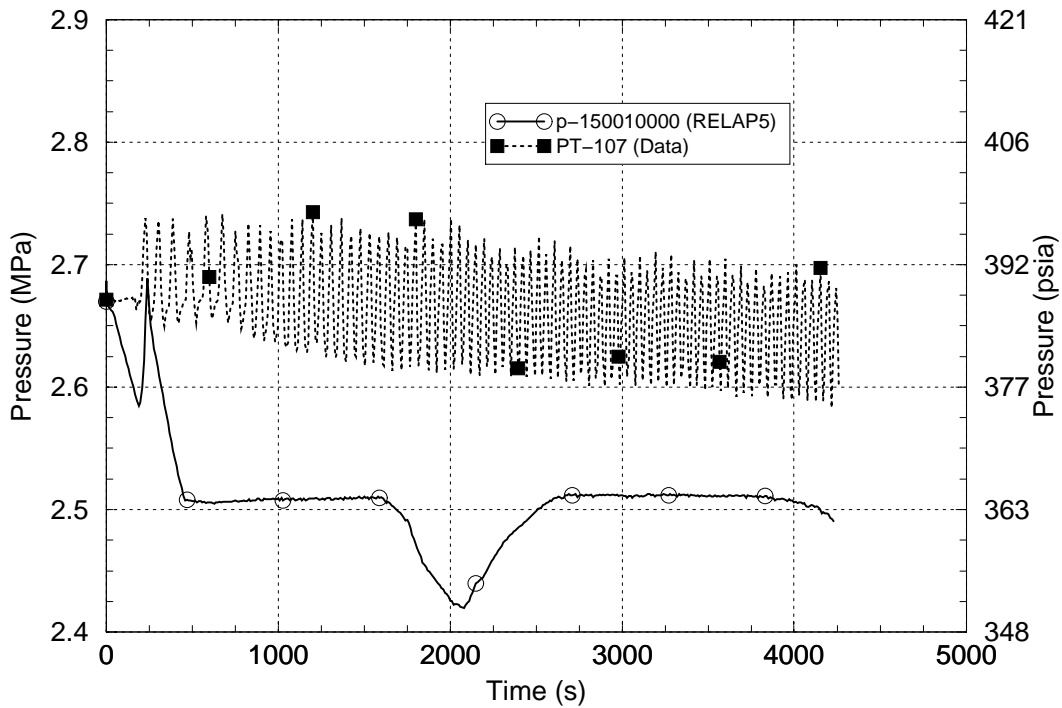
Figure 3-52   Reactor Vessel Upper Head Pressure - APEX-CE-05
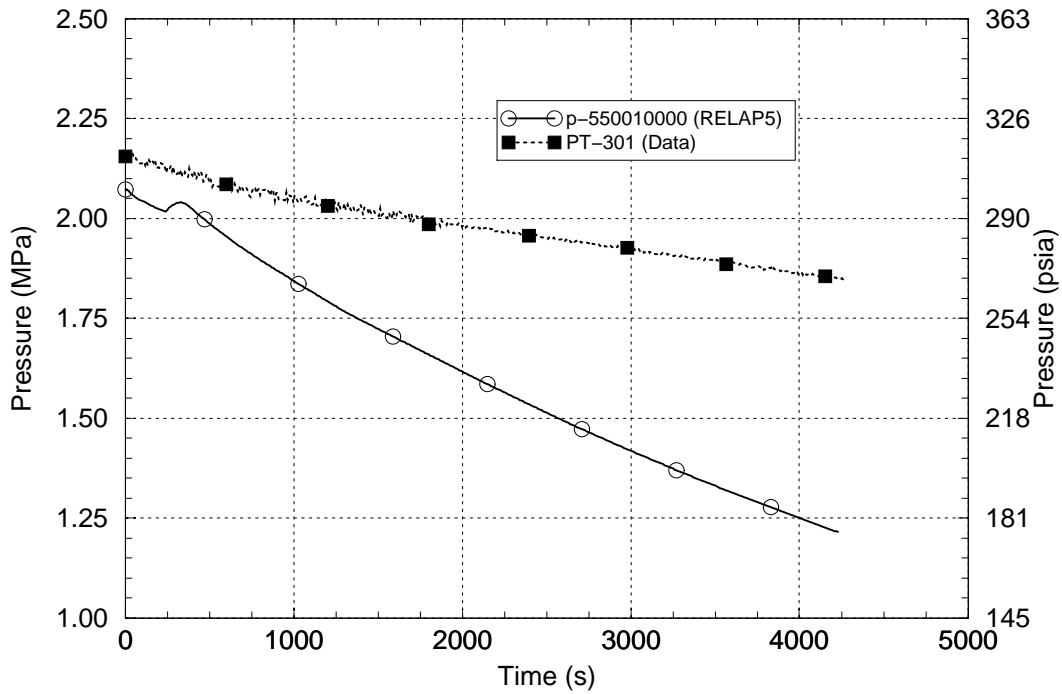
Figure 3-53   Steam Generator 1 Secondary Pressure - APEX-CE-05
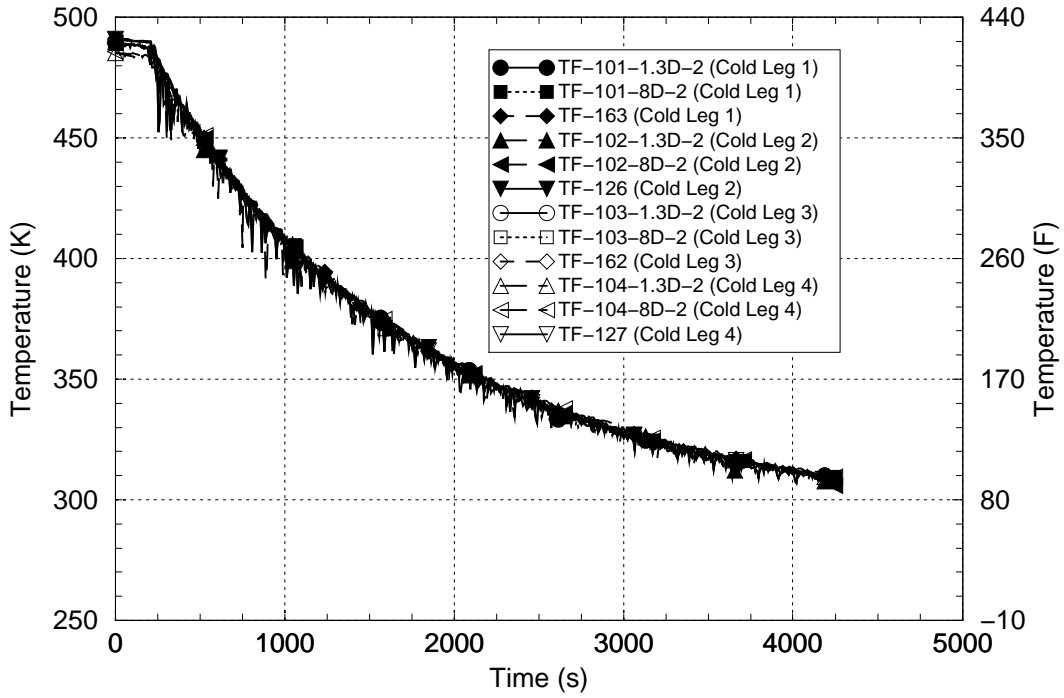
Figure 3-54   Measured Reactor Reactor Vessel Downcomer Fluid Temperatures - APEX-CE-05
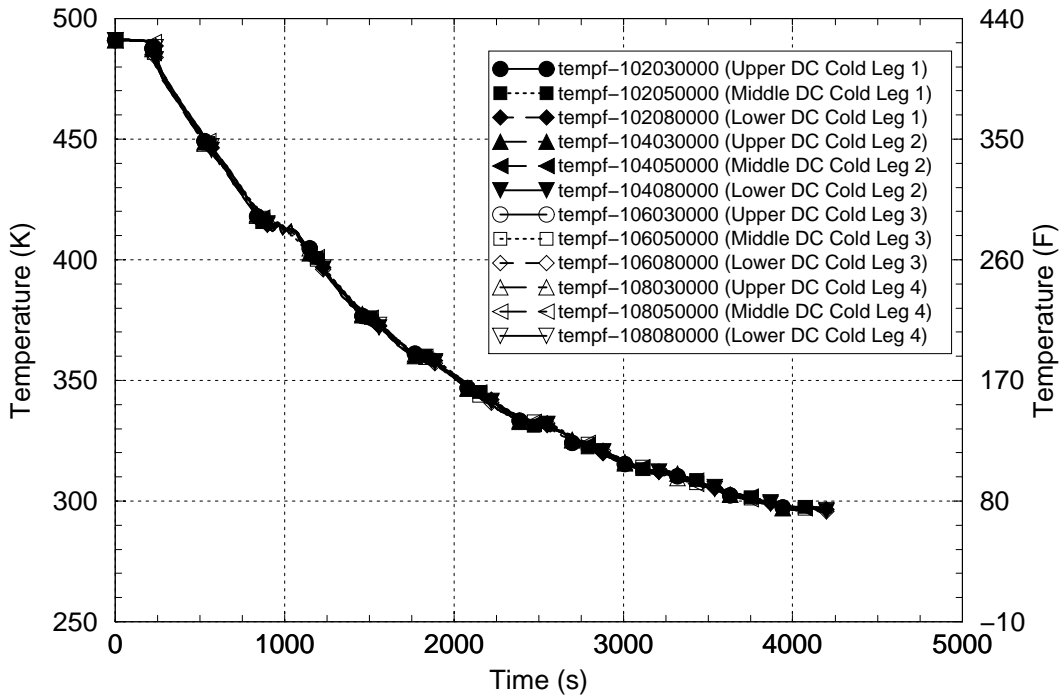
Figure 3-55   RELAP5-Calculated Reactor Vessel Downcomer Fluid Temperatures - APEX-CE-05
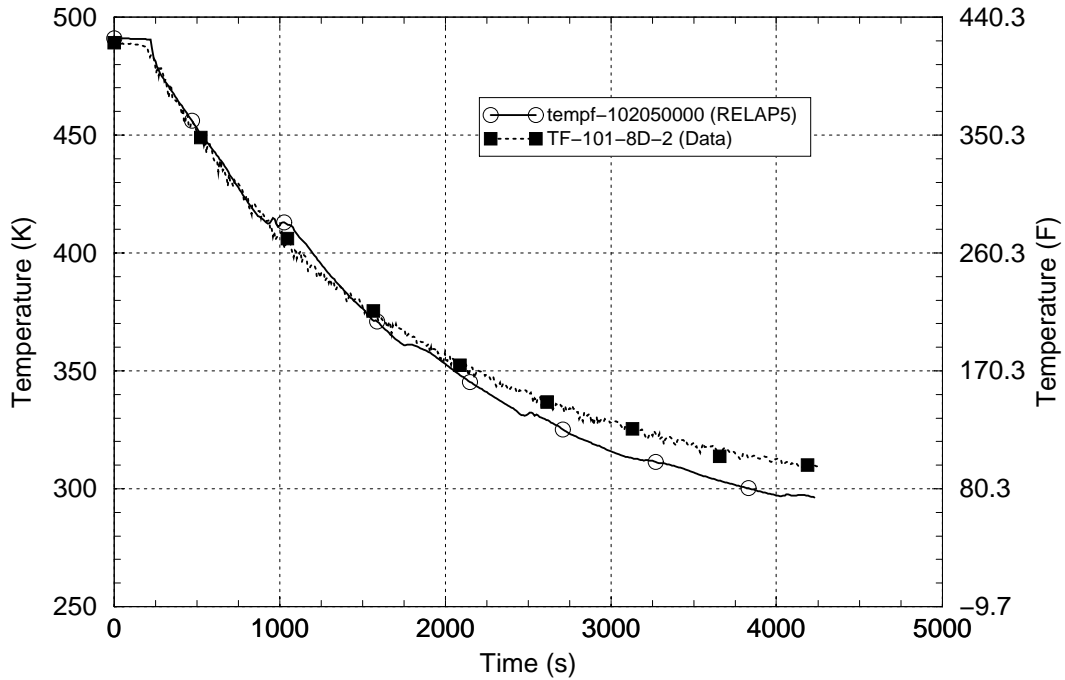
Figure 3-56   Comparison of Representative Measured and Calculated Reactor Vessel Downcomer Fluid Temperatures - APEX-CE-05
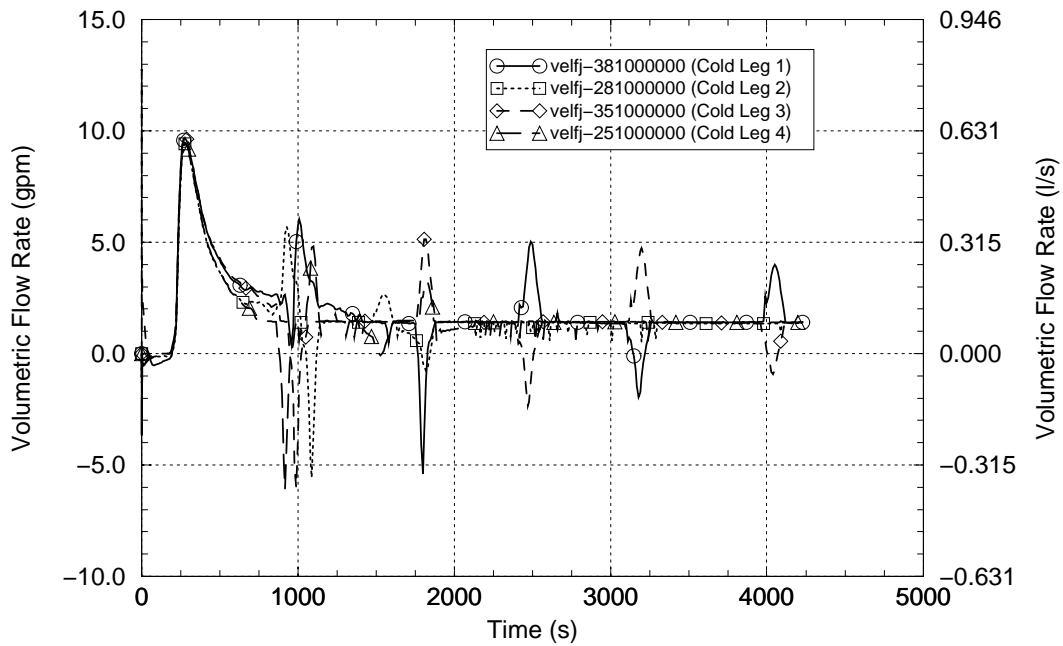
Figure 3-57   RELAP5-Calculated Cold Leg Flow Rates Between ECC Injection Nozzle and Reactor Vessel - APEX-CE-05
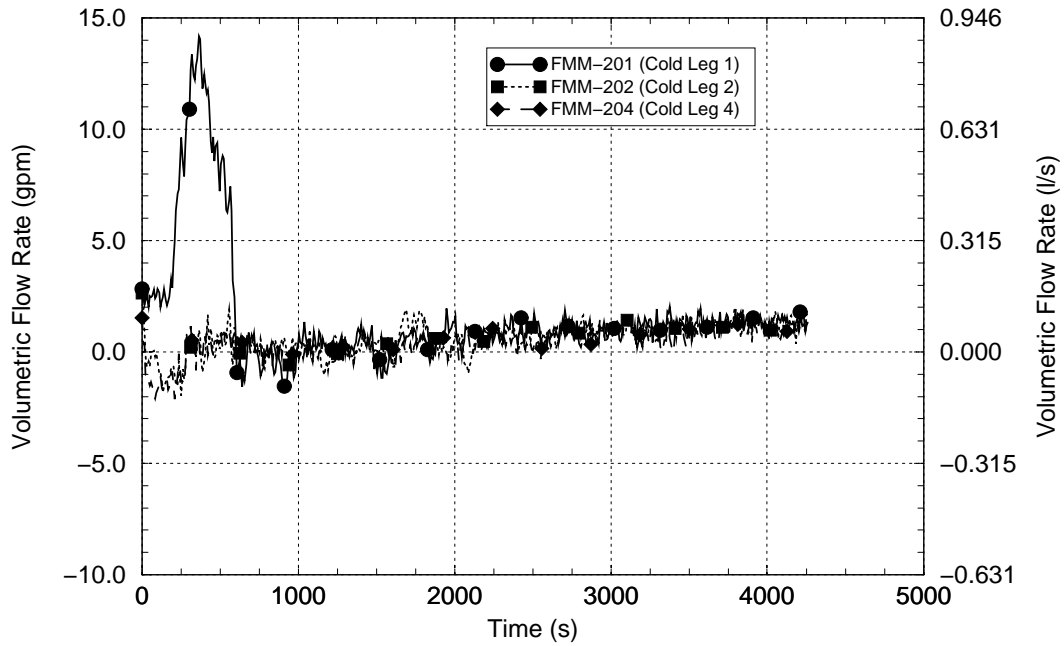
Figure 3-58   Measured Cold Leg Flow Rates Between ECC Injection Nozzle and Reactor Vessel - APEX-CE-05
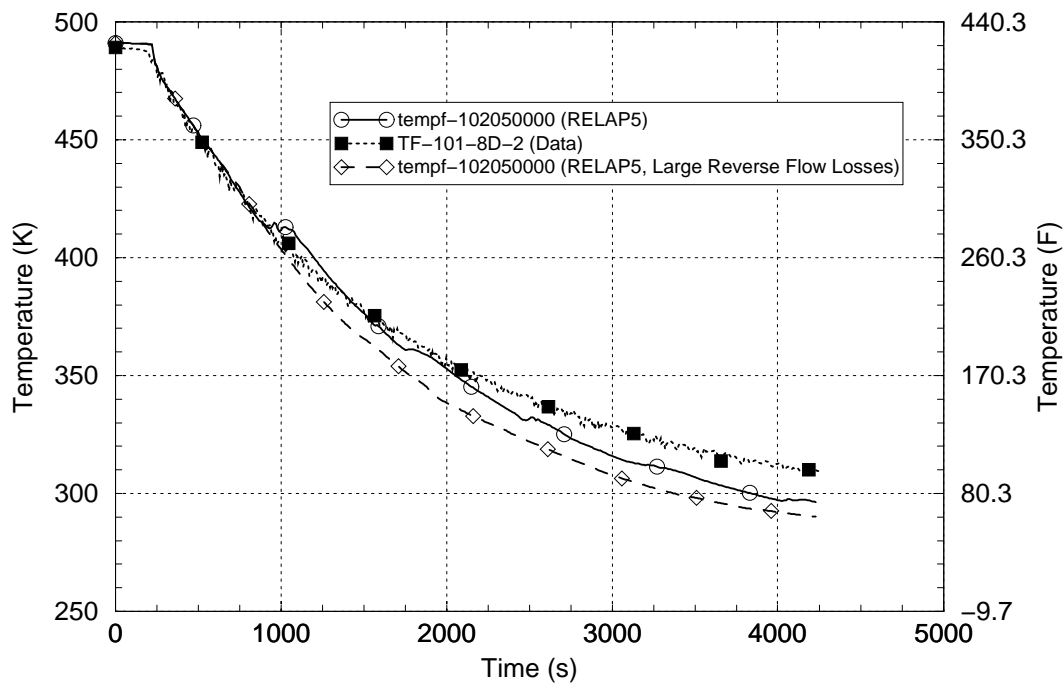
Figure 3-59   Effect of Large Reverse Loop Flow Losses on RELAP5-Calculated Reactor Vessel Downcomer Fluid Temperatures - APEX-CE-05

3.7 LOFT Test L3-7

The Loss of Fluid Test (LOFT) Facility was a 50 MWt volumetrically-scaled PWR system. LOFT was designed to obtain data on the performance of the engineered safety features of a commercial four-loop PWR system during postulated accidents, including LOCAs. A schematic of the LOFT facility is shown in Figure 3-60.

The LOFT nuclear core was approximately 1.68 m [5.51 ft] in height and 0.61 m [2 ft] in diameter and was composed of nine fuel assemblies containing 1,300 fuel rods of representative PWR design. Three intact loops were simulated using a 1/60 volume-to-power ratio scaled by the single circulating (intact) loop in the LOFT primary system. The broken loop was simulated by the scaled LOFT blowdown loop.

An ECC system was provided to simulate the engineered safety features in PWRs. A HPI system centrifugal pump and a nitrogen-pressurized accumulator supplied ECC. The LPI system and accumulator discharge lines included flow orifices in order to simulate the delivery characteristics of various PWR ECCS. The LOFT facility configuration is described in Reference 3-9.

Three LOFT tests were used in the assessment of RELAP5 for the PTS application. The first test, LOFT L3-7 represented the recovery of a plant from a 2.54 cm [1 in] diameter small break LOCA in the cold leg of a PWR. The primary purpose of this test was to establish a break flow about equal to the HPI flow when the RCS pressure is about 6.9 MPa [1,000 psia] and to isolate the break and demonstrate stabilization of the plant at cold shutdown conditions. Prior to transient initiation, the core was operating at a power of 49 MW. Other key initial conditions for Test L3-7 were a system pressure at 14.90 MPa [2,160 psia], a hot leg temperature of 576 K [577°F] and an intact loop flow rate of 481.3 kg/s [1,059 lbm/s].

During Test L3-7, the break was opened and the reactor was tripped on attainment of a low RCS pressure signal. The reactor coolant pumps were tripped manually 3 s after the reactor trip, leading to coolant loop natural circulation flow. At 1,800 s the AFW and HPI flows were terminated to hasten the loss of RCS fluid inventory and to establish the conditions leading into the system recovery to the cold shutdown condition. At 3,603 s, the AFW flow was reinstated and a steam bleed operation begun to effect a controlled depressurization of the intact loop SG secondary system. The HPI flow was reinstated at 5,974 s and the blowdown isolation valve was closed at 7,302 s, which terminated the RCS break boundary condition. The complete test procedure and the results for LOFT Test L3-7 are described the experiment data report, Reference 3-10.

The nodalization of the RELAP5 LOFT system model for Test L3-7 is shown in Figures 3-61 and 3-62. The existing LOFT L3-7 RELAP5 model employed a one-dimensional reactor vessel downcomer nodalization scheme and that was not changed for this assessment. See Section 3.9 for an assessment evaluating one- and two-dimensional modeling approaches. Table 3-13 lists the initial conditions for the test and calculation. The calculated and measured data for all parameters except the hot and cold leg temperatures and feedwater/steam flow rate are in excellent agreement. The calculated initial loop temperatures were 2 to 3 K [3.6 to 5.4°F] lower than the measured values and the calculated feedwater/steam flow rate was 8.6% lower than the measured flow rate. The test data, particularly for the initial hot leg and feedwater temperatures, were subject to considerable uncertainty. Overall, the comparison between the initial measured and RELAP5-calculated data was judged to be acceptable for the purposes of this assessment.

A simulation of LOFT Test L3-7 was performed using the RELAP5/MOD3.2.2Gamma code. The RELAP5 simulation of the test was ended when the blowdown isolation valve was closed since the re-closure of a cold leg break is not included in the PTS event sequences. A summary of the measured and calculated sequences of events is presented in Table 3-14. The comparison shows good agreement between the calculated and measured event times.

Figure 3-5.   LOFT thermal-hydraulic instrumentation for broken loop.
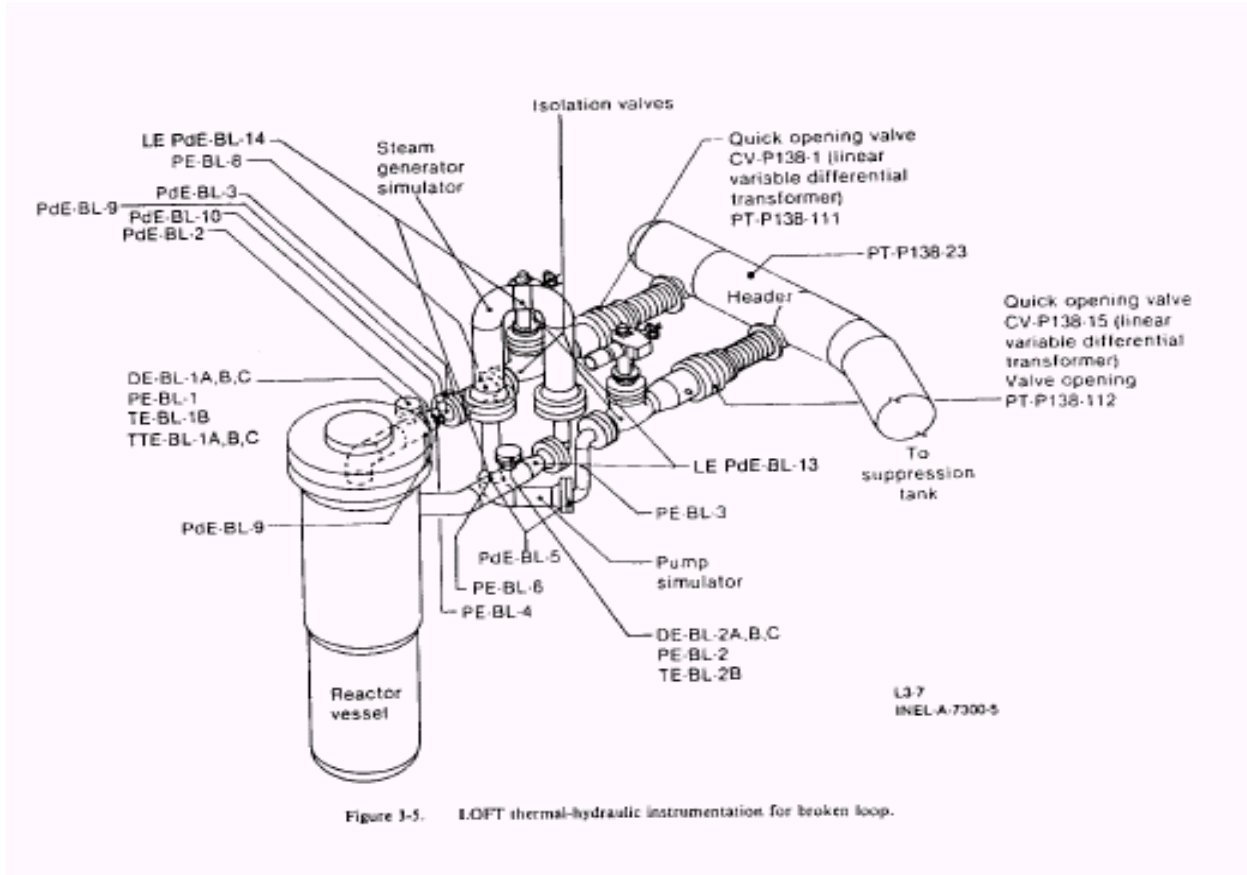
Figure 3-60   Schematic of the LOFT Test Facility
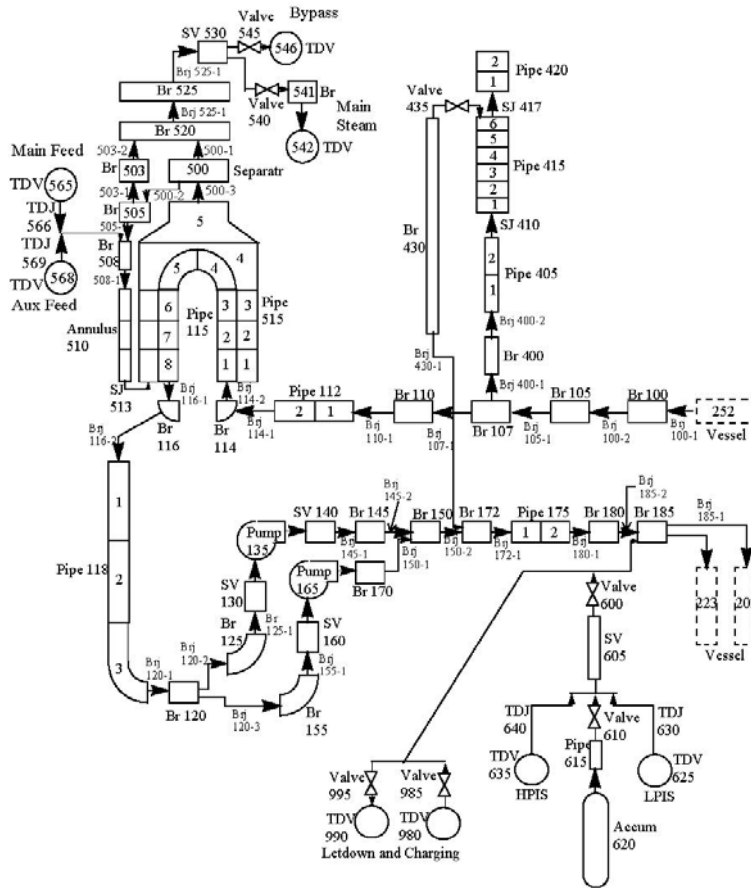
Figure 3-61   RELAP5 Nodalization of the LOFT Test Facility Intact Loop
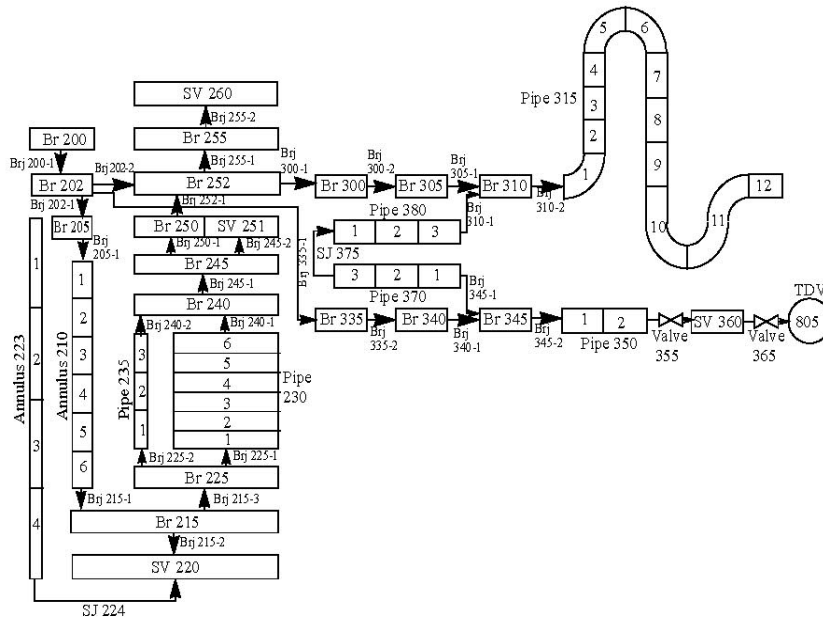
Figure 3-62   RELAP5 Nodalization of the LOFT Test Facility Vessel and Broken Loop for Test L3-7

Table 3-13   Comparison of Measured and Calculated Initial Conditions for LOFT Test L3-7

Parameter	Initial Condition	
	Measured	RELAP5
Reactor Power	49.0 MW	49.0 MW
Intact Loop Mass Flow Rate	481.3 kg/s [1058.9 lbm/s]	481.29 kg/s [1058.8 cm]
Intact Loop Hot Leg Pressure	14.90 MPa [2161.0 psia]	14.98 MPa [2172.7 psia]
Intact Loop Hot Leg Temperature	577.3 K [579.5°F]	575.0 K [575.3°F]
Intact Loop Cold Leg Temperature	559.4 K [547.3°F]	556.0 K [541.1°F]
Pressurizer Level	1.10 m [3.61 ft]	1.097 m [3.60 ft]
SG Secondary Pressure	5.576 MPa [808.7 psia]	5.421 MPa [786.2 psia]
SG Secondary Level	3.20 m [10.50 ft]	3.196 m [10.49 ft]
SG Feedwater and Steam Flow Rate	28.0 kg/s [61.6 lbm/s]	25.593 kg/s [56.3 lbm/s]

Table 3-14   Summary of Measured and Calculated Sequences of Events for LOFT Test L3-7

Event Description	Event Time (s)	
	Measured	RELAP5
Break valve opened	0	0
Scram signal (RCS pressure < 14.19 MPa)	36	28
Reactor coolant pumps tripped manually after scram	39	31
HPI flow begins (RCS pressure < 13.159 MPa)	65.4	80.1
AFW flow begins	75	75
AFW and HPI flows terminated	1,800	1,800[1]
AFW flow reinstated, intact SG steam bleed initiated	3,603	3,603[1]
HPI flow reinstated	5,974	5,974[1]
Break isolated, RELAP5 simulation ended	7,302	7,300

1 – These events represent boundary conditions on the RELAP5 calculation.

The calculated and measured break flow responses are shown in Figure 3-63. Experimental break flow data are only available over the first 1,800 s of the transient test and the measurement uncertainty is +10%. Over this period, the measured and calculated break flows are in excellent agreement.

The RCS pressure comparison is shown in Figure 3-64. The measurement uncertainty is +0.223 MPa [+33.8 psi]. The calculated pressure is in excellent agreement with the measured pressure over the first 1,800 s of the test for which measured break flow data was recorded. Afterward, the calculated pressure falls about 1.0 MPa [145 psi] below the measured pressure but the two pressures then trend downward in a similar manner. This difference in the pressure responses could result from many factors, such as system heat loss, break flow, HPI-induced condensation and SG feed-and-bleed effects. The calculated RCS pressure is judged to be in good agreement with the measured pressure after 1,800 s.

Figure 3-65 compares the calculated and measured HPI flow rates. HPI is deactivated at 1,800 s and reactivated at 5,974 s in both the test and calculation. The measured HPI flow rate for this test may be in error. Difficulties were encountered in matching the RCS pressure, break flow and HPI responses in the test data with RELAP5. The best overall match of the calculated and measured parameters was obtained when using HPI flow rates of 0.500 kg/s [1.102 lbm/s] at RCS pressures below 7.725 MPa [1120 psia] and 0.315 kg/s [0.672 lbm/s] at RCS pressures above 8.36 MPa [1212 psia]. As shown in Figure 3-65, this HPI modeling approach resulted in an apparent overprediction of HPI flow prior to the time it was deactivated and a good prediction of HPI flow after it was reactivated.

The intact loop SG secondary pressures are compared in Figure 3-66. The measurement uncertainty is +0.110 MPa [+16 psi]. The calculated and measured data are in excellent agreement up to 1,800 s, when the AFW flow is terminated. From 1,800 s to 3,603 s the calculated pressure declined moderately while the measured pressure increased moderately. This difference is perhaps due to an overprediction of secondary system heat loss effects. After 3,603 s when the SG feed-and-bleed process was initiated, the rates of decline in both pressures are comparable. Overall, the calculated and measured SG secondary pressure responses were judged to be in acceptable agreement.

The calculated intact hot leg liquid and vapor velocity responses are compared with the measured fluid velocity response in Figure 3-67. The uncertainty in the measured data is +20%. The figure shows excellent agreement between the calculated liquid velocity and the measured fluid velocity. The calculated vapor velocity was higher, indicating steam flowing more rapidly than liquid toward the SG in the intact coolant loop natural circulation flow. The calculated hot leg void fraction was in a range from about 0.1 to 0.2 after the HPI was terminated at 1,800 s. The primary system pressure remained above the intact loop SG secondary pressure and loop natural circulation flow continued throughout the test and calculation periods.

Figure 3-68 compares the calculated and measured downcomer fluid temperatures. Comparisons are made at elevations in the downcomer corresponding to the top and middle of the core (data channels for an elevation corresponding to the bottom of the core are not available for Test L3-7). Measured data are shown from the intact-loop and broken-loop sides of the downcomer and are compared with the RELAP5-calculated data using the one-dimensional downcomer nodalization scheme. Both the test data and calculated data exhibit virtually no downcomer temperature variation between the top-core to mid-core elevations. The test data exhibit only a small

temperature difference (about 2 K [3.6 °F]) between the downcomer temperatures on the intact-loop and broken-loop sides. The uncertainty in the measured temperatures is ±2.6 K [4.7 °F]. The figure shows that RELAP5 consistently underpredicted the downcomer fluid temperatures. For this test, RELAP5 underpredicted the measured downcomer temperature by a maximum of 15 K [27 °F] and overpredicted it by a maximum of 0.48 K [0.86 °F]. Over the full test period, RELAP5 underpredicted the measured downcomer temperature by an average of 8.1 K [15 °F] and varied from the measured downcomer temperature by an average of 8.1 K [15 °F]. The agreement between measured and calculated downcomer temperatures was judged to be good. The lack of any significant difference in the measured temperatures between the intact and broken loop sides of the downcomer indicates that a one-dimensional downcomer modeling scheme is acceptable for simulating very small LOCA accident scenarios such as represented with LOFT Test L3-7.

In summary, this assessment indicated no major differences between the calculated and measured data for LOFT Test L3-7. The RELAP5 prediction of the reactor vessel downcomer fluid temperature is in good agreement with the measured data. The RELAP5 prediction of the RCS pressure is in good-to-excellent agreement with the measured data. The assessment of RELAP5/MOD3.2.2 Gamma using experimental data from LOFT Test L3-7 indicates that the code is capable of acceptably simulating the behavior of the key PTS parameters.
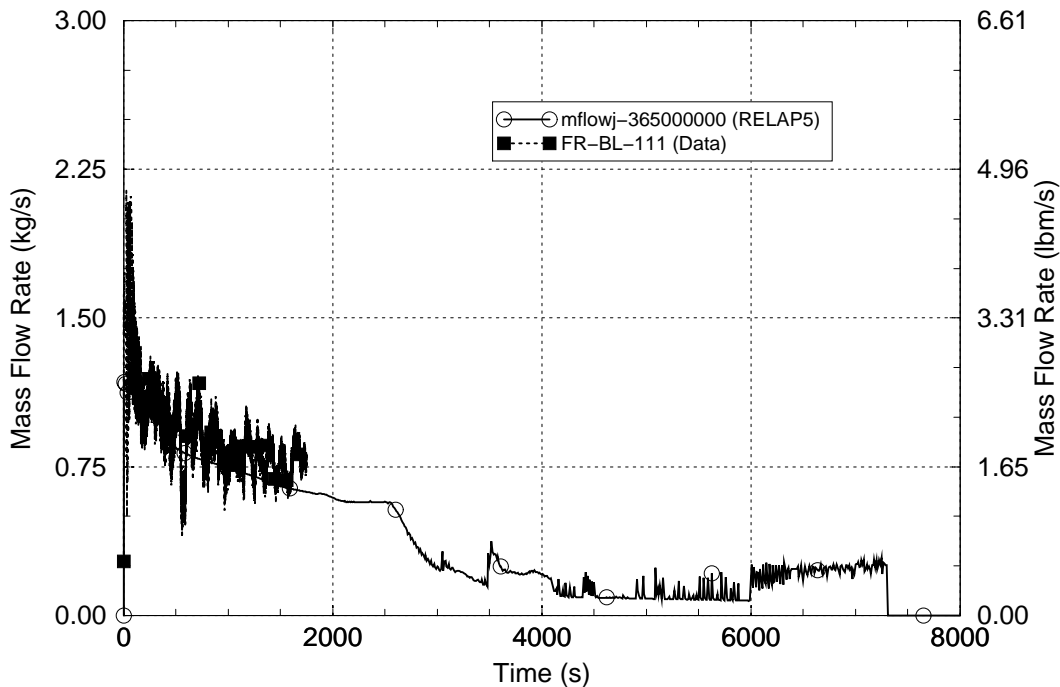
Figure 3-63   Break Flow – LOFT Test L3-7
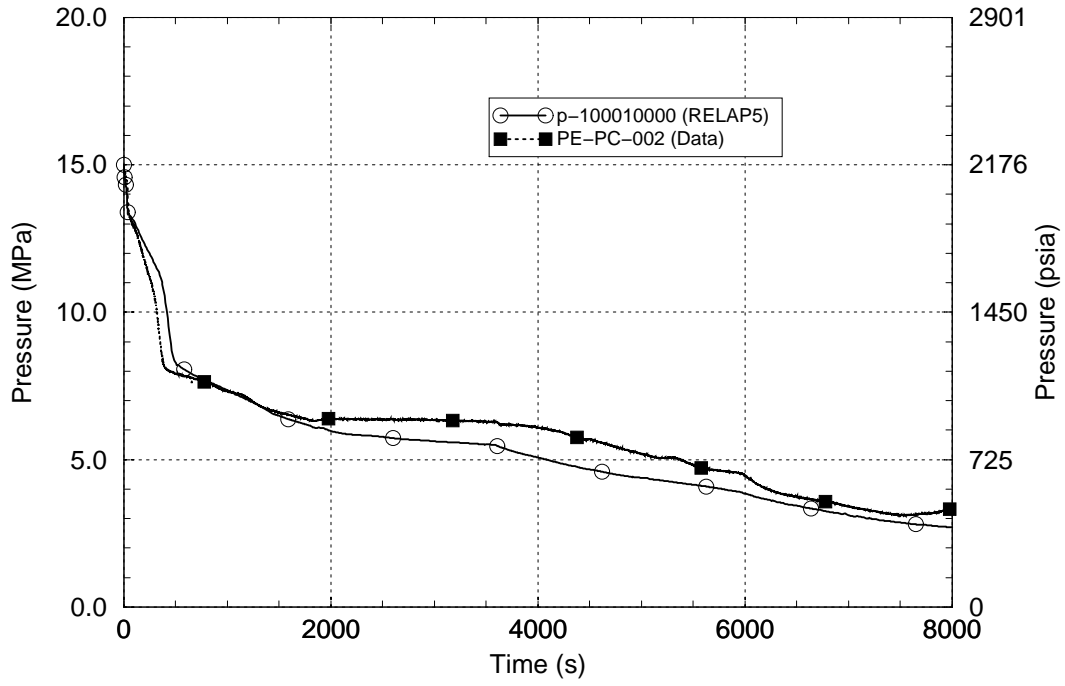
Figure 3-64   RCS Hot Leg Pressure – LOFT Test L3-7
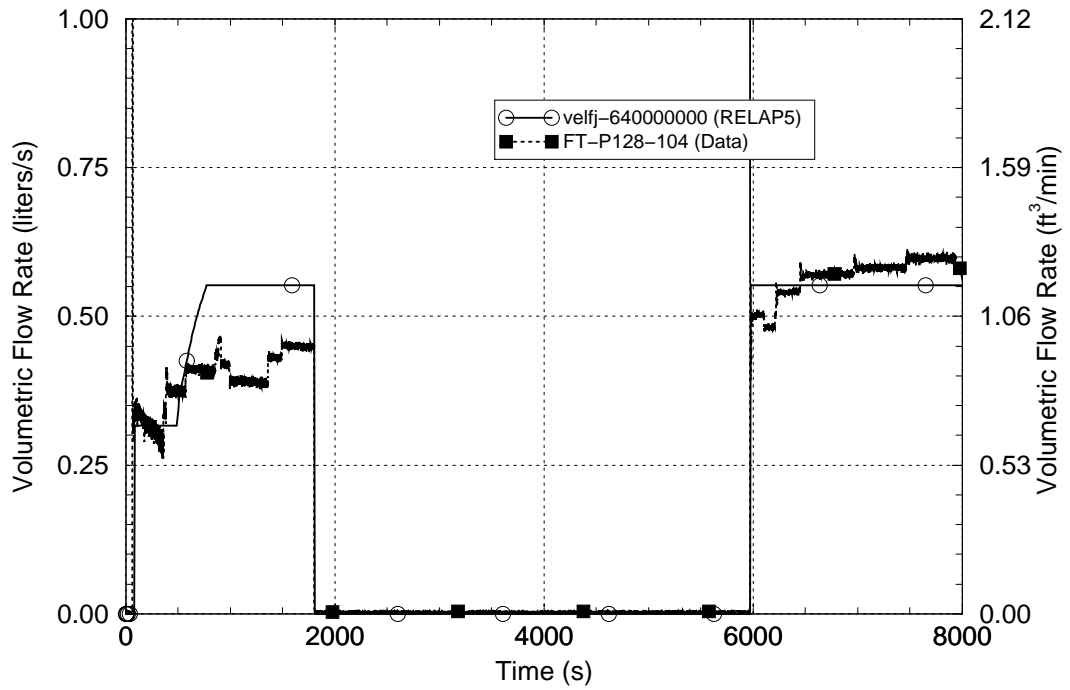
Figure 3-65   HPI Flow – LOFT Test L3-7
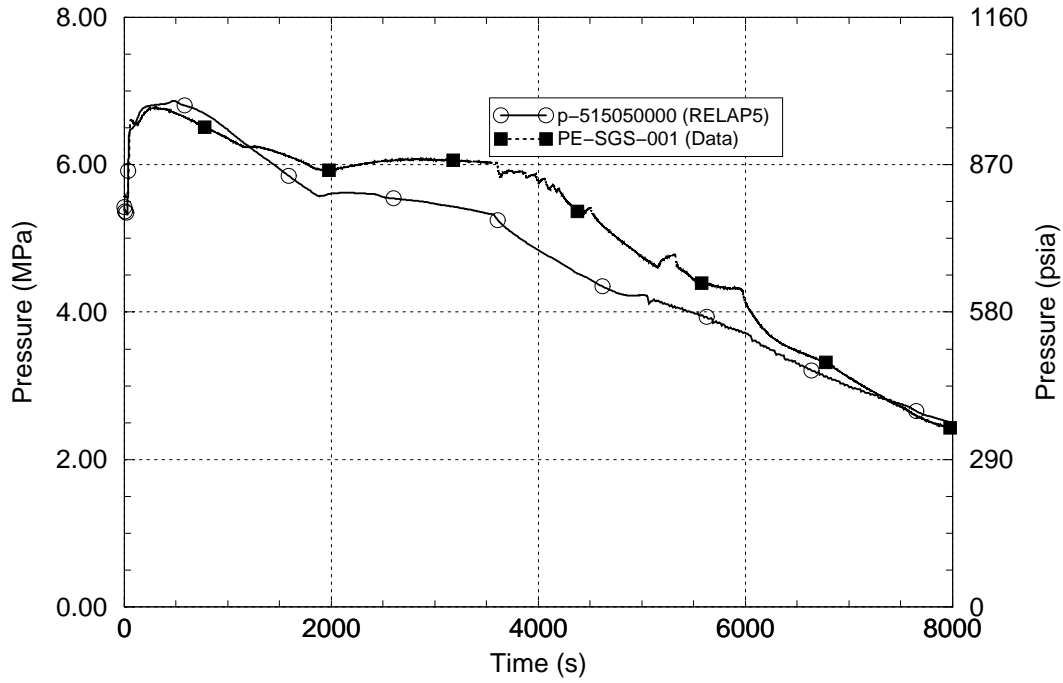
Figure 3-66   Intact Loop SG Pressure – LOFT Test L3-7
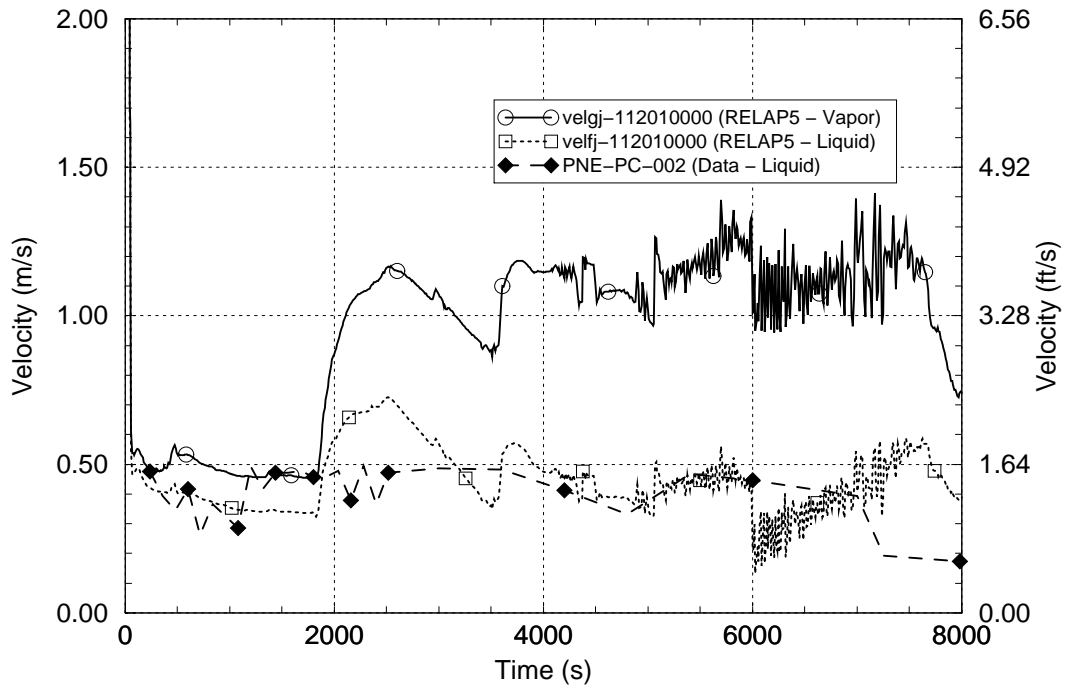
Figure 3-67   Intact Loop Hot Leg Velocities – LOFT Test L3-7
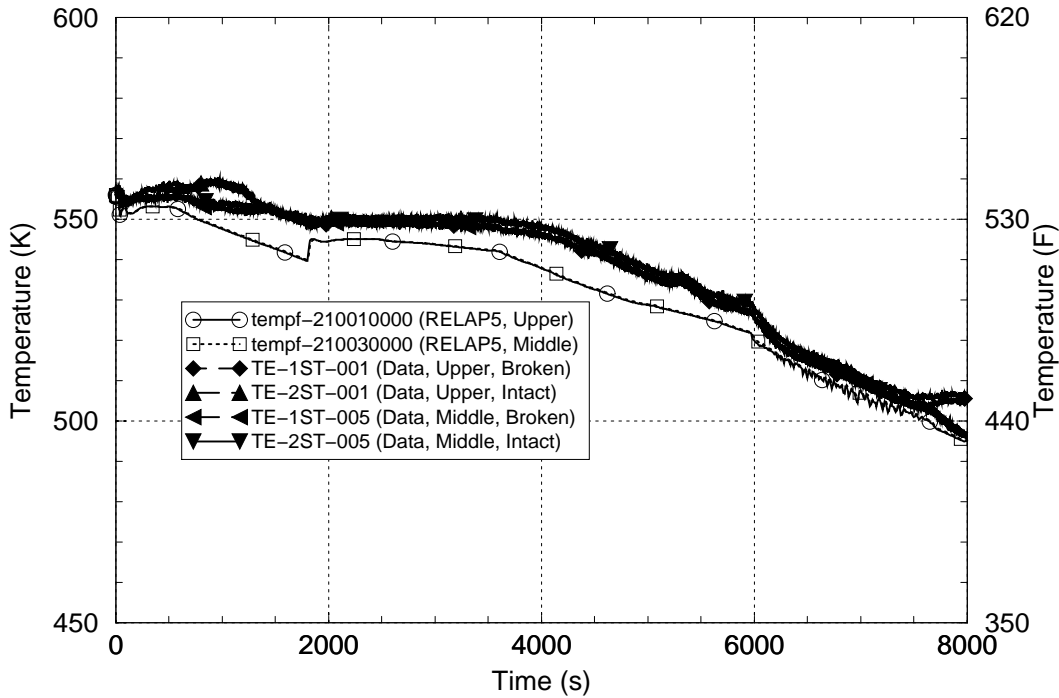
Figure 3-68   Liquid Temperatures in Reactor Vessel Downcomer – LOFT Test L3-7

3.8   LOFT Test L2-5

The LOFT facility is described in Section 3.7. Three LOFT tests were used in the assessment of RELAP5 for the PTS application. The second test, LOFT L2-5, represents a 200% double-ended guillotine break LOCA in the cold leg of a PWR. The primary purpose of this test was to evaluate the performance of the ECCS for cooling the core. For the purposes of the PTS assessment, this test provides data for the very rapid blowdown and refilling of the RCS with cold ECCS which accompanies a very large break in the RCS. Prior to the test initiation the LOFT core was operating at a power of 36 MW. Other key initial conditions for Test L2-5 were a system pressure at 14.95 MPa [2,168 psia], a core outlet temperature of 589.7 K [601.8°F] and an intact loop flow rate of 192.4 kg/s [424.2 lbm/s].

During the test, the break was opened and the reactor was tripped upon attainment of a RCS low-pressure signal. The reactor coolant pumps were tripped manually 0.94 s after the reactor trip. Accumulator injection began when the RCS pressure had declined below the initial accumulator pressure. Delayed injection of HPI and LPI ECC coolant began at 23.9 s and 37.3 s, respectively. The complete test procedure and the results for LOFT Test L2-5 are described the experiment data report, Reference 3-11.

The nodalization of the RELAP5 LOFT system model used for Test L2-5 is shown in Figures 3-61 and 3-69. (Note that the same intact loop nodalizations were used for Tests L3-7 and L2-5 but that an expanded vessel nodalization including a two-channel downcomer noding scheme is used for Test L2-5). Table 3-15 lists the initial conditions for the test and calculation. The calculated and measured initial condition data for all parameters are in excellent agreement.

A simulation of LOFT Test L2-5 was performed using the RELAP5/MOD3.2.2Gamma code. A summary of the measured and calculated sequences of events is presented in Table 3-16. The comparison shows good agreement between the calculated and measured event times. The very early depressurization rate was overpredicted by RELAP5 and as a result the reactor trip setpoint RCS pressure was reached 0.226 s earlier in the calculation than in the test. The reactor coolant pump trip signal was actuated 0.81 s later in the calculation than indicated in the test data so as to provide a best possible match between the initial declines in the calculated and measured intact loop coolant flows.

The calculated and measured broken-loop cold leg and hot leg flow responses are shown in Figures 3-70 and 3-71, respectively. Referring to Figure 3-69, note that these comparisons are made for locations within the piping system (at RELAP5 Components 340 and 305) which are considerably upstream of the break valves. However, these comparisons may be effectively used to evaluate the break valve flow responses since flow through the break valves must pass through these piping regions. The figures indicate good-to-excellent agreement between the calculated and measured flow rates through the two break paths.

The intact loop hot leg average density responses are shown in Figure 3-72 and the reactor vessel upper plenum fluid temperature responses are shown in Figure 3-73. Good agreement is seen between the calculated and measured responses for these parameters, indicating that the rate of RCS voiding and the RCS thermal response are generally well predicted with RELAP5.
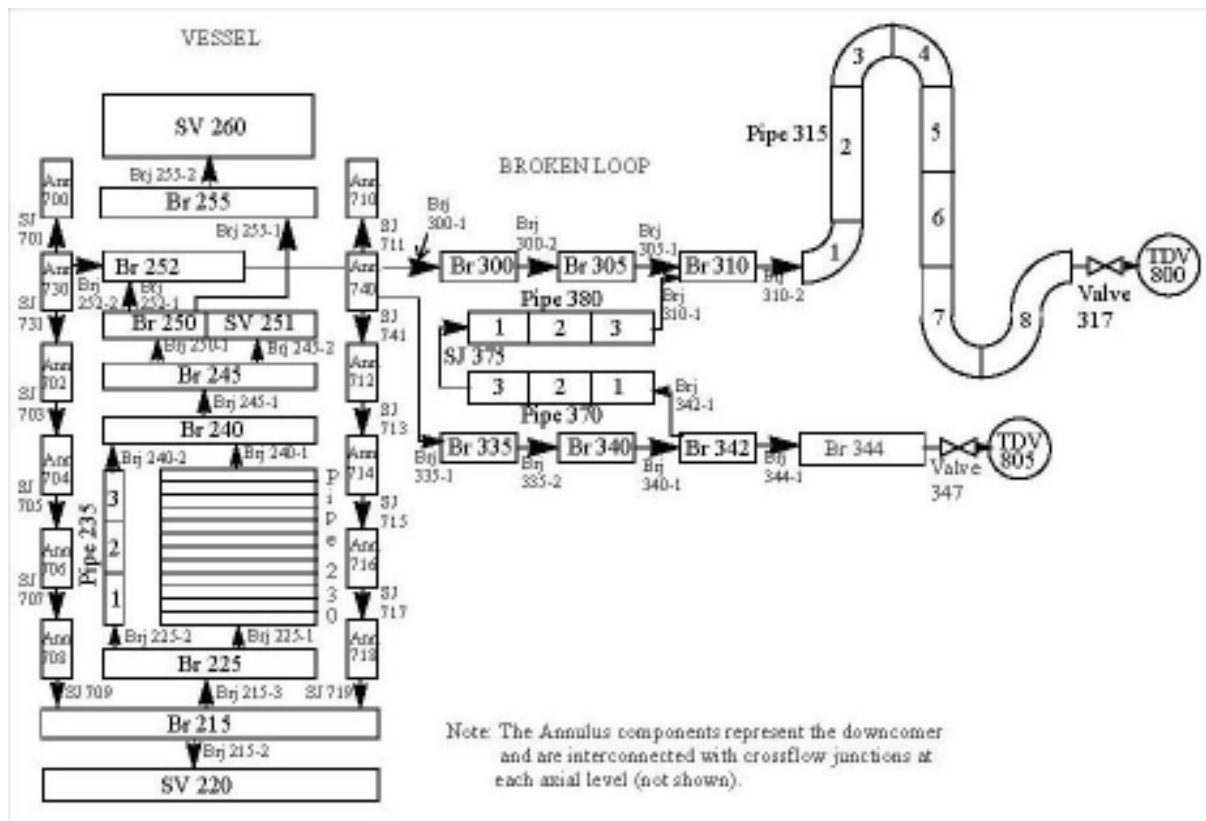
Figure 3-69   RELAP5 Nodalization of the Loft Test Facility Vessel and Broken Loop for LOFT Test L2-5

Table 3-15   Comparison of Measured and Calculated Initial Conditions for LOFT Test L2-5

Parameter	Initial Condition	
	Measured	RELAP5
Reactor Power	36.0 MW	36.0 MW
Intact Loop Mass Flow Rate	192.4 kg/s [423.3 lbm/s]	192.4 kg/s [423.3 lbm/s]
Intact Loop Hot Leg Pressure	14.95 MPa [2168.3 psia]	14.96 MPa [2169.7 psia]
Intact Loop Hot Leg Temperature	589.7 K [601.8°F]	590.45 K [603.1°F]
Intact Loop Cold Leg Temperature	556.6 K [542.0°F]	557.19 K [543.3°F]
Pressurizer Level	1.14 m [3.74 ft]	1.145 m [2.52 ft]
SG Secondary Pressure	5.85 MPa [848.5 psia]	5.846 MPa [847.9 psia]
SG Feedwater and Steam Flow Rate	19.1 kg/s [42.0 lbm/s]	18.63 kg/s [40.99 lbm/s]

Table 3-16   Summary of Measured and Calculated Sequences of Events for LOFT Test L2-5

Event Description	Event Time (s)	
	Measured	RELAP5
Break valve opened	0	0
Scram signal (RCS pressure < 14.19 MPa)	0.24	0.0141
Reactor coolant pumps tripped manually after scram	0.94	1.75
Primary system pressure falls below intact loop SG secondary pressure	10.2	17.1
Pressurizer empty	15.4	15.18
Accumulator flow initiated	16.8	12.81
HPI flow initiated after specified time delay	23.9	23.9
LPI flow initiated after specified time delay	37.3	37.3
Accumulator empty	49.6	51.42
Test, RELAP5 simulation ended	107.1	107.1
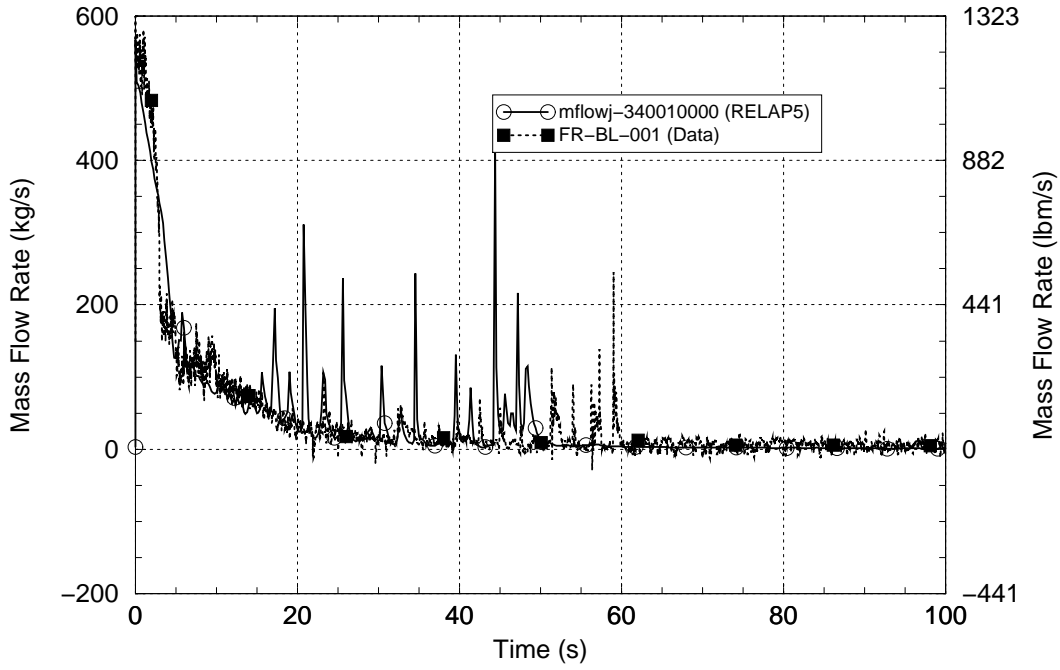
Figure 3-70   Broken Loop Cold Leg Flow – LOFT Test L2-5
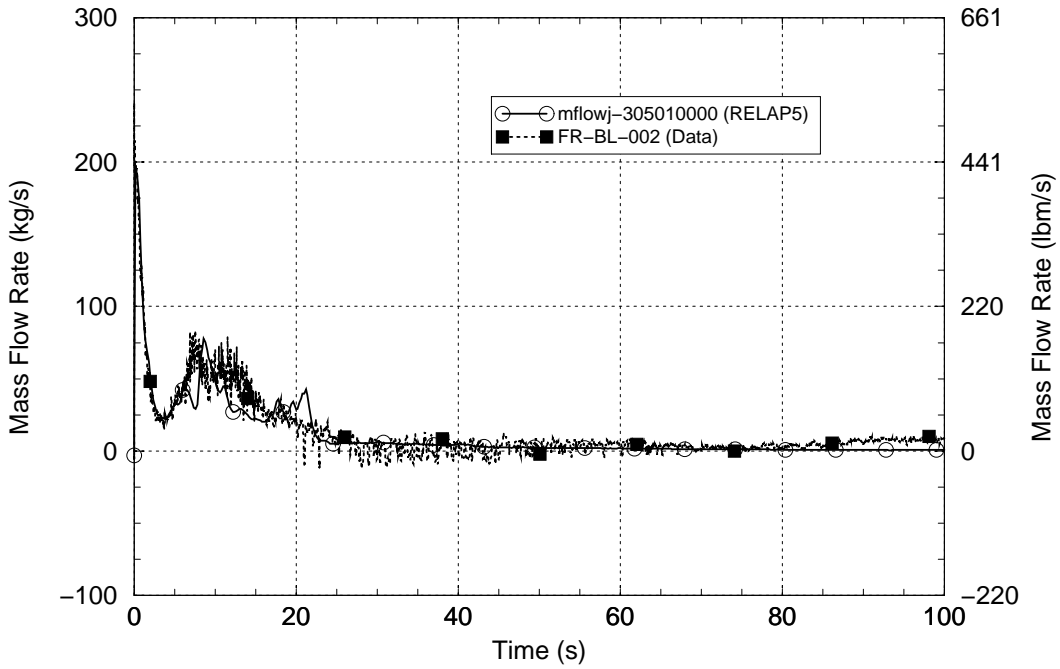
Figure 3-71   Broken Loop Hot Leg Flow – LOFT Test L2-5
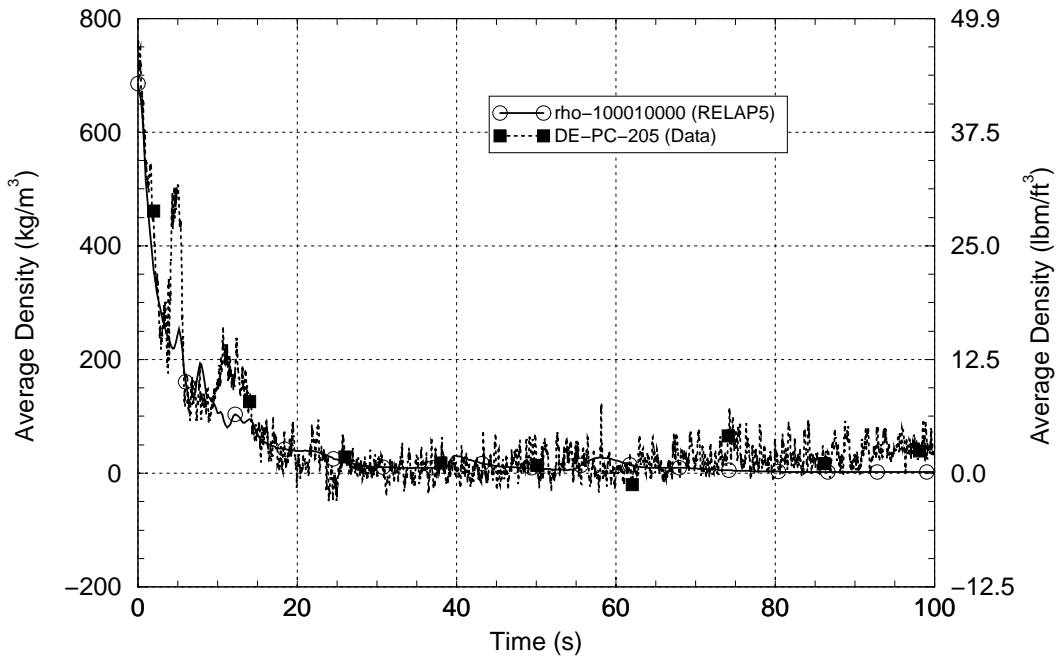
Figure 3-72   Intact Loop Hot Leg Density – LOFT Test L2-5
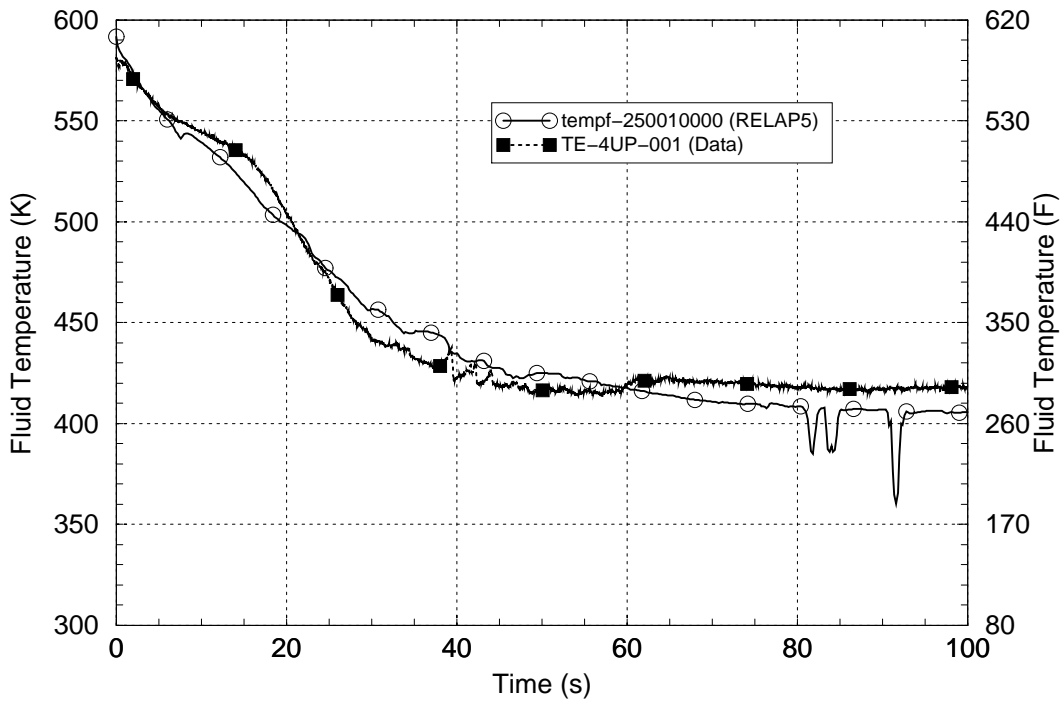
Figure 3-73   Reactor Vessel Upper Plenum Fluid Temperature – LOFT Test L2-5

The RCS pressure responses are shown in Figure 3-74. The data shown are located in the reactor vessel upper plenum region. Good agreement is indicated between the calculated and measured pressure data. From 10 s to 20 s, RELAP5 momentarily underpredicted the RCS pressure by up to about 1.0 MPa [145 psi]. Referring to Figures 3-71 and 3-72, this is the same period during which RELAP5 underpredicted the flow rates through the two break paths by up to 40%. These figures suggest that the RCS pressure underprediction from 10 s to 20 s resulted from more liquid being present at the break in the experiment than in the calculation. In the experiment this liquid momentarily retarded the depressurization and this effect was not seen in the calculation. Overall, the RELAP5 predictions for both the RCS pressure and break flows are considered good.

The SG secondary pressure responses are shown in Figure 3-63. The calculated and measured data are in excellent agreement. Coolant flow in the intact loop is lost quickly when the primary system pressure fell below the intact SG secondary pressure in both the test and calculation, see Table 3-16.

Figure 3-76 shows the cladding temperature responses at an elevation 0.13 m [5.1 in] above the bottom of the heated core length. This comparison is shown because the evaluation of issues relating to core cooling during a LBLOCA were the main purpose for performing the experiment, even though they are not specifically pertinent for the PTS application. The figure shows that the RELAP5 simulation for this test includes representations of core voiding and fuel rod heatup that were observed in the experiment. RELAP5 well-predicted the timing of the fuel rod heatup and rewet but underpredicted the peak cladding temperature.

Referring to Table 3-16, RELAP5 predicted the onset of accumulator flow about 4 s earlier than seen in the test and the emptying of the accumulator about 2 s later than seen in the test. The accumulator level responses, shown in Figure 3-77 confirm that RELAP5 moderately underpredicted the rate of accumulator discharge but that emptying proceeded via a very regular process in both the test and calculation. The RELAP5 accumulator level prediction is considered good to excellent.

The calculated and measured reactor vessel downcomer fluid temperatures are compared in Figure 3-78. Data are shown at three elevations, corresponding to the elevations of the top, middle, and bottom of the core, on the broken-loop side of the downcomer. Downcomer fluid temperature data is not available for Test L2-5 for the intact-loop side of the downcomer. Both the measured and calculated data indicate transient variations of about 12 K [22°F] in the temperatures between the top and middle downcomer axial elevations (and to a much lesser extent between the middle and bottom downcomer axial elevations). These variations reflect the effects of surging accumulator injection flows. The uncertainty in the measured temperatures is ±2.6 K [±4.7°F]. Between 5 s and 25 s, the code underpredicted the temperature by up to 15 K [27°F] and between 25 s and 50 s the code overpredicted the temperature to a similar extent. These differences are caused by the underprediction of the accumulator injection rate from 20 to 50 s (see Figure 3-67). After 50 s, when the accumulators are empty in both the test and calculation, the RELAP5-predicted temperature fell slowly while the measured temperature rose slowly. The differences between the calculated and measured downcomer temperature behavior after about 50 s are consistent with the underprediction of the RCS pressure during this period (see Figure 3-64). Although the pressure difference is small, the calculated temperature is lower than the measured temperature because the calculated saturation temperature is lower than the measured saturation temperature. Overall, the agreement between the calculated and measured downcomer fluid temperatures for this test was judged to be good. For this test, RELAP5 underpredicted the measured downcomer

temperature by a maximum of 17 K [30°F] and overpredicted it by a maximum of 21 K [37°F]. Over the full test period, RELAP5 overpredicted the measured downcomer temperature by an average of 2.0 K [3.6°F] and varied from the measured downcomer temperature by an average of 8.4 K [15°F].
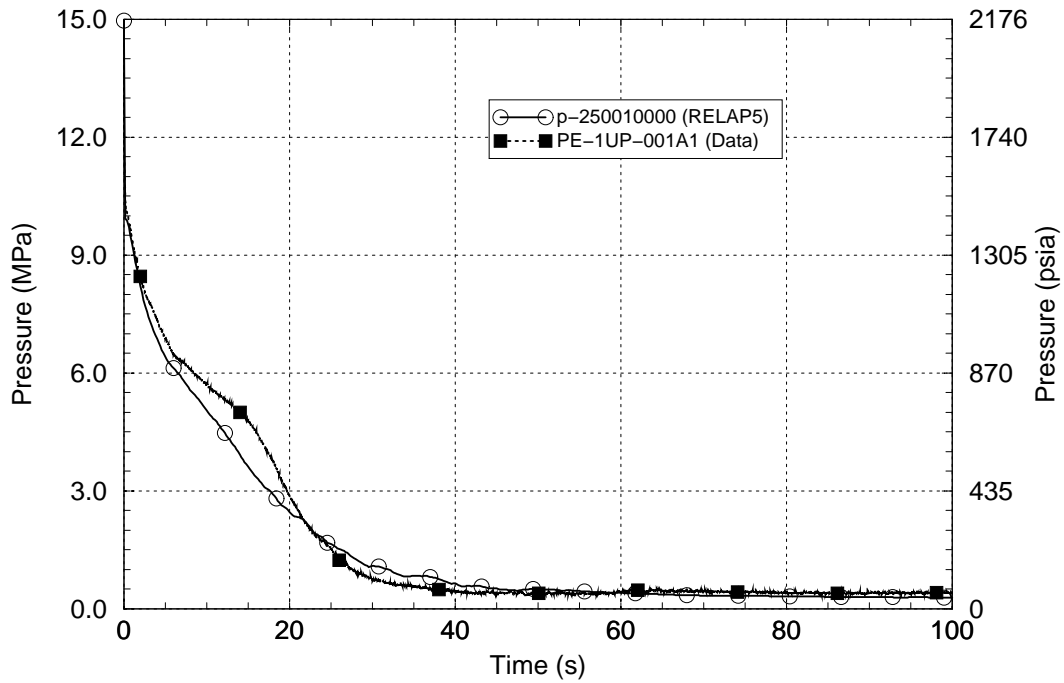
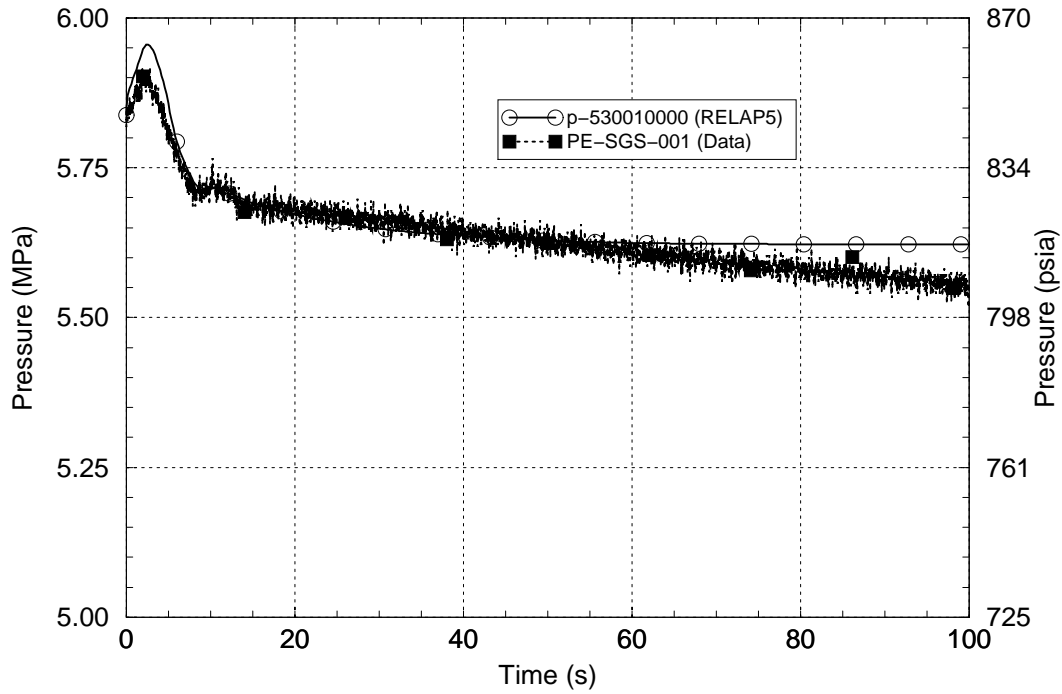**Figure 3-74   RCS Pressure – LOFT Test L2-5**

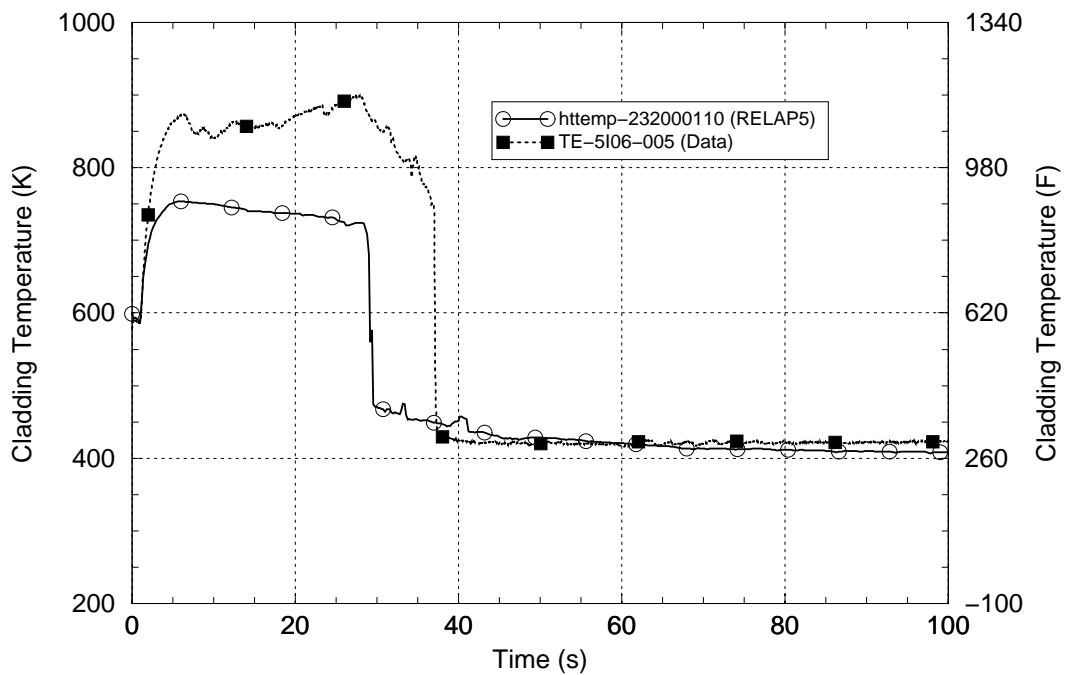**Figure 3-75　SG Secondary Pressure – LOFT Test L2-5**

Figure 3-76　Fuel Rod Cladding Temperature at 0.13 m Above the Bottom of the Core – LOFT Test L2-5
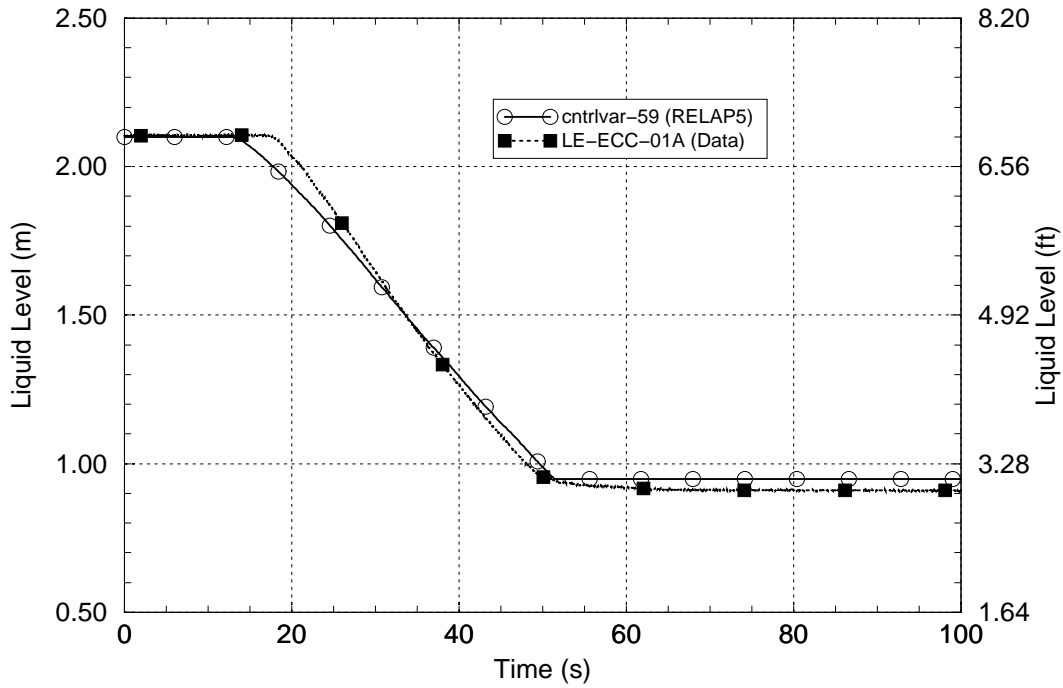
Figure 3-77 Accumulator Level – LOFT Test L2-5
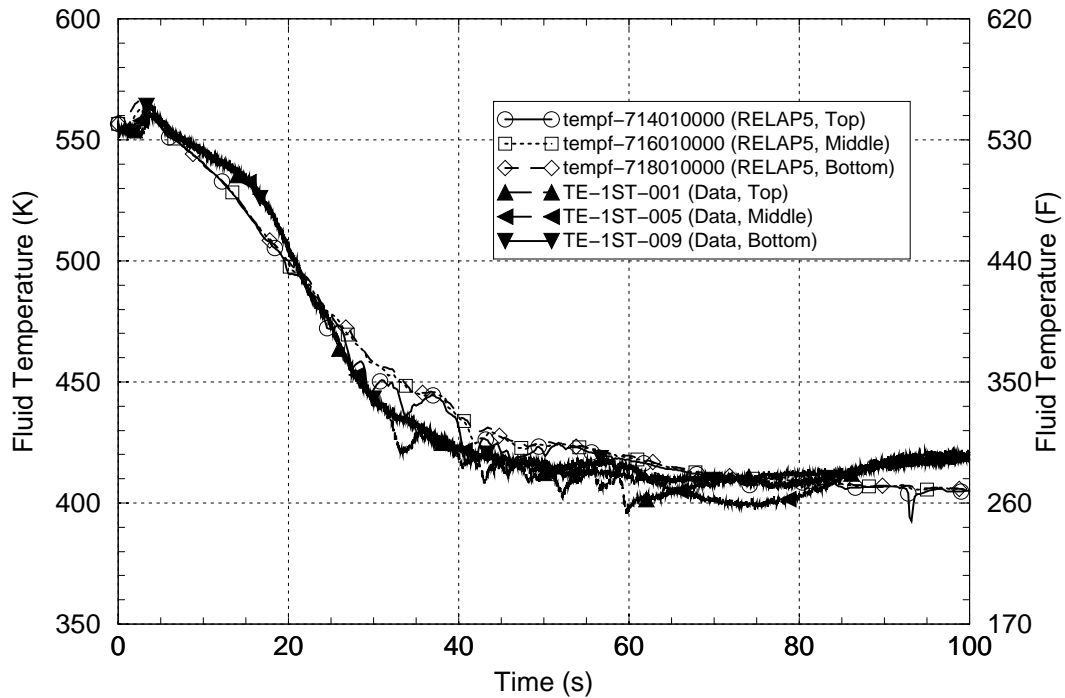
Figure 3-78 Liquid Temperatures in Reactor Vessel Downcomer – LOFT Test L2-5

In summary, this assessment indicated no major differences between the calculated and measured data for LOFT Test L2-5. The RELAP5 predictions of the reactor vessel downcomer fluid temperature and RCS pressure are in good agreement with the measured data. The assessment of RELAP5/MOD3.2.2Gamma using experimental data from LOFT Test L2-5 indicates that the code is capable of acceptably simulating the behavior of the key PTS parameters.

3.9 LOFT Test L3-1

The LOFT Facility is described in Section 3.7. Three LOFT tests were used in the assessment of RELAP5 for the PTS application. The third test, LOFT L3-1, represents an equivalent 10.16 cm [4 in] diameter break LOCA in the cold leg of a PWR. The primary purpose of this experiment was to evaluate the performance of the ECCS for cooling the core.

Prior to the test initiation the LOFT core was operating at a power of 48.9 MW. Other key initial conditions for Test L3-1 were an RCS system pressure of 14.85 MPa [2154 psia], a hot leg temperature of 574.0 K [573°F] and an intact loop flow rate of 484.0 kg/s [1067 lbm/s].

During the experimental procedure, the reactor was manually tripped just prior to the opening of the break and the reactor coolant pumps were manually tripped at the time of break opening. ECC flows from the HPI and accumulator systems were produced as the RCS pressure declined. The usable water inventory of the accumulator (that which is above the standpipe elevation) was fully discharged and the experiment was continued using HPI flow alone until 3,623 s. At that time a feed-and-bleed SG cooling process was implemented and the experiment was concluded at 4,368 s. The complete experiment procedure and the results for LOFT Test L3-1 are provided in the experiment data report, Reference 3-12.

For the purposes of the PTS assessment, this test provides data for the rapid blowdown and stabilization of the RCS with ECCS injection for a break size that is toward the larger end of the small-break LOCA spectrum. Of particular interest for the PTS study is an evaluation of RELAP5 simulation capabilities using one-dimensional and two-dimensional reactor vessel downcomer modeling approaches for the specific break size and location of this test. RELAP5 PTS plant simulations have shown variation in the calculated downcomer temperatures depending upon which downcomer modeling approach is used. For most classes of accident sequences, only minor temperature differences were observed using the two modeling approaches. Here, the word "minor" is referenced to the uncertainty in the calculated downcomer fluid temperature as generally indicated through the collective assessments documented in this report. However, much larger temperature differences were observed between plant simulations using the two different downcomer modeling approaches for cold leg LOCA sequences with a break size near the 4 in diameter equivalent break size represented by LOFT Test L3-1. Therefore the code assessment presented in this section is specifically intended to evaluate whether a one-dimensional or two-dimensional reactor vessel downcomer modeling approach provides the better simulation capability for cold leg breaks of this size.

For this assessment, RELAP5 simulations of LOFT Test L3-1 are performed using both one-dimensional and two-dimensional reactor vessel downcomer modeling approaches with the RELAP5/MOD3.2.2Gamma code. The RELAP5 LOFT system model nodalization with one-dimensional downcomer modeling is the same as used for the LOFT Test L3-7 assessment (for a 2.54 cm [1 in] diameter cold leg break) in Section 3.7; this nodalization is shown in Figures 3-61 and 3-62. Note that the LOFT facility reactor vessel contains a filler-gap region that separates

the fluid in the main region of the downcomer from the reactor vessel wall. The purpose of the filler-gap region, is to displace excess coolant in the downcomer region in order to maintain the same ratio between the downcomer and core fluid volumes in LOFT as in the PWR. The filler-gap region also insulates the downcomer fluid from the vessel wall, which in LOFT is both thicker and subject to more heat loss on a scaled basis than in a PWR. A minor portion of the vessel flow is routed through the filler-gap region in the model (represented by Annulus Component 223 in Figure 3-62). In the RELAP5 model, heat structures representing the filler blocks are connected to the downcomer fluid on the inside and to the filler-gap fluid on the outside.

For two-dimensional downcomer modeling, the RELAP5 components in the reactor vessel downcomer region (Branch Components 200, 202 and 205, and Annulus Component 210 as shown in Figure 3-62) were modified. The downcomer nodalization scheme was expanded to six azimuth sectors, comparable to the two-dimensional downcomer nodalization schemes used in the PTS RELAP5 plant models. Crossflow junction components were added to couple the vertical downcomer sectors together. Momentum flux was disabled in all downcomer internal junctions in both the axial and azimuth directions. Consistent changes were made to the hydraulic and heat structure components related to the downcomer region of the model. The azimuth sector using the node numbers shown in Figure 3-62 was defined to be that which is connected to the intact cold leg. The added RELAP5 components were numbered in a manner consistent with the existing numbering scheme. For example, Component 200 in the one-dimensional noding was converted into Components 200, 700, 750, 800, 900, and 950 in the two-dimensional noding. The broken cold leg is therefore connected to Component 802. The cross-flow junctions were input using Multiple Junction Components 714 (connecting the azimuth sectors at the Component-200 elevation), 715 (at the Component-202 elevation), 716 (at the Component 205-elevation) and 717 (at the six Component-210 elevations). Because flow in the azimuth direction is blocked by the penetrations of the hot legs through the downcomer annulus, in Multiple Junction 715 no flow paths are modeled between Cells 702 and 752 and between Cells 902 and 952. The flow loss coefficients for the reactor vessel downcomer crossflow junctions were selected by starting with a representative corresponding loss coefficient from a RELAP5 PTS plant model and scaling it, based upon the differences in the azimuth-direction flow lengths and hydraulic diameters between the full-scale plant and LOFT.

Steady-state calculations with one- and two-dimensional downcomer modeling were first performed to simulate the system conditions present at the start of LOFT Test L3-1. Table 3-17 compares the initial conditions from the test and calculations. The calculated and nominal measured data for all parameters except the hot and cold leg temperatures are in excellent agreement. The calculated initial hot leg and cold leg temperatures were respectively 1.0 K and 1.9 K higher than the nominal measured values from the experiment. The measurement uncertainties for the intact loop hot and cold leg temperatures are listed as ±1 K and ±3 K, respectively, in Table 3 of Reference 3-12. Since the calculated initial temperatures are within the uncertainties of the nominal initial measured temperatures, the comparison between the initial measured and RELAP5-calculated data was judged to be acceptable for the purposes of this assessment. As an aside, the 200 kW total LOFT facility heat loss is represented in the RELAP5 model and is distributed 6 kW in the pressurizer region, 20 kW in the intact SG region and 174 kW in the reactor vessel and coolant loop piping regions. Table 3-17 also shows that the initial conditions from the two RELAP5 steady-state calculations are virtually identical.

RELAP5 simulations of Loft Test L3-1 were performed using the system model with the one- and two-dimensional reactor vessel nodalization schemes described above. A summary of the

measured and calculated sequences of events is presented in Table 3-18. The comparison shows very good agreement between the measured event times and the calculated event times from the two RELAP5 runs up to about 700 s. The onset of accumulator injection was 67 s later in the calculations than in the test and this, coupled with more erratic accumulator discharge behavior in the calculations than in the test, led to longer delays in the calculated times for sequence events during and after the accumulator injection period.

Figure 3-79 compares the RCS pressure responses from the test and the two RELAP5 calculations. The measurement uncertainty is +0.223 MPa. The calculated pressures are judged to be in very good agreement with the measured pressure over the entire test period. The differences in the measured and calculated pressure responses could result from many factors, such as system heat loss, break flow and HPI or accumulator-induced condensation effects. Although the calculated and measured pressures agree well on an absolute basis, the derivatives of the pressures do not compare particularly well over the first 1,000 s of the test period. Between about 100 s and 650 s, the shape of the measured pressure curve is concave downward and between 650 s and 1,000 s it is concave upward. Just the opposite behavior is noted in the calculations over these two periods, which are before and during the accumulator injection period, respectively. As discussed below, the RELAP5-calculated pressures show variations during the period from about 1,000 s to 2,000 s which affect the discharge of the last 2/3 of the accumulator liquid inventory.

The intact loop SG secondary pressures are compared in Figure 3-80. The measurement uncertainty is +0.110 MPa. Auxiliary feedwater is delivered at 0.5 kg/s [1.1 lbm/s] from 75 s to 1,870 s both in the test and in the calculations. The calculated and measured data are in excellent agreement up to about 500 s. Afterward, the calculated pressures decline moderately below the measured pressure, perhaps due to an overprediction of condensation within the SG secondary system caused by injection of cold auxiliary feedwater. RELAP5 models the SG secondary region with relatively large fluid cells, which promotes this condensation.

Due to a lack of suitable instrumentation, the timing of the interruption of intact loop natural circulation flow in the experiment cannot be reliably established. In the test, the RCS pressure falls below the SG secondary pressure at 375 s; afterward neither full-loop and reflux-cooling natural circulation cooling modes can be supported. Because the RELAP5 calculated RCS pressures fall more slowly than in the test this pressure condition is reached later, but only by about 44 s, in the calculations. The flow through the pump suction cold leg region stops at about 147 s in the RELAP5 calculations. Although less than conclusive, this comparison between the calculated and measured data indicates a generally-acceptable prediction of the loss of loop natural circulation flow behavior in the test.

The accumulator level responses are compared in Figure 3-81. The measurement uncertainty is +0.02 m. Once the accumulator inventory has been depleted, nitrogen flows from the accumulator into the RCS both in the test and in the calculations. The moderately slower RCS depressurization in the calculations results in the accumulator injection beginning 67 s later in the calculations than in the experiment. More importantly, during the discharge of the first 1/3 of the accumulator liquid inventory, the injection rate of the test is seen to be very well predicted in the calculation with the two-dimensional downcomer model but overpredicted in the calculation with the one-dimensional downcomer model.

The discharge of the remaining 2/3 of the accumulator liquid inventory is seen to be erratic in both calculations but smooth in the experiment. This discharge occurs during the period after about

1,000 s, when the RCS pressure has fallen below about 2.7 MPa [392 psia] and the depressurization has slowed, as seen in Figure 3-79. The erratic accumulator discharge during this portion of the calculations is related to effects of the vapor density becoming smaller as the pressure declines. As the RCS pressure falls, both the accumulator injection rate and the volume of steam that is condensed become more sensitive to variations in the RCS pressure. An increasing feedback develops between the accumulator injection rate and the steam volume removed by the condensation resulting from injecting cold water into the RCS. The smooth injection behavior seen in the test data at the lower RCS pressures cannot be replicated with RELAP5 because the model consists of discrete fluid cells in which the fluid is considered to be homogeneous. The model therefore tends to: (1) underestimate the existence of thin liquid layers that been warmed by steam condensation and which impede further condensation and (2) overestimate the incremental volumes of steam that are available to be condensed.

Figure 3-82 shows the fluid temperature responses in the pump-discharge intact cold leg between the ECC injection nozzle and reactor vessel. The measurement uncertainty is $\pm$6.4 K. Test data from thermocouples near the top and bottom of the horizontal cold leg cross section are provided. The cold leg fluid temperatures in both RELAP5 calculations are seen to fall dramatically from the effects of HPI injection following the interruption of loop natural circulation flow and then recover with the onset of accumulator injection flow. The test data exhibit considerable thermal stratification in the horizontal cold leg, with cold fluid in the lower portion of the cold leg cross section and with warmer fluid in the upper portion of the cold leg cross section. Since the ECCS temperatures in the experiment are cold (304.7 K [89°F]), the temperatures exhibited in the top-of-cold leg test data indicate a mixing of warm water and/or steam with the cold ECCS within the intact cold leg and adjacent regions of the reactor vessel during most of the test period.

RELAP5 modeling of the cold leg region is one-dimensional and the code cannot represent thermal stratification effects seen within the LOFT intact loop cold leg pipe. The fluid within each RELAP5 hydrodynamic cell must be characterized using only a single set of liquid and steam temperatures. Figure 3-82 shows that the RELAP5-calculated liquid temperatures in the intact cold leg lay between the test data reflecting cold water in the bottom cold leg and warmer water in the top of the cold leg.

Figures 3-83 through 3-88 show the reactor vessel downcomer fluid temperature comparisons. Fluid temperature measurements in the LOFT downcomer are taken in two vertical thermocouple "stalks" that are near (but not directly beneath) the intact and broken loop reactor vessel cold leg nozzles. The six figures present comparisons for three elevations (just under the cold leg nozzles, near the mid-plane of the core and near the bottom of the downcomer) for each of the two stalks. The comparisons between the code predictions and experimental data are much the same for all six locations. Results from both RELAP5 calculations are mostly consistent with the test data before about 700 s, when the accumulator injection begins. However from about 700 s to 950 s the RELAP5-calculated temperatures fall about 10 to 20 K [18 to 36°F] below the measured temperatures and remain lower until the accumulators are depleted of liquid. The reason for the temperature underprediction relates to the difference noted between the calculated and measured cold leg behavior due to thermal stratification.

Figure 3-89 compares the measured fluid temperature data in the top and bottom regions of the intact cold leg pipe and the upper downcomer region the intact side of the vessel. The figure indicates that the downcomer temperature is slightly above the temperature of the warm water in the upper region of the cold leg. This result indicates that there is significant fluid mixing occurring

in the experiment within the intact cold leg, within the upper region of the vessel downcomer, or in both locations. This mixing leads to a relatively warm downcomer temperature that more reflects the temperature at the top of the cold leg than it does the colder temperature at the bottom of the cold leg or some average of the upper and lower cold leg temperatures.

Figure 3-90 shows the comparable RELAP5-calculated data for the temperature in the one-dimensional cold leg and in the upper downcomer region (on the intact side for the two-dimensional RELAP5 calculation). The results for both calculations are similar. The cold leg temperature response prior to the onset of accumulator injection at 701 s reflects a period of relatively low flow with a pooling of cold HPI water in the cold leg. After the accumulator injection begins, however, the situation becomes highly turbulent. First, the slug of cold water that had pooled in the cold leg is swept into the downcomer, leading to the rapid decline in the downcomer temperatures in Figures 3-83 through 3-88. As the accumulator continues its injection the condensation produced mixes up the fluid in the entire region (including both the downcomer and cold leg) and this leads to the increase in calculated cold leg temperatures seen in Figure 3-90.

Figure 3-91, which overlays the six measured downcomer fluid temperatures, shows a relatively small spread (about 9 K [16°F]) among the measured temperatures. The same comparisons are made for the RELAP5 one-dimensional downcomer fluid temperatures in Figure 3-92 and for the RELAP5 two-dimensional downcomer fluid temperatures in Figure 3-93. The spread of calculated temperatures is about 8 K with the one-dimensional downcomer modeling and about 11 K [20°F] with the two-dimensional downcomer modeling.

Figure 3-94 compares the break mass flow responses of the experiment and two calculations. The experimental data for LOFT L3-1 break flow was derived from other measurements and presented in Figure 170 of Reference 3-12. The measured break flow results shown here were digitized from that figure. RELAP5 overpredicts the break flow rate from about 100 s to 400 s and this is despite the calculated pressures being lower than the measured pressure during this period as shown in Figure 3-79. The break flow remains moderately overpredicted between about 400 s and 700 s and this delays the onset of accumulator injection in the calculations. Overall, the break flow predictions are considered good.

Figure 3-95 compares the void fractions in the intact and broken-loop sides of the reactor vessel downcomer at the cold leg elevation from two RELAP5 calculations. The figure shows that in general the downcomer region at this elevation is highly-voided, which provides a potential for condensation effects resulting from the onset of accumulator injection leading to a more turbulent flow solution. This comparison also shows for the two-dimensional downcomer model that from about 700 s to 950 s the broken-loop side of the two-dimensional downcomer model is steam filled, while the intact-loop side of the downcomer includes some liquid content. With the one-dimensional model, the steam-filled condition does not occur. The two-dimensional downcomer model provides a capability for simulating this void difference from one side of the downcomer to the other, which has a potential to affect the break flow. However, no significant break flow differences between the two calculations are observed in Figure 3-94 during this period.

Figure 3-96 compares the lower downcomer flow responses and Figure 3-97 compares the core inlet flow responses between the two RELAP5 calculations. The flow rates shown in these figures are relatively small; for perspective, the flow rate at the start of the experiment with the reactor coolant pumps operating is 484 kg/s [1067 lbm/s]. Both figures indicate that the flow behavior becomes significantly more turbulent and oscillatory when the accumulator injection begins at 701

s, as described above. The figures show that the one-dimensional downcomer model leads to larger manometer-type oscillations which mix fluid between the downcomer and core regions than does the two-dimensional model. However, unlike the one-dimensional downcomer model, the two-dimensional downcomer model provides the necessary additional flow paths to allow for circulation to go on within the downcomer region itself. Therefore, both models provide mechanisms for mixing the water in the downcomer region, but the mechanisms with the two models are different. The net effect of the mixing in the calculations is seen in the downcomer fluid temperature responses in Figures 3-83 through 3-88. Generally, the two-dimensional model leads to slightly cooler downcomer fluid temperatures than the one-dimensional model. This temperature difference on average is about 10 K [18°F].

This assessment indicates that the behavior in the reactor vessel downcomer region is particularly difficult to predict for a break of this size and location. Accumulator injection has a potential for directly influencing the downcomer temperature, but mixing within the cold leg and upper downcomer regions significantly affects that influence. The effects of this mixing are evident in the test data and also in the calculations, although no claim is made that the actual mixing locations and mechanisms in the experiment are well represented in either of the RELAP5 calculations. In particular, the prediction of mixing that occurs within the thermally-stratified cold leg region is beyond the capability of RELAP5 models. The break is large enough that the RCS depressurizes sufficiently to result in accumulator injection, but not so large as to allow for an accumulator discharge that is insensitive to the RCS pressure. There are feedback effects among the downcomer injection rate, the break flow rate and RCS pressure responses. Further, the break location in the cold leg adds to the difficulty for the code prediction because the most direct path for steam to reach the break is upward through the downcomer, against the downward flow of cold accumulator water. Therefore, interphase condensation modeling, known to be a weakness of RELAP5, appears to be a particularly important process when predicting the vessel downcomer temperature for this break size and location.

In summary, the results from assessing RELAP5/MOD3.2.2 Gamma capabilities for predicting the behavior in LOFT Test L3-1 indicate a reasonable prediction capability for most of the reactor coolant system parameters. The assessment indicates that the two-dimensional reactor downcomer modeling approach provides a better match with the measured accumulator injection response over period when the first 1/3 of the accumulator liquid inventory is discharged. Both modeling approaches led to similar injection predictions that were more erratic than in the test data during the period when the second 2/3 of the accumulator liquid inventory is discharged. The additional capabilities provided by a two-dimensional downcomer model, which are needed to represent different fluid conditions on the intact and broken loop sides of the reactor vessel downcomer, were not seen to result in a better prediction of break flow or other parameters. The assessment indicates that the downcomer fluid temperatures in the test were underpredicted using both one- and two-dimensional downcomer modeling approaches. For this test, RELAP5 underpredicted the measured downcomer temperature by a maximum of 41 K [74°F] and overpredicted it by a maximum of 9.1 K [16°F]. Over the full test period, RELAP5 underpredicted the measured downcomer temperature by an average of 12 K [21°F] and varied from the measured downcomer temperature by an average of 12 K [22°F].

Given: (1) the better accumulator injection behavior it produced, (2) the capability it provides for predicting different fluid behavior in the intact and broken-loop sides of the reactor vessel downcomer (which can affect both mixing within the downcomer and the break flow) and (3) the more conservative downcomer fluid temperature predictions it produces, two-dimensional modeling

of the reactor vessel downcomer region is judged to be the more appropriate approach for RELAP5 PTS applications.

Table 3-17   Comparison of Measured and Calculated Initial Conditions for LOFT Test L3-1

Parameter	Initial Condition	
	Measured	RELAP5 1D-DC
		RELAP5/2D-DC
Reactor Power	48.9 MW	48.9 MW
		48.9 MW
Intact Loop Mass Flow Rate	484.0 kg/s [1064.8 lbm/s]	481.3 kg/s [1058.9 lbm/s]
		481.3 kg/s [1058.9 lbm/s]
Intact Loop Hot Leg Pressure	14.85 MPa [2153.8 psia]	15.01 MPa [2177.0 psia]
		15.01 MPa [2177.0 psia]
Intact Loop Hot Leg Temperature	574.0 K [573.5°F]	575.0 K [575.3°F]
		575.0 K [575.3°F]
Intact Loop Cold Leg Temperature	554.0 K [537.5°F]	555.9 K [541.0°F]
		555.9 K [541.0°F]
Pressurizer Level	1.10 m [3.61 ft]	1.097 m [3.60 ft]
		1.097 m [3.60 ft]
SG Secondary Pressure	5.43 MPa [787.6 psia]	5.417 MPa [785.7 psia]
		5.417 MPa [785.7 psia]
SG Secondary Level	3.15 m [10.33 ft]	3.202 m [10.51 ft]
		3.203 m [10.51 ft]
SG Feedwater and Steam Flow Rate	25.0 kg/s [55.0 lbm/s]	26.77 kg/s [58.59 lbm/s]
		26.77 kg/s [58.59 lbm/s]

Table 3-18   Summary of Measured and Calculated Sequences of Events for LOFT Test L3-1

| Event Description	Event Time (s)	
	Measured	RELAP5 1D-DC/ RELAP5/2D-DC
Break valve opened	0	0 / 0
Primary coolant pumps tripped	0.04	0 / 0
HPI flow initiated	4.6	4.6 / 4.6
Pressurizer empty	17.0	23.5 / 23.5
Primary coolant pump coast-down completed, loop natural circulation begins	19.0	29.3 / 29.3
Upper plenum pressure reaches saturation	24.4	36.2 / 36.2
Auxiliary feedwater flow initiated	75.0	75.0 / 75.0
Loop natural circulation flow stops	---	146 / 147
Primary system pressure falls below secondary system pressure	375	420 / 418
Accumulator flow initiated	634	701 / 701
Accumulator empty (level below standpipe)	1,570	1,825 / 2,055
Accumulator injection line empty	1,741	2,128 / 2,110
Auxiliary feedwater flow terminated	1,870	1,870 / 1,870
SG secondary blowdown initiated	3,623	--- / ---
Termination of experimentor calculation	4,368	3,600 / 3,600
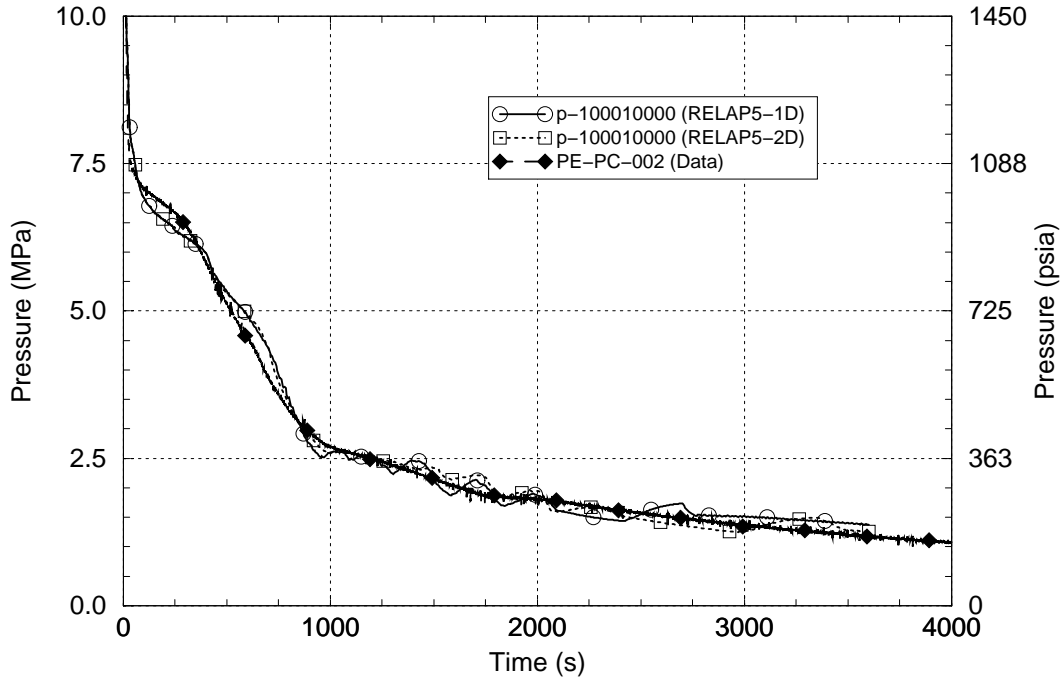
Figure 3-79   RCS Hot Leg Pressure – LOFT Test L3-1
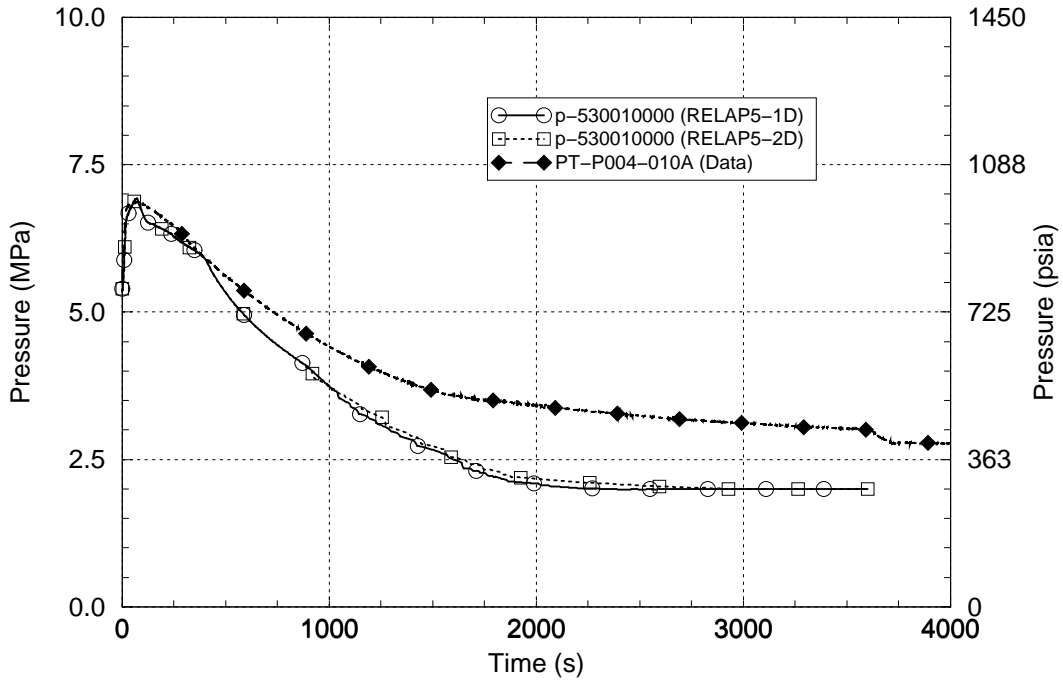

Figure 3-80   Intact Loop SG Secondary Pressure – LOFT Test L3-1
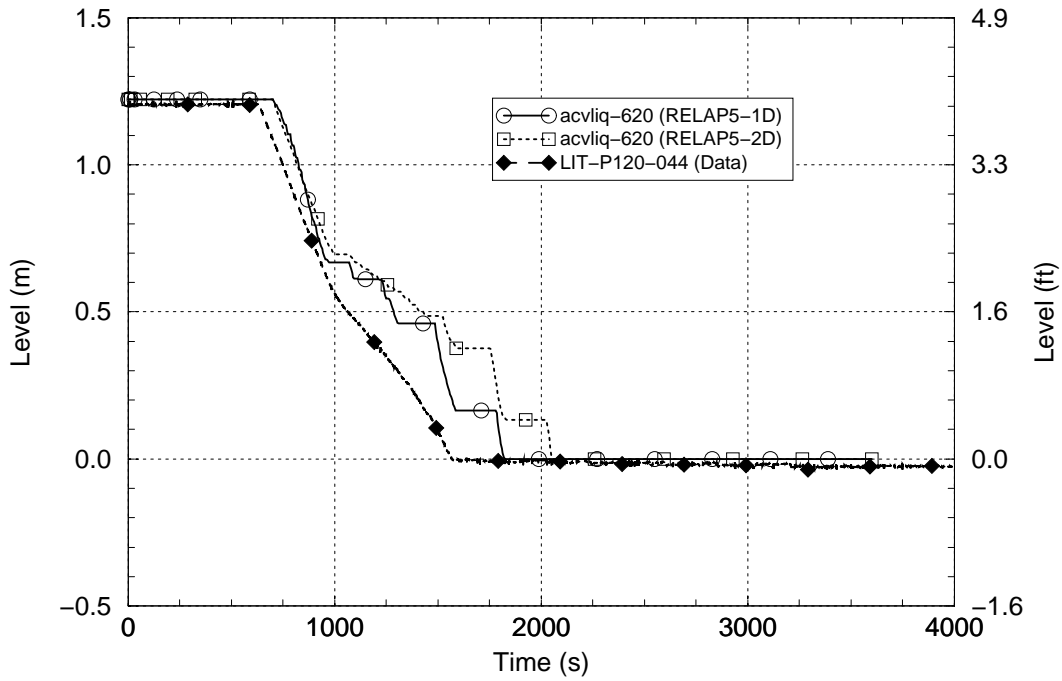
Figure 3-81   Accumulator Level – LOFT Test L3-1
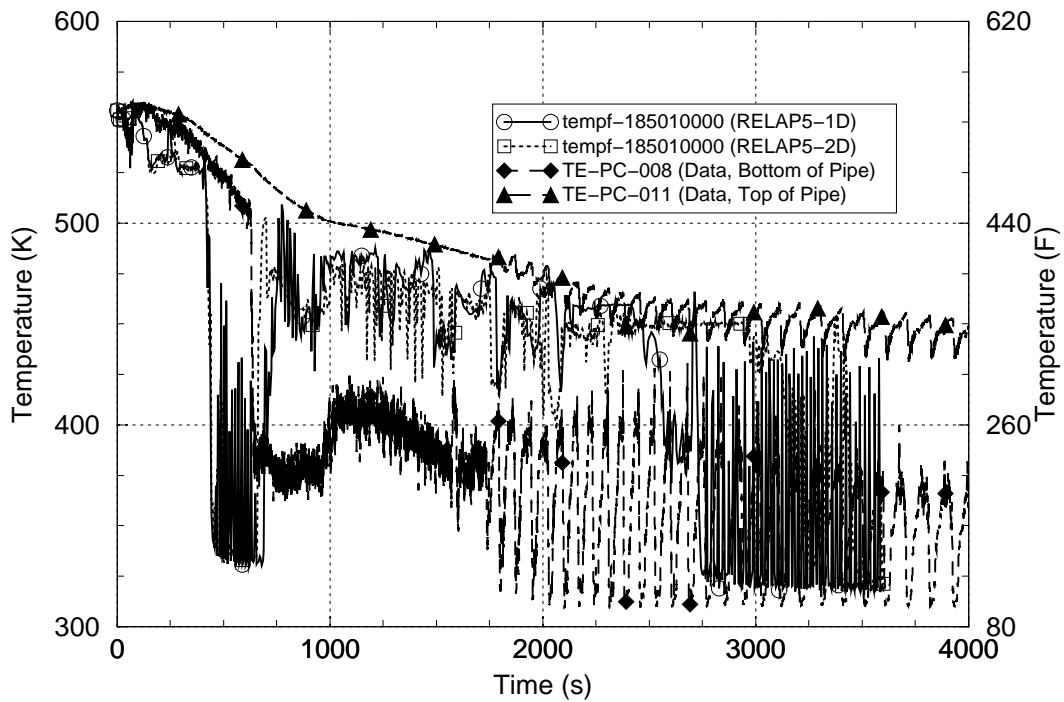

Figure 3-82   Intact Loop Cold Leg Fluid Temperature – LOFT Test L3-1

Figure 3-83   Upper Downcomer Fluid Temperature, Intact Loop Side – LOFT Test L3-1

Figure 3-84   Middle Downcomer Fluid Temperature, Intact Loop Side – LOFT Test L3-1
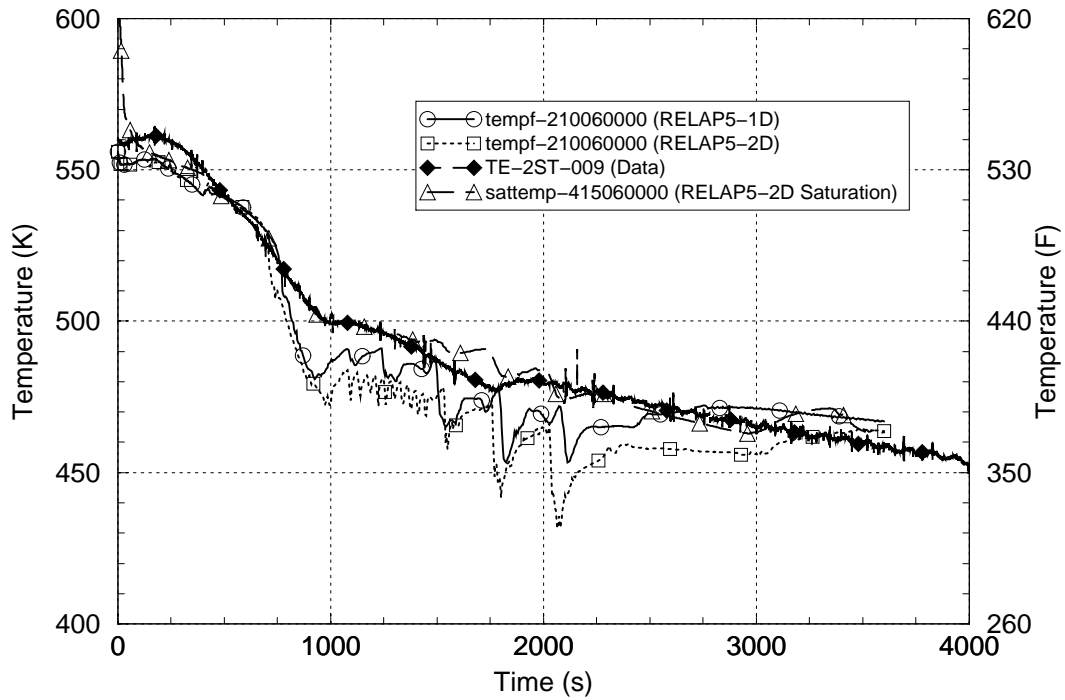
Figure 3-85   Lower Downcomer Fluid Temperature, Intact Loop Side – LOFT Test L3-1
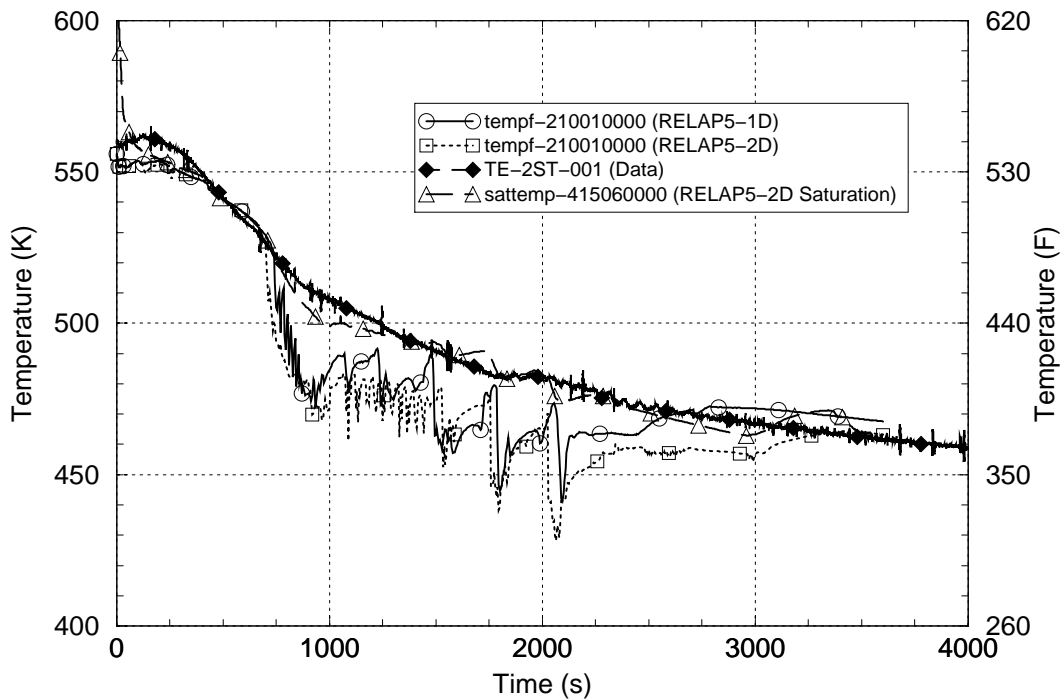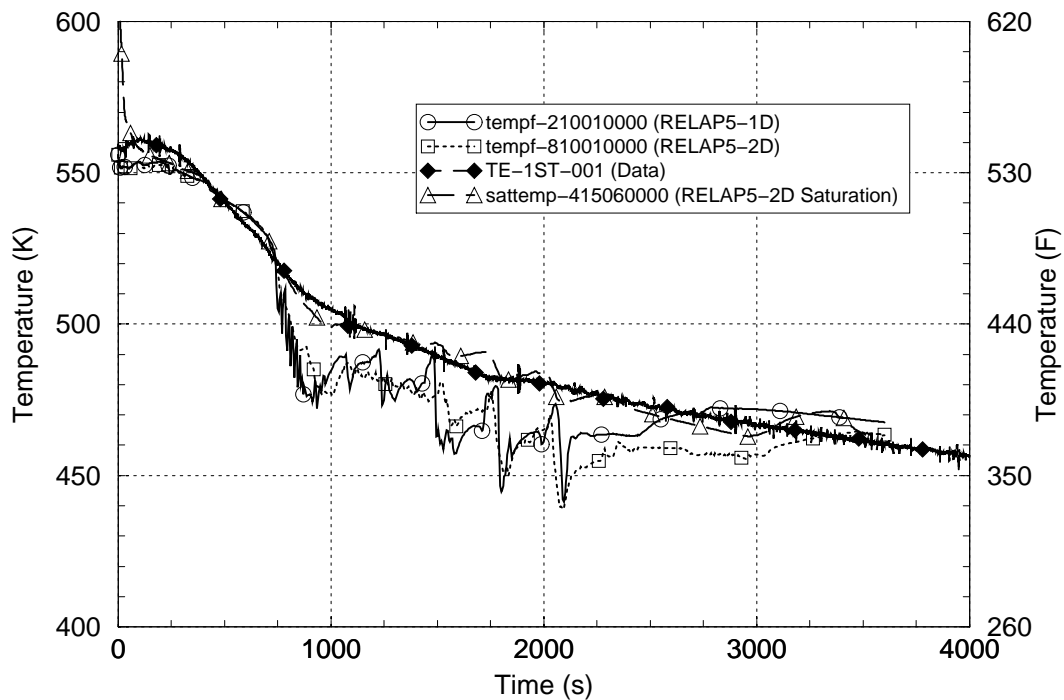

Figure 3-86   Upper Downcomer Fluid Temperature, Broken Loop Side – LOFT Test L3-1

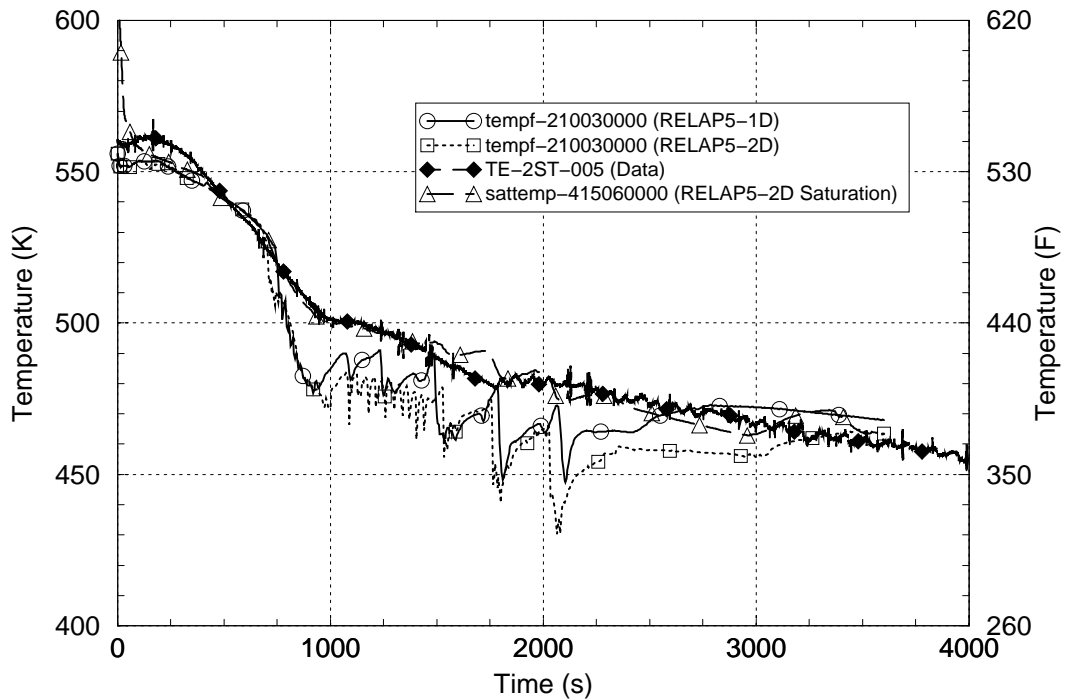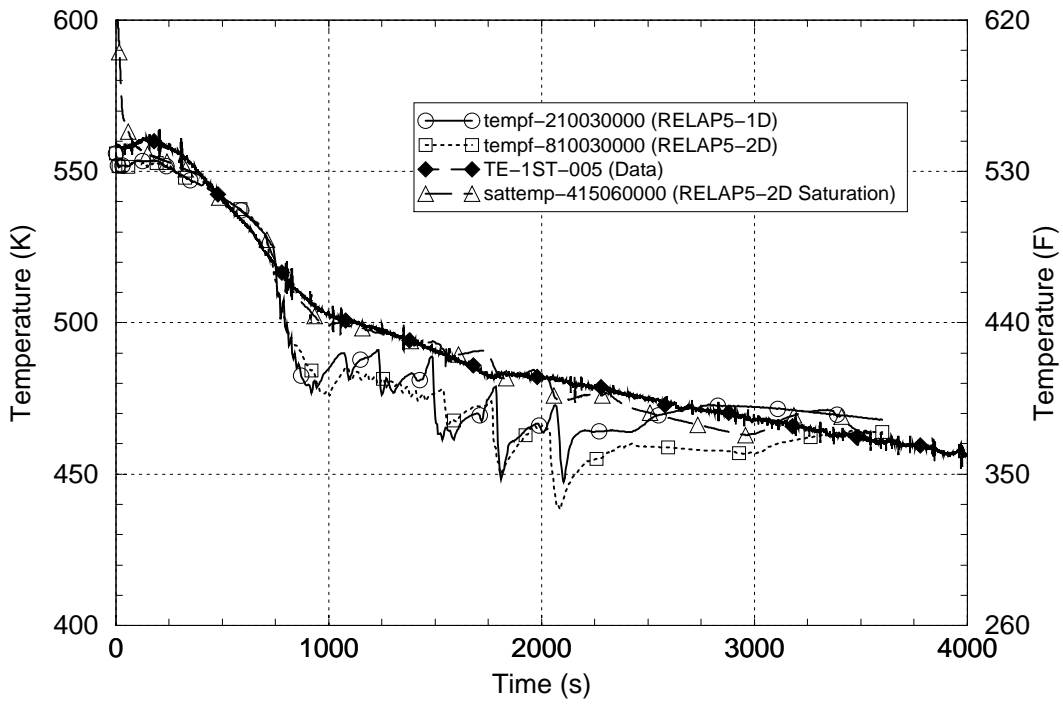**Figure 3-87   Middle Downcomer Fluid Temperature, Broken Loop Side – LOFT Test L3-1**
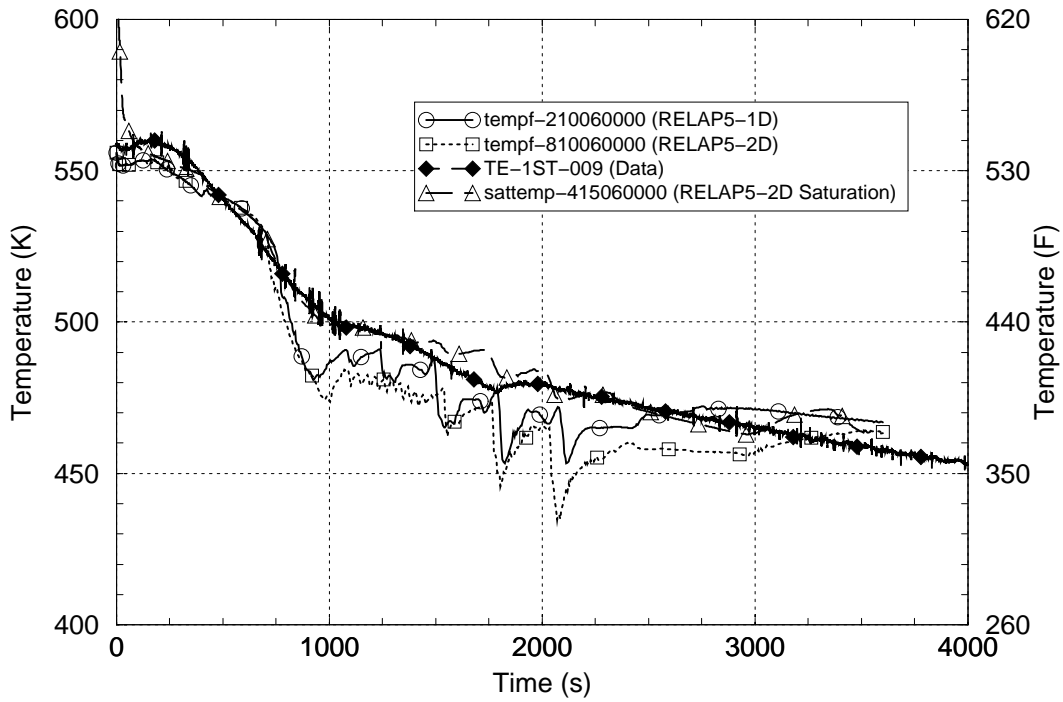
Figure 3-88   Lower Downcomer Fluid Temperature, Broken Loop Side – LOFT Test L3-1
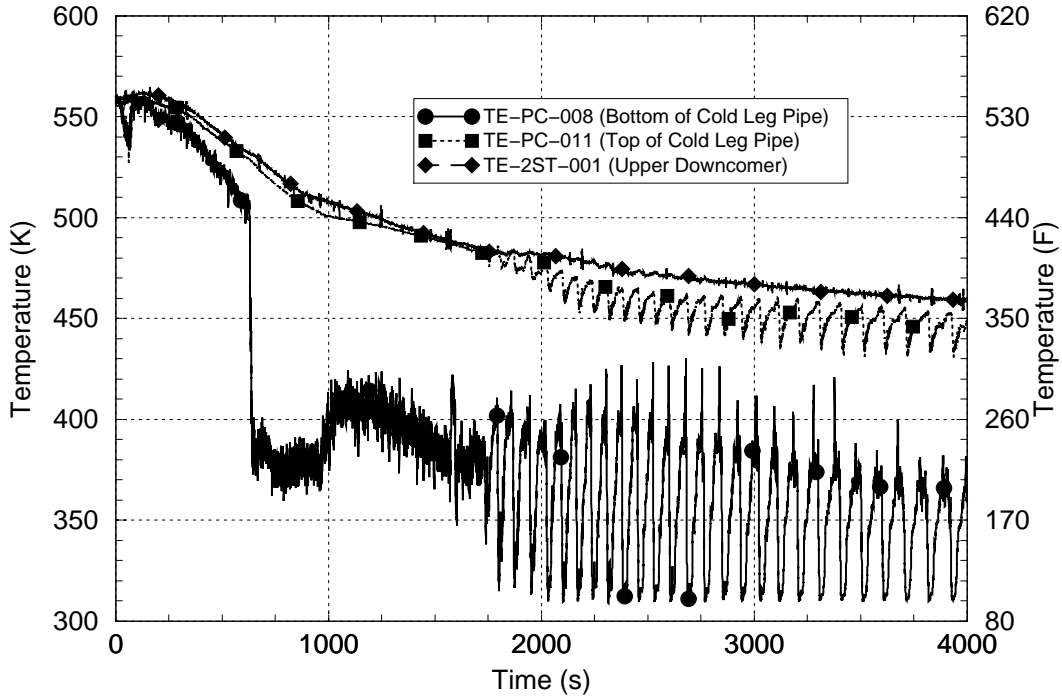
Figure 3-89   Intact Side Measured Cold Leg and Upper Downcomer Fluid Temperatures – LOFT Test L3-1
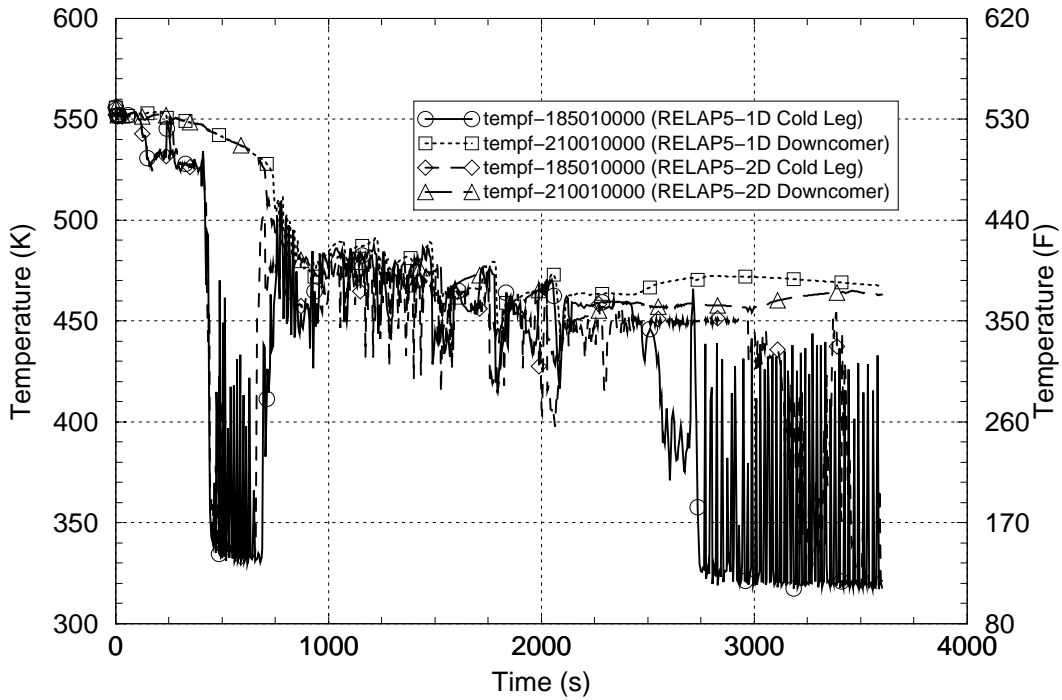
Figure 3-90   Intact Side RELAP5 Calculated Cold Leg and Upper Downcomer Fluid Temperatures – LOFT Test L3-1
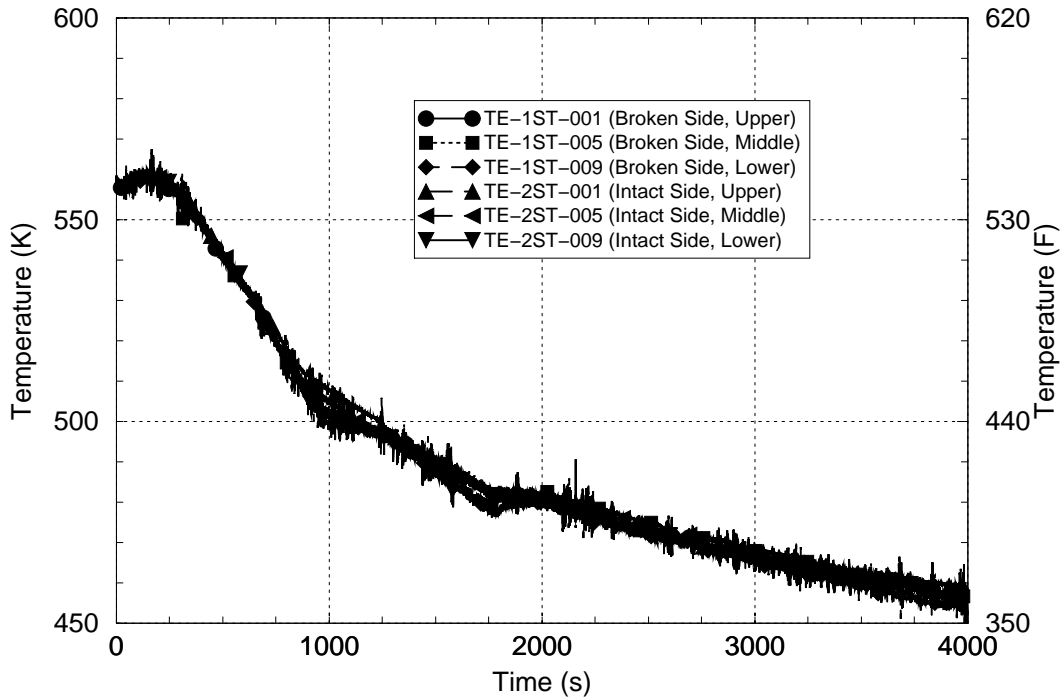
Figure 3-91   Measured Fluid Temperatures in the Downcomer – LOFT Test L3-1
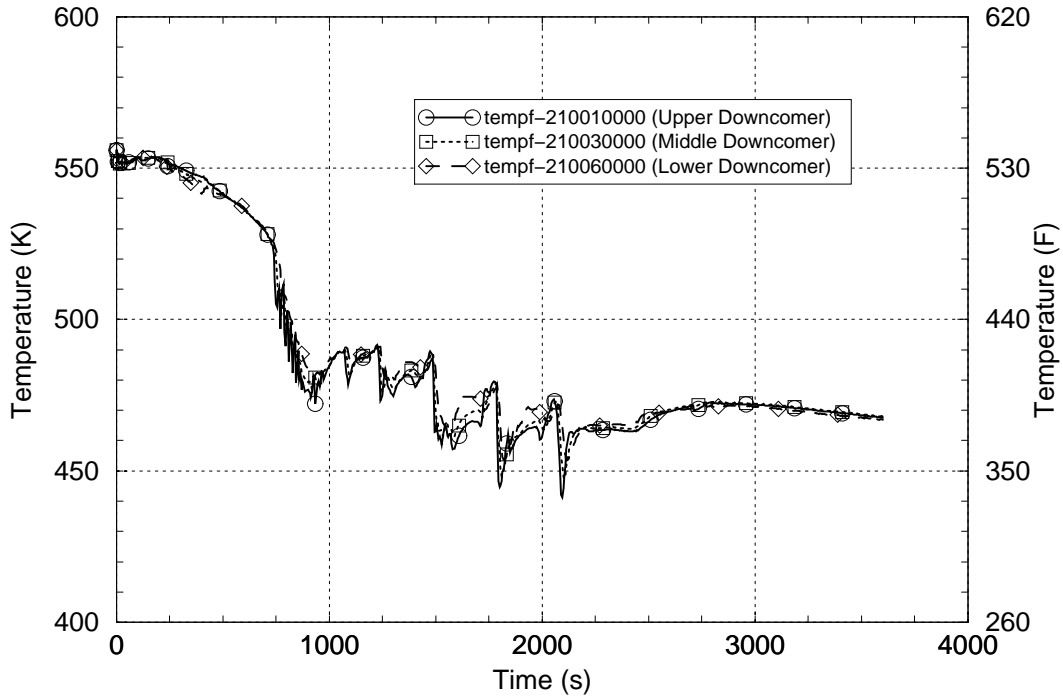
Figure 3-92   RELAP5 Calculated Fluid Temperatures in the 1-D Downcomer – LOFT Test L3-1
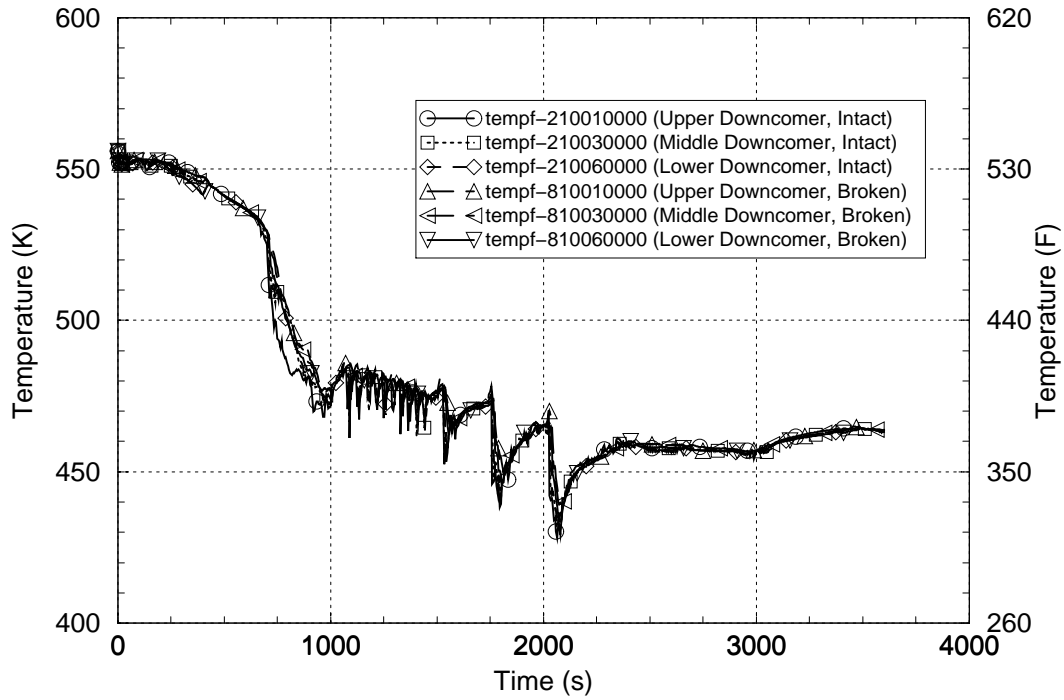
**Figure 3-93   RELAP5 Calculated Fluid Temperatures in the 2-D Downcomer –
LOFT Test L3-1**
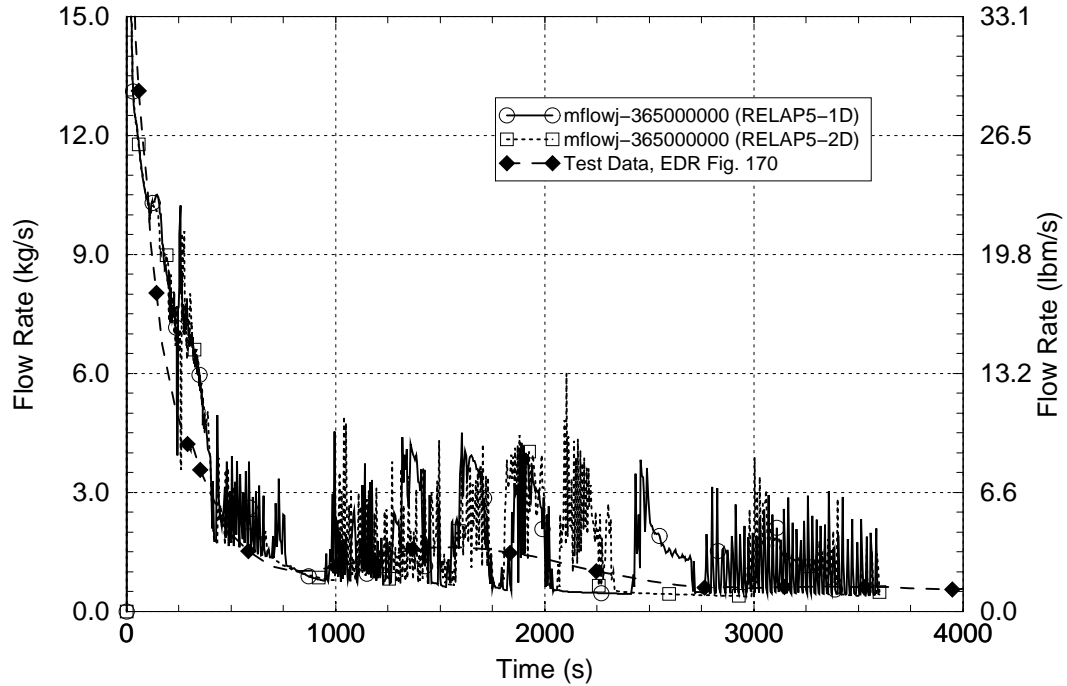
Figure 3-94   RELAP5 Calculated Break Mass Flow – LOFT Test L3-1
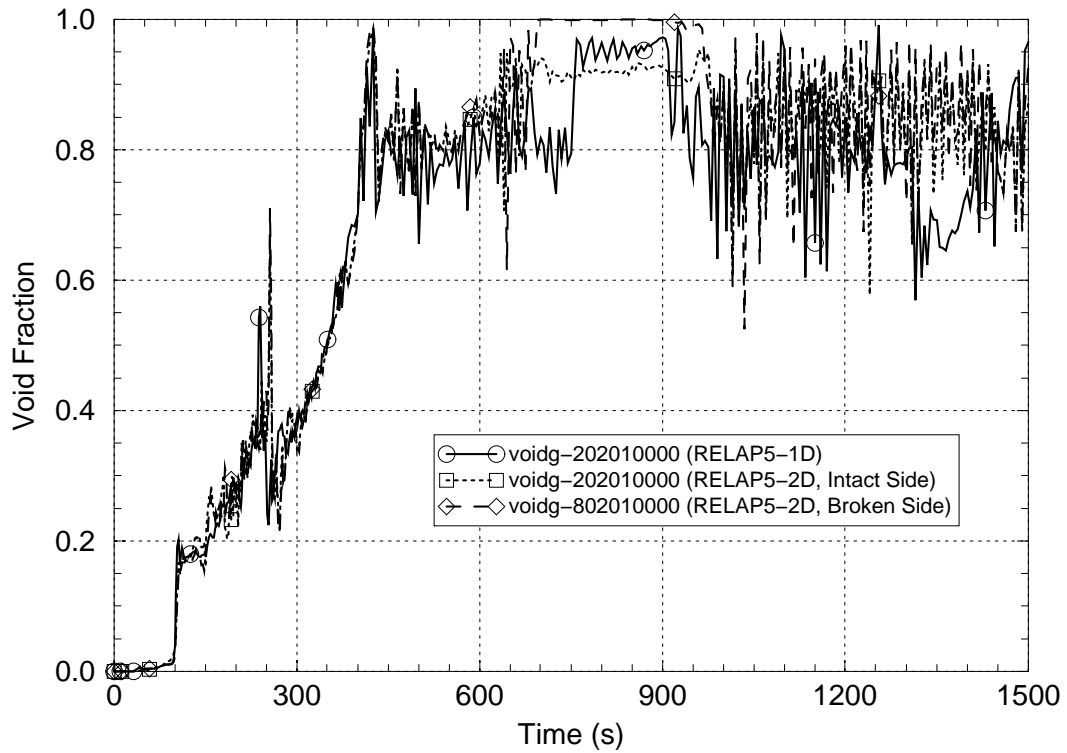
**Figure 3-95   RELAP5 Calculated Void Fractions in Downcomer at Cold Leg Elevation –
LOFT Test L3-1**
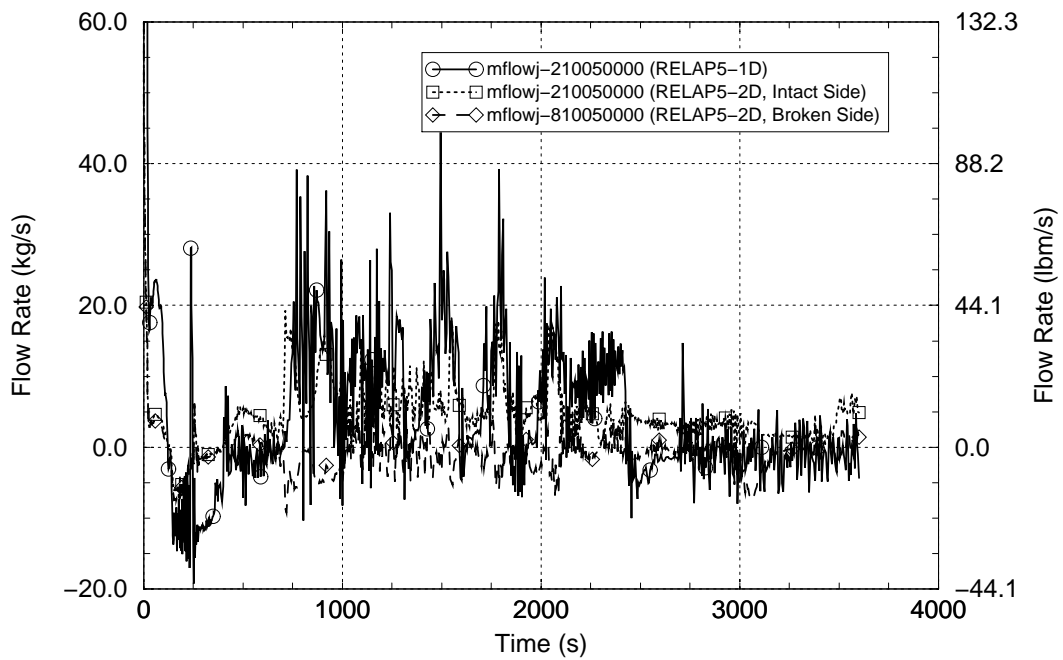
Figure 3-96   RELAP5 Calculated Flows in the Lower Downcomer – LOFT Test L3-1
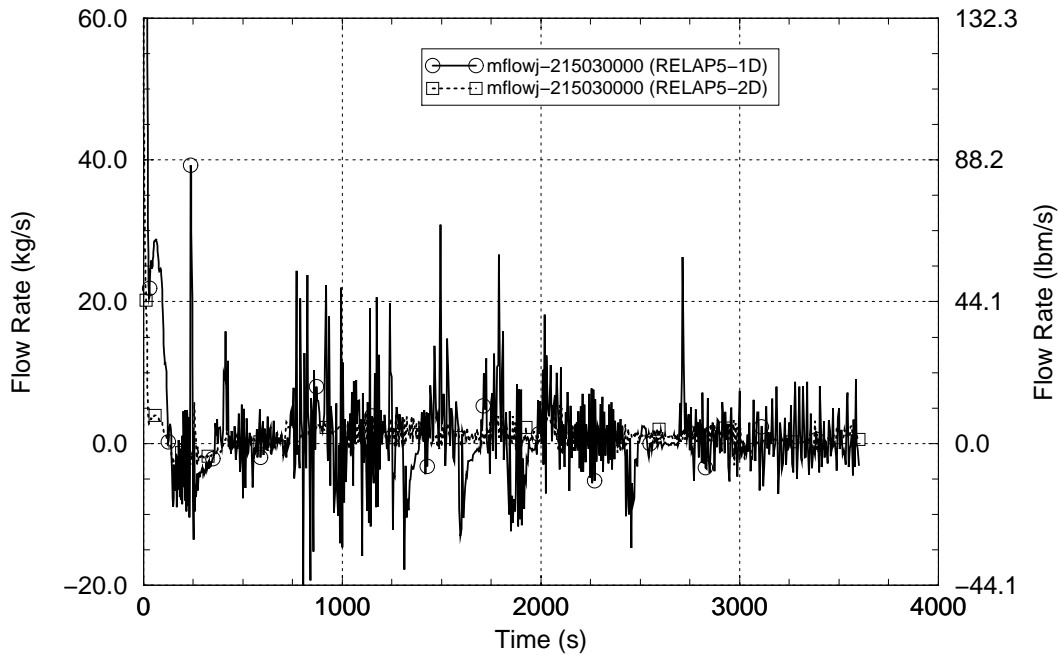
Figure 3-97   RELAP5 Calculated Core Inlet Flow Rates – LOFT Test L3-1

3.10   MIST Test 360499

MIST (Multi-loop Integral System Test) is a scaled, full-pressure experimental facility that represents a Babcock and Wilcox (B&W) lowered-loop plant design with two hot legs and four cold legs. The plant-to-test facility power scaling factor is 817 and the plant-to-test facility volume scaling factor is 620 for the total primary system volume, excluding the core flood tanks (CFTs). Figures 3-98 and 3-99 show the arrangement of the MIST experimental facility. Major components in MIST include two once-through steam generators (OTSGs) with full-length tubes, two hot leg piping segments, four cold leg piping segments, four reactor coolant pumps, a reactor vessel with an external downcomer, a pressurizer with spray and PORV connections and one CFT. Boundary systems provide simulation of the HPI, LPI and emergency feedwater (EFW) systems, and various types of failures such as steam generator tube ruptures and LOCAs. The configuration of the MIST facility is described in Reference 3-13.

Three MIST tests are used in the assessment of RELAP5/MOD3.2.2Gamma for PTS applications. The first test, 360499, represents HPI/pressurizer PORV feed-and-bleed cooling operation in a B&W PWR. At the beginning of the test, the MIST facility was operating at 110% scaled reactor coolant flow and 10% scaled power. The initial RCS pressure for the test was 14.82 MPa [2,150 psia] and the core exit subcooling margin was 47.2 K [85.0°F]. The feed-and-bleed operation was initiated by interrupting all feedwater flow and isolating the steam flow paths on both steam generators. The core power decay was initiated 9 s into the transient event sequence. The test procedures and results are described in Volume 8 of Reference 3-14.

STEAM GENERATOR B

PUMP

PUMP

COLD LEG B1

COLD LEG B2

HOT LEG B

N

VESSEL

DOWNCOMER

COLD LEG A1

HOT LEG A

COLD LEG A2

PRESSURIZER

PUMP

PUMP

STEAM GENERATOR A

Reactor Coolant System Layout

Figure 3-98   Layout View of the MIST Test Facility Reactor Coolant System

Figure 3-99   Elevation View of the MIST Test Facility Reactor Coolant System

The system behavior for this test resembles a stuck-open pressurizer PORV accident event with continued HPI injection and HPI throttling based on the RCS subcooling ma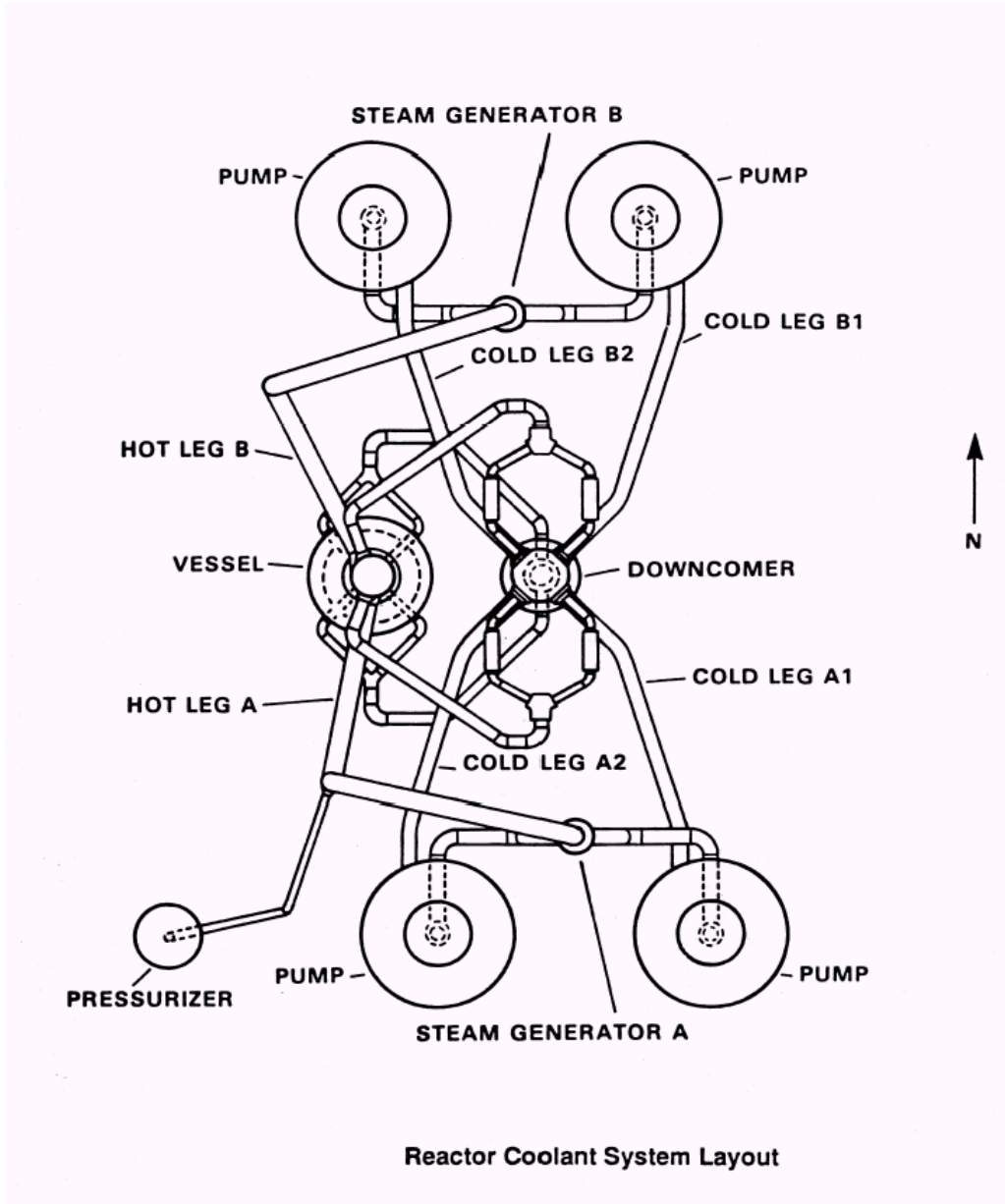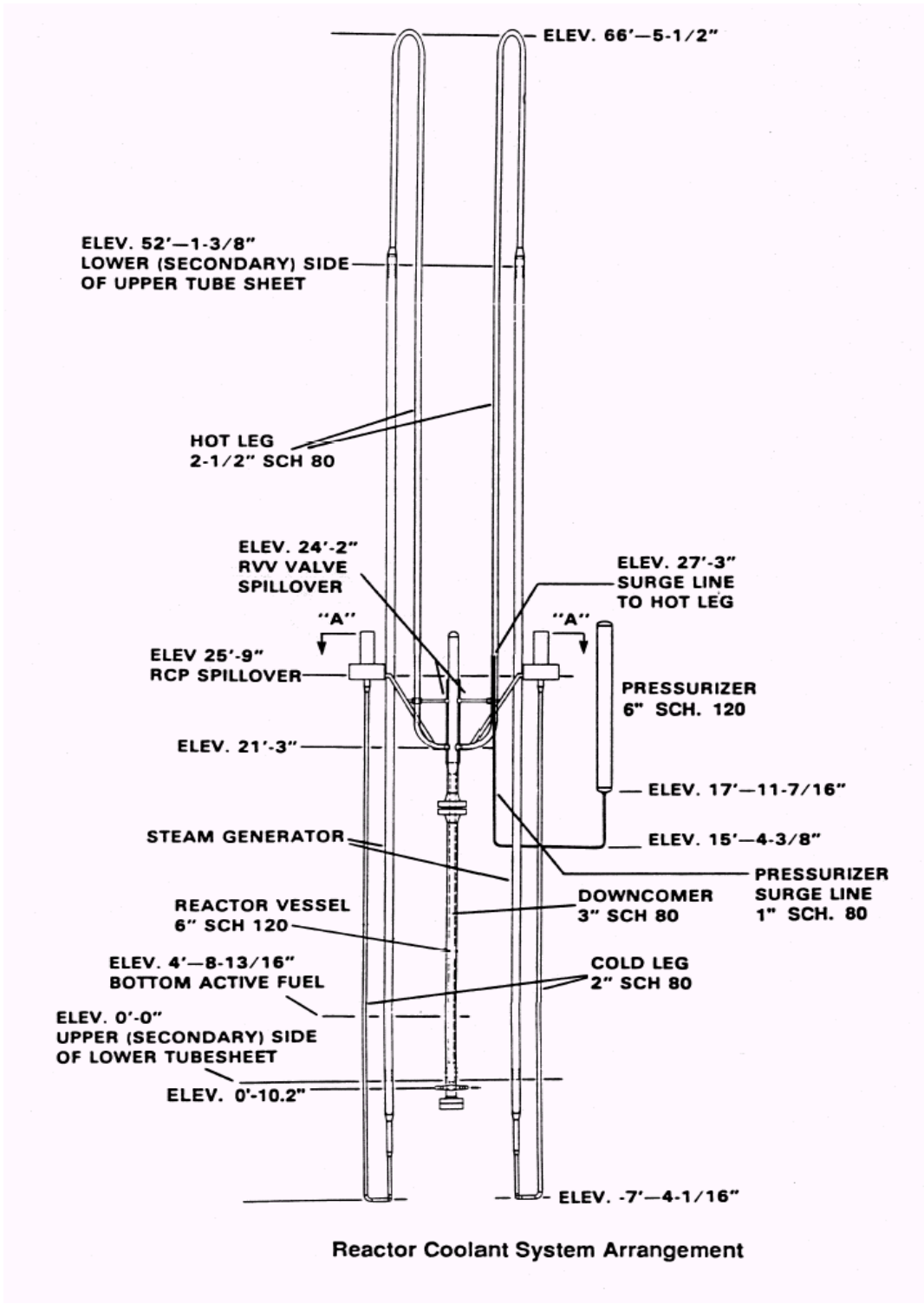rgin. Accident events such as this are significant contributors to the risk of PTS vessel failure, particularly for accidents in which the PORV is postulated to subsequently re-close.

A simulation of MIST Test 360499 was performed using the RELAP5/MOD3.2.2Gamma code. The RELAP5 nodalization for the MIST facility is shown in Figure 3-100. Table 3-19 lists the initial conditions for the test; the comparison shows good agreement between the measured and RELAP5-calculated data. A summary of the measured and calculated transient sequences of events for the test is presented in Table 3-20. The comparison shows good agreement between the calculated and measured event times.

The calculated and measured pressurizer PORV and HPI flow responses are shown in Figures 3-101 and 3-102, respectively. The HPI flow rates presented represent the sum of the HPI flows delivered to the cold legs on the four coolant loops. The RELAP5-calculated responses for these parameters are excellent agreement with the experimental data.

The calculated and measured RCS pressure responses are shown in Figure 3-103.   The RELAP5-calculated response is in excellent agreement with the experimental data.

The calculated Loop A and B cold leg flow rate responses are shown in Figures 3-104 and 3-105, respectively. The calculated data presented are for cold leg locations between the HPI injection nozzles and the reactor vessel. The figures show that coolant loop circulation flow continued throughout the calculation in Loop A and was interrupted at 6,232 s in Loop B. Figure 3-105 also shows that, for about 10,000 s after Loop B stagnated, the RELAP5 simulation included a circulation around the flow loop formed by the SG B outlet plenum, the two Loop-B cold legs and the reactor vessel downcomer. Issues relating to this same-loop cold leg flow circulation and its effects are discussed in detail in Section 3.11. The cold leg flow data channels failed during this test so no measured data is shown on these figures.

Although the cold leg flow instrumentation failed during this test, the main characteristics of the cold leg flow behavior during the experiment may be inferred from the Loop A and B measured cold leg temperature responses, which are compared with the corresponding RELAP5-calculated temperature responses in Figures 3-106 and 3-107. The sharp drop in the measured temperature response in Loop A is an indicator that coolant loop circulation was lost at 6,963 s during the test. The temperature drop results when the loop flow is interrupted because the flow of warmer fluid from the SG outlet plenum slows or stops and the influence of the cold HPI fluid on the cold leg temperature becomes much greater. Similarly, in Loop B the temperature drop occurs at 4,285 s, indicating that loop circulation was lost at that time during the test.   The measured cold leg temperature responses suggest that the loop flow stagnations in the test may not have been complete because the cold leg temperatures did not fall dramatically toward the HPI injection temperature. It is postulated that the small temperature drops reflect a loss of loop flow circulating through the hot legs, but that same-loop cold leg circulation (similar to what was observed in the calculation for Loop B) was present to some extent in both loops during the experiment.

The Loop A cold leg temperature comparison in Figure 3-106 shows the effects of coolant loop flow continuing in the calculation but not in the test. The warmer calculated cold leg temperature response reflects the effects of the small continuing coolant loop flow (see Figure 3-104) while the measured cold leg temperature response reflects the greater influence of the HPI temperature

caused by the loop flow stagnation. The RELAP5 overprediction of the Loop A cold leg temperature is characterized as about 22 K [40°F].
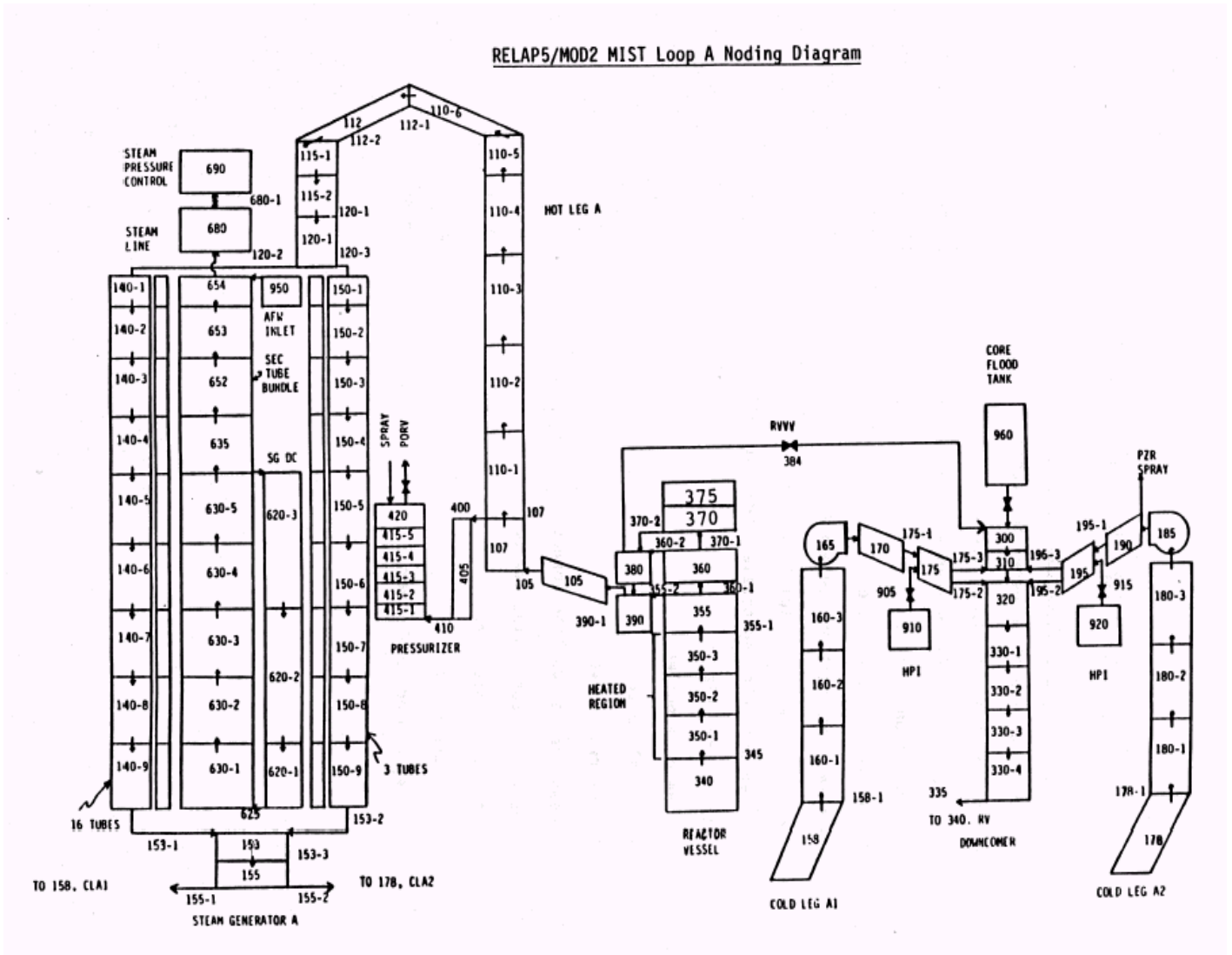
Figure 3-100   RELAP5 Nodalization for the MIST Test Facility

Table 3-19   Comparison of Measured and Calculated Initial Conditions for MIST Test 360499

Parameter	Initial Condition	
	Measured	RELAP5
Core power	384.2 kW	384.2 kW
Pressurizer Pressure	14.893 MPa [2160.0 psia]	14.380 MPa [2085.6 psia]
Hot leg subcooling	47.22 K [85.0°F]	45.57 K [82.0°F]
Core flow	22.85 kg/s [50.27 lbm/s]	22.85 kg/s [50.27 lbm/s]
Pressurizer collapsed level	1.372 m [4.50 ft]	1.367 m [4.48 ft]
SG pressure	7.00 MPa [1015.3 psia]	6.965 MPa [1010.2 psia]
SG 1 level	0.5791 m [1.90 ft]	0.5883 m [1.93 ft]
SG 2 level	0.6706 m [2.20 ft]	0.6782 m [2.22 ft]

Table 3-20   Summary of Measured and Calculated Sequences of Events for MIST Test 360499

Event	Event Time (s)	
	Measured	RELAP5
Stop EFW pumps and isolate SGs	0	0
Reactor trip signal (start core power decay)	9	9
Pressurizer sprays actuated	48	141
Pressurizer PORV locked open	282	240
HPI flow begins	286	286
Reactor coolant pumps tripped	338	280
Liquid flow begins at pressurizer PORV	516	251
Flow stagnation in Coolant Loop B	4,285	6,232
RCS pressure falls below SG pressures in both loops	6,035	Not Predicted
Flow stagnation in Coolant Loop A	6,963	Not Predicted
HPI flow throttled	8,728	9,701
High point vents opened, experiment and calculation ended	28,800	28,800

Figure 3-101   Pressurizer PORV Flow Rate – MIST Test 360499

Figure 3-102   HPI Flow Rate – MIST Test 360499

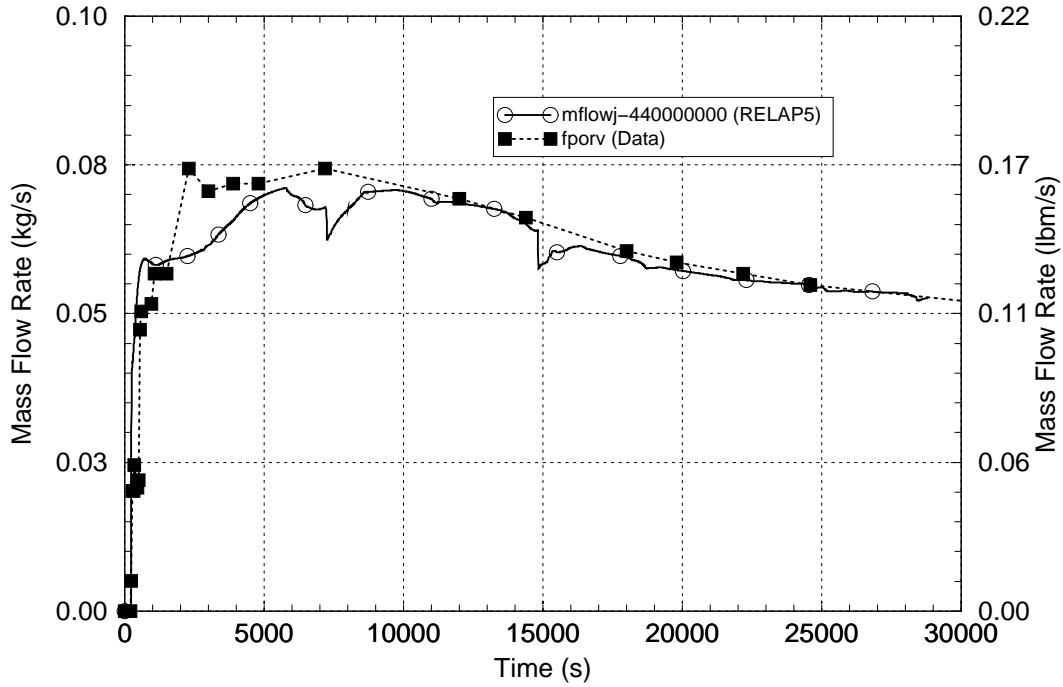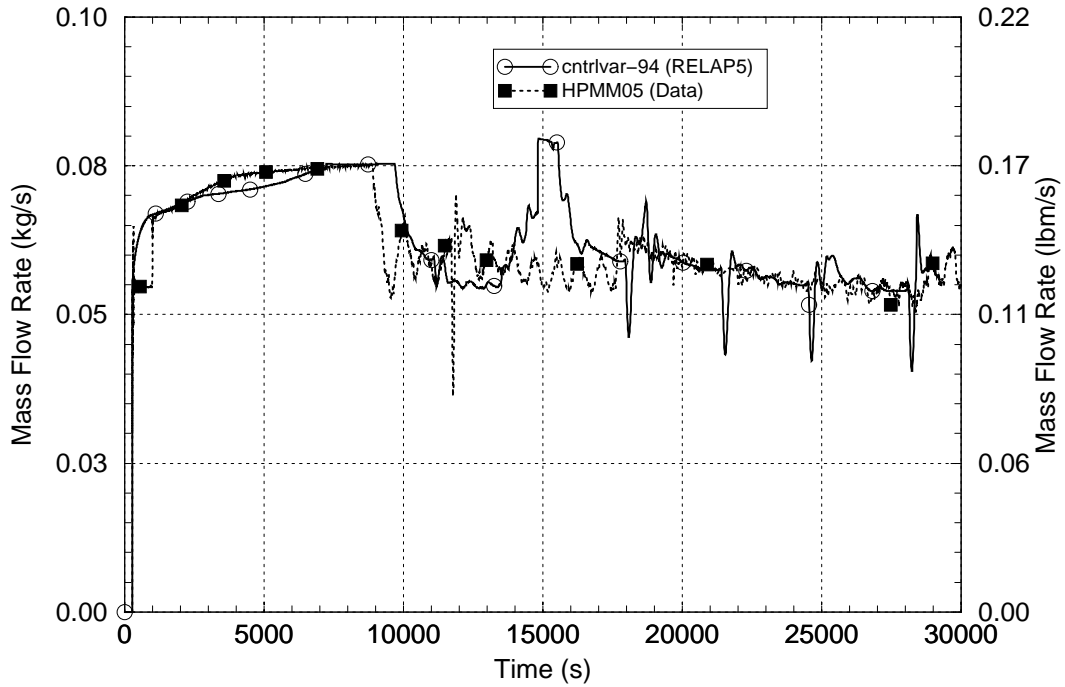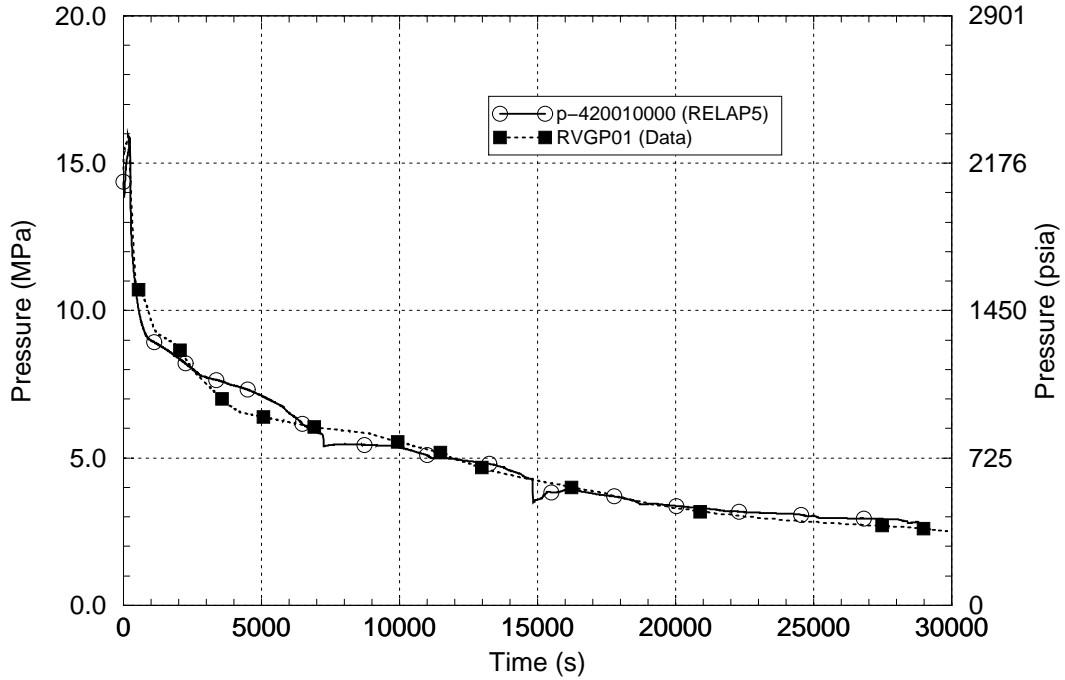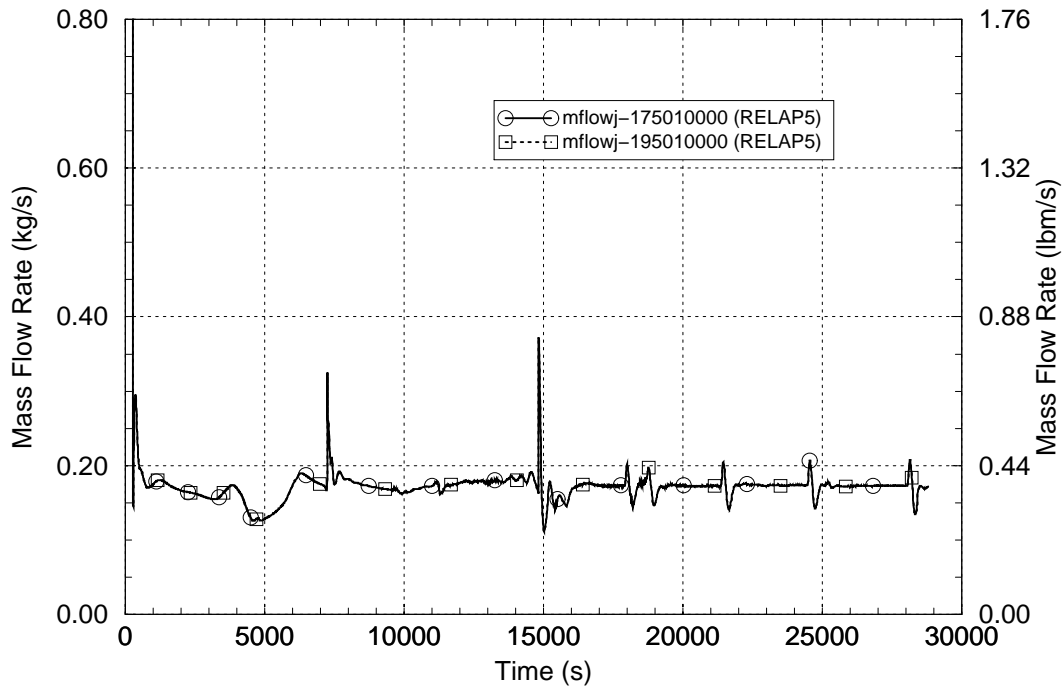**Figure 3-103   RCS Pressure – MIST Test 360499**

Figure 3-104   Loop A Cold Leg Flow Rate – MIST Test 360499
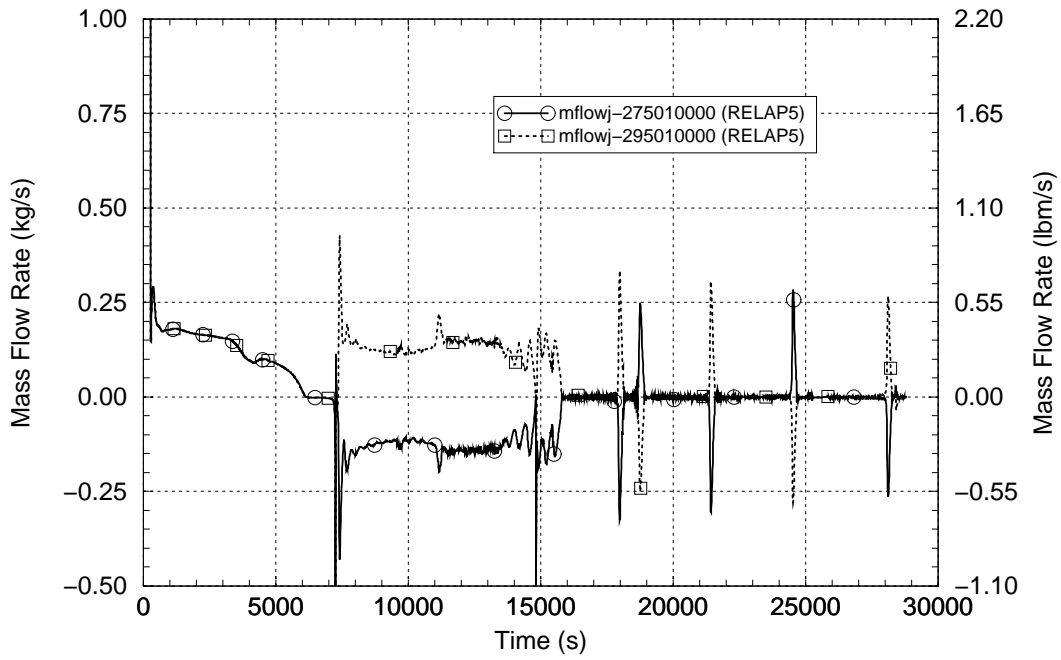
Figure 3-105   Loop B Cold Leg Flow Rate – MIST Test 360499
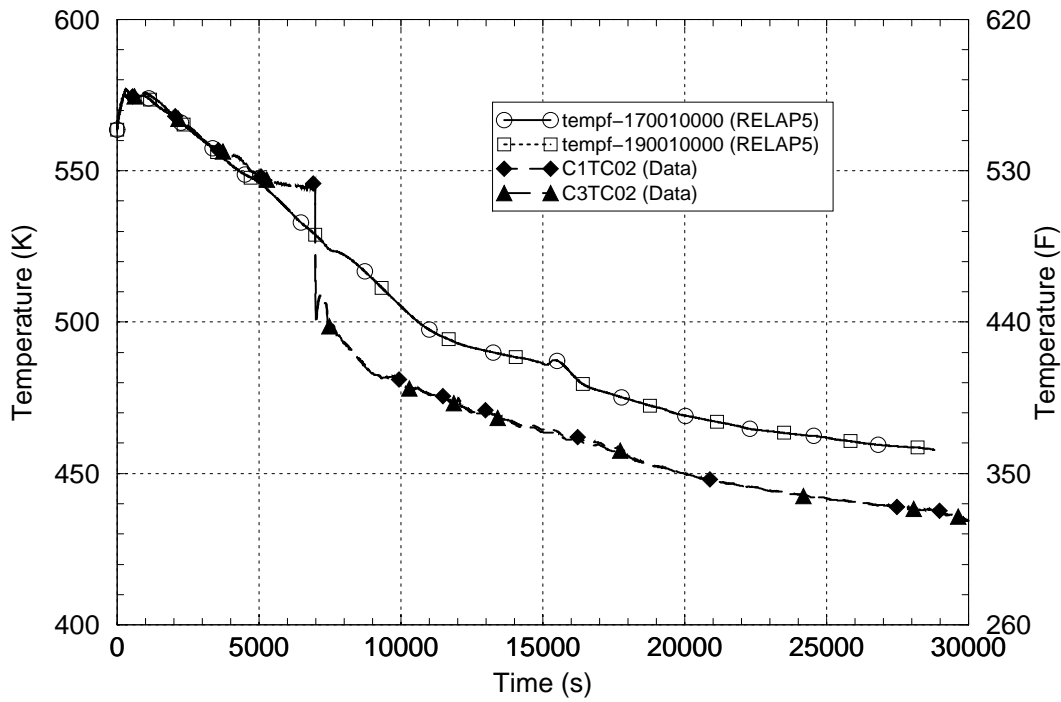

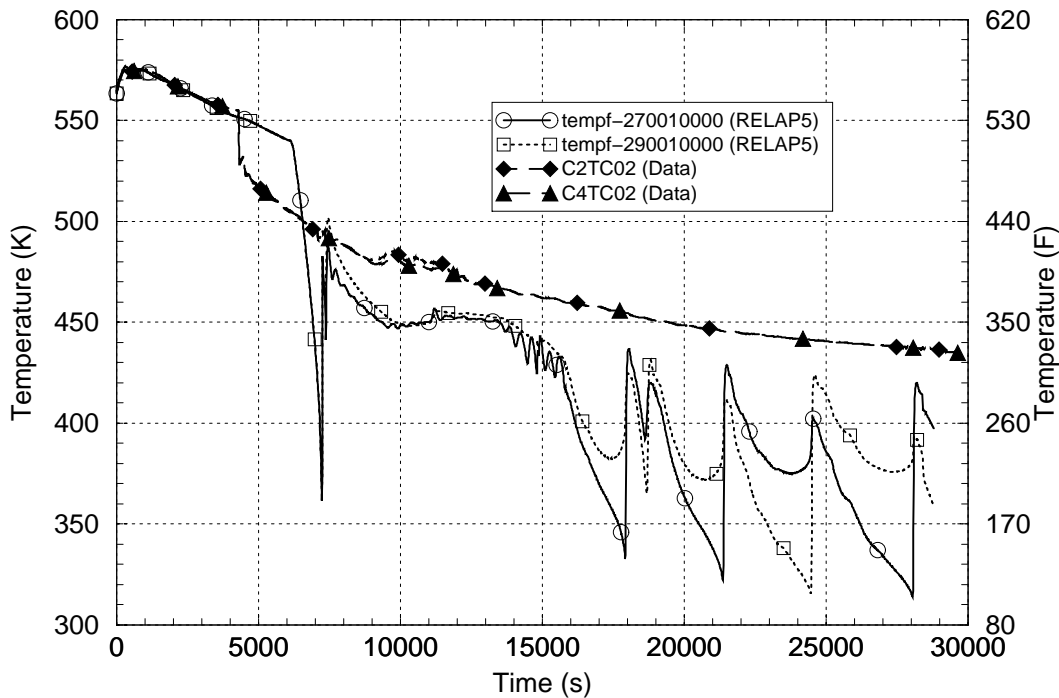**Figure 3-106   Loop A Cold Leg Fluid Temperature – MIST Test 360499**

Figure 3-107   Loop B Cold Leg Fluid Temperature – MIST Test 360499

The Loop B cold leg temperature comparison in Figure 3-107 shows that the loop flow stagnation occurred earlier in the test than in the calculation and also that RELAP5 underpredicted the Loop B cold leg temperature by about 22 K [40°F] from the time of loop stagnation up to about 16,000 s and by an average of about 100 K [180°F] afterward. The difference in the calculated behavior before and after 16,000 s reflects the complete stagnation of the Loop B flow at that time as shown in Figure 3-105 (and the dominant influence of cold ECC water afterward).

The fluid temperature responses in the upper and lower reactor vessel downcomer regions are shown in Figures 3-108 and 3-109, respectively. The data shown are for elevations in the downcomer corresponding to the elevations of the top and bottom of the heated core. The RELAP5-calculated data are in good agreement with the measured data. RELAP5 generally overpredicted the downcomer fluid temperatures over the entire period of the test but the deviations between calculated and measured data were small. When the cold leg flows are mixed together in the upper reactor vessel downcomer, the effects of the RELAP5 cold leg temperature overprediction in Loop A and underprediction in Loop B thus tended to compensate one another, leading to relatively good predictions for the downcomer fluid temperatures.

In summary, this assessment indicated major differences between the calculated and measured responses within the cold legs on the two coolant loops for MIST Test 360499. RELAP5 overpredicted the cold leg temperature in Loop A and did not predict the coolant loop flow stagnation seen in the experiment. RELAP5 underpredicted the cold leg temperature in Loop B and did predict the coolant loop flow stagnation seen in the experiment. The RELAP5 prediction of the reactor vessel downcomer fluid temperature, which represents a mixture of the cold leg temperatures, was judged to be good. For this test, RELAP5 underpredicted the measured downcomer temperature by a maximum of 11 K [19°F] and overpredicted it by a maximum of 15 K [27°F]. Over the full test period, RELAP5 overpredicted the measured downcomer temperature by an average of 3.5 K [6.3°F] and varied from the measured downcomer temperature by an average of 4.1 K [7.4°F]. The RELAP5 prediction of the RCS pressure was judged to be excellent. The

assessment of RELAP5/MOD3.2.2 Gamma using experimental data from MIST Test 360499 indicates that the code is capable of acceptably simulating the behavior of the key PTS parameters.
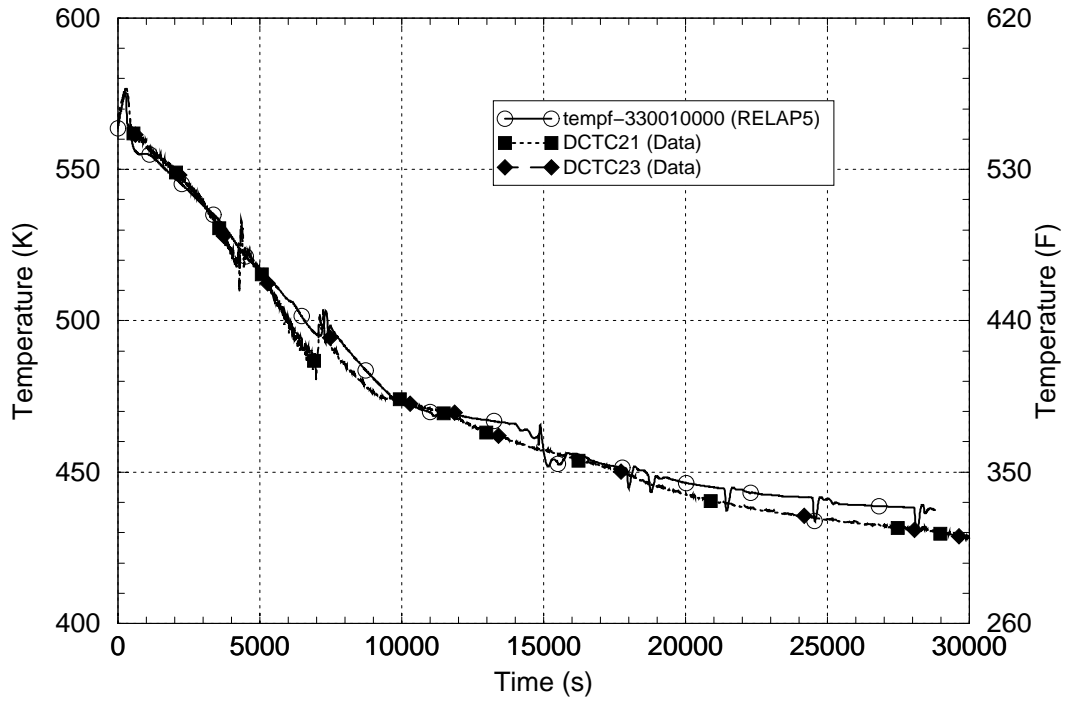
**Figure 3-108   Fluid Temperature in Upper Reactor Vessel Downcomer –
MIST Test 360499**
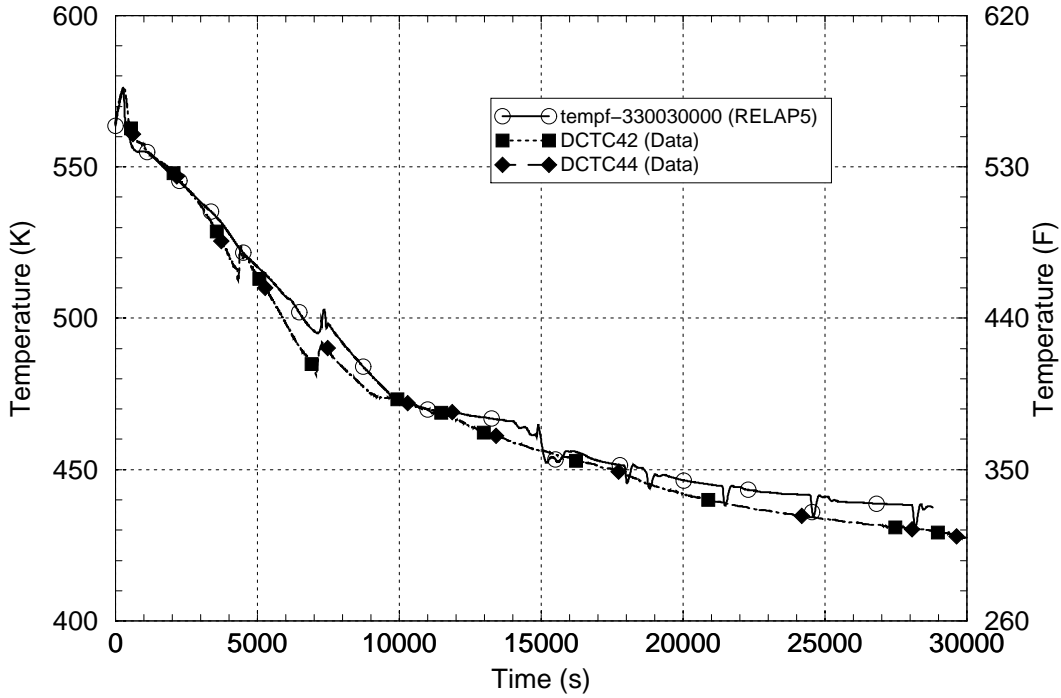
**Figure 3-109   Fluid Temperature in Lower Reactor Vessel Downcomer –
MIST Test 360499**

3.11   MIST Test 3109AA

The MIST test facility is described in Section 3.10. Three MIST tests are used in the assessment of RELAP5/MOD3.2.2Gamma for PTS applications. The second test, 3109AA, represents a 10 cm^2 small-break LOCA in a B&W PWR. This break size is sufficiently small that HPI flow can compensate for break flow.

MIST Test 3109AA simulated a 3.59 cm [1.4 in] diameter break in the Loop B-2 reactor coolant pump discharge cold leg piping. The test was initiated from 3.5% scaled core power and coolant loop natural circulation conditions with the reactor coolant pumps stopped and with the pump rotors locked in position. The initial RCS pressure was 11.9 MPa [1,726 psia], the SG secondary pressure was 7.0 MPa [1,015 psia] and the hot leg subcooling was 12.4 K [22.3°F]. The initial core exit temperature was 584.5 K [592.4°F] and the total core flow was 0.86 kg/s [1.9 lbm/s]. The initial pressurizer collapsed level was 1.372 m [4.501 ft]. The test was initiated by opening the cold leg break and when the pressurizer level had dropped below 0.3048 m [1.0 ft] the SG level setpoint was increased from 2.94 m [9.63 ft] to 9.63 m [31.6 ft], the HPI flow was started and the core power decay was initiated. The test procedures and results are described in Volume 10 of Reference 3-14.

A simulation of MIST Test 3109AA was performed using the RELAP5/MOD3.2.2Gamma code. The RELAP5 nodalization for the MIST facility is shown in Figure 3-100. Table 3-21 lists the initial conditions for the test; the comparison shows good agreement between the measured and RELAP5-calculated initial condition data. A summary of the measured and calculated

transient sequences of events for the test is presented in Table 3-22. The comparison shows good agreement between the calculated and measured event times.

The calculated and measured break flow responses are compared in Figure 3-110. The comparison indicates that the code underpredicted the break flow by about 10% prior to 800 s and overpredicted the break flow by about 10% after 3000 s. Overall, this was judged to be a good break flow prediction.

Figure 3-111 compares the calculated and measured HPI flow rates. HPI was initiated 71 s earlier in the calculation than in the test because the initial pressurizer level decline was faster in the calculation than in the test. This difference is not considered to be significant. After 1,400 s, the calculated HPI injection rate is about 4% lower than the measured value, which results from the RCS pressure overprediction shown in Figure 3-112. It is noted that these two effects reinforce each other, with the lower calculated HPI flow rate leading to less condensation of steam and, thereby, higher RCS pressure. The comparisons of both the HPI flow rate and RCS pressure are judged to indicate acceptable code predictions for those parameters.

The SG A and SG B secondary system pressures are shown in Figures 3-113 and 3-114, respectively. The pressure responses of the two SGs are different because of the different loop flow interruption behavior of the two loops (see Table 3-22). Interruption of natural circulation flow through Loop A occurs very early during the event sequence, which significantly reduces the SG A heat load. Natural circulation through Loop B continues much longer and the SG B heat load tends to keep the SG B pressure up. The same SG A and SG B behavior is observed in the test and calculation and the SG pressure predictions are judged to be very good. The RCS pressure remains above the SG A and SG B secondary pressures throughout the test and calculation.

The SG A and SG B secondary level responses are shown in Figures 3-115 and 3-116, respectively. The levels rise because the setpoint level increases as a part of the test procedure when the low pressurizer level condition has been attained. The figures show that the setpoint level reset occurred earlier in the calculation than in the test, but that the influence of this deviation on the level responses is not significant. The SG level predictions are judged to be very good.

Table 3-21   Comparison of Measured and Calculated Initial Conditions for MIST Test 3109AA

Parameter	Initial Condition	
	Measured	RELAP5
Core power	134.47 kW	134.47 kW
Pressurizer Pressure	11.9 MPa [1725.9 psia]	11.49 MPa [1666.5 psia]
Hot leg subcooling	12.4 K [22.3°F]	12.43 K 22.4°F
Core flow	0.86 kg/s [1.89 lbm/s]	0.9820 kg/s [2.16 lbm/s]
Pressurizer collapsed level	1.372 m [4.50 ft]	0.7617 m [2.50 ft]
SG pressure	7.00 MPa [1015.3 psia]	6.964 MPa [1010.0 psia]
SG 1 level	1.524 m [5 ft]	1.531 m [5.02 ft]
SG 2 level	1.524 m [5 ft]	1.531 m [5.02 ft]

Table 3-22   Summary of Measured and Calculated Sequences of Events for MIST Test 3109AA

| Event	Event Time (s)	
	Measured	RELAP5
Break opened	0	0
Low pressurizer level signal, HPI and core power decay initiated	126	55
Hot leg A flow interruption	228	143
SG level reaches 31.6 ft setpoint level	552	532
Hot leg B flow interruption	1,020	1,362
Complete loss of loop natural circulation flow	1,560	1,373
Flow reversal in Coolant Loop B	1,606	1,515
Flow reversal in Coolant Loop A	2,662	4,447
Test and calculation ended	4,800	4,800
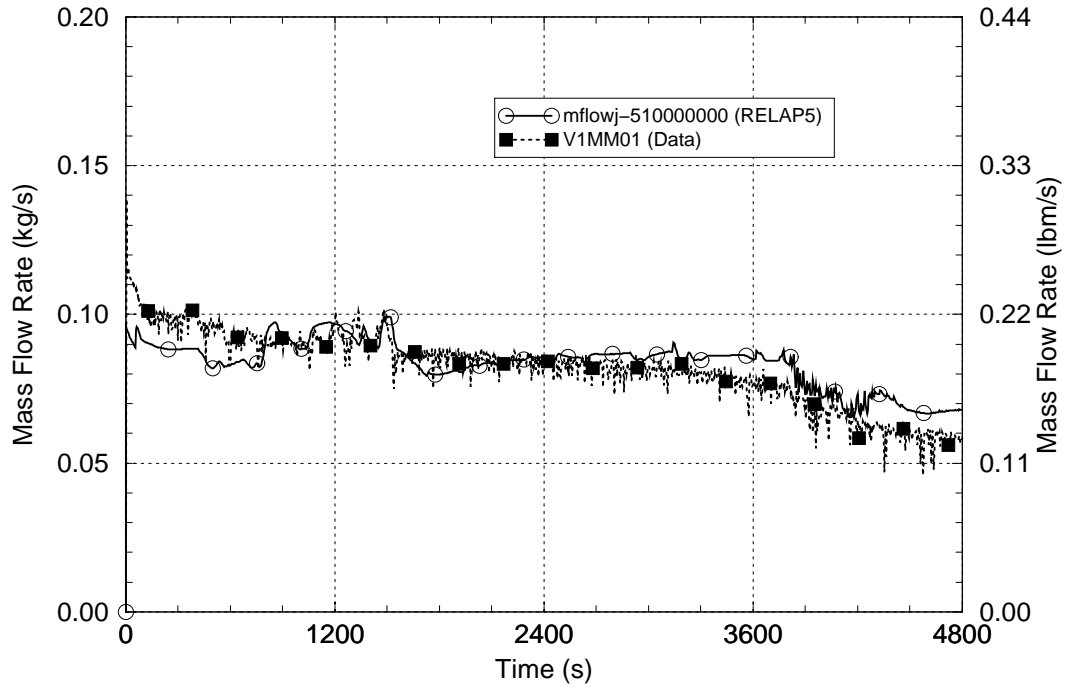
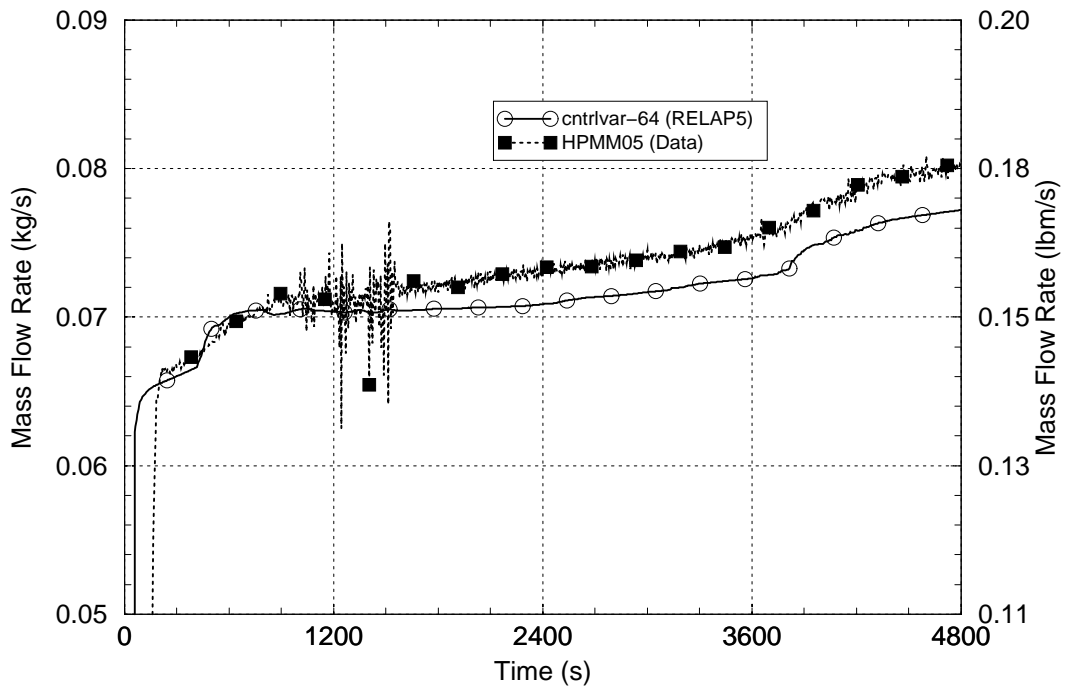**Figure 3-110   Break Flow – MIST Test 3109AA**

Figure 3-111   HPI Flow – MIST Test 3109AA
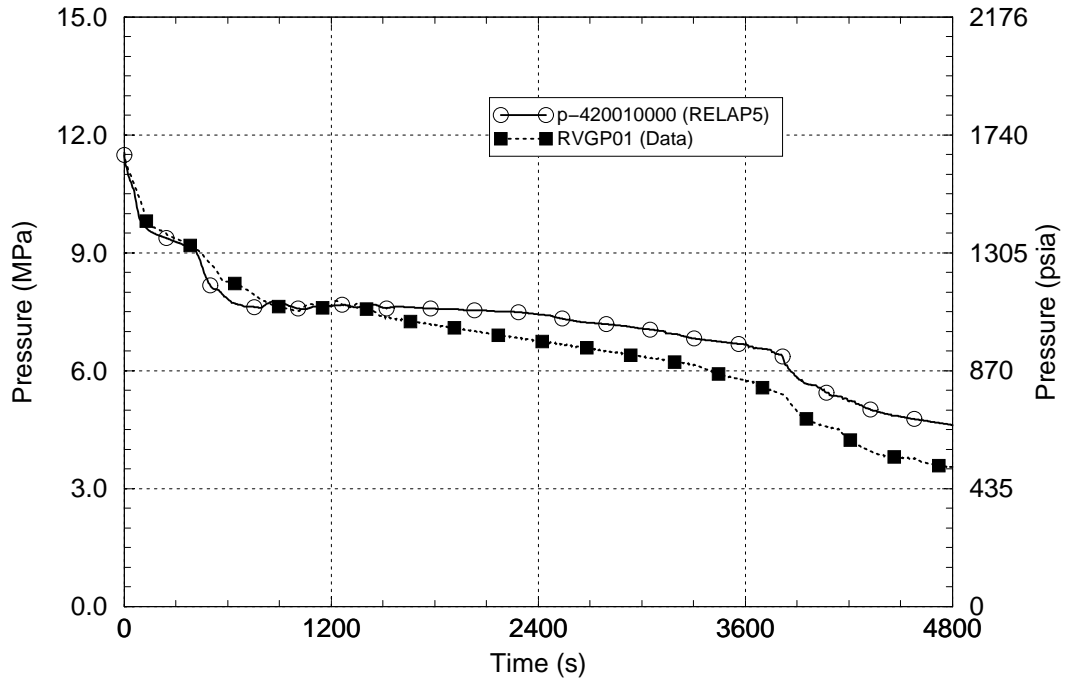
Figure 3-112   Pressurizer Pressure – MIST Test 3109AA
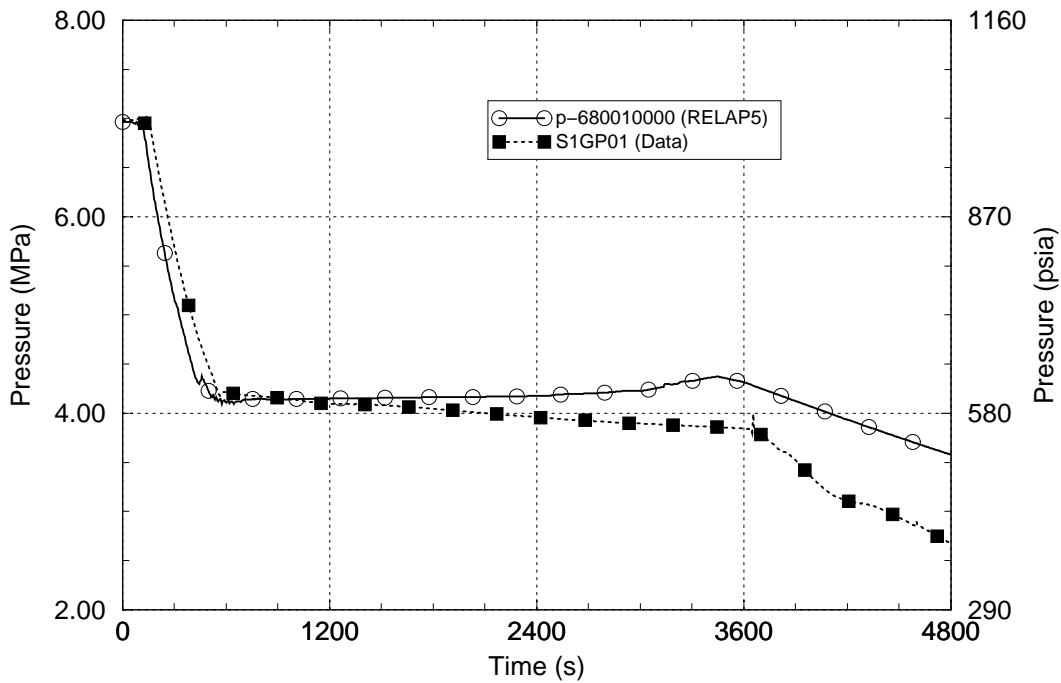

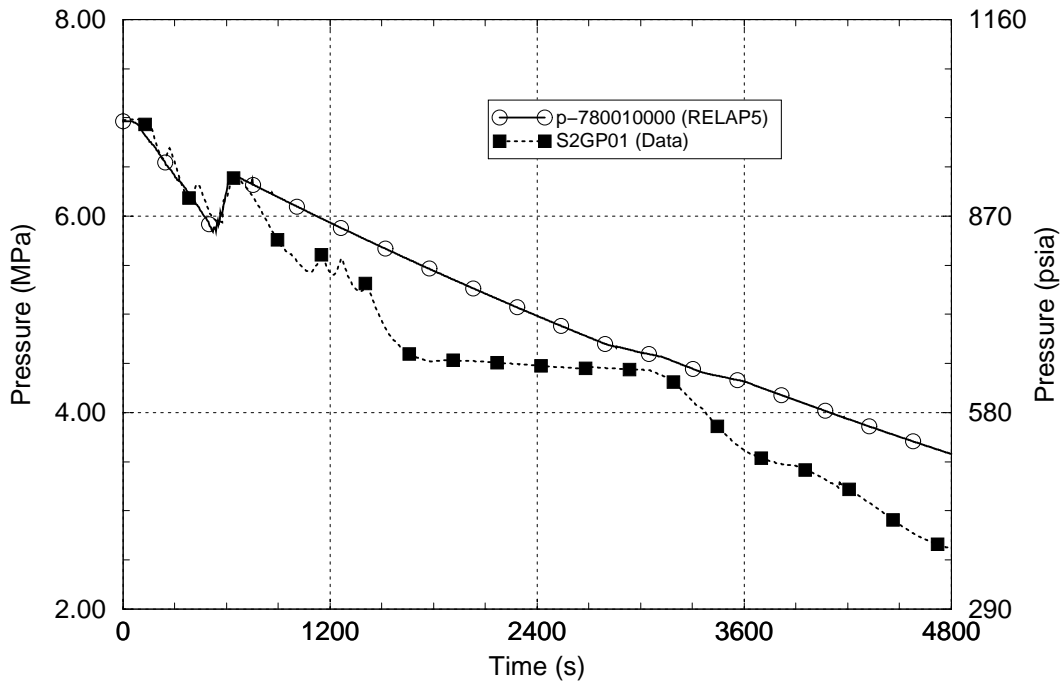**Figure 3-113   SG A Pressure – MIST Test 3109AA**

Figure 3-114   SG B Pressure – MIST Test 3109AA
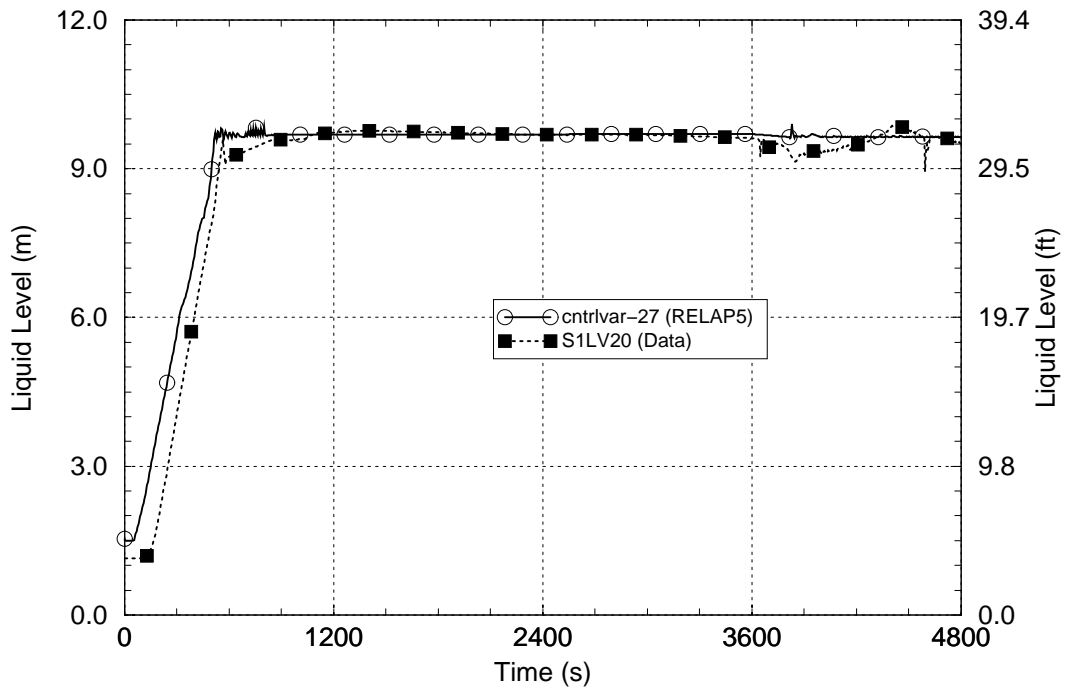
Figure 3-115   SG A Secondary Level – MIST Test 3109AA
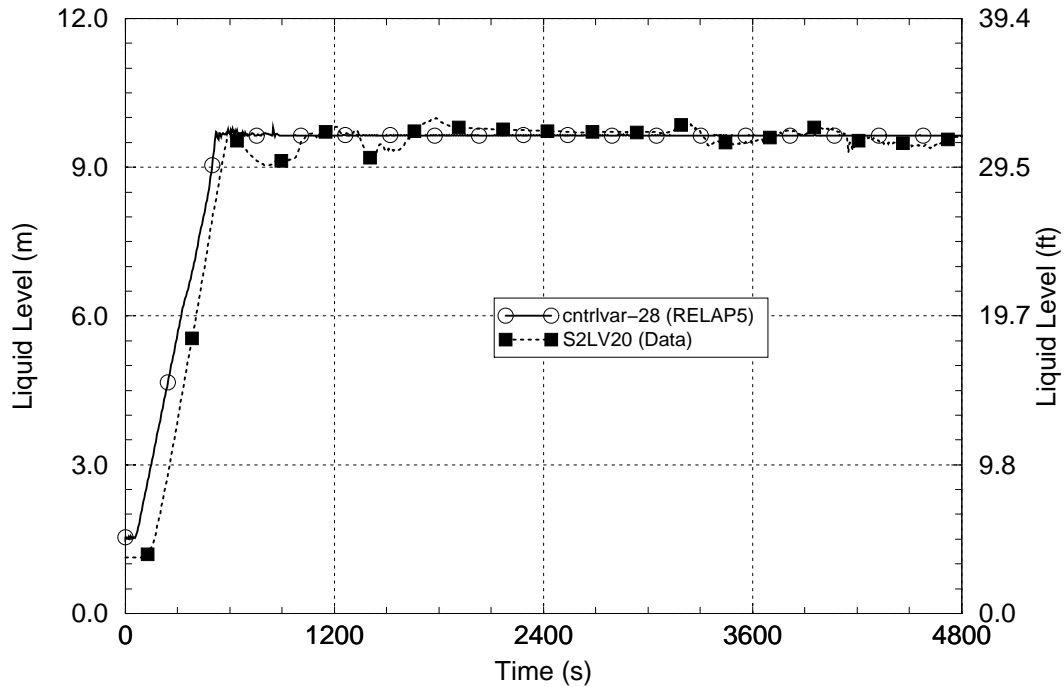
Figure 3-116   SG B Secondary Level – MIST Test 3109AA

The core-side reactor vessel level response is shown in Figure 3-117. The code prediction of the vessel level response is judged to be excellent.

The Loop A and B cold leg flow responses are shown in Figures 3-118 and 3-119, respectively. The data shown are for the pump discharge cold legs at a location between the HPI injection nozzles and the reactor vessel. The comparisons between the calculated and measured flow rates are very good. Prior to about 1,200 s, the data reflect the interruption of Loop A natural circulation flow and the continuance of the Loop B natural circulation flow. After 1,200 s, both the measured and calculated data reflect a circulating flow condition, in which one of the cold legs on each coolant loop reverses direction. When this happens, the circulation mixes coolant in the pump discharge cold legs, SG outlet plenum and upper downcomer on each loop, thus preventing a worst-case situation regarding pooling of cold HPI fluid locally in the cold leg and downcomer regions. The magnitude of the recirculating flows in the test and calculation agree very well, although the direction of the circulation is predicted correctly only in Loop B.

The existence of these cold leg circulations in RELAP5 simulations was originally reported during the first PTS evaluation study (Reference 3-15). Once the circulation has started, the buoyancy forces created by the difference in temperatures in the vertical sections of the circulation loop are sufficient to sustain the circulation. The circulation rate is that which balances the buoyancy driving head and the friction pressure drop created by the loop flow resistance.

Figure 3-117   Reactor Vessel Level – MIST Test 3109AA

Figure 3-118   Cold Leg A Flow – MIST Test 3109AA
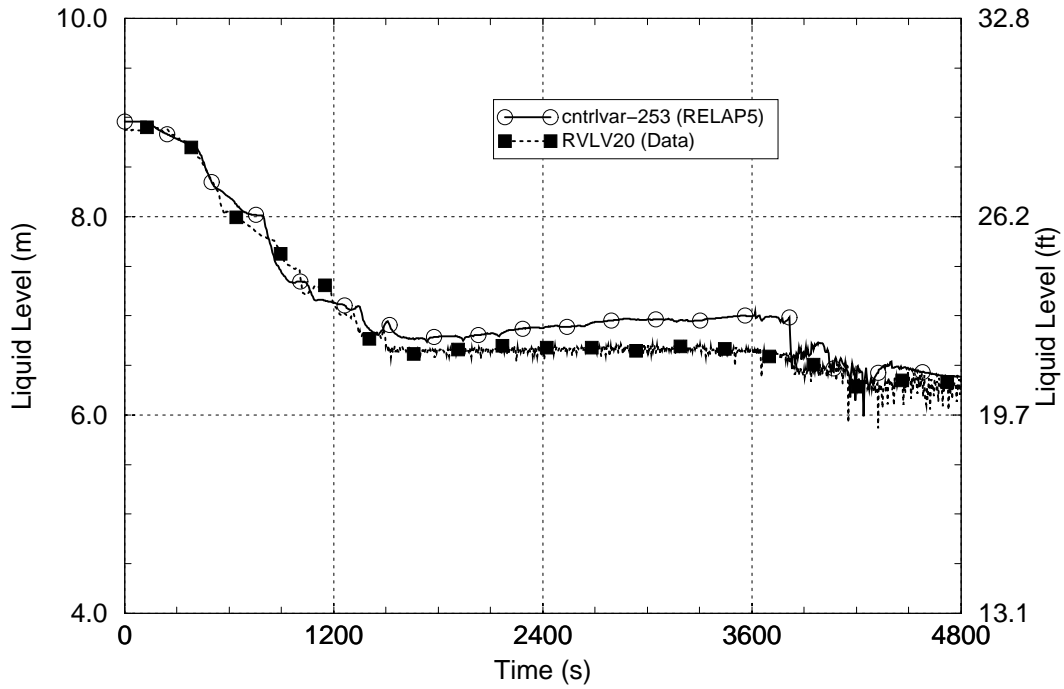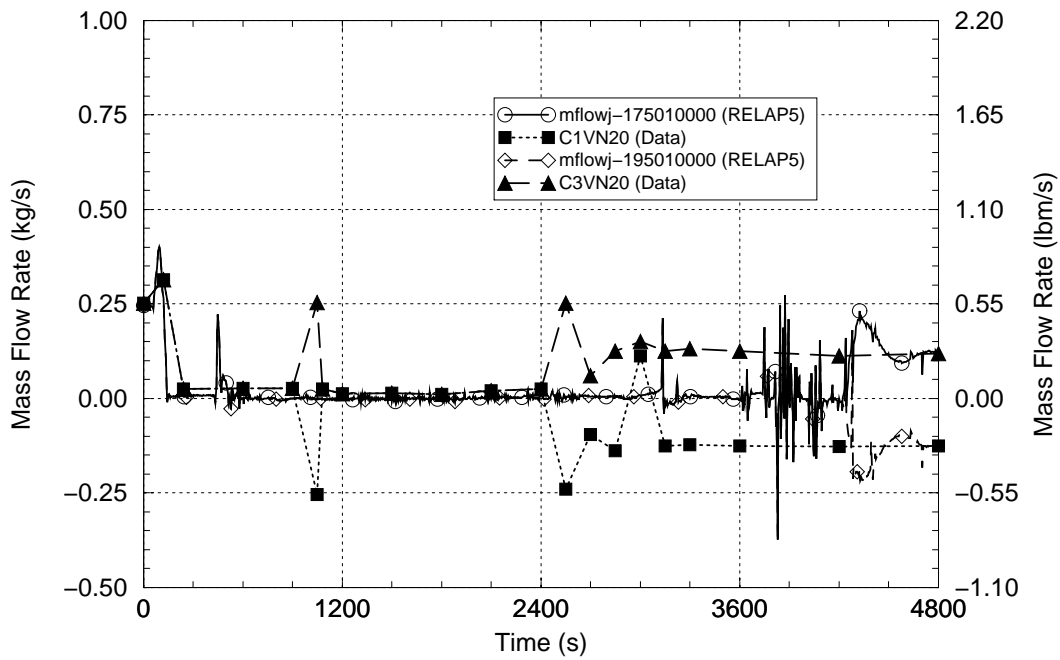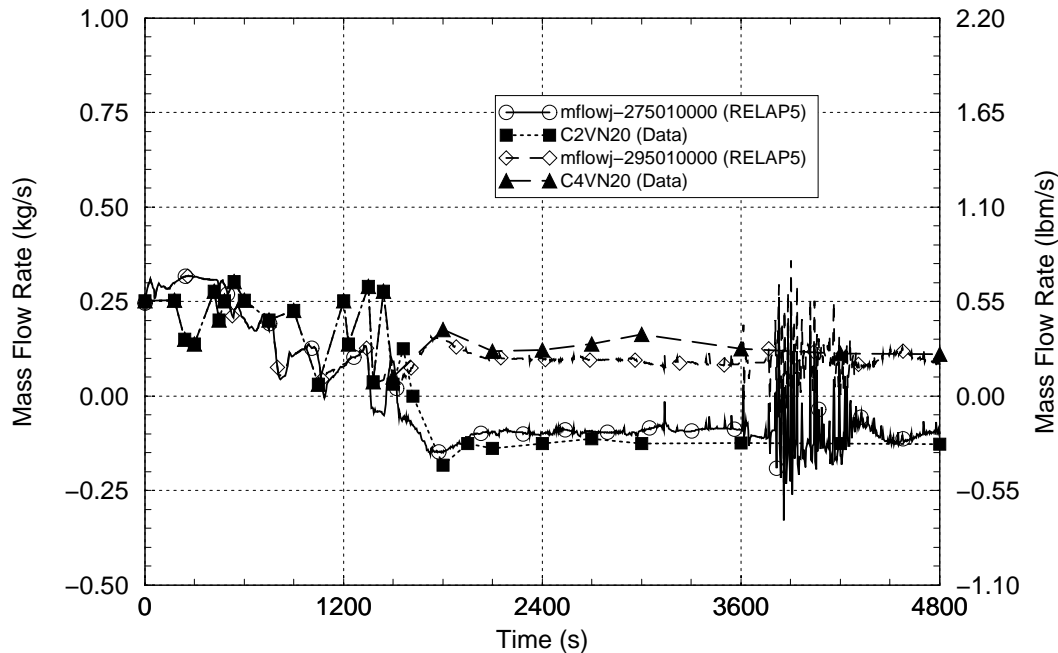
Figure 3-119   Cold Leg B Flow – MIST Test 3109AA

While the Test 3109AA experimental data show apparent flow circulations between the cold legs on the same loops and the code similarly predicts those circulations, it was elected not to credit the PTS plant analyses for the warming effects these circulations provide for the RELAP5-predicted reactor vessel downcomer fluid temperatures. Two concerns remain regarding the veracity of these circulations. First is the issue of initiating events for the circulations. While one could speculate that slight irregularities in the configurations or fluid conditions between the two cold legs on the same loop might be present, with RELAP5 the cold legs are modeled identically and the circulations appear to be initiated by numerical effects, such as round-off error. Thus no assurance can be given that sufficient asymmetries will be present in the physical system to initiate circulations. Second, while the test data do appear to be demonstrating that circulations existed during this experiment, there is significant difference in the length scales of the experimental facility and the PWR. Even if it does exist in the sub-scale experiment, there is no assurance that the circulation will be present in the full-scale plant configuration. Because of these concerns and because the effect of including the circulation in the analysis is non-conservative for PTS (i.e., it results in warmer reactor vessel downcomer temperatures), same-loop circulation was prevented in the PTS plant analysis using artificially-high reverse flow loss coefficients in the reactor coolant pump regions of the models.   See Section 3.6 for more information regarding the magnitude of conservatism introduced by preventing the cold leg circulation in the RELAP5 model.

The upper reactor vessel downcomer fluid temperature responses for Test 3109AA are shown in Figure 3-120. The data shown are for an elevation in the downcomer corresponding to the elevation of the top of the heated core. The comparison shows that after about 1,200 s RELAP5 overpredicted the downcomer temperature.   This overprediction is consistent with the underprediction of HPI flow rate shown in Figure 3-111. The RELAP5 prediction of the downcomer temperature is considered to be adequate.
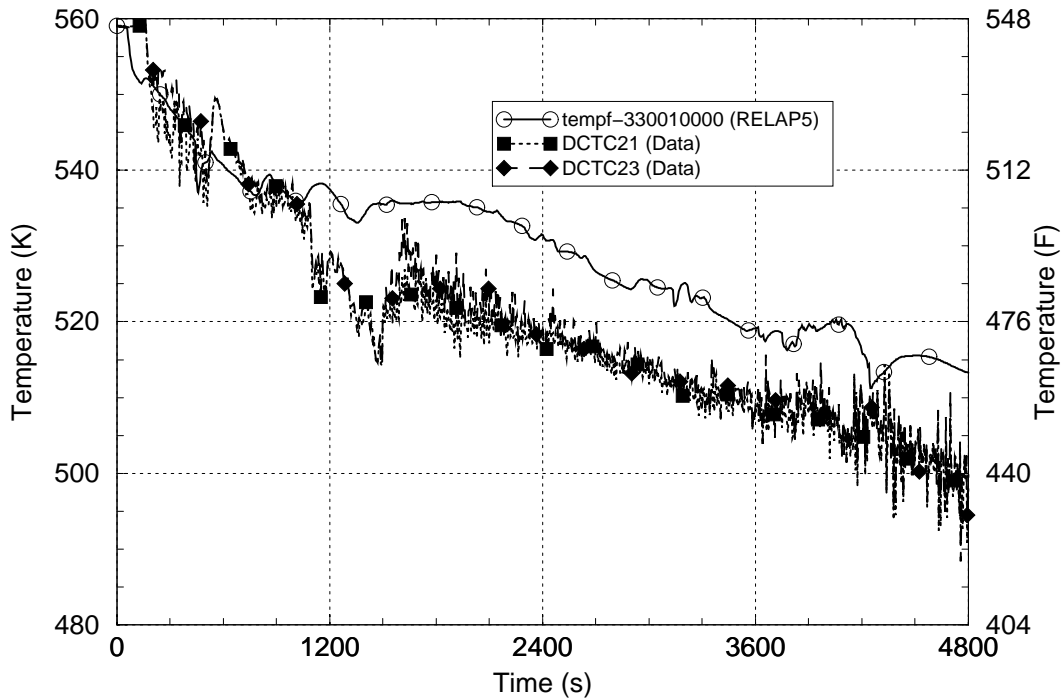
Figure 3-120   Fluid Temperature in Upper Reactor Vessel Downcomer – MIST Test 3109AA

In summary, this assessment indicated no major differences between the calculated and measured data for MIST Test 3109AA. For this test, RELAP5 underpredicted the measured downcomer temperature by a maximum of 8.3 K [15°F] and overpredicted it by a maximum of 23 K [42°F]. Over the full test period, RELAP5 overpredicted the measured downcomer temperature by an average of 9.6 K [17°F] and varied from the measured downcomer temperature by an average of 10 K [18°F]. The RELAP5 prediction of the RCS pressure is in good agreement with the measured data. The code well-predicted the interruption of loop natural circulation flow in both of the coolant loops. The assessment of RELAP5/MOD3.2.2 Gamma using experimental data from MIST Test 3109AA indicates that the code is capable of acceptably simulating the behavior of the key PTS parameters.

3.12   MIST Test 4100B2

The MIST test facility is described in Section 3.10. Three MIST tests were used in the assessment of RELAP5/MOD3.2.2Gamma for PTS applications. The third test, 4100B2, represents a 100 cm^2 [15.5 in^2] small-break LOCA in a B&W PWR. This break size is sufficiently large that HPI flow cannot compensate for break flow.

MIST Test 4100B2 simulated a 11.28 cm [4.4 in] diameter break in the Loop B-2 reactor coolant pump discharge cold leg piping. The test was initiated from 3.5% scaled core power and coolant loop natural circulation conditions with the reactor coolant pumps stopped and with the pump rotors locked in position. The initial RCS pressure was 11.9 MPa [1,726 psia], the SG secondary pressure was 7.0 MPa [1,015 psia] and the hot leg subcooling was 12.8 K [23.1°F]. The initial core exit

temperature was 584.5 K [592.4°F] and the total core flow was 0.86 kg/s [1.9 lbm/s]. The initial pressurizer collapsed level was 1.524 m [5.00 ft]. The test was initiated by opening the cold leg break and when the pressurizer level had dropped below 0.3048 m [1.0 ft] the SG level setpoint was increased from 2.94 m [9.63 ft] to 9.63 m [31.6 ft], the HPI flow was started and the core power decay was initiated. The test procedures and results are described in Volume 11 of Reference 3-14.

A simulation of MIST Test 4100B2 was performed using the RELAP5/MOD3.2.2Gamma code. The RELAP5 nodalization for the MIST facility is shown in Figure 3-100. Table 3-23 lists the initial conditions for the test; the comparison shows good agreement between the measured and RELAP5-calculated initial condition data. A summary of the measured and calculated transient sequences of events for the test is presented in Table 3-24. The comparison shows good agreement between the calculated and measured transient event times for this test.

The calculated and measured break flow responses are shown in Figure 3-121. The calculated beak flow is in excellent agreement with the measured break flow.

The ECCS response comparisons are shown in Figures 3-122 (HPI flow), 3-123 (LPI flow), 3-124 (CFT flow) and 3-125 (CFT level). The calculated responses for HPI flow, CFT flow and CFT level are in excellent agreement with the measured data. The calculated response for LPI flow is in good agreement with the measured data, with the overprediction of the LPI flow rate after about 2,600 s resulting from the underprediction of RCS pressure during this period as shown in Figure 3-126.

Because the break size for this test is relatively large, the RCS depressurization is rapid. The RELAP5 predictions for this depressurization and the rates at which ECCS entered the system during the depressurization were excellent. However, once the large volume of cold water ECCS water had entered the RCS, so much condensation potential existed that RELAP5 did not well predict the repressurization of the system after 2,600 s.

Thermal stratification effects that were present in the experiment but could not be simulated with RELAP5 may have caused this difference in repressurization behavior. The situation is somewhat similar to the issue of thermal stratification in liquid-filled cold legs of the ROSA/AP600 facility for Tests AP-CL-03 and AP-CL-09 as described in Sections 3.3 and 3.4. RELAP5 cannot represent thermal stratification effects in liquid-filled regions (with warm liquid residing over cold liquid) because the only one temperature can be assigned for the liquid phase within each RELAP5 hydrodynamic cell. The simulation of the refill process in MIST Test 4100B2 is especially difficult because stratified liquid columns are moving upward into steam-filled spaces through fixed nodalization grids. The rapid influx of cold ECCS is expected to refill the upper regions of the reactor vessel (downcomer, upper plenum and upper head) and partially refill the higher-elevation regions of the RCS (pressurizer, hot legs and SG tubes). In the physical system, as the liquid rises into these regions, steam condensation will warm the leading edge of the liquid front but not the bulk of the liquid. RELAP5 cannot simulate this behavior, resulting in the bulk of the liquid becoming involved in the condensation process and thereby an underprediction of the repressurization process. These code limitations may be partially overcome by employing much more detailed nodalization schemes in affected regions, but the RELAP5 single-liquid-temperature assumption remains and therefore RELAP5 simulations for rapid depressurization and refill events are generally susceptible to these over-condensation and under-pressurization effects. RELAP5 did predict a delayed and more moderated RCS repressurization after 2,600 s. On a relative basis, the pressure error during this period is large. However, on an absolute basis the pressure error

shown in Figure 3-126 is moderate, about 0.68 MPa [98 psi], and this value may be taken as an indication of the typical uncertainty in RELAP5 capabilities for predicting RCS pressures for SBLOCA event sequences with break sizes toward the upper end of the SBLOCA break-spectrum range.

The SG pressure and level responses are shown in Figures 3-127 through 3-130. The RELAP5-calculated responses for these parameters are in excellent agreement with the experimental data. The primary system pressure quickly falls below the SG secondary pressures in both the test and calculation, see Table 3-24.

The reactor vessel downcomer level responses are shown in Figure 3-119. The RELAP5-calculated level response is in good agreement with the experimental data.

Table 3-23   Comparison of Measured and Calculated Initial Conditions for MIST Test 4100B2

Parameter	Initial Condition	
	Measured	RELAP5
Core power	134.47 kW	134.47 kW
Pressurizer Pressure	11.9 MPa [1725.9 psia]	12.07 MPa [1750.6 psia]
Hot leg subcooling	12.4 K [22.3°F]	12.29 K [22.1°F]
Core flow	0.86 kg/s [1.89 lbm/s]	0.8328 kg/s [1.83 lbm/s]
Pressurizer collapsed level	1.524 m [5 ft]	1.373 m [4.50 ft]
SG pressure	7.00 MPa [1015.3 psia]	6.964 MPa [1010.0 psia]
SG 1 level	1.402 m [4.60 ft]	1.402 m [4.60 ft]
SG 2 level	1.433 m [4.70 ft]	1.432 m [4.70 ft]
CFT pressure	4.14 MPa [600.5 psia]	4.14 MPa [600.5 psia]
CFT level	5.812 m [19.07 m]	5.812 m [19.07 m]

Table 3-24   Summary of Measured and Calculated Sequences of Events for MIST Test 4100B2

Event	Event Time (s)	
	Measured	RELAP5
Break opened	0	0
Initiate HPI and core power decay	Manual (within 20 sec)	0
Loss of loop natural circulation flow	~120	114
SG level reaches 31.6 ft setpoint level	~530	532
Primary system pressure falls below SG secondary pressure in both loops.	779	823
Accumulator injection begins	~1,000	991
LPI flow begins	2,043	2,093
HPI flow throttled on high subcooling	2,986	N/A
Simulation ended	4,800	4,800
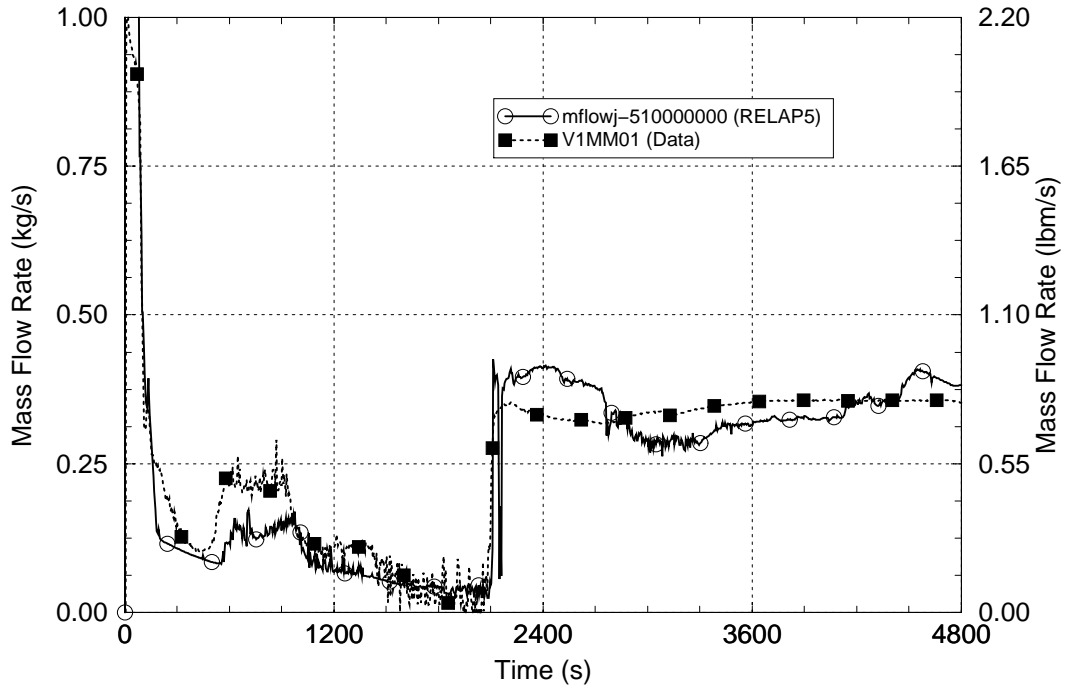
Figure 3-121   Break Flow – MIST Test 4100B2
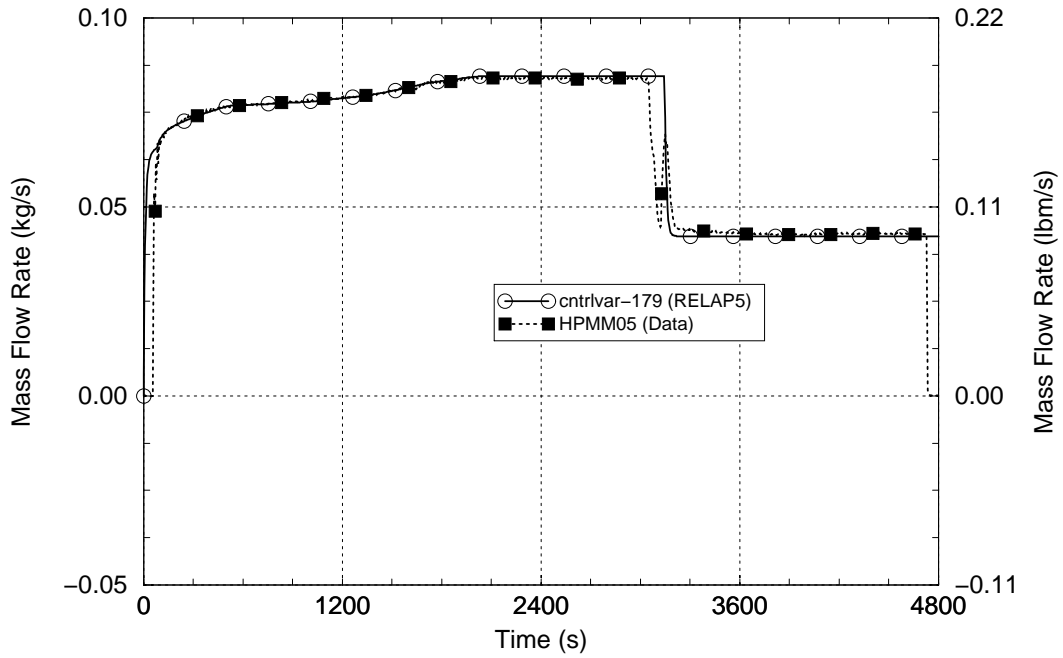
Figure 3-122   HPI Flow – MIST Test 4100B2

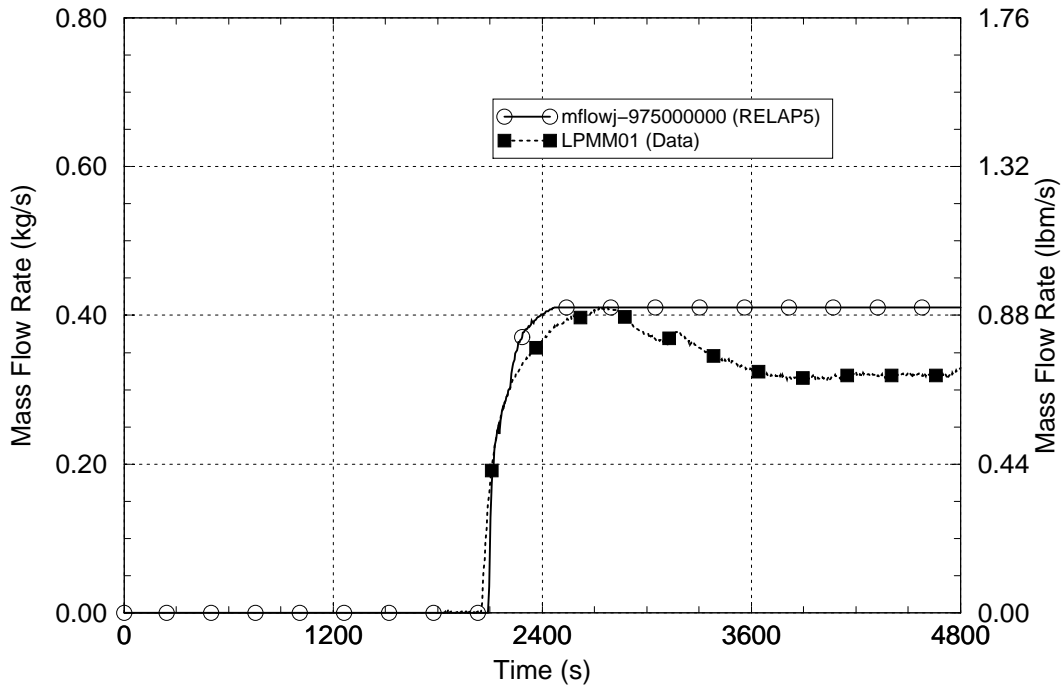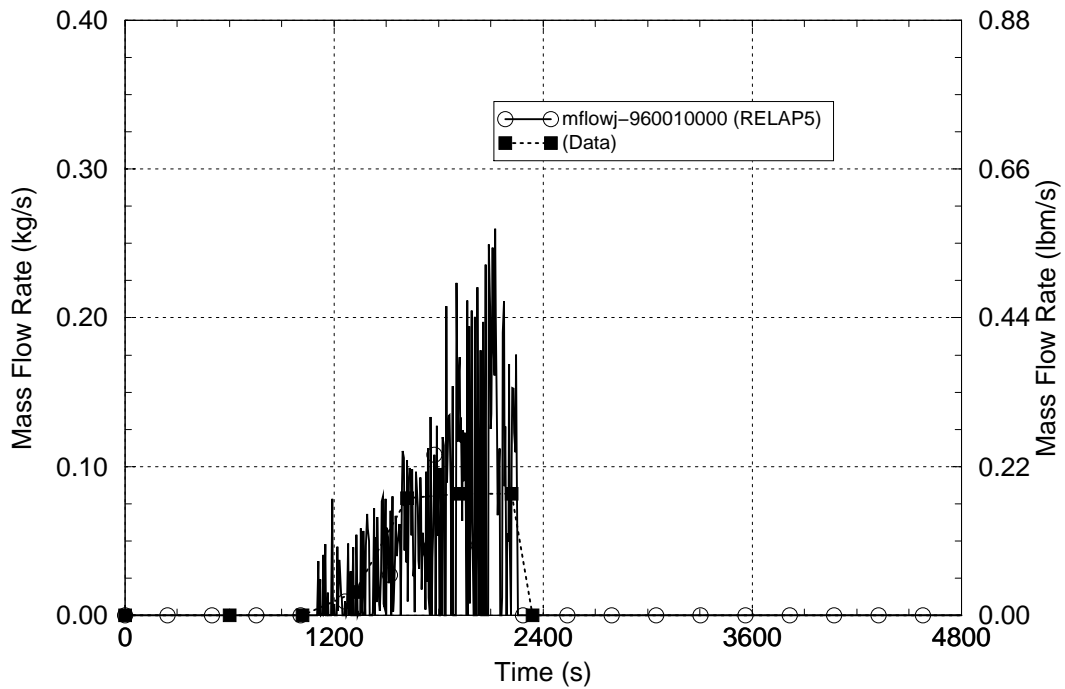**Figure 3-123 LPI Flow – MIST Test 4100B2**

Figure 3-124 CFT Flow – MIST Test 4100B2
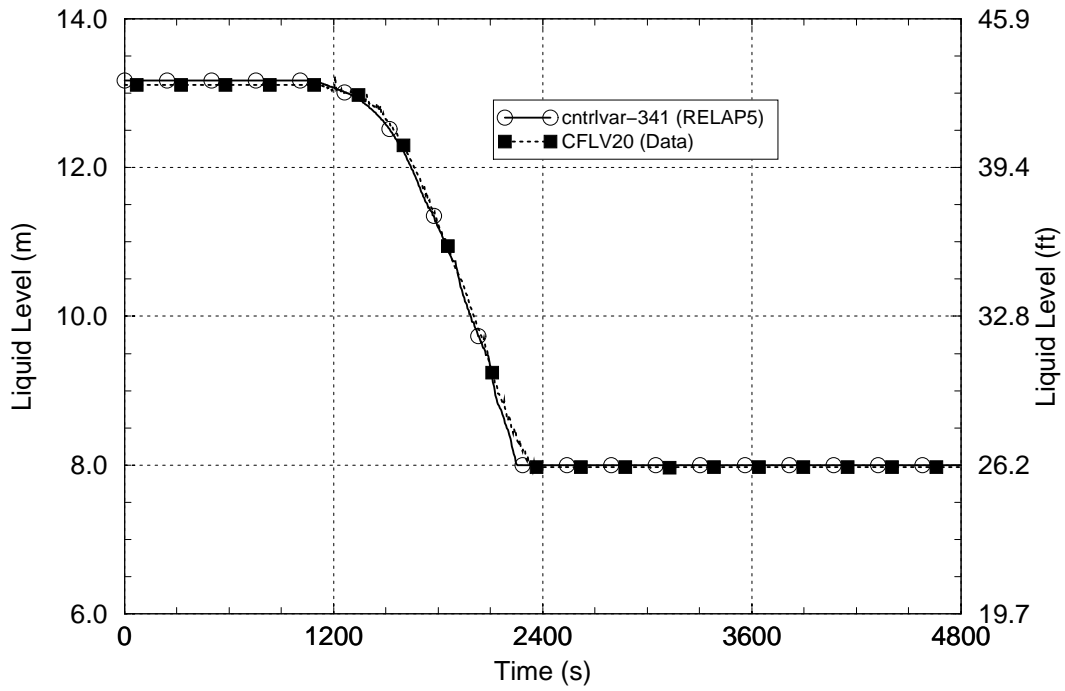
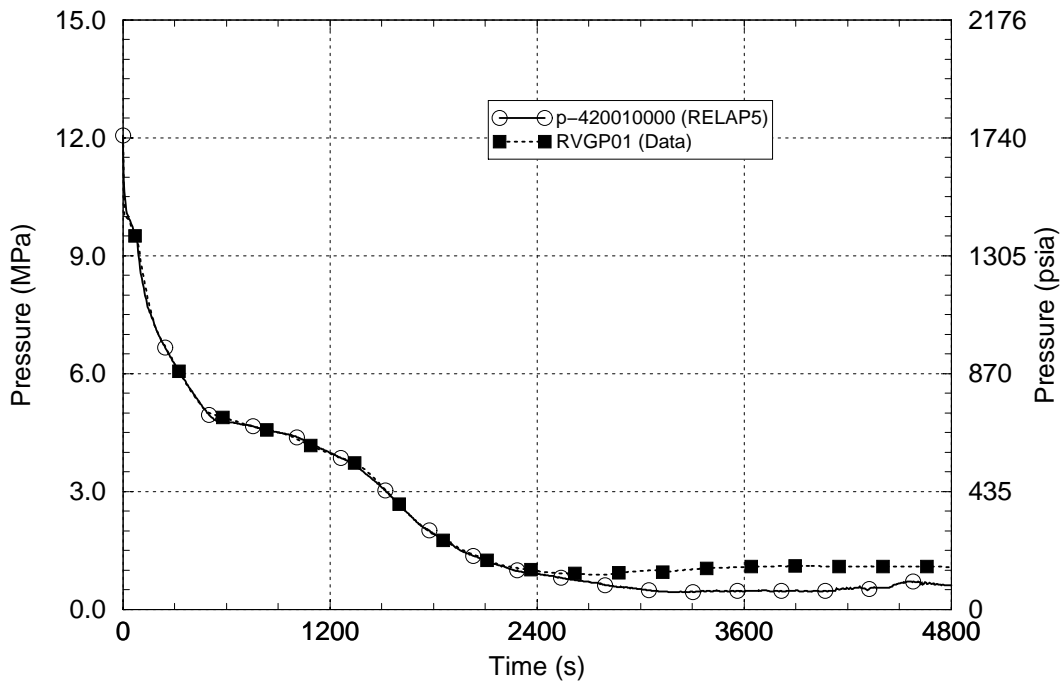**Figure 3-125   CFT Level – MIST Test 4100B2**

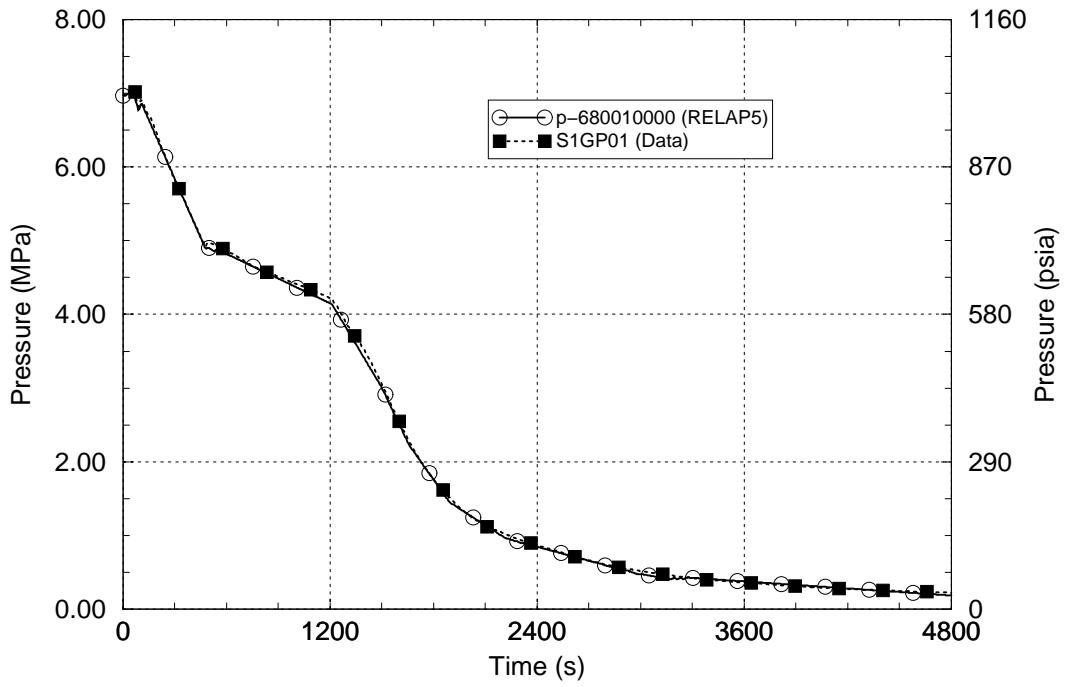**Figure 3-126   Pressurizer Pressure – MIST Test 4100B2**
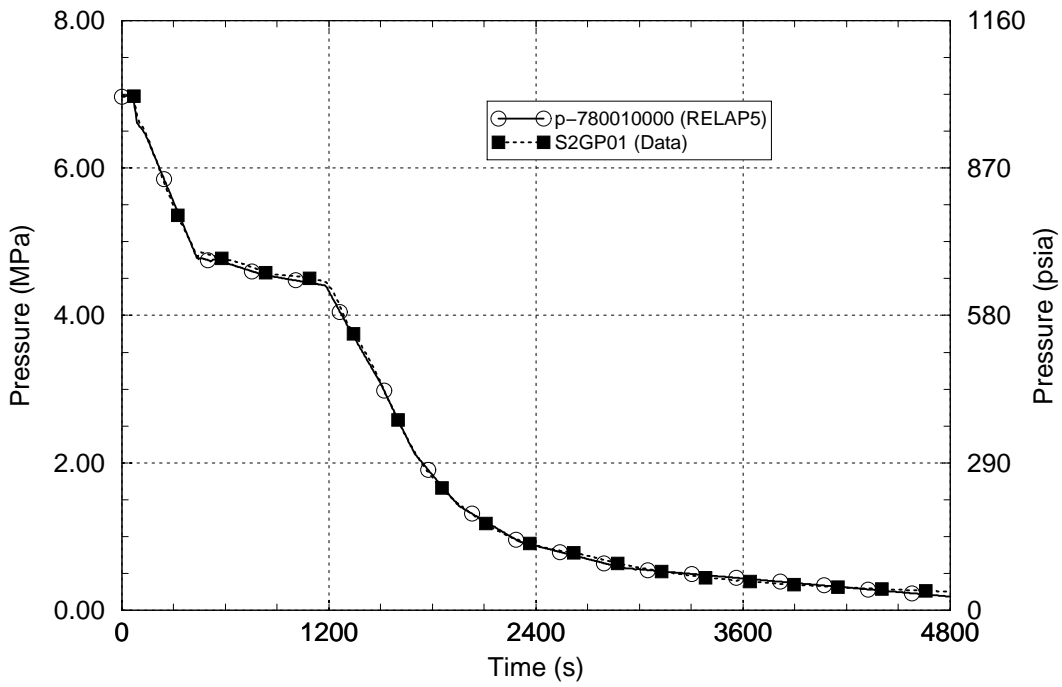
Figure 3-127   SG A Pressure – MIST Test 4100B2

Figure 3-128   SG B Pressure – MIST Test 4100B2
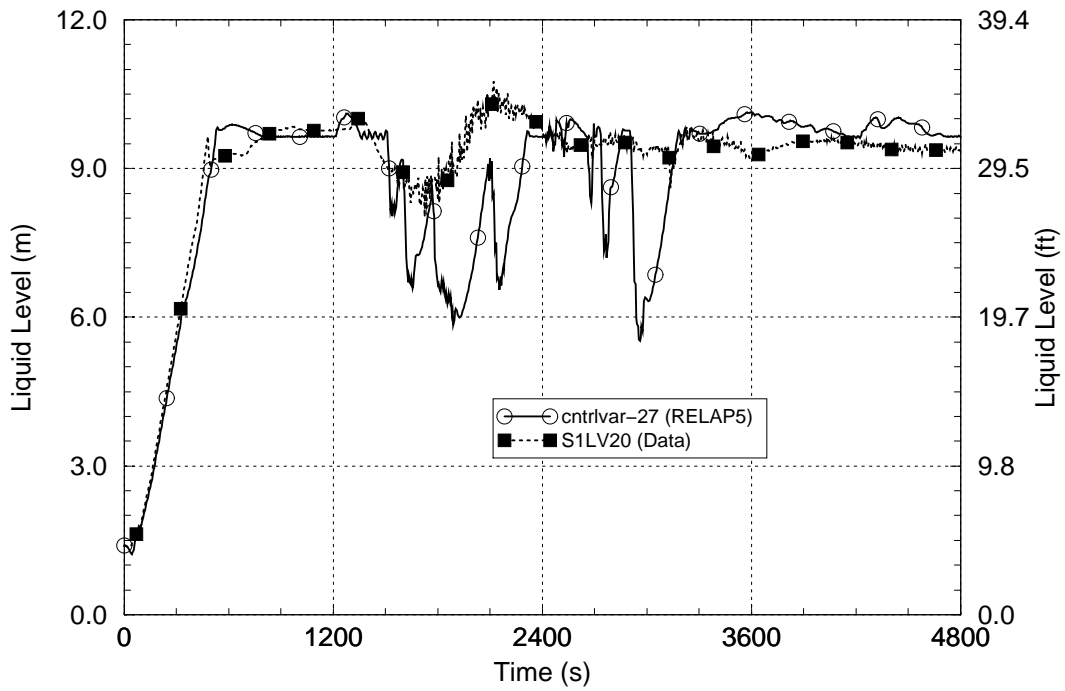
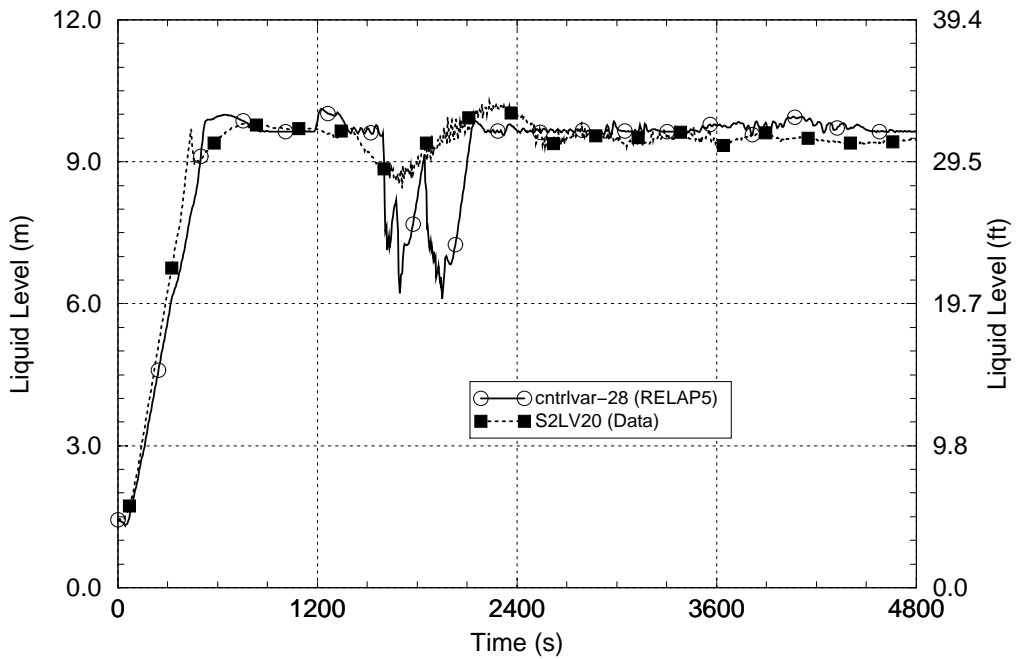**Figure 3-129   SG A Level – MIST Test 4100B2**

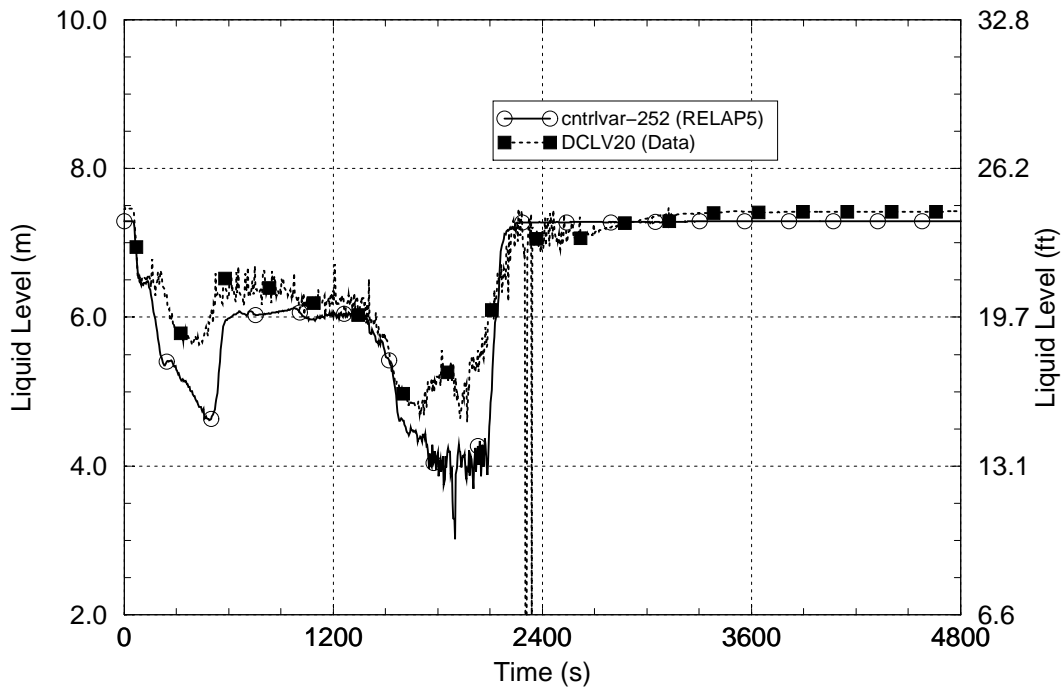**Figure 3-130   SG B Level – MIST Test 4100B2**

Figure 3-131 Reactor Vessel Downcomer Level – MIST Test 4100B2

The fluid temperature responses in the upper region of the reactor vessel downcomer are shown in Figure 3-132. The data shown are for an elevation in the downcomer corresponding to the elevation of the top of the heated core.   Prior to about 2,600 s and after 3,300 s, the RELAP5-calculated fluid temperature is in excellent agreement with the measured data. However, between about 2,600 s and 3,300 s, RELAP5 overpredicts the downcomer fluid temperature. The overprediction of the fluid temperature results from the fluid-warming caused by overpredicting the condensation behavior, as described above. The maximum overprediction of the downcomer fluid temperature is 32 K [57°F] and this value may be taken as an indication of the typical maximum uncertainty in RELAP5 capabilities for predicting the downcomer temperature for SBLOCAs with break sizes toward the upper end of the SBLOCA break-spectrum range.

The difficulties in obtaining better code-to-data comparisons for the RCS pressure and downcomer temperature for this test are indicative only for scaled break diameters of around 4 inches. For smaller breaks, the RCS does not depressurize sufficiently to involve flow from the high-capacity ECC systems (CFTs and LPI) so that the condensation potential inside the RCS is much lower. For larger breaks, the break flow area is large enough that the ECCS systems cannot refill the RCS above the elevation of the cold legs and cannot repressurize the RCS. Assessments covering LOCAs for these smaller and larger break diameters appear in other sections of this report.

In summary, this assessment shows good and excellent agreement between the calculated and measured data for many parameters for MIST Test 4100B2. However, for the most important PTS parameters (RCS pressure and downcomer temperature) the assessment showed moderate differences between the calculated and measured responses. Following the RCS blowdown, basic limitations of RELAP5 resulted in an underprediction of the RCS pressure by about 0.68 MPa [98

psi]. For this test, RELAP5 underpredicted the measured downcomer temperature by a maximum of 16 K [29°F] and overpredicted it by a maximum of 32 K [57°F]. Over the full test period, RELAP5 overpredicted the measured downcomer temperature by an average of 0.37 K [0.67°F] and varied from the measured downcomer temperature by an average of 9.0K [16°F]. The assessment of RELAP5/MOD3.2.2 Gamma using experimental data from MIST Test 4100B2 indicates that the code is capable of simulating the behavior of the key PTS parameters. The differences in RCS pressure and downcomer fluid temperature behavior listed here should be taken as indications of the typical maximum uncertainties in these key PTS parameters for RELAP5 simulations of SBLOCAs with break sizes near the upper end of the SBLOCA break-spectrum range.
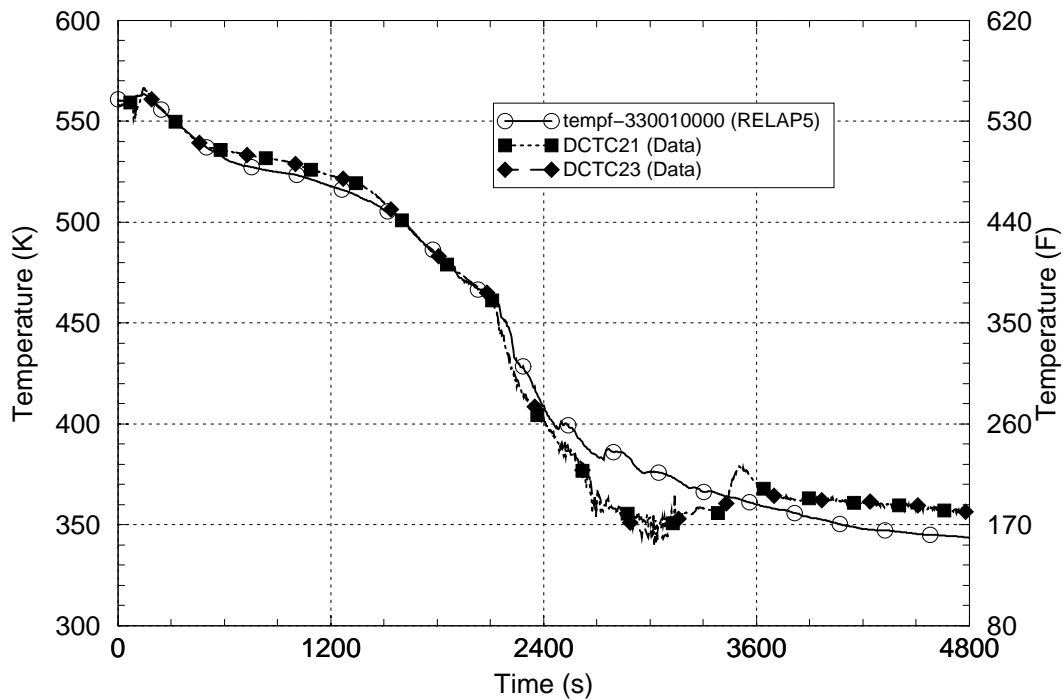

**Figure 3-132   Fluid Temperature in Upper Reactor Vessel Downcomer –
MIST Test 4100B2**

4. CONCLUSIONS

This report documents the assessment of the RELAP5/MOD3.2.2Gamma computer code for predicting the parameters of importance for evaluating PTS risk during PWR plant accident scenarios. The most important thermal-hydraulic parameters for the PTS application are the RCS pressure and the temperature of the fluid in the reactor vessel downcomer region. The assessment is performed by comparing the results from RELAP5 simulations of pertinent separate-effects and integral-effects tests with measured test data for experiments in facilities scaled to PWRs. Qualitative judgements are made regarding the overall fidelity of the RELAP5 test predictions. Quantitative estimates are made of the average uncertainties in the RELAP5 predictions for the important PTS parameters, along with estimates of additional specific uncertainties that are indicated from certain assessment cases for which the RELAP5 test predictions are particularly poor.

The RELAP5 PTS assessments use data from seven experiments in four different separate-effects experimental facilities and from 12 experiments in five different integral-effects experimental facilities. The separate-effects experiments specifically address: (1) pressurizer draining and filling, (2) critical break flow, (3) steam and water behavior in the reactor vessel lower plenum and downcomer regions during the end-of-blowdown and refill periods of LBLOCAs, (4) fluid-fluid mixing in the downcomer, and (5) single-phase, two-phase and reflux cooling mode loop natural circulation phenomena under primary-side and secondary-side degraded inventory conditions. These represent phenomena that are significant for the prediction of the important PTS parameters. The integral-effects experiments address phenomena in coolant-system configurations specifically representing the geometries of Westinghouse, Combustion Engineering and Babcock & Wilcox PWR plant designs. The integral-effects tests simulated PWR behavior under conditions expected during small, medium and large break LOCAs, stuck-open pressurizer SRV events and feed-and-bleed cooling operation scenarios. These sequence categories make up the majority of the risk-dominant sequences in the PTS evaluation study for the Oconee-1, Beaver Valley-1 and Palisades PWRs.

The results of the 19 assessment cases generally indicated good and excellent agreement between the RELAP5 calculations and the measured test data. The average uncertainty in predicting the RCS pressure is characterized as $\pm$0.2 MPa [$\pm$29 psi]. The average uncertainty in predicting the reactor vessel downcomer fluid temperature is characterized as $\pm$10 K [$\pm$18°F].

The results for certain of the assessment cases indicated poor or fair agreement between the RELAP5 calculations and measured test data. The RELAP5 vessel pressure and critical break flow predictions for the two Marviken blowdown tests are characterized as fair. RELAP5 underpredicted the vessel pressure by about 0.3 MPa [43.5 psi] and the break flow prediction was only within about $\pm$ 20% of the measured break flow. These differences were attributed to numerical diffusion effects in the modeling of the Marviken vessel blowdown response. Break flow modeling uncertainties are directly accounted for in the PTS evaluations because the plant analyses cover a complete spectrum of break sizes. The RELAP5 loop flow predictions for the two Semiscale steady natural circulation tests are characterized as poor, with RELAP5 overpredicting the loop flow rate by a factor of about two under certain conditions. This difference was attributed to RELAP5 overpredicting interfacial drag and wall condensation. The effect of this loop flow uncertainty is estimated to be a reactor vessel downcomer fluid temperature overprediction of about 19 K [35°F]. This estimated uncertainty is applicable only during periods of steady coolant-loop natural circulation flow with degraded inventory on the primary or secondary side of the SG tubes. Such

periods are occasionally encountered during PTS transient event sequences, however they typically are short. Evaluations of the effects of any loop flow underpredictions are automatically included in the RELAP5 assessments using the transient integral effects experiments. For ROSA/AP600 Test AP-CL-03, RELAP5 overpredicted the fluid temperature in certain regions of the reactor vessel downcomer by about 20 K [36°F]. This overprediction was related to effects of thermal stratification in liquid-filled cold legs, a phenomenon that basic code limitations prevent RELAP5 from simulating.

The assessment of cold water injection into a stagnant reactor coolant system in test APEX-CE-05 indicated that the downcomer fluid temperature conservatism added by using large artificial reverse flow losses to prevent same-loop cold leg circulations is 8 K [14°F].

In the PTS plant calculations, results obtained for cold leg breaks with a diameter of about 4 inches were found to vary considerably when using one-dimensional and two-dimensional reactor vessel downcomer modeling approaches. An assessment was performed for this break size and location using experimental data from LOFT Test L3-1. This assessment judged two-dimensional downcomer modeling to be the more appropriate approach for the PTS application.

The conclusion from the RELAP5/MOD3.2.2Gamma PTS assessment is that the code is capable of well predicting the phenomena of importance for evaluating PTS risk in PWRs. The average uncertainty in the RCS pressure prediction is characterized as about $\pm$ 0.2 MPa [$\pm$ 29 psi]. The average uncertainty in the reactor vessel downcomer fluid temperature prediction is characterized as about $\pm$ 10 K [$\pm$ 18°F].

5. REFERENCES

1-1   RELAP5/MOD3 Code Manual, "Volume II: Appendix A Input Requirements," RELAP5/MOD3.2.2Gamma, NUREG/CR-5535, Scientech, Inc., June 1999.

2-1   L. Erickson, et al., "The Marviken Full-Scale Critical Flow Tests Interim Report: Results from Test 22," MXC222, March 1979.

2-2   L. Erickson, et al., "The Marviken Full-Scale Critical Flow Tests Interim Report: Results from Test 24," MXC224, May 1979.

2-3   RELAP5/MOD3.3 Code Manual, "Vol III: Developmental Assessment Problems," NUREG/CR-5535/Rev 1 - Vol. III, December 2001.

2-4   H. R. Saedi and P. Griffith, "The Pressure Response of a PWR Pressurizer During an Insurge Transient, Transactions of the American Nuclear Society," 1983 Annual meeting, Detroit, MI, June 12-16, 1983.

2-5   R. Shumway, M. Bolander and B. Aktas, "Prediction of MIT Pressurizer Data using RELAP5 and TRAC-M", ICONE-10 22580, Proceeding of ICONE-10, 10th International Conference on Nuclear Engineering, April 14-18, 2002, Alexandria, VA.

2-6   Siemens AG, "2D/3D Program Upper Plenum Test Facility, Test No. 6, Downcomer Countercurrent Flow Test," Quick Look Report, U9 316/89/2, March 1989

2-7   Kraftwerk Union AG, "Upper Plenum Test Facility, Test No. 1, Fluid-Fluid Mixing Test," R515/87/09, April 1987.

2-8   System Design Description for the Mod-A Semiscale System, Addendum 1: "Mod-A Phase I Addendum to Mod-3 System Design Description," Idaho National Engineering Laboratory, EG&G Idaho, Inc., December 1980.

2-9   R. A. Dimenna, "RELAP5 Analysis of Semiscale Mod-A Single-Loop Single-Component Steady-State Natural Circulation Tests," Idaho National Engineering Laboratory, EG&G Idaho, Inc., EGG-SEMI-6315, June 1983.

3-1   JAERI, "ROSA-IV Large Scale Test Facility (LSTF) System Description," Japan Atomic Energy Research Institute, JAERI-84-237, January 1985.

3-2   ISP-26, "OECD/NEA/CSNI International Standard Problem No. 26, ROSA-IV LSTF Cold-Leg Small-Break LOCA Experiment, Comparison Report," OECD Nuclear Energy Agency, NEA/CSNI/R(91)13, February 1992.

3-3   JAERI, "ROSA-IV Large Scale Test Facility (LSTF) System Description for Second Simulated Fuel Assembly," Japan Atomic Energy Research Institute, JAERI-90-176, October 1990.

3-4   L. S. Ghan, et al., "Large Scale Test Facility: System Description for the ROSA/AP600 and ROSA-V Configuration (for the Third Installed Core)," Japan Atomic Energy Research Institute, JAERI-memo-09-070, March 1996.

3-5   R. A. Shaw, et al., "Quick Look Report for ROSA/AP600 Experiment AP-CL-03," Japan Atomic Energy Research Institute, JAERI Memo 06-249, October 1994.

3-6   Y. Anoda, L. S. Ghan and Y. Kukita, "Quick Look Report for ROSA/AP600 Experiment AP-CL-09, Japan Atomic Energy Research Institute, JAERI Memo 07-232, November 1995.

3-7   "APEX-CE Stuck Open Pressurizer Safety Relief Valve (SRV) from Full Power with Subsequent Reclosure," OSU-CE-13, Oregon State University, October 19, 2001.

3-8   "APEX-CE Palisades Baseline Fluid Mixing Test with 4 Injection Lines, OSU-CE-05," Oregon State University, February 13, 2001.

3-9   D. L. Reeder, "LOFT System and Test Description (5.5-ft Nuclear Core 1 LOCAs)," Idaho National Engineering Laboratory, EG&G Idaho, Inc., NUREG/CR-0247, TREE-1208, July 1978.

3-10   D. L. Gills and J. M. Carpenter, "Experimental Data Report for LOFT Nuclear Small Break Experiment L3-7," Idaho National Engineering Laboratory, EG&G Idaho, Inc., NUREG/CR-1570, August 1980.

3-11   P. D. Bayless and J. M. Devine, "Experiment Data Report for LOFT Large Break Loss of Coolant Experiment L2-5," Idaho National Engineering Laboratory, NUREG/CR-2826, EGG-2210, August 1982.

3-12   P. D. Bayless, J. B. Marlow and R. H. Averill, "Experiment Data Report for LOFT Nuclear Small Break Experiment L3-1," Idaho National Engineering Laboratory, NUREG/CR-1145, EGG-2007, January 1980.

3-13   T. F. Habib, et al., "Multiloop Integral System Test (MIST): MIST Facility Functional Specification," NUREG/ CR-5670, April, 1991.

3-14   J. A. Klingenfus and M. V. Parece, "Multiloop Integral Systems Test, Final Report," NUREG/CR-5395, December 1989.

3-15   C. D. Fletcher, et al., "RELAP5 Thermal-Hydraulic Analyses of Pressurized Thermal Shock Sequences for the Oconee-1 Pressurized Water Reactor," Idaho National Engineering Laboratory, NUREG/CR-3761, EGG-2310, June 1984.

2. TITLE AND SUBTITLE

RELAP5/MOD3.2.2 Gamma Assessment for Pressurized Thermal Shock Applications

3. DATE REPORT PUBLISHED

MONTH	YEAR
October	2004

4. FIN OR GRANT NUMBER
Y6533

5. AUTHOR(S)

C.D. Fletcher, D.A. Prelewicz, W.C. Arcieri

6. TYPE OF REPORT

Final, technical

7. PERIOD COVERED *(Inclusive Dates)*

8. PERFORMING ORGANIZATION - NAME AND ADDRESS *(If NRC, provide Division, Office or Region, U.S. Nuclear Regulatory Commission, and mailing address; if contractor, provide name and mailing address.)*

Information Systems Laboratories, Inc.
11140 Rockville Pike, Suite 500
Rockville, MD 20852

9. SPONSORING ORGANIZATION - NAME AND ADDRESS *(If NRC, type "Same as above"; if contractor, provide NRC Division, Office or Region, U.S. Nuclear Regulatory Commission, and mailing address.)*

Division of Systems Analysis and Regulatory Effectiveness
Office of Nuclear Regulatory Research
U. S. Nuclear Regulatory Commission
Washington, DC 20555-0001

10. SUPPLEMENTARY NOTES

1 1. ABSTRACT *(200 words or less)*

The RELAP5/MOD 3.2.2Gamma computer code has been used to simulate overcooling and/or pressurization events that have the potential to result in pressurized thermal shock (PTS) in the reactor vessels of pressurized water reactors. An assessment of this code version is reported here to establish the suitability of the computer code for analyzing transients that may be significant PTS risk contributors. Code assessment principally consists of performing calculations for a specific test in an experimental facility and comparing the calculated results to the measured data from the experimental facility.

Prior assessment of the RELAP5 code series has been performed for a wide variety of transients over the 20-year development history of the code. In this assessment, the focus is on the temperature and pressure conditions in the reactor vessel downcomer which are key parameters for PTS assessment. The assessment reported here focuses on comparing RELAP5 results with experimental data for conditions in the downcomer.

This report presents assessments that demonstrate the suitability of RELAP5/MOD3.2.2 Gamma for analyzing PTS transients.

12. KEY WORDS/DESCRIPTORS *(List words or phrases that will assist researchers in locating the report.)*

pressurized thermal shock, RELAP5, thermal hydraulic analysis, reactor pressure vessels

13. AVAILABILITY STATEMENT
unlimited

14. SECURITY CLASSIFICATION

(This Page)
unclassified

(This Report)
unclassified

15. NUMBER OF PAGES

16. PRICE

NRC FORM 335 (2-89)